

Mechanisms and Design in Homogeneous Catalysis

Students: Sillars, D.; Batterton, J.; Hall, J.

Collaborators: Piers, W.

Department of Chemistry, University of Wisconsin-Madison, Madison, WI 53706

landis@chem.wisc.edu

Goal

Elucidation of fundamental reactivity patterns of transition metal alkyls in metallocene-catalyzed alkene polymerization and novel ligand development.

Recent Progress

Metallocene-catalyzed alkene polymerization is rapidly becoming the largest scale application of homogeneous catalysts in the world. Despite enormous investments in the development of new catalysts, ligand systems, and co-catalysts for alkene polymerizations, many fundamental aspects of catalytic polymerization remain unclear. In the last year of support, we have made significant progress in several areas: direct observation of polymerization events by NMR methods, identification of the mechanism by which polypropene isotacticity is lost during polymerization, and examination of the relative reactivities of various primary and secondary alkyls.

Direct Observation of Catalytic Events. Direct observation of polymer growth at the metallocene center enables “molecular level” characterization of catalyst structure and dynamics. We recently reported *the first example of the interception and characterization of the propagating species in a commercially-relevant metallocene-catalyzed polymerization reaction.* In this case, it is the propagating species for (EBI)ZrMe(MeB(C₆F₅)₃)-catalyzed polymerization of 1-hexene, propene, and ethene. Characterization of the propagating species using various labeled compounds (summarized in the adjacent graphic) is comprehensive and compelling. At temperatures < -40°C, the propagating species is stable for tens of hours and constitutes a living catalyst. By simultaneous monitoring of the consumption of alkene and conversion of the uninitiated catalyst to the propagating one, the rate laws and rate constants for initiation and propagation *are measured directly for the first time.* Importantly, for 1-hexene and (EBI)ZrMe(MeB(C₆F₅)₃) we find that *the rate constants and rate laws for initiation, propagation, and termination determined at low temperature by direct NMR observation correspond with those determined previously* over the temperature range of 0-50°C. Thus, we have found a rapid method for generating fundamental kinetic parameters for this important reaction.

Powerful mechanistic insights result from direct observation. One example is the nature of propagation: does the polymer grow continuously at a single center or is the growth, as suggested by Brintzinger, sporadic with stops and starts driven by ion-pair dissociation/association events? Careful labeling studies based on direct observation of the propagating species provide the answer: propagation is a continuous event.

Loss of Stereoregularity in Propene Polymerization. One of the more interesting and surprising proposals from the past decade of isotactic propene polymerization catalysis concerns loss of stereoregularity at low concentrations of propene. The proposal, chain-epimerization of the growing polymer, poses that low tacticity results primarily from epimerization of a correctly inserted monomer rather than insertion of the wrong enantioface. In effect, the catalyst first makes the correct decision and then changes its mind. Using direct-observation methods and extensive isotopic labeling, we have been able to “watch” chain-end epimerization events at metallocene-polymeryl intermediates for the first time. These studies confirm epimerization via tertiary alkyls and provide quantitative data for the overall rates of epimerization vs. termination. Importantly, extrapolation of these data to higher temperatures confirms that the *primary process for loss of stereoregularity in propene polymerization is chain-end epimerization* via a complex process with a high degree of nuclear motion.

Regioerrors, Catalyst Activity, and H₂ Responsivity. More recently we have examined the relative reactivity of secondary alkyls at metallocenes. Secondary alkyls result from 2,1-insertions of monosubstituted alkenes. Such regioerrors are thought by many to have dire consequences for catalysis according to the following logic: secondary alkyls are slow to insert monomers which leads to accumulation of catalyst in this dormant state. As a result, less of the catalyst lies in the active pool and the overall activity declines (estimates for the activity decrease are in the 10- to 100-fold range). The primary evidence for these hypotheses comes from hydrooligomerization and labeled ethene incorporation studies. In both types of studies, there is an over-representation of products from reaction of H₂ and/or C₂H₄ with secondary alkyls.

In contrast, our quench-label approaches to active site counting consistently demonstrate little accumulation of catalyst in the form of secondary alkyls. To resolve this important dilemma we have taken a direct approach: generate secondary alkyls in situ and directly measure their rates of isomerization, hydrogenolysis, and alkene insertion. Each direct measurement that we have made refutes the “conventional wisdom”. We find: (1) reaction of secondary alkyls with 1-hexene and propene at –80°C *not* slower than reaction of primary alkyls (such as Zr-polypropenyl or Zr-polyhexenyl cations) (2) *secondary alkyls are more reactive than primary alkyls toward H₂ and ethene by 1-3 orders of magnitude* (3) secondary alkyls are thermodynamically unstable with respect to primary alkyls and (4) secondary alkyls undergo β-H elimination with *significantly lower activation enthalpies* than primary alkyls. What does this mean? One clear implication is that secondary alkyls do not constitute “dormant” sites into which most of the catalyst is pooled. Equally importantly, the much higher reactivity of secondary alkyls toward H₂ means that *responsivity of a catalyst to H₂ as a chain transfer agent is critically dependent on the catalyst regioselectivity*. Less regioselective catalysts will be more responsive to H₂-based chain transfer.

Novel Ligands for Highly Selective Catalysis. Highly selective catalysts increase atom economy and energy efficiency while decreasing waste. Our goal is to develop new phosphorus chemistry that will enable broadened catalyst discovery via large phosphine ligand libraries. This project was seeded with DOE funding and so is briefly mentioned here.

We have shown that 3,4-diazaphospholanes provide a pathway to making enormous libraries of novel, chiral phosphine ligands. Recently we have demonstrated that monophosphine libraries of diazaphospholanes form highly effective ligands for Pd-catalyzed asymmetric allylic alkylation reactions. These studies have been extended to bead-based catalysts and demonstrate state-of-the-art selectivity while supported on beads. In the near future, we will report highly active, regio-, and enantio-selective alkene hydroformylation promoted by diazaphospholane ligands.

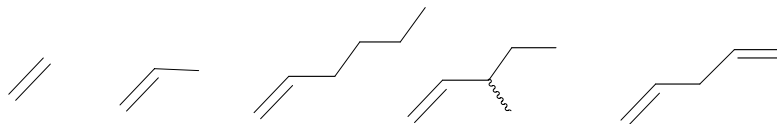
DOE Interest

Patterns in transition metal alkyl formation and reactivity control product selectivity in the largest worldwide catalytic transformations of organic feedstocks. This research program develops (1) a fundamental understanding of these patterns (2) specific, detailed mechanisms of actual (non-model) catalysts for the commodity-scale process of alkene polymerization and (3) novel techniques for studying catalytic transformations.

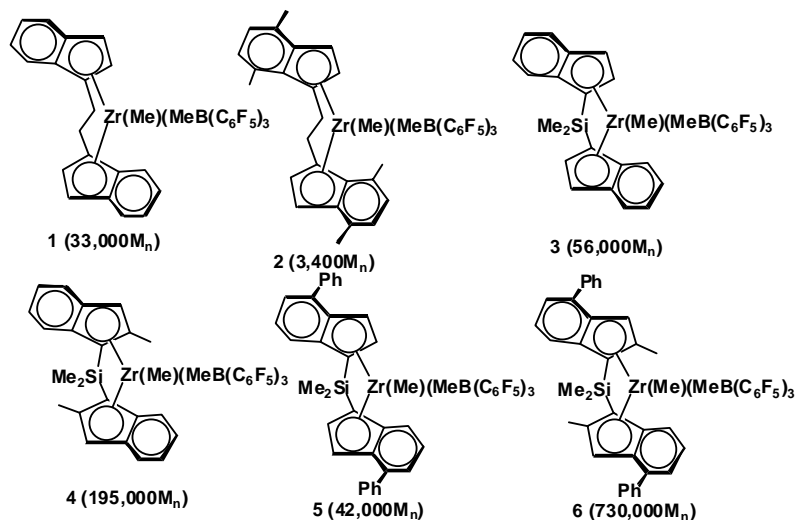
Future Plans

Quantitative Structure-Activity Relationships. Direct observation of polymer growth at the metallocene center enables “molecular level” characterization of catalyst structure and dynamics. We have previously demonstrated that one can intercept the propagating species for (EBI)ZrMe(MeB(C₆F₅)₃)-catalyzed polymerization of 1-hexene, propene, and ethene and *directly measure rates of initiation, propagation, and termination*. Furthermore, we have rigorously proven that the rates, rate laws, activation parameters, and rate constants obtained under low temperature conditions apply can be extrapolated to “real” polymerization conditions.

We now are accumulating quantitative data for insertion and termination rates as a function of alkene structure:



The second dimension of our study on structure-activity relationships concerns the influence of metallocene-ligand structure on the kinetics of elementary steps. The collection of ligands (along with polymer molecular weights obtained with these catalysts) under ongoing investigation is shown below.



The third dimension of our examination of structure-activity relationships concerns the influence of co-catalyst on polymerization rates. We are in the process of collecting data with non-coordinating anions (both $\text{B}(\text{C}_6\text{F}_5)_4^-$ and some of Warren Piers diboryl anions).

Publications Citing DOE Support

1. 'A ^2H -Labeling Scheme for Active-Site Counts in Metallocene-Catalyzed Alkene Polymerization.' Liu, Z.; Somsook, E.; Landis, C. R. *J. Am. Chem. Soc.* **2001**, *123*(12), 2915-2916.
2. 'Kinetics of initiation, propagation, and termination for the $[\text{rac}-(\text{C}_2\text{H}_4(1\text{-indenyl})_2)\text{ZrMe}][\text{MeB}(\text{C}_6\text{F}_5)_3]$ -catalyzed polymerization of 1-hexene' Liu, Z. X.; Somsook, E.; White, C. B.; Rosaaen, K. A.; Landis, C. R. *J. Am. Chem. Soc.* **2001**, *123*, 11193-11207.
3. 'A Rapid Quenched-Flow Device for the Study of Homogeneous Polymerization Kinetics', White, C. B.; Rosaaen, K. A.; Landis, C. R. *Rev. of Sci. Instr.*, **2002**, *73*, 411-415.
4. 'Diverse Mechanisms of Chemical Exchange for Group 4 Metallocene-Based Alkene Polymerization Catalysts' Somsook, E.; Landis, C. R. *J. Am. Chem. Soc.*, submitted for publication.
5. 'Counterion Influence on the Kinetics of Initiation, Propagation, and Termination for Polymerization of 1-Hexene as Catalyzed by $[\text{rac}-(\text{C}_2\text{H}_4(1\text{-indenyl})_2)\text{ZrMe}]$ Cations' Landis, C. R.; Liu, Z.; White, C. B. *Polymer Preprints* **2002** *43*, 301-302.
6. 'Direct Observation of the Propagating Species in the $(\text{EBI})\text{Zr}(\text{Me})(\text{MeB}(\text{C}_6\text{F}_5)_3)$ -catalyzed Polymerization of 1-Hexene' Landis, C. R.; Rosaaen, K. A. *Polymer Material Science and Engineering*, **2002**, *43*, 301-302.
7. 'Heavy Atom Kinetic Isotope Effects, Cocatalysts, and the Propagation Transition State for Polymerization of 1-Hexene Using the $\text{rac}-(\text{C}_2\text{H}_4(1\text{-indenyl})_2)\text{ZrMe}_2$ Catalyst Precursor' Landis, C. R.; Rosaaen, K. A.; Uddin, J. *J. Am. Chem. Soc.*, **2002**, *124*, 12062-12063.
8. 'Direct Observation of Insertion Events at $(\text{EBI})\text{Zr}(\text{MeB}(\text{C}_6\text{F}_5)_3)$ -Polymeryl Intermediates: Distinction Between Continuous and Intermittent Propagation Modes' Clark R. Landis, Kimberly A. Rosaaen, Douglass R. Sillars *J. Am. Chem.*

- Soc.* **2003**, *125*, 1710-1711.
9. 'Catalytic Propene Polymerization: Determination of Propagation, Termination, and Epimerization Kinetics by Direct NMR Observation of the (MeB(C₆F₅)₃)propenyl Catalyst Species' Douglass R. Sillars and Clark R. Landis, *J. Am. Chem. Soc.* **2003**, *125*, 9894-9895.
 10. 'Resolved Chiral 3,4-Diazaphospholanes and Their Application to Catalytic Asymmetric Allylic Alkylation' Thomas P. Clark, Clark R. Landis, *J. Am. Chem. Soc.* **2003**, *125*, 11792-11793.
 11. 'Solid Phase Synthesis of Chiral 3,4-Diazaphospholanes and Their Application to Catalytic Asymmetric Allylic Alkylation' *Proc. Nat. Acad. Sci.* (in press).

This page intentionally left blank.

primary amine, secondary amine, urea, isocyanate, vinyl, and nitrile, with high reproducibility.^{2,3} We discovered that the particle morphology of the resulting materials could be directed to different particle shapes and sizes, such as spheres (**Figure 1a**), tubes, and rods (**Figure 1b**), simply by introducing different organoalkoxysilane precursors into our co-condensation reactions.^{2,3}

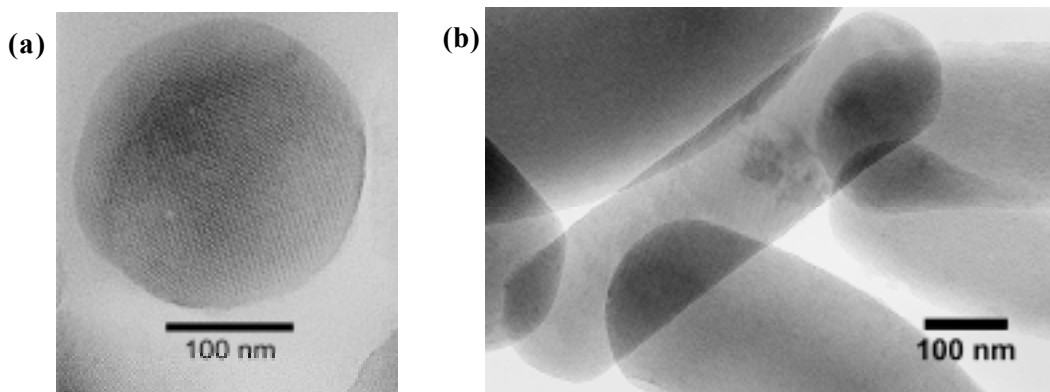


Figure 1. TEM micrographs of mercaptopropyl- and cyanopropyl-functionalized mesoporous silica materials (**a** and **b**, respectively).

Progress 3. Multi-functionalization: incorporation of multiple organic functional groups with precisely controlled relative concentrations

As previously described, the difference in “the hard/soft acid/base electrostatic matching” abilities of various organoalkoxysilane precursors with CTAB surfactant micelles can not only influence the loading of a particular functional group under our co-condensation condition, but also dictate the pore and particle morphology of the resulting mesoporous material. By introducing two organoalkoxysilanes with different structure-directing abilities as precursors of our co-condensation reaction, we can take advantage of such a difference between the two organoalkoxysilanes and utilize one precursor with *stronger structure-directing ability* to create the desired pore and particle morphology and employ the *other* for selective immobilization of catalysts. This strategy allows us to generate a series of multi-functionalized mesoporous silica materials with *control of both morphology and functionalization*.⁴

Progress 4. Tethering transition metal complex catalyst onto organically functionalized mesoporous silicas for formation-directing polymerization

To demonstrate the feasibility of using the morphologically defined silicas with precise control of the density and location of the organic functional groups as a support for *single-site heterogeneous catalysts*, we have used the aforementioned co-condensation method with *N*-[3-(trimethoxysilyl)propyl]-ethylenediamine (AAPTMS), as the precursor.⁵ The AAPTMS groups then served as chelating ligands to bind with Cu^{2+} and form the catalytically active complexes. The resulting AAPTMS-functionalized particles (**Cu-MCM**) had a spherical shape with an average diameter of 500 nm and a BJH pore diameter of 25.6 Å.⁵ As depicted in **Figure 2**, the Cu-MCM served as a catalytic scaffold to direct and orient the conformation of the “molecular wire” formed through oxidative

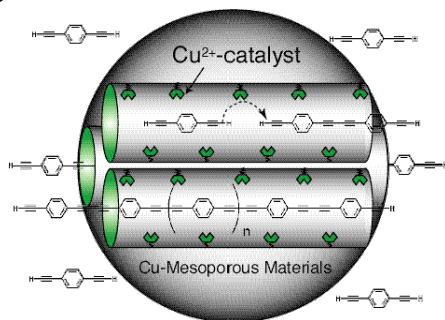


Figure 2. Schematic representation of Cu^{2+} -functionalized mesoporous silica (**Cu-MCM**) catalysts for oxidative polymerization of 1,4-diethynylbenzene into conjugated oligo(phenylene butadiynylene).

coupling reactions of 1,4-diethynylbenzene to a highly conjugated poly(phenylene butadiynylene) polymer (PPB). Fluorescence and ^{13}C solid state NMR provided spectroscopic evidence that isolated molecular wires with a high degree of alignment were formed within the parallel channels of our mesoporous catalyst.⁵ These results indicated that proper adjustment of the pore diameter and the distribution of catalytic groups are vital in order to prevent clogging of the pores with aggregated and/or cross-linked polymers.

Progress 5. Control of the selectivity of mesopore-tethered catalysts (*Gatekeeping Effect*)

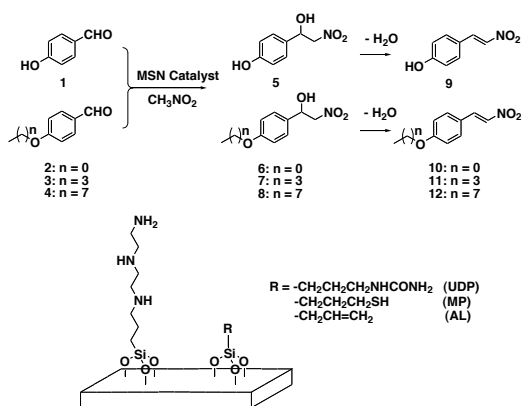


Figure 3. Bi-functionalized MSNs catalyzed competitive nitroaldol reaction.

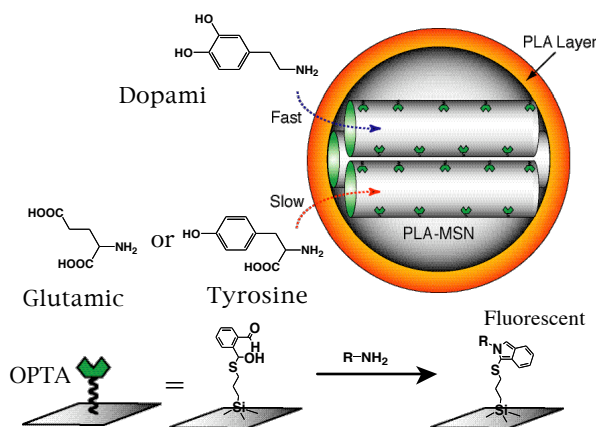


Figure 4. Schematic representation of the synthesis of PLA-coated MSN-based fluorescence sensor system for detection of amine-containing neurotransmitters, i.e., dopamine, glutamic acid, and tyrosine ($R-NH_2$).

highly efficient and selective catalysts. This research can also provide new fundamental knowledge about catalysis in general by deconvoluting the key factors that affect selectivity, reactivity and kinetics.

Future Plans

- *Control of the orientation and activity of tethered transition metal complex catalysts.* In order to understand the activity and selectivity of metal complex catalysts tethered on the walls of mesopores, we will characterize and control the location and the exact structure of the tethered catalysts on the surface.
- *Influence of the mesopore environment on catalyst selectivity and activity.* Our ability to anchor two types of groups on mesopore walls allows us to tether not only the catalyst but also other functional moieties. The influence of these auxiliary groups will be directed toward achieving various catalyst functions, such as enantioselectivity. These studies will use the concept of gatekeepers, which will be tested in the development of catalysts for the stereochemically controlled polymerization, selective hydrolysis, etc.

Publications (2002-present)

1. D. R. Radu, C.-Y. Lai, J. Huang, J. W. Wiench, M. Pruski, and V. S.-Y. Lin,* “Controlled Functionalization of MCM-41 Type of Mesoporous Silica with Anionic Organotrioxysilanes via Interfacial Electrostatic Designed Co-condensation” *Chem. Comm. (Cambridge, U.K.)*, **2004**, submitted.

We have demonstrated that the reaction selectivity of mesoporous catalysts can be controlled by using the novel concept of *gatekeepers*.^{6,7} Specifically, we prepared a series of bifunctionalized mesoporous silica nanosphere-based (MSN) catalysts for nitroaldol (Henry) reaction.⁶ In these catalysts (**Figure 3**), a common 3-[2-(2-aminoethylamino)ethylamino]propyl (AEP) primary group served as a catalyst, while three different secondary groups, ureidopropyl (UDP), mercaptopropyl (MP), and allyl (AL) functionalities, were incorporated as gatekeepers to control the reaction selectivity. We demonstrated that the selectivity of these bifunctionalized MSN catalysts could be systematically tuned simply by varying the polarity and hydrophobicity of the gatekeepers. In a separate study (**Figure 4**),⁷ we demonstrated a unique “sieving” effect of the poly(lactic acid) layer that was covalently attached to the exterior surface of mesoporous silica nanospheres. By utilizing this layer as a gatekeeper, we investigated the molecular recognition events between several structurally similar neurotransmitters, i.e., dopamine, tyrosine, and glutamic acid and a pore surface-anchored *o*-phthalic hemithioacetal (OPTA) group.⁷

DOE Interest

Developing catalytic systems that can coherently unite the best features of the homogeneous and heterogeneous areas of catalysis has been a key interest of DOE. By controlling the structure, reactivity and morphology of the mesoporous solid support and its interaction with the active sites, one can provide truly unique opportunities for the design of a new generation of

2. S. Huh, J. W. Wiench, J.-C. Yoo, M. Pruski, and V. S.-Y. Lin,* “Organic Functionalization and Morphology Control of Mesoporous Silica Materials via a Co-condensation Synthesis Method”, *Chem. Mater.* **2003**, *15*, 4247-4256.
3. C.-Y. Lai, D. M. Jeftinija, K. Jeftinija, S. Xu, S. Jeftinija, and Victor S.-Y. Lin,* “A Mesoporous Silica Nanosphere-Based Carrier System with Chemically Removable CdS Nanoparticle Caps for Stimuli Responsive Controlled Release of Neurotransmitters and Drug Molecules”, *J. Am. Chem. Soc.* **2003**, *125*, 4451-4459.
4. S. Huh, J. W. Wiench, B. G. Trewyn, S. Song, M. Pruski, and V. S.-Y. Lin,* “Tuning of Particle Morphology and Pore Properties in Mesoporous Silicas with Multiple Organic Functional Groups”, *Chem. Comm. (Cambridge, U.K.)*, **2003**, *18*, 2364-2365.
5. V. S.-Y. Lin,* D. R. Radu, M.-K. Han, W. Deng, S., Kuroki, D. R. Radu, B. H. Shanks, and M. Pruski, “Oxidative Polymerization of 1,4-Diethynylbenzene into Highly Conjugated Oligo(phenylene butadiynylene) Polymer Within the Channels of Surface-functionalized Mesoporous Silica and Alumina Materials” *J. Am. Chem. Soc.*, **2002**, *124*, 9040-9041
6. S. Huh, H.-T. Chen, J. W. Wiench, M. Pruski, and V. S.-Y. Lin,* “Controlling the Selectivity of Competitive Nitroaldol Condensation by Using a Bifunctionalized Mesoporous Silica Nanosphere-Based Catalytic System”, *J. Am. Chem. Soc.*, **2004**, *126*, 1010-1011.
7. D. R. Radu, C.-Y. Lai, J. W. Wiench, M. Pruski, and V. S.-Y. Lin,* “Gatekeeping Layer Effect: A Poly(lactic acid)-coated Mesoporous Silica Nanosphere-Based Fluorescence Sensor for Detection of Amino-Containing Neurotransmitters”, *J. Am. Chem. Soc.*, **2004**, *126*, 1640-1641.

Basic Investigations into the Reactivity of CO₂: New Methods of Activation of CO₂

Postdocs: Main, A. D. and Getty, A.

Students: Bott, E. and Weaver, M.

Collaborators: Jessop, P. G. and Bitterwolf, T. E.

Molecular Interactions and Transformations, Fundamental Sciences Division, Pacific Northwest National Laboratory, Richland, WA 99352

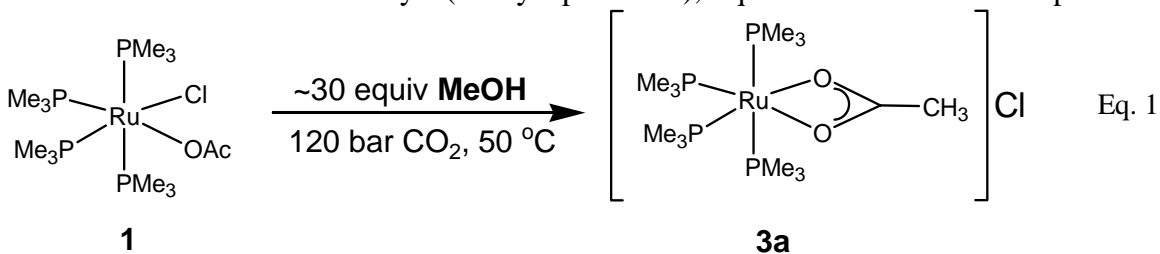
john.linehan@pnl.gov

Goal

Develop a fundamental understanding of the mechanisms of activation of relatively inert substrates.

Recent Progress

Ruthenium-based catalysts for CO₂ hydrogenation. Ruthenium-based catalysis of the hydrogenation of CO₂ to produce formic acid has been reported to be enhanced in the presence of protic co-catalysts, such as alcohols. We have used *in situ* high-pressure NMR spectroscopy to determine that the alcohol acts to produce cationic ruthenium complexes which appear to be a more active form of the catalyst (catalyst precursor), Equation 1. The cationic species **3**



gives the same high rates of CO₂ hydrogenation as does **1**, even in the absence of an alcohol additive.

In situ spectroscopy has also allowed us to interrogate the ruthenium complexes formed during catalysis. We have found little evidence for the involvement of a phosphine loss pathway for this series of catalysts. A proposed catalytic scheme based on our studies is shown in Figure 1. The chelated ruthenium formate cation **8** is only observed under H₂ and CO₂ pressure.

Reaction of CO₂ with alcohols. Alcohols and CO₂ have been found to be in equilibrium with the half-acid, R-O-C(O)-OH with the equilibrium far to the reactant side. In the presence of bases the half-acid salts can be observed using high-pressure NMR and IR spectroscopy. The equilibrium constant of this reaction is dependent upon the base, the alcohol, the CO₂ overpressure and the polarity of the solvent. The methyl carbonate DBU salt can be

DOE Interest

The mechanisms of interactions of relatively inert substrates such as CO₂, ethane, methane, etc. are of fundamental interest for U.S. chemical and energy production. Fundamental understanding of reaction chemistry is necessary for efficient utilization of chemical feedstocks.

Future Plans

Interfacial catalysis. Initial studies into the complex reactions in multi-phase media are being conducted. While studies of homogeneous reaction systems still yield important fundamental information, the more complex multi-phase systems need to be better understood. These systems, which include liquid-liquid, gas-liquid, solid-liquid, solid-gas and more complex mixtures, may or may not follow similar reaction pathways to their homogeneous analogs. In a relatively simple case from our laboratory the addition of small amounts of hydrogen to a homogeneous supercritical solution of ethylene containing a manganese organometallic compound led to a separation into three phases, all of which contained at least some of each of the three reagents. In this and other multi-phase systems the paramount question is: Do the reagents behave as in a homogeneous system or are there other pathways for reaction? This question is being applied to both supercritical fluid systems and more mundane systems in which homo- and heterogeneous catalysis occurs. Time-resolved spectroscopy in combination with *in situ* high-pressure spectroscopy are being applied to this complex problem.

Publications

Munshi P, Main AD, Linehan JC, Tai CC, Jessop PG, "Hydrogenation of carbon dioxide catalyzed by ruthenium trimethylphosphine complexes: The accelerating effect of certain alcohols and amines", *J. Am. Chem. Soc.*, **2002**, *124* (27): 7963-7971.

Bitterwolf TE, Scallorn WB, Bays JT, Weiss CA, Linehan JC, Franz J, Poli R," Photochemical intermediates of trans-Rh(CO)L₂Cl where L = PMe₃, PBu₃, and i-Pr₂HN and cis-Rh(CO)(2)(i-Pr₂HN)Cl in frozen organic glasses", *J. Organomet. Chem.*, **2002**, *652* (1-2): 95-104.

Yonker CR, Linehan JC, " Investigation of the hydroformylation of ethylene in liquid carbon dioxide", *J. Organomet. Chem.* , **2002**, *650* (1-2): 249-257.

Tai CC, Pitts J, Linehan JC, Main AD, Munshi P, Jessop PG, "In situ formation of ruthenium catalysts for the homogeneous hydrogenation of carbon dioxide", *Inorg. Chem.*, **2002**, *41* (6): 1606-1614.

This page intentionally left blank.

Photocatalysis with Microporous ETS-10 Materials

Students: Michael Nash and Anne Marie Zimmerman

PIs: Raul F. Lobo and Douglas Doren

Center for Catalytic Science and Technology

Departments of Chemical Engineering, and Chemistry and Biology

University of Delaware

Goal

Develop the physical basis for understanding the photocatalytic properties of ETS-10 and related microporous titanosilicates containing wires of TiO₂ octahedra.

Background and Recent Progress

ETS-10 is a crystalline microporous semiconductor containing one-dimensional units of TiO₂ octahedra. These semiconducting wires act as photocatalysts and promote intermolecular reactions between adsorbed species. We are conducting a comprehensive investigation of photocatalysis in ETS-10 consisting of five interconnected research focuses. Firstly we are studying surface species formed in the micropores upon irradiation of ETS-10 with UV light. These studies will rely mostly on DRIFT spectroscopy, UV/Vis-diffuse-reflectance spectroscopy and EPR to characterize the species formed inside the pores. Second we will study the mechanisms of photooxidation of methanol and ethanol in the pores of ETS-10 (in its sodium and proton forms) and compare them to the well-understood mechanism of decomposition in TiO₂ anatase. Third, we will prepare new forms of ETS-10 containing other transition metals (Fe, V, Nb, etc.) with the objectives of reducing the bandgap, increasing the quantum yield, changing the nature of the excited species formed upon irradiation and changing the hydrophilic character of the pores (i.e. to make it more organophilic).

The interpretation of the experimental results and the selection of specific dopants will be closely tied to electronic structure calculations. We have recently begun first-principles calculations of dopant effects on the electronic structure of anatase and we are applying the same methods to understand the photochemistry of ETS-10. Modeling will be a proactive part of the research driving guiding the synthesis efforts of the research.

Our aims are that at the end of the funded period we will have a well-organized body of experimental data and modeling results that will let us make useful predictions about the photocatalytic properties of ETS-10 isostructural materials. The information should also help in the prediction of photocatalytically relevant steps in the oxidation of small molecules in the pores of different materials.

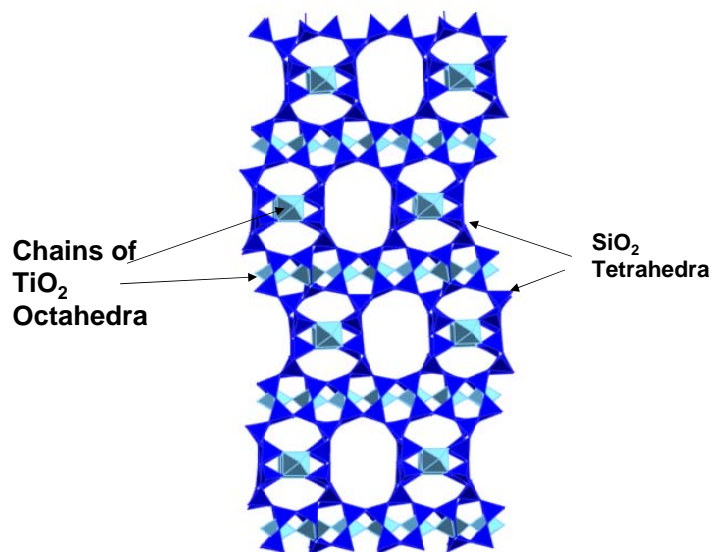


Figure 1: Framework structure of ETS-10.

**Cluster-Expanded Solids:
A Strategy for Assembling Functional Porous Materials**

Postdoctoral Associate: Stéphane A. Baudron

Graduate Students: Laurance G. Beauvais, Miriam V. Bennett, Louise A. Berben, Nathan R. M. Crawford, Allan G. Hee, Eric G. Tulsy, Eric J. Welch

Undergraduate Students: Mary Faia, Shaun Wong, Chun Liang Yu

Collaborators: Patrick Batail, Robert G. Bergman, Sophia E. Hayes

Department of Chemistry, University of California, Berkeley, CA 94720-1460
jlong@cchem.berkeley.edu

Goal

The intention of the research is to explore the use of molecular cluster precursors in the assembly of microporous coordination solids that function as sieves, sensors, or catalysts.

Recent Progress

Cyano-Bridged Frameworks Incorporating Mixed-Metal Clusters. Reactions of the face-capped octahedral clusters $[\text{Re}_5\text{OsSe}_8\text{Cl}_6]^{3-}$ and $[\text{Re}_4\text{Os}_2\text{Se}_8\text{Cl}_6]^{2-}$ with NaCN in a melt of NaNO_3 afford the cyano-terminated clusters $[\text{Re}_5\text{OsSe}_8(\text{CN})_6]^{3-}$ and $[\text{Re}_4\text{Os}_2\text{Se}_8(\text{CN})_6]^{2-}$. The former species reacts with $[\text{Ni}(\text{H}_2\text{O})_6]^{2+}$ in aqueous solution to yield the cluster-expanded Prussian blue analogue $\text{Ni}_3[\text{Re}_5\text{OsSe}_8(\text{CN})_6]_2 \cdot 33\text{H}_2\text{O}$. In addition, these clusters can be reduced by one electron to give the first 25-electron clusters of their type. As demonstrated with the synthesis and characterization of $\{\text{Re}_4\text{Os}_2\text{Se}_8[\text{CNCu}(\text{Me}_6\text{tren})]_6\}^{9+}$, the reduced diosmium cluster is capable of engaging in ferromagnetic exchange interactions, indicating its potential utility in the synthesis of a microporous magnet.

Cyano-Bridged Frameworks Incorporating $[\text{Zr}_6\text{BCl}_{12}]^{2+}$ Cluster Cores. The reaction between $[\text{Zr}_6\text{BCl}_{18}]^{4+}$ and $[\text{Cr}(\text{CN})_6]^{3-}$ in aqueous solution, leads to the immediate precipitation of the cluster-expanded Prussian blue analogue $(\text{Et}_4\text{N})[\text{Zr}_6\text{BCl}_{12}][\text{Cr}(\text{CN})_6] \cdot \text{Et}_4\text{NCl} \cdot 3\text{H}_2\text{O}$. The cubic Prussian blue type structure of this compound was confirmed via Rietveld profile analysis of X-ray powder diffraction data, and magnetization measurements reveal the onset of long-range magnetic ordering at 2 K.

Trigonal Prismatic Cluster Building Units. Simultaneous reduction of WCl_6 and CCl_4 with bismuth metal at 450 °C, leads, upon work-up, to the carbon-centered trigonal prismatic cluster $[\text{W}_6\text{CCl}_{18}]^{2-}$. Cyclic voltammetry experiments performed on solutions

containing this cluster show that it possesses five chemically-accessible redox states. Related reactions incorporating NaN_3 in place of CCl_4 led to the analogous nitrogen-centered cluster $[\text{W}_6\text{NCl}_{18}]^{2-}$.

New Metal-Chalcogen Cluster Building Units. Evaporation of binary transition metal chalcogenides and cocondensation of the vapor with PEt_3 has led to a range of new metal-chalcogen clusters. For example, evaporation of Cu_2Se enables isolation of $[\text{Cu}_{26}\text{Se}_{13}(\text{PEt}_3)_{14}]$ and $[\text{Cu}_{70}\text{Se}_{35}(\text{PEt}_3)_{21}]$, containing surface-ligated fragments of the original solid.

Prussian Blue Analogues Incorporating $[\text{Co}(\text{CN})_5]^{3-}$. The reaction between $[\text{Co}(\text{H}_2\text{O})_6]^{2+}$ and the square pyramidal complex $[\text{Co}(\text{CN})_5]^{3-}$ in deoxygenated water yields the Prussian blue analogue $\text{Co}_3[\text{Co}(\text{CN})_5]_2 \cdot 8\text{H}_2\text{O}$, containing a high concentration of lattice vacancies. Upon dehydration, the compound retains crystallinity and exhibits a Type I dinitrogen sorption isotherm, characteristic of a microporous solid. Magnetic measurements showed it to behave as a ferrimagnet with an ordering temperature of 48 K, which is reduced to 38 K in the dehydrated solid. This is the first truly microporous material shown to exhibit magnetic hysteresis.

New Cyanomolybdate Building Units. Octahedral coordination of molybdenum(III) was achieved by limiting the amount of cyanide available upon complex formation. Reaction of $\text{Mo}(\text{CF}_3\text{SO}_3)_3$ with LiCN in DMF affords $\text{Li}_3[\text{Mo}(\text{CN})_6] \cdot 6\text{DMF}$, featuring the previously unknown octahedral complex $[\text{Mo}(\text{CN})_6]^{3-}$. Further restricting the available cyanide in a reaction between $\text{Mo}(\text{CF}_3\text{SO}_3)_3$ and $(\text{Et}_4\text{N})\text{CN}$ in DMF, followed by recrystallization from DMF/MeOH, yields $(\text{Et}_4\text{N})_5[\text{Mo}_2(\text{CN})_{11}] \cdot 2\text{DMF} \cdot 2\text{MeOH}$.

New Cyanorhenate Building Units. Reaction of $(\text{Bu}_4\text{N})\text{CN}$ with $[\text{ReCl}_6]^{2-}$ in acetonitrile affords yellow $(\text{Bu}_4\text{N})_3[\text{Re}(\text{CN})_7]$, featuring the pentagonal bipyramidal complex $[\text{Re}(\text{CN})_7]^{3-}$. In aqueous solution, this compound reacts with Mn^{2+} ions to generate the porous, and potentially photomagnetic, three-dimensional solid $[\text{fac-Mn}(\text{H}_2\text{O})_3][\text{cis-Mn}(\text{H}_2\text{O})_2][\text{Re}(\text{CN})_7] \cdot 3\text{H}_2\text{O}$. Addition of KIO_4 to the reaction solution, originally intended to prevent reduction of the rhenium during solid formation, instead yields white $(\text{Bu}_4\text{N})_3[\text{Re}(\text{CN})_8]$, featuring the square antiprismatic complex $[\text{Re}(\text{CN})_8]^{3-}$.

Homoleptic Trimethylsilylacetylde Complexes. Reactions between simple transition metal salts and LiCCSiMe_3 have been shown to generate three new octahedral complexes: $[\text{Cr}(\text{CCSiMe}_3)_6]^{3-}$, $[\text{Fe}(\text{CCSiMe}_3)_6]^{4-}$, and $[\text{Co}(\text{CCSiMe}_3)_6]^{3-}$. Spectroscopic characterization of these molecules has enabled us to establish the ligand field strength of trimethylsilylacetylde as lying just below methyl in the spectrochemical series.

DOE Interest

The new microporous materials resulting from these studies may be of utility in a range of applications, including molecular sieving, detection of volatile organic compounds, ion exchange, and homogeneous catalysis.

Future Plans

Synthesis of a Microporous Magnet. Our efforts to produce molecular cluster building units capable of delivering strong magnetic coupling with surrounding metal ions will continue. The goal here is to generate solids with ordering temperatures at or above room temperature for use in performing magnetic separations (e.g., for the noncryogenic separation of dioxygen from dinitrogen). New targets of particular interest here include the clusters $[\text{Gd}_6\text{CCl}_{18}]^{9-}$, $[\text{Re}_{6-n}\text{M}_n\text{Q}_8\text{Cl}_6]^{(4+n)-}$ ($\text{M} = \text{Mo}, \text{W}$), $[\text{M}_6\text{Q}_8(\text{CN})_6]^{n-}$ ($\text{M} = \text{Cr}, \text{Fe}, \text{Co}$), $[\text{W}_6\text{CCl}_{12}(\text{CN})_6]^{3-}$, and $[\text{B}_6(\text{CN})_6]^{1-}$. Relatedly, dioxygen-binding experiments will be carried out on porous phases incorporating $[\text{Co}(\text{CN})_5]^{3-}$.

Homogeneous Catalysis in Cluster-Expanded Prussian Blue Type Solids. Attempts will be made to exploit the coordinatively-unsaturated metal sites within dehydrated cluster-expanded Prussian blue solids for homogeneous catalysis.

Characterization of Photomagnetic Solids. The photomagnetic properties of porous solids incorporating $[\text{Re}(\text{CN})_7]^{3-}$ and $[\text{Re}(\text{CN})_8]^{3-}$ will be further characterized, with the intention of developing potential sensing applications.

Synthesis of Acetylenediide-Bridged Solids. The new trimethylsilylacetylide complexes obtained recently will be used in coupling reactions intended to produce unprecedented frameworks featuring acetylenediide bridges.

Publications (2002-2004)

1. "Cyanide-Limited Complexation of Molybdenum(III): Synthesis of Octahedral $[\text{Mo}(\text{CN})_6]^{3-}$ and Cyano-Bridged $[\text{Mo}_2(\text{CN})_{11}]^{5-}$ " Beauvais, L. G.; Long, J. R. *J. Am. Chem. Soc.* **2002**, *124*, 2110-2111.
2. "Co₃[Co(CN)₅]₂: A Microporous Magnet with an Ordering Temperature of 38 K" Beauvais, L. G.; Long, J. R. *J. Am. Chem. Soc.* **2002**, *124*, 12096-12097.
3. "Cluster Synthesis via Ligand-Arrested Solid Growth: Triethylphosphine-Capped Fragments of Binary Metal Chalcogenides" Crawford, N. R. M.; Hee, A. G.; Long, J. R. *J. Am. Chem. Soc.* **2002**, *124*, 14842-14843.
4. "New Cyanometalate Building Units: Synthesis and Characterization of $[\text{Re}(\text{CN})_7]^{3-}$ and $[\text{Re}(\text{CN})_8]^{3-}$ " Bennett, M. V.; Long, J. R. *J. Am. Chem. Soc.* **2003**, *125*, 2394-2395.
5. "New Routes to Transition Metal-Carbido Species: Synthesis and Characterization of the Carbon-Centered Trigonal Prismatic Clusters $[\text{W}_6\text{CCl}_{18}]^{n-}$ ($n = 1, 2, 3$)" Welch, E. J.; Crawford, N. R. M.; Bergman, R. G.; Long, J. R. *J. Am. Chem. Soc.* **2003**, *125*, 11464-11465.
6. "Cluster-to-Metal Magnetic Coupling: Synthesis and Characterization of 25-Electron $[\text{Re}_{6-n}\text{Os}_n\text{Se}_8(\text{CN})_6]^{(5-n)-}$ ($n = 1, 2$) Clusters and $\{\text{Re}_6$

$\text{Os}_n\text{Se}_8[\text{CNCu}(\text{Me}_6\text{tren})]_6\}^{9+}$ ($n = 0, 1, 2$) Assemblies” Tulskey, E. G.; Crawford, N. R. M.; Baudron, S. A.; Batail, P.; Long, J. R. *J. Am. Chem. Soc.* **2003**, *125*, 15543-15553.

7. “Atomlike Building Units of Adjustable Character: Solid State and Solution Routes to Manipulating Hexanuclear Transition Metal Chalcogenide Clusters” Welch, E. J.; Long, J. R. *Prog. Inorg. Chem.*, submitted.
8. “Determination of ^{77}Se - ^{77}Se and ^{77}Se - ^{13}C J -Coupling Parameters for the C_{4v} -Symmetry Selenocyanide Cluster $[\text{Re}_5\text{OsSe}_8(\text{CN})_6]^{3-}$ ” Ramaswamy, K.; Tulskey, E. G.; Kao, L.-F.; Long, J. R.; Hayes, S. E. *Inorg. Chem.*, submitted.
9. “Homoleptic Trimethylsilylacetylide Complexes of Chromium(III), Iron(II), and Cobalt(III): Syntheses, Structures, and Ligand Field Parameters” Berben, L. A.; Long, J. R. *J. Am. Chem. Soc.*, submitted.

New Vistas for Functionalized Polyoxometalates

Postdoc: Louis Wojcinski

Ph.D. Students: Jeffery Karcher, Kristopher Mijares

Undergraduate Student: Sean Tomlinson

Collaborators: Anna Proust, Pierre Gouzerh (University of Paris VI)

Department of Chemistry, Kansas State University, Manhattan, KS 66506-3701

eam@ksu.edu

Goals

The development of rational methods for incorporating functionality into polyoxometalate (POM) systems and to employ the resulting species to catalytic advantage.

Recent Progress

Our principal recent efforts have focused on the synthesis and characterization of new classes of POM complexes incorporating nitrido ligands. Prototypical structures of these systems are shown below in Chart 1.

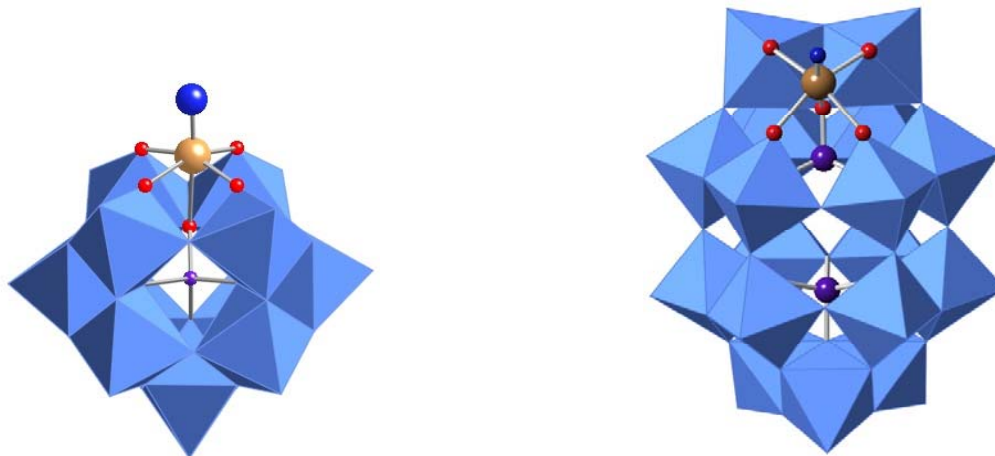


Chart 1. Nitrido-POM structures of the Keggin (left) and Dawson (right) families.

Osmium Nitrido-Keggin systems: Introduction of the $[\text{Os}^{\text{VI}}\equiv\text{N}]^{3+}$ unit into a Keggin POM framework has been accomplished in a straightforward reaction between $[\text{TBA}][\text{OsNCl}_4]$ and $[\text{TBA}]_4[\text{H}_3\text{PW}_{11}\text{O}_{39}]$ in acetonitrile in the presence of Et_3N . A single-crystal X-ray diffraction study of the product $[\text{TBA}]_4[(\text{Os}^{\text{VI}}\text{N})\text{PW}_{11}\text{O}_{39}]$ reveals, as expected, a twelve-fold orientational disorder in the solid state, but the identity and structure of the material has been established by a variety of techniques including electrospray MS and multinuclear (^{15}N , ^{31}P , ^{183}W) NMR studies.¹

Rhenium Nitrido-Keggin systems: Reaction of the classical Chatt nitride complex $[\text{Re}^{\text{V}}\text{NCl}_2(\text{PPh}_3)_2]$ with $[\text{TBA}]_4[\text{H}_3\text{PW}_{11}\text{O}_{39}]$ proceeds smoothly to yield the $[\text{Re}^{\text{VI}}\equiv\text{N}]^{3+}$ derivative $[\text{TBA}]_4[(\text{Re}^{\text{VI}}\text{N})\text{PW}_{11}\text{O}_{39}]$. A transient, extremely reactive $[(\text{Re}^{\text{V}}\text{N})\text{PW}_{11}\text{O}_{39}]^{5-}$ intermediate can be detected by ^{31}P NMR. The fully oxidized system $[\text{TBA}]_3[(\text{Re}^{\text{VII}}\text{N})\text{PW}_{11}\text{O}_{39}]$ has been isolated upon treatment of the Re^{VI} species with $[\text{TBA}][[\text{Br}_3]$. Cyclic voltammetry studies indicate that the corresponding $[\text{Re}^{\text{IV}}\equiv\text{N}]$ and $[\text{Re}^{\text{III}}\equiv\text{N}]$ derivatives can be generated upon electrochemical reduction.¹

Manganese Nitrido-Keggin and Nitrido-Dawson systems. Our most exciting recent result is the generation of the $[\text{Mn}^{\text{V}}\equiv\text{N}]^{2+}$ unit within both the Keggin and Dawson POM frameworks. Irradiation of the azido precursor $[(\text{Mn}^{\text{III}}\text{N}_3)\text{P}_2\text{W}_{17}\text{O}_{61}]^{8-}$ smoothly induces N_2 extrusion forming deep blue $[(\text{Mn}^{\text{V}}\text{N})\text{P}_2\text{W}_{17}\text{O}_{61}]^{8-}$. Isolation and purification of this material is difficult because of its high reactivity; we also suspect that it may be susceptible to photodegradation during its preparation. ^{31}P NMR spectra confirm the diamagnetism expected for $d^2 \text{Mn}^{\text{V}}$, and IR spectra reveal $\nu_{(\text{Mn}=\text{N})}$ at 1059 cm^{-1} . Photolysis of $[(\text{Mn}^{\text{III}}\text{N}_3)\text{PW}_{11}\text{O}_{39}]^{5-}$ similarly affords a deep blue material tentatively formulated as $[(\text{Mn}^{\text{V}}\text{N})\text{PW}_{11}\text{O}_{39}]^{5-}$.

Chromium Nitrido-Keggin system: We have recently prepared a Keggin-type POM incorporating the $[\text{Cr}^{\text{V}}\equiv\text{N}]^{2+}$ unit. The complex $[(\text{Cr}^{\text{V}}\text{N})\text{PW}_{11}\text{O}_{39}]^{5-}$ has been characterized by ESR and its electrochemistry indicates that the Cr^{VI} analogue should be easily accessible. Preliminary studies indicate that the nitrido ligand exhibits electrophilic character, reacting with PR_3 to generate the phosphorane iminato systems $[(\text{Cr}^{\text{III}}\text{N}=\text{PR}_3)\text{PW}_{11}\text{O}_{39}]^{5-}$.²

Nitrogenous Hexametalate Derivatives. We have reported the preparation, characterization and structure of a hexatungstate diazoalkane derivative namely, $[\text{TBA}]_2[\text{W}_6\text{O}_{18}(\text{NNC}(\text{CH}_3)\text{C}_6\text{H}_4\text{OCH}_3)]$.³ This complex is the first diazoalkane derivative of a tungsten POM, and the second diazoalkane POM derivative of any type.

POMs as Polymer Pendants. We previously demonstrated that the POM-bound styrylimido ligand in the system $[\text{Mo}_6\text{O}_{18}(\text{NC}_6\text{H}_4\text{CH}=\text{CH}_2)]^{2-}$ could serve as reactive entity allowing the preparation of various soluble styrenic co-polymers bearing POM units as backbone substituents. A patent application covering these materials has recently been allowed by the USPTO.⁴ We have extended these ideas to the preparation of other styrylimido systems including those of rhenium and gold.

DOE Interest

The POM framework is thermally and oxidatively robust, and can be tailored for solubility in aqueous or non-aqueous media by counteranion variation. As such, it presents an attractive and stable platform for metal-mediated catalytic transformations, provided that suitable functionality can be appended.

Future Plans

Reactivity of Nitrido-Polyoxometalates. The $[\text{Mn}^{\text{V}}\equiv\text{N}]$ -substituted Dawson and Keggin systems will be examined for olefin aziridination activity. Our initial approach will be to generate the species in the presence of trifluoroacetic anhydride and a suitable olefin, and then screen the reaction mixture for the desired trifluoroacyl aziridine product. Simple alkylations

will be also be pursued in an effort to access the long-sought organoimido-Keggin and -Dawson systems. Preliminary results on the $[(\text{Cr}^{\text{V}}\text{N})\text{PW}_{11}\text{O}_{39}]^{5-}$ species suggest that reactions of this complex with nucleophiles will be productive.

New Metal-nitrido POM systems. Keggin and Dawson POMs incorporating $[\text{W}^{\text{VI}}\equiv\text{N}]^{3+}$, $[\text{Mo}^{\text{VI}}\equiv\text{N}]^{3+}$, $[\text{V}^{\text{V}}\equiv\text{N}]^{2+}$, and $[\text{Fe}^{\text{V}}\equiv\text{N}]^{2+}$ units are current targets of exploratory synthesis in our laboratory.

Incorporating Remote Functionality into Organoimido-POMs. We are interested in creating multi-functional POM derivatives in which secondary metal centers can be tethered covalently to a POM anion through the intervention of an organoimido ligand bearing appropriate functionality. Our attention is now focused on incorporating bipyridyl-imido ligands into various POM frameworks.

Publications (2002-3)

1. Kwen, H.; Tomlinson, S.; Maatta, E. A.; Dablemont, C.; Thouvenot, R.; Proust, A.; Gouzerh, P. "Functionalized heteropolyanions: High-valent metal nitrido fragments incorporated into a Keggin polyoxometalate structure", *Chem. Commun.* **2002**, 2970-2971.
2. Karcher, J. D.; Maatta, E. A., in preparation.
3. Moore, A. R.; Kwen, H.; Hamaker, C. G.; Mohs, T. R.; Beatty, A. M.; Harmon, B.; Needham, K.; Maatta, E. A. "New Classes of Functionalized Polyoxometalates: Organo-Nitrogen Derivatives of Lindqvist Systems", in: *Polyoxometalates for Nano-Composite Design*, Pope, M. T., Yamase, T., Wang, E., Eds.; Kluwer Academic / Plenum Publishing: New York (2002); pp. 129 - 138.
4. Maatta, E. A.; Moore, A. R. "Polymers Incorporating Covalently Attached Organoimido Polyoxometalates", *U.S. Patent Application 09/609,863* allowed 10/03/03.

This page intentionally left blank.

Nanoscale Phenomena in Surface Chemistry: Structure, Reactivity and Electronic Properties

Postdocs: Ally S. Y. Chan, Wenhua Chen, Jamie Quinton

Students: Robin Barnes, Ivan Ermanoski, Hao Wang, Qifei Wu

Collaborators: J. E. Rowe, R. Blaszczyszyn, Jingguang Chen, Gilles Renaud, Elsebeth Schroder

Department of Physics and Astronomy, Rutgers, the State University of New Jersey, Piscataway NJ 08854

Madey@physics.rutgers.edu

Goal

Identify the relations between nanometer-scale surface features (e.g., faceted structures and clusters) and heterogeneous chemistry.

Recent Progress

Our emphasis is on atomically-rough morphologically unstable surfaces [e.g., bcc W(111), fcc Ir (210), hcp Re (12-31)] that can undergo nanoscale faceting when covered by adsorbed gases or ultrathin films of metals (~1 monolayer thick), and annealed. Our objectives are:

(a) to identify the causes of faceting and other nanometer-scale growth phenomena on metallic surfaces, adsorbate-covered surfaces, and sulfided surfaces, and

(b) to correlate surface reactivity, surface structure, and surface electronic properties of surfaces with nanometer-scale features (facets, metallic clusters).

We use a surface science approach, including scanning tunneling microscopy (STM), low energy electron diffraction (LEED), temperature programmed desorption (TPD), and high resolution soft x-ray photoemission (HRSXPS), using synchrotron radiation at the National Synchrotron Light Source (NSLS). Details of recent results include:

Faceting of Ir and structure sensitive reactions: Ir (210) surfaces are unstable when covered with oxygen and heated to > 600K; nanometer scale pyramids having {311} and {110} facets cover the surface (identified by LEED and STM); see Figure 1. We have developed a novel chemical procedure to remove the oxygen and retain the atomically-clean, faceted Ir surface. By studying reactions over the clean *planar* surface and the clean *faceted* surface, several structure sensitive processes have been identified (see Figure 2), including the recombination and desorption of hydrogen, the thermal decomposition of acetylene, and the thermal decomposition of ammonia. In all cases, there are substantial differences in reaction kinetics over planar versus faceted surfaces.

Faceting of Re and structure sensitive reactions: The atomically-rough Re(12-31) surface, when covered with oxygen and heated to $T > 700\text{K}$, develops ridge-like nanoscale facets having $(01\bar{1}0)$ and $(11\bar{2}1)$ orientations. HRXPS is used to characterize the transition from an oxygen atom-covered surface to the onset of oxidation (ReO, Re₂O₃). Supported Re oxides have recently been shown to catalyze the oxidation of methanol to methylal (dimethoxymethane, CH₃OCH₂OCH₃). Using TPD, we have investigated the reaction of methanol over planar and faceted O-covered Re(12 $\bar{3}$ 1) to probe for structure sensitivity in this elementary step in methylal synthesis. We find that methanol reacts on O-covered Re(12 $\bar{3}$ 1) via two competing pathways: selective dehydrogenation to evolve gaseous CO and formaldehyde, and non-selective decomposition to deposit surface C, O and H. The data demonstrate clear evidence for structure

sensitivity associated with nanoscale facets, manifested by a substantially reduced activity of the faceted surface towards methanol dehydrogenation.

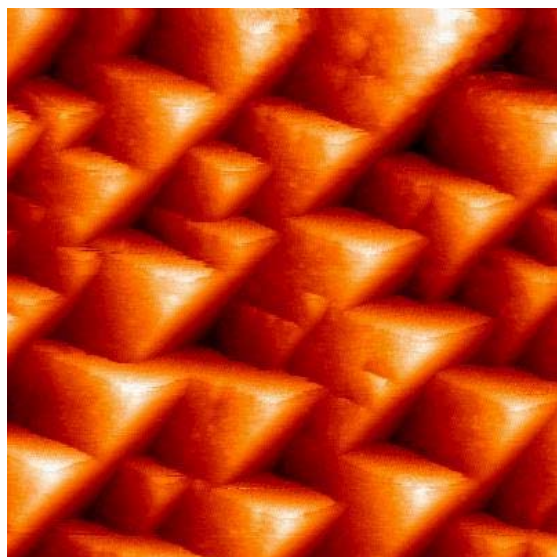


Figure 1. STM image of faceted Ir(210) surface, (100 nm x 100nm).{311} and {110} facets are formed by annealing the oxygen-covered surface to $T > 600\text{K}$.

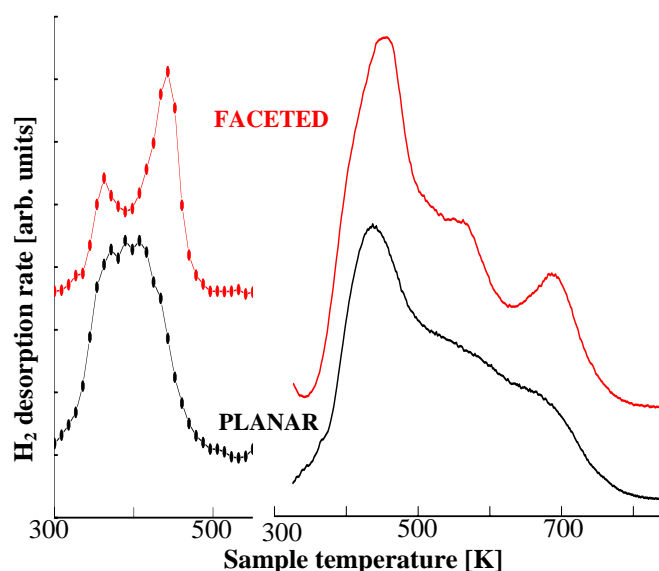


Figure 2: TPD spectra displaying structure sensitivity of planar and faceted Ir surfaces. Left, recombinative desorption of hydrogen; right, thermal decomposition of acetylene and desorption of hydrogen.

Bimetallic systems, from segregated monolayers to surface alloys: Monolayer metallic films that cause faceting of W(111) and Mo(111) are generally found to "float" on the outer surface, with little or no alloy formation. Multilayer films (Pt, Pd, Ir, Rh, ...) on W surfaces form alloys upon annealing. Theory and experiment have been combined to identify the conditions under which multilayers of Pt, Pd, Ru form surface alloys with unstable W surfaces, while monolayers remain segregated.

Growth of nanoscale metal clusters on sulfided surfaces: Both Cu and Ni atoms, when deposited onto the highly-textured sulfided S(4x4)/W(111) surface, form subnanometer-scale clusters at specific sites and exhibit self-limiting growth. Clear evidence for non-random nucleation is found, which may imply long-range interactions in nanocluster growth.

DOE Interest

These results provide new understanding of dynamic structural rearrangements at the surfaces of high area bimetallic and sulfide catalysts, and are clarifying the role of nanometer-scale size effects in energy-related surface reactions such as hydrogen generation, hydrocarbon reforming, and hydrodesulfurization.

Future Plans

Surface structure: We will use STM to determine the temperature-dependent shapes, orientations, size distributions and atomic structure of oxygen-induced facets on both Ir and Re surfaces. A new variable temperature STM system will allow us to determine the growth of facets and the relaxation of facets back to the planar surface, in real time. This has never been accomplished before! In a collaboration at U. of Illinois, LEEM (low energy electron microscopy) will be used to complement the STM studies: we will characterize nucleation and growth of faceted regions in real time over micrometer distance scales. These studies are important for determining the stability of nanometer-scale supported metal Ir and Re catalysts. A

longer-term prospect is the use of O-faceted surfaces as templates for growth of nanoscale metal clusters, including bimetallics.

Reactivity: Our reactivity studies will involve effects of facet size on acetylene chemistry and methanol oxidation over Ir and Re, respectively. A new direction is ammonia surface chemistry on planar and faceted Ir(210) (decomposition of ammonia will produce CO_x-free hydrogen, which has potential fuel cell applications). We are also developing Monte Carlo simulation methods to model reactions on nanoscale surface features.

Synchrotron radiation: Future work using synchrotron radiation will include the interaction of S overlayers on Re(12-31), the growth of Pt on both O-modified and S-modified Re surfaces, and a search for reaction intermediates in methanol chemistry over Re. Conditions for surface alloy formation on Re, Ir and W substrates will be established. We will collaborate with a group at the European Synchrotron Radiation Facility in France, in innovative studies of Grazing Incidence Small Angle X-Ray Scattering (GISAXS) to characterize faceted surfaces. This novel method can provide unprecedented insights into structure, dispersion, size distributions and orientation of nanoscale features on surfaces.

Publications (2003-2004)

1. "Adsorption and Decomposition of Acetylene on Planar and Faceted Ir(210)", W. Chen, I. Ermanoski, Q. Wu, T. E. Madey, H. Hwu, J. G. Chen, *J. Phys. Chem B* **107** (2003) 5231-5242.
2. "High Resolution Photoemission Study of Growth, Alloying, and Intermixing of Ultrathin Ruthenium Films on W(111) and W(211)", M. J. Gladys, G. Jackson, J. E. Rowe, and T. E. Madey, in press, *Surface Science* **544** (2003) 193-208.
3. "Ultrathin Pd and Pt Films on W(211)", J. Block, J. J. Kolodziej, J. E. Rowe, T. E. Madey, E. Schroder, *Thin Solid Films* **428** (2003) 47-51.
4. "Elucidation of the active surface and origin of the weak metal-hydrogen bond on Ni/Pt(111) bimetallic surfaces: A surface science and density functional theory study", J. R. Kitchin, N. A. Khan, M. A. Barteau, J. G. Chen, B. Yakshinskiy, T. E. Madey, *Surface Science* **544** (2003) 295-308.
5. "Oxygen induced nano-faceting of Ir(210)", I. Ermanoski, K. Pelhos, W. Chen, J. S. Quinton, T. E. Madey" *Surface Science* **549** (2004) 1-23.
6. "Pt-Induced faceting of tungsten field emitter tips " G. Antczak, R. Blaszczyzyn, T. E. Madey, in press, *Progress in Surface Science* **74** (2003) 81-95.
7. "Site Specific Nucleation of Ni Nanoclusters on S(4x4)/W(111)", Qifei Wu and Theodore E. Madey, *Surface Science* (2004), in press
8. "A High Resolution Photoemission Study of Surface Core-Level Shifts (SCLS) in Clean and Oxygen Covered Ir(210) Surfaces", M. J. Gladys, I. Ermanoski, G. Jackson, J. S. Quinton, J. E. Rowe, and T. E. Madey, *J. Electron Spectroscopy and Related Phenomena* (2004), in press.
9. "Methanol Reactions over Oxygen-modified Re Surfaces: Influence of Surface Structure and Oxidation", Ally S. Y. Chan, Wenhua Chen, Hao Wang, John E. Rowe and Theodore E. Madey, *Journal of Physical Chemistry*, submitted

This page intentionally left blank.

The Dynamics of Adsorption on Clean and Adsorbate-modified Transition Metal Surfaces

Postdocs: Xing-Cai Guo, Chia-ling Kao

Students: James Stinnet, Jason Weaver, Anders Carlsson, Chia-ling Kao

Goal

An understanding of molecular adsorption processes on surfaces is important for heterogeneous catalysis, thin film and crystal growth, and surface lubrication processes. Due to the industrial importance of reactions of alkanes on platinum catalysts, trapping of small molecules on the platinum group metals has been studied by the use of both molecular beam methods and stochastic molecular dynamic simulations in recent years. The goal of this work is to develop a methodology for predicting the adsorption probabilities of alkanes on metal surfaces.

Background and previous work

The trapping dynamics of small alkanes on Pt(111) and Pt(110)-(1×2) have been extensively investigated. To better understand the energy transfer process involved in adsorption, realistic molecular simulations of alkane adsorption were initially undertaken by Stinnett et al. for ethane trapping on Pt(111). By adjusting the parameters in the Morse potential used to represent the ethane-Pt interaction in the united atom approximation, good agreement between experiment and simulation was obtained. Subsequently, these potential parameters were used to successfully predict the trapping probabilities of ethane on Pt(110)-(1×2), Pt(111)-S, and Pt(111)-O. Stinnett et al. also extend their calculations to methane and propane on Pt(111) and Pt(110)-(1×2), finding excellent agreement between experiment and the predictions of theory over a wide range of incident energies and angles. Later, Weaver et al. extended the united-atom approximation to model the dynamics of n-butane, isobutane, and neopentane on Pt(111) using the same simulation methods. In the latter work the Morse potential was adjusted slightly to give a better fit of theory and experiment for all the alkanes, C₁ – C₅.

Recent results

More recently we began studies of the predictive capability of the theory to scale trapping probabilities for the alkanes from metal to metal. The first metal studied was palladium. Many physical properties of Pd(111) and Pt(111) are similar, such as the lattice parameter and the Debye temperature, the measure of the metal-metal force constants. Thus these two surfaces differ primarily in their atomic masses. In addition, the binding energies of alkanes to the two surfaces are nearly identical, so the interaction between small alkanes and the surfaces should be governed by nearly the same, if not identical, Morse potential parameters. We successfully predicted the trapping probabilities of several alkanes on Pd(111) to within 30% with *no* adjustment of the potential parameters obtained from Pt(111). The simulations clearly indicate that the excitation of lattice phonons plays a more important role in trapping than on Pt(111); this result appears to originate from the lower mass of the palladium atoms.

Although nickel is in the same group as platinum and palladium, the prediction of alkane trapping on Ni(111) offers a more stringent test of the scaling from one surface to another. First, the atomic mass of nickel is much lower (58.69 amu) than either platinum (195.05 amu) or palladium (106.4 amu). According to mass matching arguments, the trapping probability would be expected to be highest on Ni(111). However, the nickel surface is much stiffer than either Pt or Pd. Thus, the dynamical response of the surface to collisions of the incident gas should be affected appreciably. Furthermore, the alkanes bind less strongly to Ni(111) than to Pt(111) or Pd(111), suggesting that different Morse potential parameters may be necessary to describe the gas-surface collision.

For methane, ethane, propane, and n-butane at a fixed incident energy and angle, the trapping probability is highest on Pd(111), followed by Pt(111) and Ni(111), a result which deviates from the prediction of simple mass matching arguments. The lower binding energy of the alkanes and the higher lattice force constant for Ni(111) compared with Pt(111) and Pd(111) give rise to the lower trapping probability. Three dimensional stochastic trajectory simulations for alkane trapping on the three metals clearly indicate that incoming molecules lose considerable energy to Pd lattice vibrations, resulting in a high trapping probability. On the other hand, the stiffer Ni lattice prevents the excitation of surface phonons, consistent with experimental results.

Future work

Dissociative adsorption of alkanes on metals proceeds via both trapping-mediated and direct pathways. The above work relates directly to the trapping-mediated channel. In the direct process bond rearrangement should occur at a distance characterized by a bond length. This distance is significantly shorter than the distance at which the repulsion between the alkane and metal set in. Accordingly, one would expect there to be energy transfer from the translational energy of the incident molecule to the lattice. Since we know that energy transfer is sensitive to both the mass of the incident alkane and to the dynamical parameters of the metal, we expect there to be different energy “thresholds” for C-H bond breaking for different alkanes on each metal. However, preliminary evidence for both Pt(111) and Ir(110) indicate the opposite. We are engaged in a comprehensive study of this effect on surfaces with widely varying dynamical characteristics.

Selected Relevant Publications

1. J. F. Weaver, M.A. Krzuzowski, R.J. Madix, *Direct dissociative chemisorption of alkanes on Pt(111): influence of molecular complexity*, J. Chem. Phys. 112 (2000) 396
2. C.-L. Kao, A.F. Carlsson, R.J. Madix, *Molecular adsorption dynamics on oxygen covered Pt(111)*, Topics in Catalysis 14 (2001) 63 - 69.
3. C.-L. Kao, R.J. Madix, *The adsorption dynamics of molecular methane, propane, and neopentane on Pd(111): theory and experiment*, Journal of Physical Chemistry 106 (2002) 8248.
4. C.-L. Kao, J.F. Weaver, R.J. Madix, *The prediction of trapping probabilities for ethane by molecular dynamics simulations: scaling from Pt(111) to Pd(111)*, Surf. Sci. 505 (2002) 115-123
6. C.L. Kao, R.J. Madix, *The adsorption dynamics of small alkanes on (111) surfaces of platinum group metals*, Surf. Sci. *submitted*

This page intentionally left blank.

“Supported Organometallic Complexes: Surface Chemistry, Spectroscopy, Catalysis and Homogeneous Models”

Postdocs: Graham Abramo, Liting Li, Michael Chen, Cristiano Zuccaccia, Aswini Dash

Graduate students: Christopher P. Nicholas, Nicholas Stahl, Hongbo Li, Neng Guo, Neraaj Saraiya, John Roberts

Collaborators: Peter Nickias (Dow Chemical Co.), Liong Tee (BP Chemicals), Ignazio Fragala (U. Catania), Alceo Macchioni (U. Perugia), Scott Collins (U. Akron), Moshe Kol (Tel Aviv U.), Jeremy Kropf (Argonne National Laboratory), Giuseppe Lanza (U. Potenza).

Department of Chemistry and the Center for Catalysis and Surface Science, Northwestern University, Evanston IL 60208-3113

t-marks@northwestern.edu

Goals

The overall goals of this project are to understand, model, and exploit the pathways by which organometallic molecules undergo chemisorption and dramatic catalytic activity enhancements on the surfaces of metal oxides and halides. Such phenomena impinge directly on the efficiency, selectivity, and “greenness” of real-world, large-scale industrial catalytic processes and our ability to produce cleaner, more environmentally acceptable products. This research program combines organometallic synthesis, surface science and catalysis with *ab initio* quantum chemistry and involves significant collaboration with industrial scientists and researchers at National Labs. The specific objectives are to: 1) Understand early transition metal and f-element hydrocarbyl molecule chemisorption on “super Brønsted acid” and related high surface area supports, 2) Develop functional, homogeneous phase, crystallographically characterizable mono- and multimetallic models for the adsorbate species formed on oxide surfaces, 3) Characterize the thermochemistry, molecular structures, molecular dynamics, and catalytic properties of such species, 4) Understand in detail the reaction mechanisms these species undergo and use this understanding to create new, useful processes, 5) Computationally analyze the formation processes, electronic structures, bonding, and catalytic reactivity of such species. The properties investigated include new, more energy-efficient routes to environmentally acceptable polymeric materials.

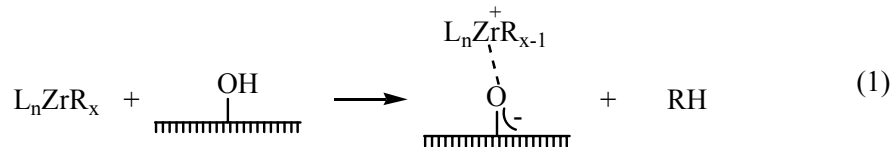
Recent Progress

In the past effort period, we focused on three primary areas: 1) Synthesis and characterization of the single-site organometallic species produced by chemisorption of early transition metal hydrocarbyls on highly Brønsted acidic metal oxides, 2) Understanding catalyst-cocatalyst structure and their interplay in single-site homogeneous polymerization catalyst function, 3) Using *ab initio* studies of single-site polymerization catalysts to understand the role of cocatalyst and solvation. A brief account of each activity is given below.

1. Metal Hydrocarbyl Chemisorption on Sulfated Metal Oxide Surfaces

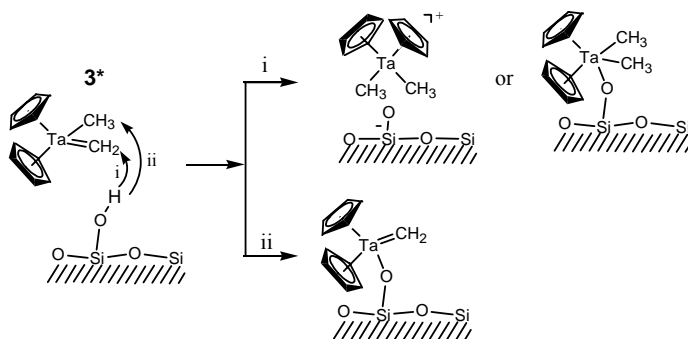
In the supported single-site catalyst area, structural studies including ^{13}C CPMAS NMR spectroscopy of the $^{13}\text{C}_\alpha$ - enriched model adsorbates, $\text{Cp}'_2\text{Th}(^{13}\text{CH}_3)_2$ (**1**^{*}), $\text{CpTi}(^{13}\text{CH}_3)_3$ (**2**^{*}) ($\text{Cp} = \eta^5\text{-C}_5\text{H}_5$, $\text{Cp}' = \eta^5\text{-(CH}_3)_5\text{C}_5$), and organozirconium adsorbates, $\text{Cp}_2\text{Zr}(^{13}\text{CH}_3)_2$ (**3**^{*}), $\text{Cp}'\text{Zr}(^{13}\text{CH}_3)_3$ (**4**^{*}), and $\text{Zr}(^{13}\text{CH}_2^t\text{Bu})_4$ (**6**^{*}) chemisorbed on sulfated zirconia (ZrS) and alumina (AlS) reveal that all adsorbates undergo M-C σ -bond protonolytic cleavage at the very strong surface Brønsted acid sites to yield “cation-like” organometallic electrophiles (e.g., eq. 1). Kinetic and mechanistic studies of olefin and arene

hydrogenation and α -olefin homopolymerization mediated by the catalysts formed by chemisorption of $\text{Cp}_2\text{Zr}(\text{CH}_3)_2$, $\text{Cp}'\text{Zr}(\text{CH}_3)_3$, $\text{Zr}(\text{CH}_2\text{TMS})_4$, $\text{Zr}(\text{CH}_2^t\text{Bu})_4$, and $\text{Zr}(\text{CH}_2\text{Ph})_4$ onto ZrS or AIS follow the



order: **4/ZRS** \gg **5/ZRS** > **6/ZRS** > **7/ZRS**, with $N_t = 970 \text{ h}^{-1}$ for **4/ZRS** making this the *most active benzene hydrogenation catalyst yet discovered*. As a function of arene substituent(s), **4/ZRS** exhibits high chemoselectivity, with hydrogenation rates following the order: benzene \gg toluene \gg *p*-xylene ~ 0 . For benzene hydrogenation by **6/ZRS**, kinetic data obey the rate law, $N_t = k_{\text{obs}}[\text{arene}]^0[\text{PH}_2]^1$ with $E_a = 10.3(8) \text{ kcalmol}^{-1}$. Partially hydrogenated products are not detected at partial conversions, with H_2 delivered pairwise to both faces of C_6D_6 , forming all-*cis* and *cis, cis, trans, cis, trans* isotopomers (1:3.1). Protonolytic poisoning experiments reveal that a maximum of $\sim 68\%$ of Zr sites in **4/ZRS400** are catalytically significant for benzene hydrogenation. Relative ethylene homopolymerization rates are: **7/ZRS** > **5/ZRS** > **6/ZRS** > **4/ZRS** for both ethylene (150 psi C_2H_4 , 60 $^\circ\text{C}$), and liquid propylene (20 $^\circ\text{C}$). Studies of similar complexes supported on highly Brønsted acidic sulfated alumina (AIS) reveal analogous chemisorption and catalytic mechanistic pathways. However, we find here that 98% of the **3/AIS** are catalytically significant for benzene hydrogenation and 88% of the sites for ethylene polymerization. To our knowledge, such high percentages of active sites are unprecedented for such catalysts (or any heterogeneous catalyst). Preliminary studies with other classes of sulfated oxides reveals rather different behavior, depending on the innate surface chemical properties of the support.

In related work, ^{13}C CPMAS NMR was employed to investigate the chemisorption of the group 5 hydrocarbyl/alkylidene complexes, $\text{Cp}'\text{Ta}(\text{}^{13}\text{CH}_3)_4$ (**1***), $\text{Cp}_2\text{Ta}(\text{}^{13}\text{CH}_3)_3$ (**2***), $\text{Cp}_2\text{Ta}(\text{}^{13}\text{CH}_2)(\text{}^{13}\text{CH}_3)$ (**3***), and $\text{Ta}(\text{}^{13}\text{CH}^t\text{Bu})(\text{}^{13}\text{CH}_2^t\text{Bu})_3$ (**4***) [$\text{Cp}' = \eta^5\text{-(CH}_3)_5\text{C}_5$, $\text{Cp} = \eta^5\text{-C}_5\text{H}_5$] supported on partially dehydroxylated silica (PDS), dehydroxylated silica (DS), or dehydroxylated γ -alumina (DA). Mono-Cp Ta hydrocarbyl **1*** undergoes chemisorption to form $\text{Cp}'\text{Ta}(\text{}^{13}\text{CH}_3)_3\text{O-Si}$ μ -oxo species on silica, and 'cation-like' $\text{Cp}'\text{Ta}(\text{}^{13}\text{CH}_3)_3^+$ and $\text{Cp}'\text{Ta}(\text{}^{13}\text{CH}_3)_3\text{O-Al}$ μ -oxo species on DA, via pathways analogous to those established for group 4 and -actinide complexes. When supported on DA, bis-Cp Ta hydrocarbyl **2*** follows the same chemisorption mode as **1***. However, when **2*** is chemisorbed on PDS and DS, a "cation-like" $\text{Cp}_2\text{Ta}(\text{}^{13}\text{CH}_3)_2^+$ species is the major adsorbate product. On PDS, bis-Cp tantalum alkylidene complex **3*** is converted predominantly to a stable $\text{Cp}_2\text{Ta}(\text{}^{13}\text{CH}_3)_2^+$ species, presumably via electrophilic addition of a surface proton from the surface as shown below. In contrast to **3***, Ta alkylidene complex **4*** forms predominantly a $\text{Ta}(\text{}^{13}\text{CH}^t\text{Bu})(\text{}^{13}\text{CH}_2^t\text{Bu})_3\text{O-Si}$ μ -oxo-alkylidene species on PDS.



2. The Significance of Ion-Pairing in on Structure, Activity, and Selectivity of Single-Site Polymerization Catalysts

The solution structures of the zirconocenium homogeneous polymerization catalyst ion-pairs $[\text{Cp}_2\text{ZrMe}]^+[\text{MeB}(\text{C}_6\text{F}_5)_3]^-$ (**1**), $[(1,2\text{-Me}_2\text{Cp})_2\text{ZrMe}]^+[\text{MeB}(\text{C}_6\text{F}_5)_3]^-$ (**2**), $[(\text{Me}_2\text{SiCp}_2)\text{ZrMe}]^+[\text{MeB}(\text{C}_6\text{F}_5)_3]^-$

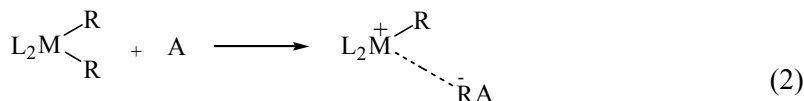
(**3**), $[\text{Me}_2\text{C}(\text{Fluorenyl})(\text{Cp})\text{ZrMe}]^+[\text{FPBA}]^-$ (FPBA = tris(2,2',2''-nonafluorobiphenyl)fluoroaluminate) (**4**), $[\text{rac-Et}(\text{Indenyl})_2\text{ZrMe}]^+[\text{FPBA}]^-$ (**5**), $[(\text{Me}_5\text{Cp})_2\text{ThMe}]^+[\text{B}(\text{C}_6\text{F}_5)_4]^-$ (**6**), $[(\text{Me}_2\text{SiCp}_2)\text{Zr}(\text{Me})(\text{THF})]^+[\text{MeB}(\text{C}_6\text{F}_5)_3]^-$ (**7**), $[(\text{Me}_2\text{SiCp}_2)\text{Zr}(\text{Me})(\text{PPh}_3)]^+[\text{MeB}(\text{C}_6\text{F}_5)_3]^-$ (**8**), $[(\text{Me}_2\text{SiCp}_2)\text{Zr}(\text{Me})(\text{THF})]^+[\text{B}(\text{C}_6\text{F}_5)_4]^-$ (**9**), $[(\text{Me}_2\text{Si}(\text{Me}_4\text{Cp})(t\text{-BuN})\text{Zr}(\text{Me})(\text{solvent}))]^+[\text{B}(\text{C}_6\text{F}_5)_4]^-$ (solvent = benzene, toluene) (**10**), $[(\text{Cp}_2\text{ZrMe})_2(\mu\text{-Me})]^+[\text{MePBB}]^-$ (PBB = tris(2,2',2''-nonafluorobiphenyl)borane) (**11**), and $[(\text{Cp}_2\text{Zr})_2(\mu\text{-CH}_2)(\mu\text{-Me})]^+[\text{MePBB}]^-$ (**12**), having the counteranion in the inner (**1**, **3**, **4**, **5**, and **6**) or outer (**7**, **8**, **9**, **10**, **11**, and **12**) coordination sphere, have been investigated for the first time in solvents with low relative permittivity such as benzene or toluene by ^1H -NOESY and ^1H , ^{19}F -HOESY NMR spectroscopy. It is found that the average interionic solution structures of the inner sphere contact ion-pairs are similar to those in the solid state with the anion B-Me (**1**, **3**) or Al-F (**5**) vectors oriented toward the free zirconium coordination site. The HOESY spectrum of complex **6** is in agreement with the reported solid-state structure. In contrast, in outer sphere contact ion-pairs **7**, **8**, **9**, and **10**, the anion is located far from the Zr-Me^+ center and much nearer to the Me_2Si bridge than in **3**. The interionic structure of **8** is concentration-dependent, and for concentrations greater than 2 mM, a loss of structural localization is observed. PGSE NMR measurements as a function of concentration (0.1-5.0 mM) indicate that the tendency to form aggregates of nuclearity higher than simple ion-pairs is dependent on whether the anion is in the inner or outer coordination sphere of the metallocenium cation. Complexes **2**, **3**, **4**, **5**, and **6** show no evidence of aggregation up to 5 mM (well above concentrations typically used in catalysis) or at the limit of saturated solutions (complexes **3** and **6**), while concentration-dependent behavior is observed for complexes **7**, **8**, **10**, and **11**. These outer sphere ion-pairs begin to exhibit significant evidence for ion-quadruples in solutions having concentrations greater than 0.5 mM with the tendency to aggregate being a function of metal ligation and anion structure. Above 2 mM, compound **8** exists as higher aggregates that are probably responsible for the loss of interionic structural specificity.

Counteranion effects on the rate and stereochemistry of syndiotactic propylene enchainment by the archetypal C_s -symmetric precatalyst $[\text{Me}_2\text{C}(\text{Cp})(\text{Flu})]\text{ZrMe}_2$ (**1**; Cp = C_5H_4 ; Flu = C_{13}H_8 , fluorenyl) are probed using the cocatalysts MAO (**2**), $\text{B}(\text{C}_6\text{F}_5)_3$ (**3**), $\text{B}(2\text{-C}_6\text{F}_5\text{C}_6\text{F}_4)_3$ (**4**), $\text{Ph}_3\text{C}^+\text{B}(\text{C}_6\text{F}_5)_4^-$ (**5**), and $\text{Ph}_3\text{C}^+\text{FAl}(2\text{-C}_6\text{F}_5\text{C}_6\text{F}_4)_3^-$ (**6**), offering greatly different structural and ion pairing characteristics. Reaction of **1** with **3** affords $[\text{Me}_2\text{C}(\text{Cp})(\text{Flu})]\text{ZrMe}^+ \text{MeB}(\text{C}_6\text{F}_5)_3^-$ (**7**). In the case of **4**, this reaction leads to formation the μ -methyl dinuclear diastereomers $\{([\text{Me}_2\text{C}(\text{Cp})(\text{Flu})]\text{ZrMe})_2(\mu\text{-Me})\}^+ \text{MeB}(2\text{-C}_6\text{F}_5\text{C}_6\text{F}_4)_3^-$ (**8**). A similar reaction with **6** results in diastereomeric $[\text{Me}_2\text{C}(\text{Cp})(\text{Flu})]\text{ZrMe}^+ \text{FAl}(2\text{-C}_6\text{F}_5\text{C}_6\text{F}_4)_3^-$ (**10**) ion pairs. The molecular structures of **7** and **10** have been determined by single-crystal X-ray diffraction. Reorganization pathways available to these species have been examined using EXSY and dynamic NMR, revealing that the cation- $\text{MeB}(\text{C}_6\text{F}_5)_3^-$ interaction is considerably weaker/more mobile than in the $\text{FAl}(2\text{-C}_6\text{F}_5\text{C}_6\text{F}_4)_3^-$ -derived analogue. Polymerizations mediated by **1** in toluene over the temperature range -10° to $+60^\circ\text{C}$ and at 1.0-5.0 atm propylene pressure (at 60°C) reveal that activity, product syndiotacticity, m and mm stereodeflect generation, and chain transfer processes are highly sensitive to the nature of the ion pairing. Thus, the complexes activated with **4** and **5**, having the weakest ion pairing, yield the highest estimated propagation rates, while with **6**, having the strongest pairing, yields the lowest. The strongly coordinating, immobile $\text{FAl}(2\text{-C}_6\text{F}_5\text{C}_6\text{F}_4)_3^-$ anion produces the highest/least temperature-dependent product syndiotacticity, lowest/least temperature-dependent m stereodeflect abundance, and highest product molecular weight. These polypropylene microstructural parameters, and also M_w , are least sensitive to increased propylene pressure for $\text{FAl}(2\text{-C}_6\text{F}_5\text{C}_6\text{F}_4)_3^-$, but highest with $\text{MeB}(\text{C}_6\text{F}_5)_3^-$. In general, mm stereodeflect production is only modestly anion-sensitive; [propylene] dependence studies reveal enantiofacial propylene misinsertion to be the prevailing mm -generating process in all systems at 60°C , being most dominant with **6**, where mm stereodeflect abundance is lowest. For 1,3-dichlorobenzene as the polymerization solvent, product syndiotacticity, as well as m and mm stereodeflects, become indistinguishable for all cocatalysts. These observations are consistent with a scenario in which ion pairing modulates the rates of stereodeflect generating processes relative to monomer enchainment, hence net enchainment syndioselectivity, and also dictates the rate of termination relative to propagation and the preferred termination pathway. In comparison to **3-6**, propylene polymerization mediated by MAO (**2**) +

1 in toluene reveals an estimated ordering in site epimerization rates as **5** > **4** > **2** > **3** > **6**, while product syndiotacticities rank as **6** > **2** > **5** ~ **4** > **3**.

3. Theoretical Studies

Computational efforts centered on understanding catalyst-cocatalyst/cation-counteranion activation processes and subsequent interactions in typical group 4 single-site catalysts, of great technological importance (eq 2).



Mechanistic aspects of ethylene insertion into the Ti-CH₃ bond of the [H₂Si(C₅H₄)(^tBuN)]TiCH₃⁺ H₃CB(C₆F₅)₃⁻ ion pair have been analyzed at the ab initio level, employing a double-zeta quality basis set, second-order perturbative Møller-Plesset methods (MP2), and including solvation effects and thermal and pressure corrections to 298 K and 1.0 atm. Three reaction pathways are identified as viable. Ethylene approach from the side opposite the H₃CB(C₆F₅)₃⁻ counteranion is energetically most favored and occurs in a concerted (intermediateless) fashion. The other two pathways involving olefin approach on the same side as the H₃CB(C₆F₅)₃⁻ counteranion are energetically similar, and each occurs via two discrete steps: i) anion displacement with formation of an intermediate π-ethylene complex, ii) ethylene insertion into the Ti-C bond (the slow step). These latter pathways are more strongly solvent-assisted because of the larger attendant ion pair separation. Structural and energetic analysis of the [H₂Si(C₅H₄)(^tBuN)]Ti(*n*-C₃H₇)⁺ H₃CB(C₆F₅)₃⁻ insertion product shows the existence of several stable conformations. All such structures can be divided into two different types depending on the [H₂Si(C₅H₄)(^tBuN)]Ti(*n*-C₃H₇)⁺⋯H₃CB(C₆F₅)₃⁻ distance. Structures with short Ti⁺⋯[H₃CB(C₆F₅)₃]⁻ contacts involve metal coordinative saturation by the CH₃ group or an aryl F atom of the counteranion. For structures with longer Ti⁺⋯[H₃CB(C₆F₅)₃]⁻ contacts, the counteranion remains out of the Ti coordination sphere, and these structures exhibit agostic interactions between the *n*-propyl chain and Ti. The relative stabilities of these structures is an index of the preferred olefin enchainment mechanism: chain migratory insertion (dissociated ion pair) versus nonmigratory insertion (associated ion pair). These results are in generally good agreement with the large breath of experimental data now available.

DOE Interest

The catalyst syntheses, mechanistic studies, and product characterization activities that are the central part of this project relate directly to the efficiency, selectivity, and “greenness” of real-world industrial catalytic processes that are practiced on a huge scale and to the ability of these processes to produce cleaner, more environmentally acceptable products. These multifaceted, highly interdisciplinary projects provide ideal training for young scientists needed as part of a highly skilled U.S. technical workforce.

Future Plans

We plan to continue our efforts in all three of the above areas. In the area of novel supports for molecule-based catalysts, we plan EXAFS studies on adsorbate structure in collaboration with Jeremy Kropf of ANL. Systems with virtually 100% active sites present a unique opportunity. We also plan to expand our studies to other types of highly Brønsted acidic supports, to use polymerization reactivity probes of the ion-pairing “tightness,” and to explore tandem supported catalytic processes in which cascade processes are turned on by virtue of the close proximity of the catalytic sites on the surface. In the area of ion-pairing studies, we plan to investigate cocatalyst-selectivity effects in other systems where ion-pairing might be intimately connected with enchainment selectivity. In the theoretical arena, we will explore whether double-layer effects at oxide surfaces may loosen ion-pairing,

hence produce the enhanced reactivities observed. We will also investigate the effects of ion-pairing on enchainment stereochemistry.

Publications (2002-Present)

1. Li, L.; Metz, M.V.; Li, H.; Chen, M.-C.; Marks, T.J.; Liable-Sands, L.; Rheingold, A.L. Catalyst/Cocatalyst Nuclearity Effects in Single-Site Polymerization. Significantly Enhanced Polyethylene Branching and α -Olefin Comonomer Enchainment in Polymerizations Mediated by Binuclear Catalysts and Cocatalysts, *J. Am. Chem. Soc.*, **2002**, *124*, 12725-12741.
2. Ahn, H.; Nicholas, C.P.; Marks, T.J. Surface Organozirconium Complexes Activated by Chemisorption on "Super Acidic" Sulfated Zirconia as Hydrogenation and Polymerization Catalysts. A Synthetic, Structural, and Mechanistic Catalytic Study" *Organometallics*, **2002**, *21*, 1788-1806.
3. Ahn, H.; Marks, T.J. High-Resolution Solid-State ^{13}C NMR Structural Studies of Chemisorbed Organometallics. Chemisorptive Formation of Organotantalum Cationic and Alkylidene Complexes on High-Surface Area Inorganic Oxides, *J. Am. Chem. Soc.*, **2002**, *124*, 7103-7110.
4. Lanza, G.; Fragala, I.L.; Marks, T.J. Energetic, Structural, and Dynamic Aspects of Ethylene Polymerization Mediated by Homogeneous Single-Site "Constrained Geometry Catalysts" in the Presence of Cocatalyst and Solvation: An Investigation at the ab Initio Quantum Chemical Level, *Organometallics*, **2002**, *21*, 5594-5612.
5. Metz, M.V.; Schwartz, D.J.; Stern, C.L.; Marks, T.J. New Perfluoroarylborane Activators for Single-Site Olefin Polymerization. Acidity and Cocatalytic Properties of a "Superacidic" Perfluorodiboraanthracene, *Organometallics*, **2002**, *21*, 4159-4168.
6. Metz, M.V.; Sun, Y.; Stern, C.L.; Marks, T.J. Weakly Coordinating Al-, Nb-, Ta-, Y-, and La-Based Perfluoroaryloxy Anions as Cocatalyst Components for Single-Site Olefin Polymerization, *Organometallics*, **2002**, *21*, 3691-3702.
7. Abramo, G.P.; Li, L.; Marks, T.J. Polynuclear Catalysis. Enhancement of Enchainment Cooperativity Between Different Single-Site Olefin Polymerization Catalysts by Ion Pairing with a Binuclear Co-Catalyst, *J. Am. Chem. Soc.*, **2002**, *124*, 13966-13967.
8. Nicholas, C.P.; Ahn, H.; Marks, T.J. Synthesis, Spectroscopy, and Catalytic Properties of Cationic Organozirconium Adsorbates on "Super Acidic" Sulfated Alumina. "Single-Site" Heterogeneous Catalysts with Virtually 100% Active Sites, *J. Amer. Chem. Soc.*, **2003**, *125*, 4325-4331.
9. Stahl, N.G.; Zuccaccia, C.; Jensen, T.R.; Marks, T.J. Metallocene Polymerization Catalyst Ion-Pair Aggregation by Cryoscopy and Pulsed Gradient Spin-Echo NMR Diffusion Measurements, *J. Am. Chem. Soc.*, **2003**, *125*, 5256-5257.
10. Chen, M.-C.; Roberts, J.A.; Marks, T.J. Marked Counteranion Effects on Single-Site Olefin Polymerization Processes. Correlations of Ion Pair Structure and Dynamics with Polymerization Activity, Chain Transfer Pathways, and Syndioselectivity, *J. Am. Chem. Soc.*, in press ASAP.
11. Jensen, T.R.; Marks, T.J. Diversity of Pathways in Ring-Opening Ziegler Polymerization. A New Single-Site Chain Transfer Mechanism, *Macromolecules*, **2003**, *36*, 1775-1778.

12. Jensen, T.R.; Yoon, S.C.; Dash, A.K.; Luo, L.; Marks, T.J. Organo-Titanium Mediated Stereoselective Coordinative/Insertive Homopolymerizations and Copolymerizations of Styrene and Methyl Methacrylate, *J. Am. Chem. Soc.*, **2003**, *125*, 14482-14494.
13. Jensen, T.R.; O'Donnell III, J.J.; Marks, T.J. d^0/f^n -Mediated Ring-Opening Ziegler Polymerization (ROZP) and Copolymerization with Mono- and Disubstituted Methylene cyclopropanes. Diverse Mechanisms and a New Chain-Capping Termination Process, *Organometallics*, **2004**, *23*, 740-754.
14. Li, H.; Li, L.; Marks, T.J. Catalyst/Cocatalyst Nuclearity Effects in Single-Site Olefin Polymerization. Significantly Enhanced 1-Octene and Isobutene Comonomer Enchainment in Ethylene Polymerizations Mediated by Binuclear Catalysts and Cocatalysts, *J. Am. Chem. Soc.*, **2003**, *125*, 10788-10789.
15. Zuccaccia, C.; Stahl, N.G.; Macchioni, A.; Chen, M.-C.; Roberts, J.A.; Marks, T.J. NOE and PGSE NMR Spectroscopic Studies of Solution Structure and Aggregation in Metallocenium Ion-Pairs, *J. Am. Chem. Soc.*, **2004**, *126*, 1448-1464.
16. Chen, M.-C. Roberts, J.A.; Marks, T.J. New Mononuclear and Polynuclear Perfluoroarylmethylate Cocatalysts for Stereospecific Olefin Polymerization, *Organometallics*, **2004**, *5*, 932-935.
17. Li, H.; Li, L.; Marks, T.J. Nuclearity Effects in Olefin Polymerization. Significantly Enhanced Polyethylene Molecular Weight and Comonomer Enchainment in Polymerizations Mediated by Binuclear Catalysts, submitted for publication.
18. Guo, N.; Li, L.; Marks, T.J. Styrene Homopolymerization and Ethylene-Styrene Copolymerization Mediated by Bimetallic "Constrained Geometry Catalysts". Exceptional Comonomer Incorporation Selectivity, submitted for publication.

Inorganic-Organic Molecules and Solids with Nanometer-Sized Pores

Postdocs: Banglin Chen and Chandu Pariya

Graduate students: Christopher Sparrow, Yixun Zhang, and James Kakoullis Jr.

Department of Chemistry, Louisiana State University, Baton Rouge LA 70803-1804

maverick@lsu.edu

Goal

We are constructing porous inorganic-organic hybrid molecules and solids that contain coordinatively unsaturated metal centers.

Recent Progress

We have prepared extended-solid and molecular porous materials based on multifunctional β -diketone ligands.

(a) Extended solids

These materials are constructed by using $M(\text{Pyac})_2$ (see Figure 1) as a "rod"-shaped building block. We completed a study of the coordination of the building block $\text{Cu}(\text{Pyac})_2$ with itself. Meanwhile, we explored the reactions of $\text{Cu}(\text{Pyac})_2$ with other metal ions M' . If M' is capable of binding four pyridine ligands, then a layer with "square-grid" topology results (Figure 2).

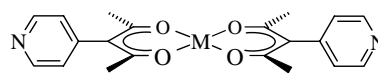


Figure 1. The "rod"-shaped molecule $M(\text{Pyac})_2$.

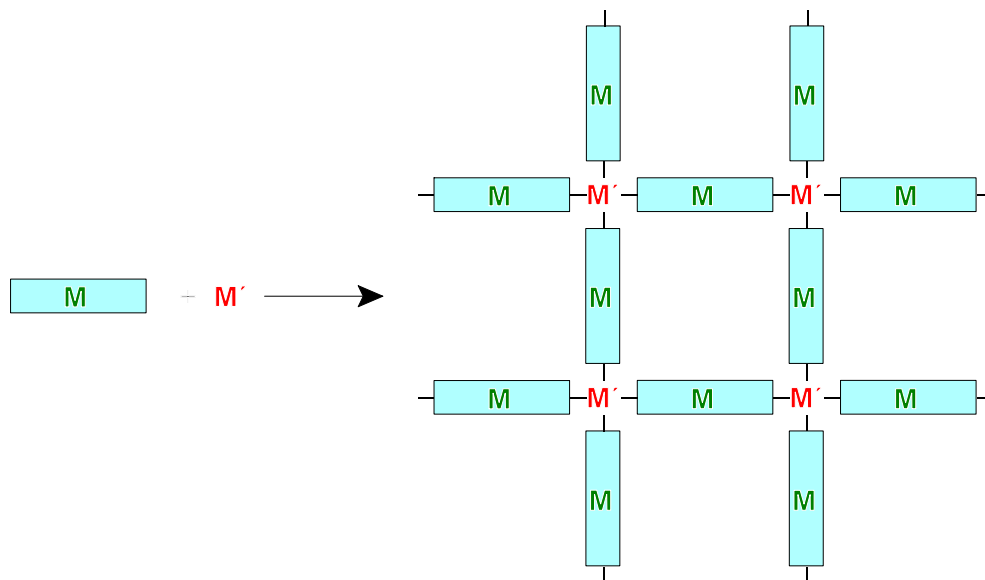


Figure 2. Formation of "square-grid" layer from "rod"-shaped molecules such as $\text{Cu}(\text{Pyac})_2$ (M) and metal "nodes" M' .

We have shown that reaction of $\text{Cu}(\text{Pyac})_2$ with CdCl_2 and $\text{Cd}(\text{NO}_3)_2$ produces 1D and 2D structures based on this square-grid arrangement. In these structures, the pores are ca. 19.7 Å in diameter, with the Cu atoms exposed to the pores.

As an alternative "building block" we have used the iron(III) complex $\text{Fe}(\text{Pyac})_3$. Its three pyridine N atoms are in an approximately trigonal arrangement around the Fe atom. Although this species is coordinatively saturated, it can still be used to construct porous materials. Reaction with AgNO_3 produces a nanoporous bimetallic crystalline solid with a 1-D "ladder" structure, $[\text{Fe}(\text{Pyac})_3]_2[\text{AgNO}_3]_3(\text{solvent})_x$ (abbreviated $\text{Fe}_2\text{Ag}_3(\text{solvent})_x$). Two examples are shown in Figure 3 below, with the solvents of crystallization in their pores (ca. 18 x 21 Å). Not only can the same type of structure be prepared with different solvents/guests, they can be interconverted: $\text{Fe}_2\text{Ag}_3(\text{bromobenzene})_5$ changes to $\text{Fe}_2\text{Ag}_3(1,2\text{-dichlorobenzene})_x$ in a *single-crystal-to-single-crystal transformation*.

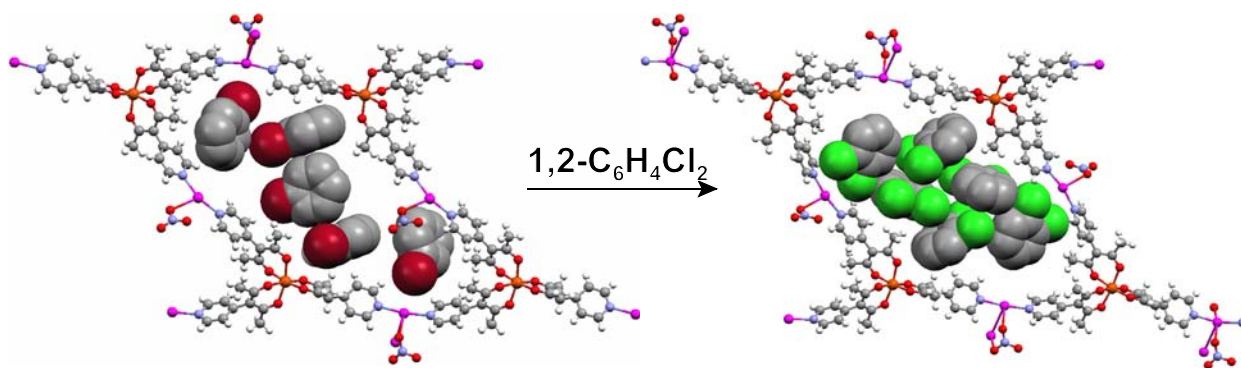


Figure 3. Crystal structures of nanoporous 1-D ladder-structure Ag-Fe compounds. Solvent/guest molecules shown as spacefilling. Crystalline $\text{Fe}_2\text{Ag}_3(\text{bromobenzene})_5$ (*left*) is transformed into crystalline $\text{Fe}_2\text{Ag}_3(1,2\text{-dichlorobenzene})_x$ (*right*) on standing in liquid 1,2-dichlorobenzene.

(b) Molecular materials

We have also studied the reaction of "rods" such as $\text{Cu}(\text{Pyac})_2$ with other metal-containing nodes, including $\text{Re}(\text{CO})_5\text{Cl}$. This reaction is expected to produce "molecular square" species, in analogy with species such as

$[(\text{CO})_3\text{ClRe}(4,4'\text{-bpy})]_4$, pioneered by Hupp et al.; see

Figure 4. Like Hupp's compounds, our Re-Cu square is expected to be neutral; preliminary results indicate that this compound has UV-vis spectral features approximately as expected for a combination of $\text{Re}(\text{CO})_3\text{Cl}(\text{py})_2$ and $\text{Cu}(\text{Pyac})_2$ moieties.

We are also studying the reaction of $\text{Cu}(\text{Pyac})_2$ (as a "4,4'-bpy equivalent") with other right-angle nodes, such as $\text{Ru}(\text{bpy})_2^{2+}$ and $\text{Pd}(\text{en})^{2+}$. In addition, building on the work of Thomas et al. with "molecular cubes" based on $\text{Ru} + 4,4'\text{-bpy}$, we are carrying out analogous reactions

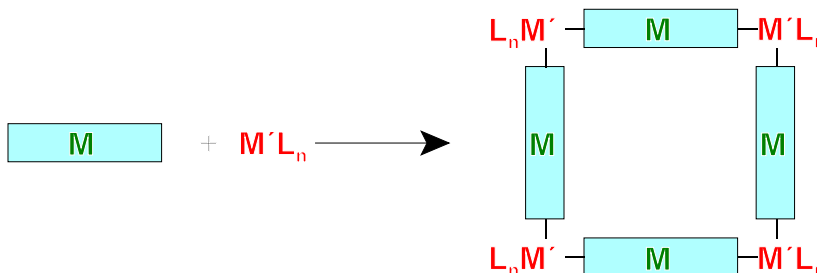


Figure 4. Proposed synthesis of bimetallic molecular squares by reaction of "rods" M with right-angle "nodes" $\text{M}'\text{L}_n$.

with Cu(Pyac)₂. These Re, Pd, and Ru systems are expected to be good molecular analogs of the extended-solid materials mentioned above.

DOE Interest

We expect to use the approaches outlined here to prepare new porous molecules and solids that expose reactive metal sites to the interiors of enclosed cavities and channels. Possible applications of the resulting materials include sensors, thin-film membranes for separations, and catalysts, all of which may derive improved selectivity from the placement of the active metal sites inside the cavities.

Future Plans

For the expended-solid species, we are now working toward porous materials that have both exposed M sites and the ability to exchange guest molecules while maintaining structural integrity. We are also preparing organic "nodes" that are suitable for both molecular and extended-solid products.

Publications

"Solvent-dependent 4⁴ square grid and 6⁴.8² NbO frameworks formed by Cu(Pyac)₂ (bis[3-(4-pyridyl)pentane-2,4-dionato]copper(II))"; Chen, B.; Fronczek, F. R.; Maverick, A. W. *Chem. Commun.* **2003**, 2166-2167.

"3-(4-Cyanophenyl)pentane-2,4-dione and its copper(II) complex"; Chen, B.; Fronczek, F. R.; Maverick, A. W. *Acta Crystallogr., Sect. C*, **2004**, C60, m147-m149.

(2 others in preparation)

This page intentionally left blank.

Reactions of Hydrocarbons on Transition Metal Surfaces

Postdocs: Y. Yang, S. A. Sardar

Students: M. Sushchikh

Collaborators: S.-H. Baeck, H. Metiu, T.F. Jaramillo, B. Cuenya, J. Chou, N. Franklin

Department of Chemical Engineering, University of California, Santa Barbara, CA 93106-5080

mcfar@engineering.ucsb.edu

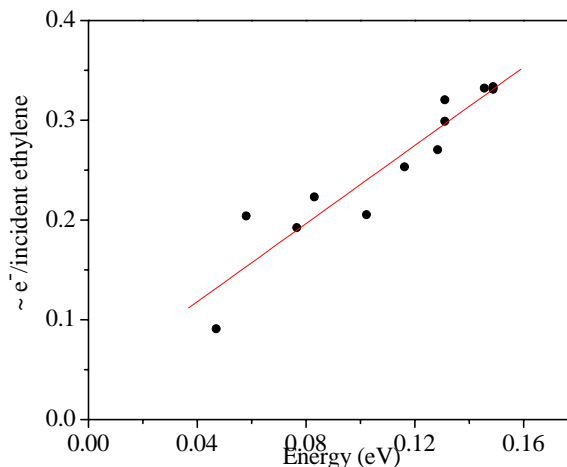
Goal

Improve our understanding of the molecular level processes and the relationships between reactivity, energy transfer, and surface electronic structure associated with hydrocarbon reactivity on transition metal surfaces representative of industrial scale heterogeneous catalysis.

Recent Progress

Reaction induced electronic energy dissipation from olefin absorption on transition metal surfaces: We have observed reaction induced hot electrons from high energy and low energy chemisorption on several metal surfaces on both M-S Schottky diodes as well as MIS and MOS device structures.¹⁻³ The observation of reaction associated “hot” charge carriers produced by hydrocarbons (low adsorption energy) appears to utilize a different electronic pathway in MOS devices compared to the high energy species (e.g. atomic H, O, NO, etc).^{1,3} With our recently upgraded molecular beam (modified with a redesigned nozzle and skimmer) we have used He seeding to produce a hyperthermal beam to observe the kinetic energy dependence of electronic excitations from ethylene adsorption on Au deposited on a silica capped Si (111) n-type substrate (MIS). The results show a dependence upon the incident molecular kinetic energy and the number of electrons observed associated with the reaction.

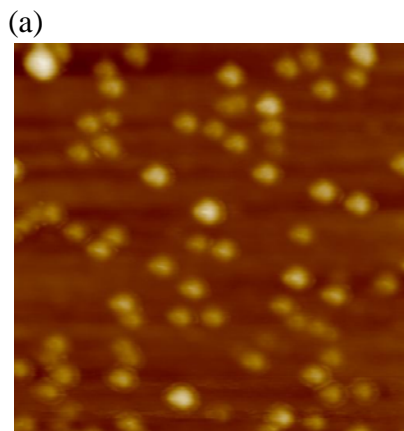
Number of observed electrons per incident ethylene molecule as a function of the ethylene kinetic energy incident upon Au. Ethylene is in a seeded molecular beam incident upon Au on a silica capped Si (111) n-type diode.



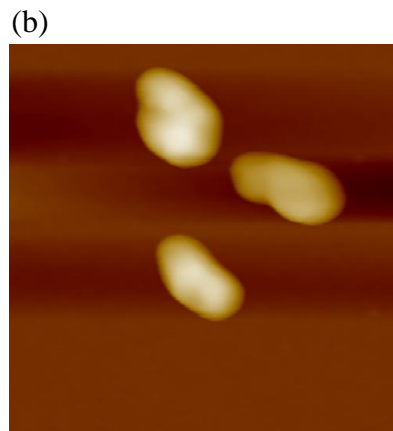
Support and Size Dependent Reactivity of Transition Metal Clusters: The low temperature reactivity of gold clusters (8-22 nm diameter) supported on different metal oxides (titanium dioxide (TiO₂), zinc oxide (ZnO), zirconium oxide (ZrO₂), and silicon dioxide (SiO₂)) was investigated in a high pressure continuous flow reactor. Clusters were encapsulated within polymer in toluene solution, impregnated onto the bulk supports, and reduced by calcination at 300 °C. Support dependent sintering (TiO₂ > ZrO₂ > ZnO) was observed following heating in air at 300 °C. For both propylene hydrogenation and CO oxidation, Au clusters on TiO₂ exhibit the highest activity compared to other supports with activity observed down to room temperature.⁸

There are clearly size dependent changes in the electronic properties of supported metal clusters that alter their catalytic performance. In the case of gold, size selected clusters prepared from micelles as particles with diameters between approximately 1 and 6 nm showed a strong dependence on both the particle size and the support for oxygen reactivity. We observed differences in the formation and stabilization of a metal-oxide, and in the activity for electro-oxidation of carbon monoxide.^{4,5} The smallest particles studied (1.5 nm) were the most active for electro-oxidation of CO and had the largest fraction of oxygen associated with gold at the surface as measured by the Au³⁺/Au⁰ X-ray photoemission intensities. Conducting and semiconducting substrates, ITO-coated glass and TiO₂, respectively, were associated with greater stabilization of Au³⁺ oxide compared to insulating, SiO₂, substrates.

Sintering is the most important limitation to practical utilization of metal cluster catalysts and we have investigated the stability of both supported Ir and Au clusters (1-4 nm diameter) prepared from micelles on several substrates (titania, silica, silicon, alumina). An unexpected, and dramatic increase in the rate of sintering, has been observed on silica and titania substrates under relatively short UV irradiation at room temperature in the presence of oxygen. In contrast, prolonged thermal oxidation in air or oxygen plasmas produced stable non-sintered clusters in all cases in the absence of UV. We have no clear idea, as yet, what is going on.



500 nm x 500 nm

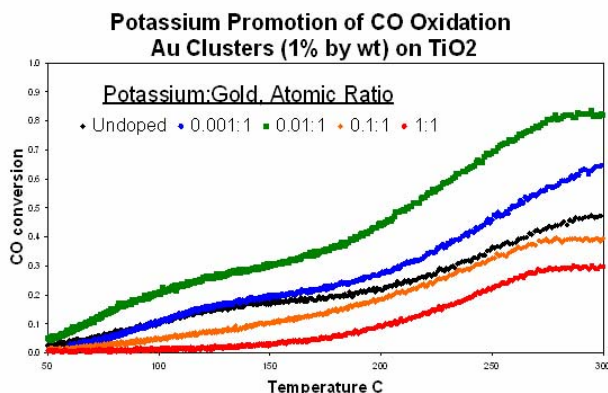


500 nm x 500 nm

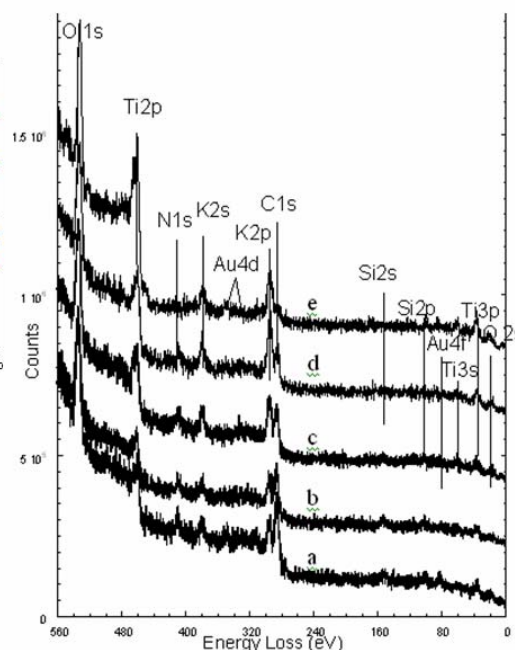
Fig. 2: AFM images of Au nanoclusters deposited from micelles on silica substrates after (a) calcination at 300° C in air, and (b) room temperature UV irradiation in the presence of oxygen.

Activity of Metal Alloy Clusters and Promoted Au Clusters: We are exploring the use of co-metal alloys and promoters to control the electronic structure of metals. Using a micelle deposition method Ag-Au, Pd-Au, Pt-Au and Rh-Au nanoclusters have been deposited on a titania support. Their activity for propylene epoxidation has been screened in a packed bed reactor. The Pd-Au alloy catalyst was found to have unusually high activity for both epoxidation and hydrogenation. The activity of Pt-Au alloys was significantly less and other alloys many of which exhibited no activity.

Initial studies with K promoted Au clusters supported on titania show that there is a significant increase in the activity for high pressure CO activity yet little change in the activation energy in otherwise identical samples (below). A model is under development to explain the kinetics as well as the similar increase in hydrocarbon partial oxidation activity. UHV studies of these potassium-promoted Au-titania catalysts show that in the presence of high pressure oxygen the K appears to “stabilize” Au availability at the surface (a). In the absence of oxygen, K will entirely cover the Au surface (b-d, explaining the observed loss of activity) up to nearly 800 K.



Above: Packed bed reactor (1 atm) activity of K promoted Au. Right: XPS of K/Au/TiO₂ surface taken after a) insert UHV from air, heating to b) 500K, c) 600 K, d) 700 K and e) 800 K. Sample is cooled back to room temperature after each heating cycle.



Investigations of hydrocarbons on transition metals supported on titania and alumina : As a first step in these investigations of partial oxidation and epoxidation in the presence of O₂ and H₂ we investigated the reactivity of TiO₂ (110) and polycrystalline anatase surfaces with molecular and ionized D and H. Thermal Desorption Spectroscopy (TDS), following exposure to more than 100 kL of molecular deuterium, showed a D₂ desorption peak at ~440 K on both single crystal rutile and polycrystalline anatase surfaces. The desorption peak was observed following exposure only at surface temperatures between 140-270 K. Ionized D₂ is significantly more reactive with the titania surface and two desorption peaks at 380 K and ~550 K were observed together with a small D₂O peak observed at ~440 K. Dosing the surfaces with hydrogen and deuterium either in succession or as a mixture showed HD

desorption with no change in the desorption peaks, consistent with dissociative adsorption of both ionized and molecular species. The experimental data was compared to DFT calculations and modeled as a two-step process of hydrogen dissociation at oxygen vacancy sites on TiO₂.⁷

DOE Interests

Understanding and predicting hydrocarbon reactivity on metal surfaces is essential to developing technical strategies to improve and optimize utilization of our fossil hydrocarbon feedstocks (oil, coal, and natural gas) for fuels and chemicals. Investigations connecting fundamental surface science on idealized surfaces to the active surfaces present in industrial scale heterogeneous catalysis are an essential link between the decades of surface chemistry performed in the 20th century and the predictive models to be developed in the 21st century.

Future Plans

In addition to completing the work in progress described above, we intend to pursue the following extensions.

Reaction induced electronic energy dissipation on transition metal surfaces: As proposed, we are now initiating parallel investigations of the incident kinetic energy of several alkanes and olefins on the continuous films and clusters of transition metals on MS and MIS devices.

Support and Size Dependent Reactivity of Transition Metal Nanoclusters: We are now ready to connect the reaction produced hot electrons to catalytic effects on the metal surface in clusters small compared to the mean free path of the electrons. In bulk material and two dimensional films the majority of the electronic energy is driven from the surface ballistically and “cools” by phonon production in the bulk. When mean free path of a hot carrier is on the order of the cluster size (~10-100 nm), multiple interactions of the hot carrier and any adsorbed species are possible. Surface reaction may not be independent of hot carrier production. Using FTIR as *in situ* monitoring tool, we will study the desorption rates of carbon monoxide in presence of inert helium and in presence of strongly physisorbed xenon at adsorption-desorption equilibrium conditions as functions of cluster size and support. We have shown that Xe produces large numbers of carriers compared to He upon collision with the surface. We have completed the installation of a Diffuse-Reflectance Infra-Red accessory (Harrick Scientific) into the external beam path of our FTIR spectrometer and are prepared to make these measurements.

Investigations of hydrocarbons on transition metals supported on titania and alumina : We have developed a complimentary means for depositing size-controlled metal nanoclusters for UHV studies by direct evaporative deposition in vacuum on to surfaces with large concentrations of defects created by sputtering. We will first investigate the size dependent absorption/desorption characteristics of propylene, ethylene, hydrogen, oxygen, and methyl-Br on Au clusters supported on rutile and anatase. Cobalt clusters will be subsequently studied.

Publications

1. X. Liu, B. Roldan Cuenya, and E. W. McFarland, “An MIS Device Structure for Detection of Chemically Induced Charge Carriers,” (accepted and in press *Sensors and Actuators B*, Jan 2004).

2. B. Roldan Cuenya and E.W. McFarland, "Sensors Based on Chemicurrents," Encyclopedia of Nanoscience and Nanotechnology, Sensors: vol1 edited by C.Grimes and E.Dicky, (2003).
3. B. Roldan Cuenya, H. Nienhaus, and Eric W. McFarland, "Chemically Induced Charge Carrier Production and Transport in Pd/SiO₂/n-Si(111) MOS Schottky Diodes," (submitted Phys. Rev. B, 2003).
4. T.F. Jaramillo, S.-H. Baeck, B.R. Cuenya, and E.W. McFarland, "Catalytic Activity of Supported Au Nanoparticles Deposited from Block Copolymer Micelles," J. Am. Chem. Soc. 125(24) 7148-7149 (2003).
5. B. Roldan Cuenya, S.-H. Baeck, T.F. Jaramillo, E.W. McFarland, "Size and Support Dependent Electronic and Catalytic Properties of Au⁰/Au³⁺ Nanoparticles Synthesized From Block Co-polymer Micelles," J. Am. Chem. Soc., 125(42); 12928-12934 (2003).
6. J. Chow, N. Franklin, and E. McFarland, "Support Dependent Propylene and CO Reactivity of Size Selected Au Nanoclusters," (accepted, in press Journal of Catalysis, Aug. 2003).
7. Y. Yang, M. Sushchikh, G. Mills, H. Metiu, and E. McFarland, "Reactivity of TiO₂ with Hydrogen and Deuterium," (submitted Surface Science, Dec 2003)
8. J. Chow, and E. McFarland, "Direct Propylene Epoxidation on Chemically Reduced Au Nanoparticles Supported on Titania ," (submitted, Chem. Com, March. 2004).

This page intentionally left blank.

Catalysis on the Nanoscale: Theoretical Studies of the Stability and Reactivity of Metcar Mo₈C₁₂ Nanoparticles

Postdocs: Liu, P.

Collaborators: Rodriguez, J.

Department of Chemistry, Brookhaven national Laboratory, Upton, NY 11973

muckerma@bnl.gov

Goal

To explore, as a representative example of early transition metal carbide species, the stability and reactivity of Mo₈C₁₂ metcar nanoparticles compared to the extended surfaces Mo(001), Mo₂C(001) and MoC(001) using density functional theory.

This work was carried out as part of the FWP Catalysis on the Nanoscale: Preparation, Characterization and Reactivity of Metal-Based Nanostructures.

Recent Progress

Considering the utility of metal carbides in catalysis, we are particularly interested in the stability and reactivity of metcar nanoparticles. We have employed density functional theory (DFT) using the DMol³ code in all-electron calculations on the Mo₈C₁₂ metcar, and extended surfaces of Mo(001), Mo₂C(001) and MoC(001) as well as their interaction with several small molecules (CO, SO₂ and thiophene) and S atoms. These calculations were carried out using a double numerical plus d-function basis (comparable in accuracy to a Gaussian 6-31G(d) basis) and the generalized gradient approximation (GGA) with the revised version of the Perdew-Burke-Ernzerhof functional (RPBE).

Our DFT calculations show that: (1) In general, the reactivity of molybdenum carbides decreases in the sequence Mo>Mo₂C>MoC because of the increasing C/Mo ratio; (2) Owing to their unique geometry, Mo₈C₁₂ nanoparticle behave quite differently from the bulk materials; (3) The special geometry of Mo₈C₁₂ attenuates the ligand effect of C atoms on metal atoms, and the nanoparticles interact with CO, S and SO₂ as well as Mo₂C does; and (4) When dealing with thiophene, the steric repulsion of the C₂ groups can overcome the intrinsic reactivity of metal atoms in corner or edge sites, and Mo₈C₁₂ becomes as inert as MoC.

Publications 2002-2003

1. K. Kobayashi, G. E. Hall, J. T. Muckerman, T. J. Sears, A. J. Merer, *The E³Π - X³Δ Transition of Jet-Cooled TiO Observed in Absorption*, J. Molec. Spectroscopy **212**, 133 (2002).
2. H. Hou, J. T. Muckerman, P. Liu, J. A. Rodriguez, *A Computational Study of the Geometry and Properties of the Metcars Ti₈C₁₂ and Mo₈C₁₂*, J. Phys. Chem. A **107**, 9344 (2003).

3. P. Liu, J. A. Rodriguez, *Interaction of Sulfur Dioxide with Titanium-Carbide Nanoparticles and Surfaces: A Density Functional Study*, J. Chem. Phys. **119**, 10895 (2003).
4. P. Liu, J. A. Rodriguez, H. Hou, J. T. Muckerman, *Chemical Reactivity of Metcar Ti_8C_{12} , Nanocrystal $Ti_{14}C_{13}$ and A Bulk $TiC(001)$ Surface: A Density Functional Study*, J. Chem. Phys. **118**, 7737 (2003).
5. P. Liu, J. A. Rodriguez, J. T. Muckerman, J. Hrbek, *Interaction of CO, O and S with Metal Nanoparticles on Au(111): A Theoretical Study*, Phys. Rev. B **67**, 155416 (2003).
6. P. Liu, J. A. Rodriguez, J. T. Muckerman, J. Hrbek, *The Deposition of Mo Nanoparticles on Au(111) from a $Mo(CO)_6$ Precursor: Effects of CO on Mo-Au Intermixing*, Surf. Sci. **530**, L313 (2003).
7. P. Liu, J. A. Rodriguez, *Effects of Carbon on the Stability and Chemical Performance of Transition Metal Carbides: A Density Functional Study*, J. Chem. Phys. (in press).

Surface Chemistry Related to Heterogeneous Catalysis

Co-Investigators: Steven H. Overbury, Jun Xu

Chemical Sciences Division, Oak Ridge National Laboratory, Oak Ridge, TN 37831-6201
mullinsdr@ornl.gov

Goal

Expand the fundamental understanding of how chemisorption and reaction occur on well-characterized surfaces, composed of metals deposited on oxide films. Of particular interest are oxidation and reduction type reactions on surfaces composed of reducible oxides, and how interactions between the adsorbates, metal and support are manifested in the reaction pathways.

Recent Progress

Our work has focused on how the mechanisms of reactions occurring at model catalyst surfaces depend upon the oxidation state of the support. The principal systems of interest are reducible mixed oxides of cerium and other rare earth elements as supports for Rh, Pt, and Au. Controlled doping of ceria with other rare earth elements or surface modifiers such as K, is used to determine the effect of oxygen vacancies, ionic conductivity, lattice strain and promoters upon support reducibility. We have also been investigating how molecules with more active functionalities, such as –OH or –SH, interact with the reducible oxide surfaces.

Oxygen Mediated Reduction of Ceria by H₂: All previous work on highly crystalline cerium oxide films grown in UHV have shown that these films are very stable to reduction in hydrogen. Addition of Rh to the surface does not enhance reduction, indicating that the mechanism is not limited solely by hydrogen activation. We have found that pre-adsorption of oxygen on Rh leads to facile reduction of cerium oxide films during a subsequent exposure to H₂. The results suggest that a hydroxyl disproportionation at the Rh-ceria interface is a key step in the reduction.

Reactions on Rh Supported on Dysprosium Oxide: Dysprosium oxide films have been prepared in UHV and used as a support to study Rh catalyzed redox chemistry. Unlike Ce, Dy does not have multiple oxidation states and therefore Dy₂O₃ should not readily undergo oxidation and reduction. The surface structure of Dy₂O₃ is believed to be similar to partially reduced ceria and therefore presents a surface containing O vacancies but no reducible cations. When Rh is deposited on the Dy₂O₃ surface, it is not active for the decomposition of CO. This suggests that the presence of O vacancy nucleation sites is not sufficient for activating supported Rh. Surprisingly, CO is produced when C₂H₄ is adsorbed and heated on Rh / Dy₂O₃. There is apparently an excess of O contained in the DyO_x film. Further, following C₂H₄ treatment, the Rh becomes partially active for CO decomposition. This activity can be eliminated following re-oxidation.

Reactions on Rh Supported on Praseodymium Oxide: Both Pr and Ce are divalent (+3 and +4) and form similar oxide structures in the fully oxidized form. Pr is harder to fully oxidize, however, and the sub-oxides have a more complex structure. CO desorption from Rh is similar on oxidized PrO_x and ceria. C_2H_4 adsorption / desorption produces CO indicative of reduction of the oxide, but there initially appears to be little effect on subsequent CO desorption. After extensive reduction by C_2H_4 the Rh does become active for CO decomposition. This behavior occurs over a fairly narrow range of C_2H_4 treatment, however, and excess ethylene exposure poisons CO uptake.

Reducibility of Mixed Oxides: The reducibility of a series of mixed oxides (Ce-X O_2 where $\text{X}=\text{Dy, Gd, Pr}$) both with and without Rh impregnation, have been studied by x-ray absorption near edge spectroscopy (XANES) and temperature programmed reduction. The goal is to understand what factors determine the oxygen storage capability in mixed oxide supports for oxidation catalysts. XANES quantitatively differentiates between Ce^{3+} and Ce^{4+} in high surface area powders. The mixed oxides were synthesized using both a polymer complexation method and a surfactant mediated method that successfully led to single phase mixed oxides. Contrary to expectations, introduction of oxide vacancies by substituting the +3 cations into the fluorite matrix did not strongly affect the reducibility of these oxides. In all cases however the Rh impregnation greatly enhanced reducibility at low temperatures.

Reduction of CeO_2 films studied by positron annihilation spectroscopy: A 100-nm thick CeO_2 film grown on a Si(111) surface was measured with beam positron lifetime spectroscopy and Doppler broadening of annihilation radiation. The positron lifetime spectra were measured before and after the sample was exposed to H_2 at $\sim 10^{-5}$ torr for about three hours at 614°C . The lifetime spectra do not show a clear difference before and after H_2 exposure, indicating that there are no oxygen vacancies generated in the sub layers of the CeO_2 film by exposing H_2 . This is consistent with our XPS experiments, which also shows no reduction of the CeO_2 surface by H_2 exposure alone.

K Co-adsorption with Rh Supported on CeO_2 : The effect of potassium on the adsorption and reaction of CO on Rh supported on CeO_2 was studied by TPD and SXPS. The key findings were that the K did not reduce the Ce^{+4} to Ce^{+3} and did not promote the dissociation of CO on the Rh. The K did promote the formation of carbonate species on the CeO_2 .

Interactions of $-\text{OH}$ and $-\text{SH}$ Groups with Cerium Oxide: The adsorption and reaction of CH_3OH , CH_3SH and H_2S on oxidized and reduced cerium oxide films was studied by TPD and SXPS. CH_3OH was a very effective reductant producing H_2O and CH_2O . H_2S also removed lattice O by producing H_2O but it left the S behind. CH_3SH did not interact strongly with the oxidized film. All of the molecules reacted with a reduced surface by breaking an OH or SH bond and forming a stable species on the surface. CH_3O decomposed to form CO and H_2 at elevated temperatures while CH_3S reacted with surface hydroxyls to form CH_4 . The decomposition of CH_3SH on reduced CeO_x is much more selective than the decomposition on metal surfaces.

DOE Interest

A detailed understanding of the interactions between adsorbates, supported metals and oxide supports is related to many catalytic processes relevant to energy utilization including emission control, lean burn catalysis, and catalysts for fuel cells and hydrogen utilization.

Future Plans

Comparison of Au with Pt and Rh on CeO_x: The work of Haruta and Goodman have established that the reactivity of Au particles on TiO₂ is dependent on the Au particle size. Recent work by Norskov and Besenbacher has shown that the particle size is influenced by the O vacancy concentration on the TiO_x surface. It is likely that O vacancies will serve as Au nucleation sites on CeO_x as they do on TiO_x. We will test the theory proposed by Norskov to generate Au particles of different sizes and to further test the reactivity of these Au particles.

Electronic Structure of Supported Catalytic Particles: The valence band spectra of Pt supported on oxidized and reduced ceria have been recorded. The goal is to understand how the electronic structure of the metal particle is affected by changes in the oxidation state of the support. In collaboration with a computational scientist at ORNL we will seek a correlation between the activity of CO and changes in the electronic structure as exhibited in the VB spectra both with and without adsorbed CO.

Speciation of Adsorbed Molecular Species by FTIR: Previous studies have revealed a rich chemistry that occurs when molecules such as NO or CH₃OH are adsorbed on ceria films or adsorbed on Rh supported by ceria films. SXPS has been useful for identifying the species that occur on the surfaces during the reactions, however in some cases the results are inconclusive. The nature of these species will be further probed by reflection absorption infra-red spectroscopy (RAIRS) in an apparatus which is capable of measuring both the RAIRS and the XPS.

Adsorption of Heteronuclear Aromatics on CeO_x: Our results have shown that hydrocarbons do not interact strongly with oxidized or reduced CeO_x. The presence of a heteroatom such as S or O allows thiols and alcohols to bind to the surface and follow a more selective decomposition pathway than adsorption on metals. A logical extension of this study is to examine heteronuclear aromatics to see if the heteroatom is able to interact with the oxide and whether this leads to selective reaction chemistry. This work will also be extended to N containing molecules since they have been proposed as potential additives for selective catalytic reduction and their interaction with CeO_x needs to be determined.

Adsorption of Alcohol on Rh/ CeO_x: Our recent study of CH₃OH on CeO₂ has shown how the interaction between the alcohol and the oxide is significantly different from the interaction of the alcohol with a metal. When the two materials are combined by supporting the metal on the oxide, new reaction pathways may open up. A desirable result for fuel cell applications may be the production of H₂ and CO₂ from CH₃OH.

Publications (2002-3)

1. Xu, J and S. H. Overbury, "H₂ Reduction of CeO₂(111) Surfaces via Boundary Rh-O Mediation," *Journal of Catalysis* (in press).
2. D. R. Mullins, "Adsorption of CO and C₂H₄ on Rh-Loaded Thin-Film Praseodymium Oxide", *Surface Science*, (in press).
3. W. T. Tysoe and D. R. Mullins, "Substituted Hydrocarbons on Metal Surfaces" in *Physics of Covered Solid Surfaces*, Vol. III / 42A3, H. P. Bonzel, ed., Landolt-Bornstein, pub., New York, 2003.

4. H. Piao, K. Adib, Z. Chang, H. Hrbek, M. Enever, M. A. Barteau and D. R. Mullins, "Multi-step reaction processes in epoxide formation from 1-chloro-2-methyl-2-propanol on Ag(110) revealed by TPXPS and TPD experiments", *J. Phys. Chem. B*, **107** (2003) 13976.
5. K. Adib, D. R. Mullins, G. Totir, N. Camillone III, J. P. Fitts, K. T. Rim, G. W. Flynn and R. M. Osgood, Jr., "Dissociative Adsorption of CCl₄ on the Fe₂O₃(111)-(2x2) Selvege of alpha-Fe₂O₃(0001)", *Surface Science*, **524** (2003) 113.
6. M. H. Zhang, H. H. Hwu, M. T. Buelow, J. G. Chen, T. H. Ballinger, P. J. Andersen and D. R. Mullins, "Decomposition Pathways of NO on Clean and Oxycarbide-Modified W(111) Surfaces", *Surface Science*, **522** (2003) 112.
7. Overbury, S.H. and D. R. Mullins . "Ceria Surfaces and Films for Model Catalytic Studies using Surface Analysis Techniques" in *Catalysis by Ceria and Related Systems* A Trovarelli, ed. Imperial College Press, (2002)
8. D. R. Mullins and K. Z. Zhang, "Metal - Support Interactions between Pt and Thin Film Cerium Oxide", *Surface Science*, 513 (2002) 163.
9. D. R. Mullins and S. H. Overbury, "Coverage Dependent Dissociation of NO on Rh Supported on Cerium Oxide Thin Films", *Surface Science*, **511** (2002) 293.
10. Moxom, J., J. Xu, R. Suzuki, T. Ohdaira, G. Brandes and J. S. Flynn, "Characterization of Mg doped GaN by positron annihilation spectroscopy." *Journal of Applied Physics* **92**(4), (2002) 1898-1901.
11. Xu, J., J. Moxom, S. H. Overbury, and C. W. White, A. P. Mills, Jr., R. Suzuki, "Quantum antidot formation and correlation to optical shift of gold nanoparticles embedded in MgO", *Phys. Rev. Lett.*, **88** (17), 175502 , 2002
12. Xu, J., J. Moxom, S. Yang, R. Suzuki and T. Ohdaira, "Dependence of porosity in methyl-silsesquioxane thin films on molecular weight of sacrificial triblock copolymer." *Chemical Physics Letters* **364**(3-4),(2002) 309-313.
13. Xu, J., J. Moxom, S. Yang, R. Suzuki and T. Ohdaira, "Porosity in porous methyl-silsesquioxane (MSQ) films." *Applied Surface Science* **194**(1-4):(2002) 189-194.

DE-FG01-03ER15461

Djamaladdin Musaev
Craig Hill
Keiji Morokuma

Principles of Selective O₂-Based Oxidation by Optimal (Binuclear) Catalytic Sites

Postdocs: Bogdan Botar, Yurii Gueletii, David Quinonero

Students: A. Khalid

Collaborators: Ira Weinstock, Stephan Irle

Department of Chemistry, Emory University, 1515 Dickey Dr., Atlanta GA 30322, dmusaev@emory.edu

Goal: To develop combined experimental and theoretical approach to enable molecular-level understanding of the mechanisms of selective (non-radical), reductant-free, O₂-based oxidation of organic substrates catalyzed by polyoxometalates (POMs) with di-metal active sites, virtually the only compounds capable of this chemistry

Progress Report: Experimental work has focused on probing the physical and electronic structures and solution chemistry of one of the 4 known catalysts capable of the low-temperature activation of O₂ for selective (non-radical-chain) oxidations. Three of the four catalysts capable of these practically and environmentally noteworthy processes are transition-metal-oxygen anion cluster compounds (polyoxometalates or “POMs”). These 3 POMs are the gamma-(FeOH₂)₂SiW₁₀O₃₈⁶⁻ complex of Mizuno and co-workers (Fe₂**1**), the (RuOH₂)₂ZnW(ZnW₉O₃₄)₂¹²⁻ sandwich-type complex of Neumann-Dahan (Ru₂**2**) and the recoverable heterogeneous catalyst ((Fe(OH₂)₂)₂(A-α-PW₉O₃₄)₂⁹⁻ supported on cationic silica nanoparticles (Fe₃**3**/CNP) of our group. Initial work has addressed the Fe₂**1** for three reasons: (1) this complex is the simplest of these 3 very complex structures; (2) it shares the Fe₂O₂ active site structural motif with methane monooxygenase (MMO) and other di-iron enzymes under continuing intense investigation; and (3) it is, in some ways the most experimentally tractable.

At the outset, we sought to elucidate whether Fe₂**1** exists in H₂O, and if so, what are its aqueous solution chemistry and catalytic activity in this economically and environmentally optimal medium. The literature studies reported the extremely attractive epoxidation catalyzed by Fe₂**1** via a dioxygenase stoichiometry (alkene + 1/2 O₂ → epoxide). However, prohibitively undesirable chlorocarbon solvents were used.

We have determined that when Fe₂**1** is placed in H₂O at natural pH, an unprecedented trimer, [(gamma-SiW₁₀O₃₆)₃Fe₆(OH)₉(H₂O)₉]¹⁵⁻, forms. The gamma-Keggin units remain largely intact in the trimer, but the Fe atoms move

out of their “pockets” defined by 5 bridging oxygen ligands and now coordinate to hydroxo ligands on the Fe atoms in two adjacent $\text{Fe}_2\text{SiW}_{10}\text{O}_{38}^{6-}$ units. If acetate (a buffer molecule but exemplary of many possible bridging ligands that could be present in such systems either naturally or by design) is present, a structurally related acetate-bridged dimer, $[(\gamma\text{-SiW}_{10}\text{O}_{36})_3\text{Fe}_4(\text{OH})_4(\text{OAc})_4]^{12-}$, forms. Both structures have been solved by X-ray crystallography. Based on many control reactions, the trimer (and not dissociated daughter species) appears to catalyze the selective O_2 -based oxidation of 2-mercaptoethanol in H_2O .

Three different theoretical approaches (models) to study several γ -Keggin POMs, with a general formula of $(\text{MOH}_2)_2\text{SiW}_{10}\text{O}_{36}^{4-}$ ($\text{M}_2\mathbf{1}$) and the lacunary POM $\gamma\text{-}[(\text{SiO})_4\text{W}_{10}\text{O}_{30}(\text{H}_2\text{O})_2]^{4-}$ have been validated. Our computational values of the physical and chemical properties of the low-lying electronic states of $\text{Mn}_2\mathbf{1}$, are in excellent agreement with the available experimental values {*M. Pope and co-workers, Inorg. Chem. 1996, 35, 30*} which substantiates the applicability of the chosen theoretical and geometrical models. These models were then used to elucidate the geometries and energetics of the low-lying electronic states of $\text{M}_2\mathbf{1}$ structures with $\text{M} = \text{Fe}, \text{Mo}, \text{Tc}, \text{Ru}$ and Rh in context with endeavoring to predict the catalytically most active γ -Keggin structures.

Our studies of the lacunary POM indicate that the reported structure (based on X-ray data) $\gamma\text{-}[(\text{SiO})_4\text{W}_{10}\text{O}_{30}(\text{H}_2\text{O})_2]^{4-}$, {*Kamata K. and co-workers, Science, 2003, 300, 964*} should be modified and described as $\gamma\text{-}[(\text{SiO})_4\text{W}_{10}\text{O}_{28}(\text{OH})_4]^{4-}$ with four terminal hydroxy groups.

References (2002-2004) (Musaev and Morokuma)

1. **Musaev, D. G.**; Morokuma, K. „Transition Metal Catalyzed σ -bond Activation and Formation Reactions“ In: *Topics in Organometallic Chemistry*. Vol: Theoretical Aspects of Transition Metal Catalysis“ Ed: G. Frenking, Wiley, **2004**, submitted
2. Khavrutskii, I. V.; **Musaev, D. G.**; Morokuma, K. „Cooperative Pull and Push Effects on the O-O Bond Cleavage in Acylperoxy Complexes of $[(\text{Salen})\text{Mn}(\text{III})\text{L}]$: How to Ensure Formation of $\text{Mn}(\text{V})$ oxo species“, *J. Am. Chem. Soc.* **2004**, submitted.
3. Prabhakar R.; **Musaev, D. G.**; Khavrutskii, I. V.; Morokuma, K. „Elucidation of the structure of Glutathione Peroxidase (GPxs) at the ONIOM level“, *J. Am. Chem. Soc.* **2004**, submitted
4. **Musaev, D. G.** „Theoretical Prediction of a New Dinitrogen Reduction Process: The Utilization of four Dihydrogen Molecules and Zr_2Pt_2 Cluster“, *J. Am. Chem. Soc.* **2004**, submitted
5. Khavrutskii, I. V.; **Musaev, D. G.**; Morokuma, K. „Epoxidation of Unfunctionalized Olefins by $\text{Mn}(\text{Salen})$ Catalyst Using Organic Peracids as Oxygen Source. A Theoretical Study“ “, *Proc. Nat. Acad. Of Sci. (USA)* **2004**, in press

6. Khavrutskii, I. V.; Rahim, R. R.; **Musaev, D. G.**; Morokuma, K. „Axial Ligand as a Mechanistic Switch of the O-O Bond Activation in Acylperoxo Complexes of [(Salen)Mn^{III}L]: Mn^{IV} versus Mn^V Oxo Species“, *J. Phys. Chem. B*, **2004**, 108, 3845-3854
7. Geletii, Yu. V.; **Musaev, D. G.**; Khavrutskii, L.; Hill, C. L. „Peroxynitrite Reactions with Dimethylsulfide and Dimethylselenide: An Experimental Study.“ *J. Phys. Chem. A*, **2004**, 108, 289-294.
8. **Musaev, D. G.**; Galloway, A. L.; Menger, F. M. „The Roles of Steric and Electronic Effects in the 2-Hydroxy-2'-Nitrodiphenyl Sulfones to 2-(o-Nitrophenoxy)-Benzene-Sulfinic acids Rearrangement(Smiles). Computational Study.“, *J. Molecular Struc (Theochem)*, **2004**, in press
9. Khavrutskii, I. V.; **Musaev, D. G.**; Morokuma, K. „Insights into the Structure and Reactivity of Acylperoxo Complexes in Kochi-Jacobsen-Katsuki Catalytic System. A Density Functional Study“*J. Am. Chem. Soc.* **2003**, 125, 13879-13889.
10. **Musaev, D. G.**; Hirao, K. „Reactivity of [1,2-benzisotellurazol-3(2H)-one] with the Peroxynitrous Acid: Comparison with their Ebselen Analogues.“ *J. Phys. Chem. A*, **2003**, 107, 9984-9990.
11. Quiñonero, D.; **Musaev, D. G.**; Morokuma, K. „Theoretical Studies of Non-Heme Iron Catalyst [(BPMEN)Fe(II)(NCCH₃)₂]²⁺ for Olefin Epoxidation and Cis-Dihydroxylation. I. Structures, Stabilities and Electronic Properties of the Catalyst“, *Inorg. Chem.* **2003**, 42, 8449-8455.
12. Hoffmann, M.; Khavrutskii, I. V.; **Musaev, D. G.**; Morokuma, K. „The Protein Effects on the O₂ Binding to the Active Site of the Methane Monooxygenase: ONIOM Studies“, *Int. J. Quant. Chem.*, **2004**, in press.
13. Khoroshun, D. V.; Inagaki, A.; Suzuki, H.; Vyboishchikov, S. F.; **Musaev, D. G.**; Morokuma, k. „Versatile and cooperative reactivity of a triruthenium polyhydride cluster. A computational study.“ *J. Am. Chem. Soc.* **2003**, 125(33), 9910-9911.
14. Menger, F. M.; Galloway, A. L.; **Musaev, D. G.** „Experimental and Computational Support for the Rate/Distance Equation“, *Chem. Comm.* **2003**, 2370-2371.
15. Sakimoto, Y.; Hirao, K.; **Musaev, D. G.**; „Reactivity of Ebtellur Derivatives with the Peroxynitrite Anion: Comparison with Their Ebselen Analogues“, *J. Phys. Chem. A*, **2003**, 107(29), 5631-5639.
16. **Musaev, D. G.**; Geletii, Yu. V.; and Hill, C. L. „ Theoretical Studies of the Reaction Mechanisms of Dimethylsulfide and Dimethylselenide with Peroxynitrite.“ *J. Phys. Chem. A*, **2003**, 107(30), 5862-5873.
17. Moc, J.; **Musaev, D. G.**; Morokuma, K. „ Activation and Adsorption of Multiple H₂ Molecules on Pd₅ Cluster, A Density Functional Study“*J. Phys. Chem. A*, **2003**, 107(24), 4929-4939.
18. Inagaki, A.; **Musaev, D. G.**; Toshifumi, T.; Suzuki, H.; Morokuma, K. „Skeletal Rearrangement in the Trinuclear nido-Ruthenacyclopentadiene Complexes: Theoretical and Experimental Studies“*Organometallics*, **2003**, 22(8); 1718-1727.

19. **Musaev, D. G.**; Geletii, Yu. V.; Hill, C. L.; Hirao, K. „Can the Ebselen Derivatives Catalyze the Isomerization of Peroxynitrite to Nitrate ? „ *J. Am. Chem. Soc.* **2003**, 125(13), 3877-3888.
20. Ilieva, S.; Galabov, B.; **Musaev, D. G.**; Morokuma, K. „Computational Study of the Aminolysis of 2-Benzoxazolinone“ , *J. Org. Chem.* **2003**, 68(9), 3406-3412.
21. **Musaev, D. G.**; Hirao, K. „ The Differences and Similarities in the Reactivity of Peroxynitrite Anion and Peroxynitrous Acid with Ebselen. A Theoretical Study.“ *J. Phys. Chem. A*, **2003**, 107, 1563-1573.
22. Khavrutskii, I. V.; **Musaev, D. G.**; Morokuma, K. „ Electronic and NMR Properties of Various Oxo- and Nitrido- Derivatives of [SalenMn(III)L]⁺, where L=None and Imidazole. A Density Functional Study“ *Inorg. Chem.* **2003**, 42(8); 2606-2621.
23. Khoroshun, D. V.; Warncke, K.; Ke, S.-C.; **Musaev, D. G.**; Morokuma, K. „Internal degrees of freedom, structural motifs, and conformational energetics of 5'-deoxyadenosyl radical: Implications for function in adenosylcobalamin-dependent enzymes. A computational study.“ *J. Am. Chem. Soc.* **2003**, 125(2), 570-579.
24. Ilieva, S.; Galabov, B.; **Musaev, D. G.**; Morokuma, K.; Schaefer III, H. F. „Computational Study of the Aminolysis of Esters. The reaction of methylformate with ammonia“ *J. Org. Chem.* **2003**, 68(4); 1496-1502.
25. **Musaev, D.G.**; Basch, H.; Morokuma, K. „The N≡N Triple Bond Activation by Transition Metal Complexes“, in *Computational Modeling of Homogeneous Catalysis*, Eds. Maseras, F.; Lledos, A., Kluwer Academic Publ., **2002**, 325-361.
26. Sheng, Y.; **Musaev, D.G.**; Reddy, K.S.; McDonald, F.E.; Morokuma, K. „Computational Studies of Tungsten-Catalyzed Endoselective Cycloisomerization of 4-Pentyn-1-ol“, *J. Am. Chem. Soc.*, **2002**, 124, 4149-4157.
27. **Musaev, D.G.**; Basch, H.; Morokuma, K. „Theoretical Study of the Mechanism of Alkane Hydroxylation and Ethylene Epoxidation Reactions Catalyzed by Diiron Bis-oxo Complexes. The Effect of Substrate Molecules“, *J. Am. Chem. Soc.*, **2002**, 124, 4135-4148.
28. Basch, H.; **Musaev, D.G.**; Morokuma, K. „Density functional studies of the electronic and geometric structures of Pt₃⁺, Pt₃O⁺, Pt₃O₂⁺ and Pt₃CH₄⁺“, *J. of Molecular Struct. (Theochem)*, **2002**, 586, 35-46 .
29. Szilagy, R.K.; **Musaev, D.G.**; Morokuma, K. "Hydrogen Scrambling in [(C₅Me₅)Os(dmmp)(CH₃)H]⁺. A Density Functional and ONIOM Study“ *Organometallics*, **2002**, 21, 555-564.
30. Torrent, M.; **Musaev, D.G.**; Basch, H.; Morokuma, K. Computational Studies of Reaction Mechanisms of Methane Monooxygenase and Ribonucleotide Reductase. *J. Computational Chem.* **2002**, 23, 59-76.
31. Khoroshun, D.V.; **Musaev, D.G.**; Morokuma, K. Is binding energy a measure of interaction strength? Sigma trans promotion effect in transition metal complexes. *Mol. Phys.* **2002**, 100, 523-532.

32. Ananikov, V. P.; **Musaev, D.G.**; Morokuma, K. „Vinyl-Vinyl Coupling on Late Transition Metals through C-C Reductive Elimination Mechanism. A Computational Study.“ *J. Am. Chem. Soc.*, **2002**, *124*, 2839-2852.
33. Torrent, M.; Vreven, T.; **Musaev, D.G.**; Morokuma, K.; Farkas, O.; Schlegel, H.B. "Effect of the Protein Environment on the Structure and Energies of Active Sites of Metalloenzymes. ONIOM Study of Methane Monooxygenase and Ribonucleotide Reductase" *J. Am. Chem. Soc.*, **2002**, *124*, 192-193.

Craig L. Hill publications (2002 – 2004)

1. Weinstock, I. A.; Grigoriev, V. A.; Cheng, D.; Hill, C. L. "Role of Alkali-Metal Cation Size in Electron Transfer to Solvent-Separated 1:1 [(M⁺)(POM)] (M⁺ = Li⁺, Na⁺, K⁺) Ion Pairs" In *Polyoxometalate Chemistry for Nanocomposite Design*, Yamase, T.; Pope, M. T., Eds., New York: Kluwer Academic/Plenum Publishers, 2002, pp 103-127.
2. Boring, E.; Geletii, Y.; Hill, C. L. "Catalysts for Selective Aerobic Oxidation under Ambient Conditions. Thioether Sulfoxidation Catalyzed by Gold Complexes" In "Advances in Catalytic Activation of Dioxygen by Metal Complexes" Simandi, L. I., Ed.; Kluwer: Dordrecht, The Netherlands, 2003, pp 227-264.
3. Song, I. K.; Shnitser, R. B.; Cowan, J. J.; Hill, C. L.; Barteau, M. A. "Nanoscale Characterization of Redox and Acid Properties of Keggin-type Heteropolyacids by Scanning Tunneling Microscopy (STM) and Tunneling Spectroscopy (TS): Effect of Heteroatom Substitution" *Inorg. Chem.* **2002**, *41*, 1292-1298.
4. Weinstock, I.A.; Barbuzzi, E.M.G.; Sonnen, D.M; Hill, C. L. "An Environmentally Benign Catalytic Polyoxometalate Technology for Transforming Wood Pulp into Paper", ACS Symposium Series (2002), 823 (Advancing Sustainability through Green Chemistry and Engineering), 87-100.
5. Adam, W.; Herold, M.; Hill, C. L.; Saha-Möller, C. R. "Allylic CH Oxidation versus Epoxidation of 2-Cyclohexenols, Catalyzed by Chromium- and Manganese-Substituted Polyoxometalates and Salen Complexes" *Eur. J. Org. Chem.* **2002**, 941-946.
6. Zhang, X.; Duncan, D. C.; Chen, Q.; Hill, C. L. "Iron Sandwich Polyoxoanion Compounds" *Inorganic Syntheses* Coucouvanis, D., Ed., **2002**, *33*, 52-55.
7. Cowan, J. J.; Hill, C. L.; Reiner, R. S.; Weinstock, I. A. "Dodecatungstoaluminic Acid and its Mono-Lacunary and Mixed Addendum Derivatives" *Inorganic Syntheses* Coucouvanis, D., Ed. **2002**, *33*, 18-26.
8. Anderson, T. M.; Zhang, X.; Hardcastle, K. I.; Hill, C. L. "Reactions of Trivacant Wells-Dawson Heteropolytungstates. Ionic Strength and Jahn-Teller Effects on Formation in Multi-Iron Complexes." *Inorg. Chem.* **2002**, *41*, 2477-2488.

9. Anderson, T. M.; Hill, C. L. "Modeling Reactive Metal Oxide Surfaces. Kinetics, Thermodynamics, and Mechanism of M_3 Cap Isomerization in Polyoxometalates." *Inorg. Chem.* **2002**, *41*, 4252-4258.
10. Okun, N. M.; Anderson, T. M.; Hill, C. L. "[$(Fe^{III}(OH_2)_2)_3(A-\alpha-PW_9O_{34})_2$] $^{9-}$ on Cationic Silica Nanoparticles, a New Type of Material and Efficient Heterogeneous Catalyst for Aerobic Oxidations" *J. Am. Chem. Soc.* **2003**, *125*, 3194-3195.
11. Tharnish, P. M.; Juodawlkis, A. S.; Hill, C. L.; Schinazi, R. F. "CD81 Receptor Expression in Human Cells: Implications for HCV Therapeutics" *Frontiers in Viral Hepatitis*, Schinazi, R. F., Rice, C.; Sommadossi, J.-P. Eds.; Elsevier: The Netherlands, 2002, pp 513-520.
12. Okun, N. M.; Anderson, T. M.; Hill, C. L. "Polyoxometalates on Cationic Silica. Highly Selective and Efficient O_2 /Air-Based Oxidation of 2-Chloroethyl Ethyl Sulfide at Ambient Temperature, *J. Mol. Catal. A. Chem.* **2003**, *197*, 283-290.
13. Neiwert, W. A.; Cowan, J. J.; Hardcastle, K. I.; Hill, C. L.; Weinstock, I. A. "Stability and Structure in α - and β -Keggin Heteropolytungstates, $[X^{n+}W_{12}O_{40}]^{(8-n)-}$, X = p-Block Cation" *Inorg. Chem.* **2002**, *41*, 6950-6952.
14. Geletii, Y. V.; Patel, A. D.; Hill, C. L.; Casella, L.; Monzani, E. "Catalysis of Ascorbic Acid Oxidation with Peroxynitrite by Biomimetic Cu Complexes" *React. Kinet. Catal. Lett.* **2002**, *77*, 277-285.
15. Mbomekalle, I. M.; Keita, B.; Nadjo, L.; Berthet, P.; Hardcastle, K. I.; Hill, C. L.; Anderson, T. M. "Multi-Iron Tungstodiarsenates. Synthesis, Characterization, and Electrocatalytic Studies of $\alpha\beta\beta\alpha$ -($Fe^{III}OH_2$) $_2Fe^{III}_2(As_2W_{15}O_{56})_2^{12-}$." *Inorg. Chem.* **2003**, *42*, 1163-1169.
16. Kim, G.-S.; Zeng, H.; Neiwert, W. A.; Weinstock, I. A.; Cowan, J. J.; VanDerveer, D.; Hill, C. L. "Dimerization of $A-\alpha-[SiNb_3W_9O_{40}]^{7-}$ by pH-Controlled Formation of Individual Nb- μ -O-Nb Bonds" *Inorg. Chem.* **2003**, *42*, 5537-5544.
17. Musaev, D. G.; Geletii, Y. V.; Hill, C. L.; Hirao, K. "Can the Ebselen Derivatives Catalyze the Isomerization of Peroxonitrite to Nitrate?" *J. Am. Chem. Soc.* **2003**, *125*, 3877-3888.
18. Mbomekalle, I. M.; Keita, B.; Nadjo, L.; Berthet, P.; Neiwert, W. A.; Hill, C. L.; Ritorto, M. D.; Anderson, T. M. "Manganous Heteropolytungstates. Synthesis and Heteroatom Effects in Wells-Dawson-Derived Sandwich Complexes." *J. Chem. Soc., Dalton Trans.* **2003**, 2646-2650.
19. Musaev, D. G.; Geletii, Y. V.; Hill, C. L. "Theoretical Studies of the Reaction Mechanisms of Dimethylsulfide and Dimethylselenide with Peroxynitrite" *J. Phys. Chem. A.* **2003**, *107*, 5862-5873.
20. Kim, Gyu-Shik.; Zeng, Huadong; Hill, C. L. "X-Ray Structure of Keggin-type Peroxo Polyoxometalate $A-\alpha-[Si(NbO_2)_3W_9O_{37}]^{7-}$ " *Bull. Korean Chem. Soc.* **2003**, *24*, 1005-1008.
21. Okun, N. M.; Anderson, T. M.; Hardcastle, K. I.; Hill, C. L. "Cupric Decamolybdodivanadophosphate. A Coordination Polymer Heterogeneous Catalyst for Rapid, High Conversion, High Selectivity Sulfoxidation Using the Ambient Environment." *Inorg. Chem.* **2003**, *42*, 6610-6612.

22. Mbomekalle, I. M.; Keita, B.; Nadjo, L.; Neiwert, W. A.; Zhang, L.; Hardcastle, K. I.; Hill, C. L.; Anderson, T. M. "Lacunary Wells-Dawson Sandwich Complexes. Synthesis, Characterization and Stability Studies of Multi-Iron Species." *Eur. J. Inorg. Chem.* **2003**, 3924-3928.
23. Tharnish, P. M.; Juodawlkis, A. S.; Hill, C. L.; Schinazi, R. F. CD81 receptor expression in human cells: Implications for HCV therapeutics" *Frontiers in Viral Hepatitis*, Schinazi, R. F.; Sommadossi, J.-P.; Rice, C. M. Eds., Elsevier, 2003, pp 485- 492.
24. DuBose, D. A.; Blaha, M. D.; Morehouse, D. H.; Okun, N.; Hill, C. L. "Effect of Potential Vesicant Antagonist Drugs on White Blood Cell Viability in Human Whole Blood Exposed to 2-Chloroethyl-Ethyl Sulfide" *J. Medical Chemical Defense*, **2003**, submitted.
25. Gelettii, Y. V.; Musaev, D. G.; Khavrutskii, L.; Hill, C. L. "Peroxynitrite Reactions with Dimethylsulfide and Dimethylselenide. An Experimental Study." *J. Phys. Chem.* **2004**, 108, 289-294.
26. Keita, B.; Mbomekalle, I. M.; Lu, Y. W.; Nadjo, L.; Berthet, P.; Anderson, T. M.; Hill, C. L. "Multi-Iron Sandwich-Type Polyoxometalates. Electron Transfer Behaviors of the Iron-Containing Core and Electrocatalytic Reduction Reactions" *J. Chem. Soc., Dalton Trans.* **2003**, in submission.
27. Fang, X.; Neiwert, W. A.; Hill, C. L.; Anderson, T. M. "Yttrium Polyoxometalates. Synthesis and Characterization of a Carbonate-Encapsulated Sandwich-Type Complex" *Inorg. Chem.* **2003**, 42, ASAP Article.
28. Ritorto, M. D.; Anderson, T. M.; Neiwert, W. A.; Hill, C. L. "Decomposition of A-type Sandwiches. Synthesis and Characterization of New Polyoxometalates Incorporating Multiple d-Electron-Centered Units" *Inorg. Chem.* **2004**, 42, 44-49.
29. Kholdeeva, O. A.; Timofeeva, M. N.; Maksimov, G. M.; Maksimovskaya, R. I.; Rodionova, A. A.; Hill, C. L. "Aerobic Formaldehyde Oxidation under Mild Conditions Mediated by Ce-Containing Polyoxometalates", In *Catalysis of Organic Reactions*, Sowa, J. R., Jr., Ed.; Marcel Dekker, Inc.: New York 2004, pages not yet assigned.
30. Hill, C. L. "Stable, Self-Assembling, Equilibrating Catalysts for Green Chemistry" *Angew. Chem. Int. Ed.* **2004**, 43, 402-404.
31. Hill, C. L. "Polyoxometalates: Reactivity" *Comprehensive Coordination Chemistry II: From Biology to Nanotechnology*, Elsevier: Amsterdam; December, 2004; pp. 679-759.
32. Okun, N. M.; Ritorto, M. D.; Apkarian, R. P.; Anderson, T. M.; Hill, C. L. "Polyoxometalates on Cationic Silica Nanoparticles. Physicochemical Properties of an Electrostatically Bound Multi-Iron Catalyst" *Chem. Mater.* **2004**, accepted pending revision.
33. Keita, B.; Mbomekalle, I. M.; Nadjo, L.; Anderson, T. M.; Hill, C. L. "Multi-Iron Wells-Dawson Heteropolytugstates. Electrochemical Probing of Siderophoric Behavior in Sandwich-Type Complexes" *Inorg. Chem.* **2004**, 42, in press.

34. Kholdeeva, O. A.; Timofeeva, M. N.; Maksimov, G. M.; Maksimovskaya, R. I.; Neiwert, W. A.; Hill, C. L. "Catalytic Aerobic Oxidation of Formaldehyde under Mild Conditions" *J. Am. Chem. Soc.* **2004**, *126*, 000. submitted
35. Kholdeeva, O. A.; Vanina, M. P.; Timofeeva, M. N.; Maksimovskaya, R. I.; Trubitsina, T. A.; Melgunov, M. S.; Burgina, E. B.; Mrowiec-Białoń, J.; Jarzębski, A. B.; Hill, C. L. "Aerobic Aldehyde Oxidation: a Comparative Study of Different Solid Co-polyoxometalate Catalysts." *J. Catal.*, **2004**, submitted.

Catalytic Applications of H• Transfer from Transition–Metal Hydride Complexes

Postdocs: M. Iimura

Students: M. Arribas, R. Petros, L.-H. Tang

Collaborators: M. -H. Baik, R. A. Friesner, J. C. Edwards

Department of Chemistry, Columbia University, MC 3102, New York, NY 10027

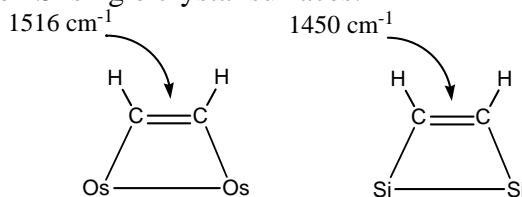
jnorton@chem.columbia.edu

Goal

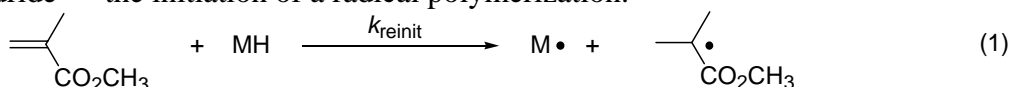
Develop better catalysts for chain transfer during free radical polymerization

Recent Progress

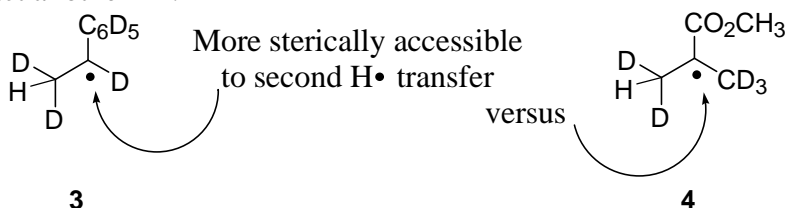
A. A Vibrational Model for Surface Acetylene.³ The vibrational frequencies of the diosmacyclobutene ring in $\text{Os}_2(\text{CO})_8(\mu_2\text{-}\eta^1, \eta^1\text{-C}_2\text{H}_2)$ and its dideuterated isotopologue $\text{Os}_2(\text{CO})_8(\mu_2\text{-}\eta^1, \eta^1\text{-C}_2\text{D}_2)$ have been measured and assigned. The results are an excellent vibrational model for C_2H_2 on Si single crystal surfaces.



B. Transfer of H• from Chromium Hydride Complexes to Methyl Methacrylate and Styrene. Strengths of Cr–H and C–H Bonds¹ The rates of H/D exchange have been measured between (a) the activated olefins methyl methacrylate-*d*₅ and styrene-*d*₈, and (b) the Cr hydrides ($\eta^5\text{-C}_5\text{Ph}_5$)Cr(CO)₃H (**1a**), ($\eta^5\text{-C}_5\text{Me}_5$)Cr(CO)₃H (**1b**), and ($\eta^5\text{-C}_5\text{H}_5$)Cr(CO)₃H (**1c**). Statistical corrections give the rate constants k_{reinit} for H• transfer to the olefin from the hydride — the initiation of a radical polymerization.

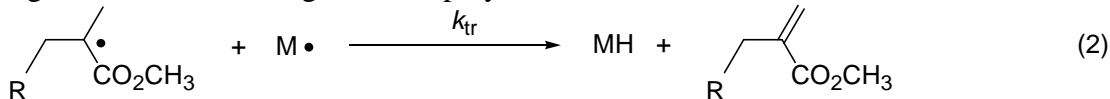


Hydrogenation is insignificant except with styrene and $\text{CpCr}(\text{CO})_3\text{H}$ (which form the intermediate radical **3**); the radical **4** arising from H• transfer to methyl methacrylate is too hindered to abstract another H•.



With MMA, k_{reinit} decreases substantially as the steric bulk of the hydride increases; with styrene, the steric bulk of the hydride has little effect. At longer times, the reaction of MMA or styrene with **1a** gives the corresponding metalloradical **2a** as termination depletes the concentration of the methyl isobutyryl radical **4** or the α -methylbenzyl radical **3**; computer simulation of [**2a**] as a function of time gives an estimate of k_{tr} , the rate constant for H• transfer

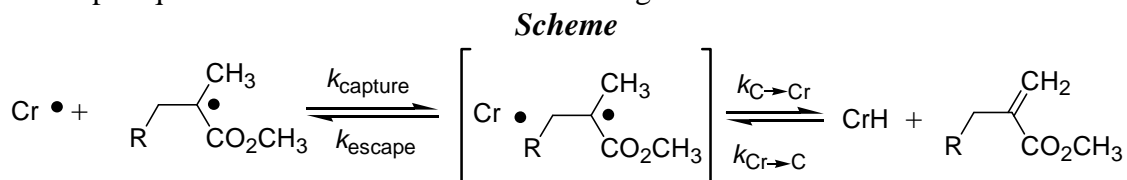
from **3** or **4** back to Cr. The value of k_{tr} measures the effectiveness of a metalloradical in catalyzing chain transfer during a radical polymerization.



The CH_3CN pK_a of **1a**, 11.7, implies a BDE for its Cr–H bond of 59.6 kcal/mol. In combination the rate constants (which give kinetic ΔG values), the experimental BDE for **2a**, and the ΔS values calculated for $\text{H} \cdot$ transfer imply a C–H BDE of 46 kcal/mol for the methyl isobutyryl radical **4**, and a C–H BDE of 48 kcal/mol for the α -methylbenzyl radical **3**.

C. Inverse Temperature Dependence of a Chain Transfer Rate Constant.

Formation of a Solvent Cage. Absence of CIDNP.² There are many reasons to assume that $\text{H} \cdot$ transfers such as k_{reinit} and k_{tr} occur within a solvent cage. (CIDNP has been observed in related reactions.) Such cage effects may explain the difference between the k_{tr} value we obtain by kinetic modeling for methyl isobutyryl radical **4** and the one we obtain from Mayo plots ($1/\text{DP}_n$ as a function of [**2a**]) for the polymer-containing radical **4-P**. We have determined the temperature dependence of k_{tr} by constructing a Mayo plot every 5 degrees between 60 and 80 °C, and have found that k_{tr} *decreases* with increasing temperature. This decrease presumably reflects the preequilibrium formation of the solvent cage in the Scheme.



With the Scheme the observed k_{tr} will be that in eq 3. The cage-forming equilibrium $k_{\text{capture}}/k_{\text{escape}}$ will lie further to the left with increasing temperature, and k_{tr} will decrease.

$$k_{tr} = \frac{k_{\text{capture}} k_{\text{C} \rightarrow \text{Cr}}}{k_{\text{escape}} + k_{\text{C} \rightarrow \text{Cr}}} \approx \frac{k_{\text{capture}} k_{\text{C} \rightarrow \text{Cr}}}{k_{\text{escape}}} \quad (3)$$

We observe no CIDNP even at 58 MHz during the reaction of the chromium hydride **1a** with MMA, presumably because the persistence of the paramagnetic chromium metalloradical **2a** causes loss of spin memory and nuclear polarization.

D. Steric Effect on the Ability of Metalloradicals to Serve as Chain Transfer Catalysts in the Polymerization of MMA.⁴ We have tried the largely monomeric $(\text{C}_5\text{Me}_5)\text{Cr}(\text{CO})_3 \cdot$ (**2b**) as a chain transfer catalyst. A Mayo plot at 70 °C shows activity six times greater than the activity of **2a**. In view of these results we have also measured the activity of $(\text{C}_5\text{H}_5)\text{Cr}(\text{CO})_3 \cdot$ (**2c**), which dissociates significantly at 70 °C. We have found **2c** to be almost as effective as the best catalyst previously reported.

After testing several other metalloradicals we believe we understand the requirements for effective catalysis of chain transfer during free radical polymerizations. The metalloradical must:

- (a) be stable at the temperature of the polymerization.
- (b) be *just crowded enough to discourage* (i) its own dimerization, (ii) the formation of an M–C bond with the chain-carrying radical, or (iii) the transfer of a second $\text{H} \cdot$ to the chain-carrying radical from its hydride M–H (resulting in hydrogenation). Additional steric hindrance will slow its abstraction of $\text{H} \cdot$ from the chain-carrying radical.

(c) form an M–H bond weak enough to permit the facile transfer of H• to monomer (suggesting that first-row metals may be preferable).

DOE Interest

This project will develop effective metalloradical catalysts for chain transfer during radical polymerizations, thus controlling molecular weight and permitting the efficient synthesis of low-molecular-weight vinyl-terminated oligomers.

Future Plans

Other Metalloradicals We will determine the M–H bond strengths of several other hydride complexes of first-row transition metals, including some water-soluble anions. With that information we will examine the reaction of these complexes with deuterated methyl methacrylate and styrene, and determine the rate of H• transfer. We should be able to predict which hydride complexes will be effective as chain transfer catalysts.

Incorporation of Macromonomers We will label the dimer of methyl methacrylate with deuterium — and see whether are incorporated when a catalyst begins a new chain. We will thus determine whether reinitiation after chain transfer catalysis can occur with oligomers.

Regulation of Molecular Weight with H₂ As some metalloradicals can be converted to the corresponding hydrides with H₂ gas, it should be possible to control the rate and molecular weight distribution of radical polymerizations by varying the H₂ pressure.

Publications (2003-2004)

1. L. -H. Tang, E. T. Papish, G. P. Abramo, J. R. Norton,* M. -H. Baik, R. A. Friesner, and A. Rappé, "Kinetics and Thermodynamics of H• Transfer From (η^5 -C₅R₅)Cr(CO)₃H (R = Ph, Me, H) to Methyl Methacrylate and Styrene," J. Am. Chem. Soc. 2003, 10093-10102.
2. L. -H. Tang, J. R. Norton*, and J. C. Edwards, "Inverse Temperature Dependence of Chain Transfer Rate Constant for a Chromium Metalloradical in Ploymerization of MMA." Macromolecules, 2003, 9716-9720.
3. C. E. Anson, N. Sheppard, R. Pearman, J. Moss, P. Stöbel, S. Koch, and J.R. Norton*, "A Vibrational Study of the Dismacrocyclobutene Complex Os₂(CO)₈(μ_2 - η^1 , η^1 -C₂H₂): The Use of Organometallic Complexes as Vibrational Models for Chemisorbed Ethyne." Physical Chemistry Chemical Physics 2004, 1070-1076.
4. L. -H. Tang and J.R. Norton*, "The Effect of Steric Congestion on the Activity of Chromium and Molybdenum Metalloradicals as Chain Transfer Catalysts during MMA Polymerization." Macromolecules, 2004, 241-243.

This page intentionally left blank.

Colin Nuckolls, Assistant Professor of Chemistry

Synthesis, Directed Assembly, and Local Probe Measurements of Dipolar, Organic Nanostructures

Post-docs: Dr. Thuc-Quyen Nguyen

Graduate Students: Chaya Ben-Porat, Mark Bushey, Dana Horoszewski, and Qian Miao

Collaborators: Phaedon Avouris, Louis Brus, and Richard Martel

*Columbia University, Department of Chemistry, New York, NY 10027**e-mail: cn37@columbia.edu*

The research program outlined below applies organic synthesis and self-assembly to create nanoscale materials. It focuses on self-assembly of complex aromatic molecules at interfaces because this allows electronic and polar properties to be investigated on molecular length-scales.

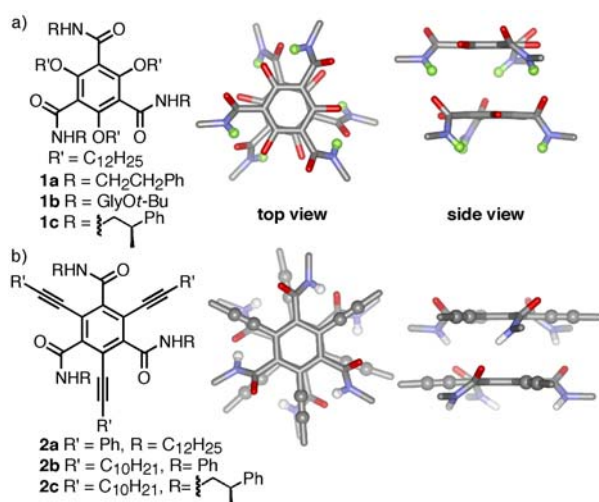


Figure 1. Crowded aromatics that utilize synergistic π -stacking and hydrogen bonding.

It focuses on molecules like **1** and **2** that in their self-assembly allow a synergy between hydrogen bonds and π -to- π interactions (shown in Figure 1). The design principle uses steric crowding to force the recognition groups—amides—out of the aromatic ring-plane and into a conformation that would allow intermolecular hydrogen bonds to form. There are three significant findings. First, the dipole moments of the disks endow the columnar stacks with a macroscopic dipole moment. Polar properties of monolayer films could be measured by means of electrostatic force microscopy. Second, because the association in the stacking direction is stronger than in typical π -stacks, it is possible to create isolated strands of molecules that can be visualized with scanning probe microscopy. Third, it is possible to create the shortest of π -stacks, dimers, on metallic surfaces through noncovalent forces.

Future work will expand the scope of the project to synthesize never versions of these molecules that have larger π -systems that can delocalize charge. In addition the polar and electrical properties will be measured as a function of film thickness from monolayer to multilayers and as the domain size is decreased to near single molecules.

Publications Recognizing Support from DE-FG02-01ER15264

(1) “STM Imaging of Self-Assembled Helical Nanostructures”, T.-Q. Nguyen, R. Martel,

- A. Carlsen, P. Avouris, M. L. Bushey, L. E. Brus, and C. Nuckolls, *in preparation*.
- (2) “Electrostatic Self-assembly of Crowded Aromatics”, T.-Q. Nguyen, J. Dickerson, M. L. Bushey, I. Herman, and C. Nuckolls, *in preparation*.
- (3) “Electric Fields on Oxidized Silicon Surfaces: Static Polarization of PbSe Nanocrystals”, C. Ben-Porat, O. Cherniavskaya, L. Brus and K.-S. Cho and C. B. Murray, *J. Phys. Chem. B.*, *accepted for publication*.
- (4) “Molecular Interactions in One-Dimensional Organic Nanostructures”, T.-Q. Nguyen, R. Martel, P. Avouris, M. L. Bushey, C. Nuckolls, and L. Brus, *J. Am. Chem. Soc.*, *accepted for publication*.
- (5) “Dimeric π -stacks on Gold using Three Dimensional Lock-and-Key Receptors,” G. S. Tulevski, M. L. Bushey, J. L. Kosky, S. J. Toshihiro-Ruter, and C. Nuckolls, *Angew. Chem. Int. Ed.*, *accepted for publication*.
- (6) “Using Hydrogen Bonds to Direct the Assembly of Crowded Aromatics,” M. L. Bushey, T.-Q. Nguyen, W. Zhang, D. Horoszewski, and C. Nuckolls, *Angew. Chem., Int. Ed.*, *accepted for publication*.
- (7) “Synthesis, Assembly, and Thin Film Transistors of Dihydrodiazapentacene—an Isostructural Motif for Pentacene,” Q. Miao, T.-Q. Nguyen, T. Someya, G. B. Blanchet, and C. Nuckolls, *J. Am. Chem. Soc.* **2003**, *125*, 10284–10287.
- (8) “A Defined Secondary Structure in Covalently-Linked Overcrowded Aromatics,” W. Zhang, D. Horoszewski, J. Decatur, and C. Nuckolls, *J. Am. Chem. Soc.* **2003**, *125*, 4870–4873.
- (9) “Synthesis, Self-Assembly, and Electro-optic Switching of One-Dimensional Nanostructures from New Crowded Aromatic,” M. L. Bushey, T.-Q. Nguyen, and C. Nuckolls, *J. Am. Chem. Soc.* **2003**, *125*, 8264–8269.
- (10) “Tuning Intermolecular Attraction to Create Polar Order and One-Dimensional Nanostructures,” T.-Q. Nguyen, M. L. Bushey, L. Brus, and C. Nuckolls, *J. Am. Chem. Soc.* **2002**, *124*, 15051–15054.
- (11) “The Consequences of Chirality in Crowded Arenes—Macromolecular Helicity, Hierarchical Ordering, and Directed Assembly,” M. L. Bushey, A. Hwang, P. W. Stephens, and C. Nuckolls, *Angew. Chem. Int. Ed.* **2002**, *41*, 2828–2831.

Nanoscale Materials for Catalysis

Principal Investigators: Ralph G. Nuzzo, Duane Johnson^{*}, Anatoly Frenkel^{},
Judith Yang^{***}**

**Graduate Students: Charles Hills, Laurent Menard, Nathan Mack
Post-doctoral Research Associate: Huiping Xu^{***}**

**Department of Chemistry, University of Illinois Urbana-Champaign, Urbana IL
61801**

*** Department of Materials Science and Engineering, University of Illinois Urbana-
Champaign, Urbana IL 61801**

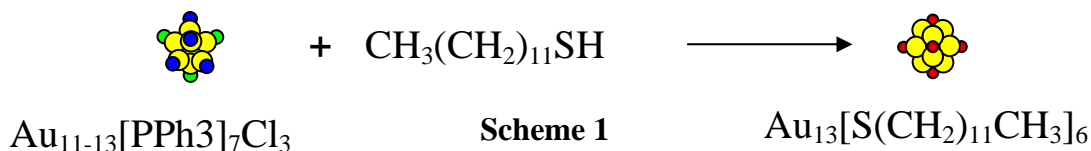
**** Department of Physics, Yeshiva University, New York City, NY, 10016**

***** Department of Materials Science and Engineering, University of Pittsburgh,
Pittsburgh, PA 15261**

Abstract

This project involves the characterization of metal nanoparticles with the goal of achieving a fundamental understanding of their dynamical and structural properties and the correlations these have with behavior seen in catalytic chemistry. In addition, the experimental studies are supported with theory and modeling. These studies employ a variety of analytical techniques, highlighted by the complementary use of electron microscopy techniques that probe nanoscale materials properties at the single particle level and x-ray absorption spectroscopy experiments that measure an ensemble of particles. As we will show, this approach has proven especially powerful in identifying metastable geometries and phases not observed in bulk systems. *In situ* studies have identified such metastable structures in several model systems and further elucidated information relevant to the dynamics of their evolution. Efforts to demonstrate the applicability and utility of these techniques to a variety of systems of fundamental and technological interest have led us to focus initially on two classes of model materials. The systems studied include ligand-protected metal nanoparticles as well as catalytically

relevant metal nanoparticles grown on high-surface-area support materials (mostly carbon). The former offers a model system providing experimental control of nanoparticle size and local environment defined by the choice of ligand. The latter is a system of obvious technological interest and also offers greater access to dynamical studies of cluster growth and structural evolution.



Small, monodisperse Au₁₃ clusters have been prepared via a ligand exchange reaction of alkanethiols onto phosphine-halide gold clusters (Scheme 1). In one synthetic protocol, two fractions separated with column chromatography exhibit very different UV-visible spectroscopy (Figure 1). The majority fraction of these exchange products showed narrow bands in the UV-visible spectroscopy – a characteristic of a so-called “molecule-like” electronic structure. The minority

fraction showed no bands in the UV-visible spectroscopy but instead exhibited an absorbance profile that increases smoothly into the UV region of the

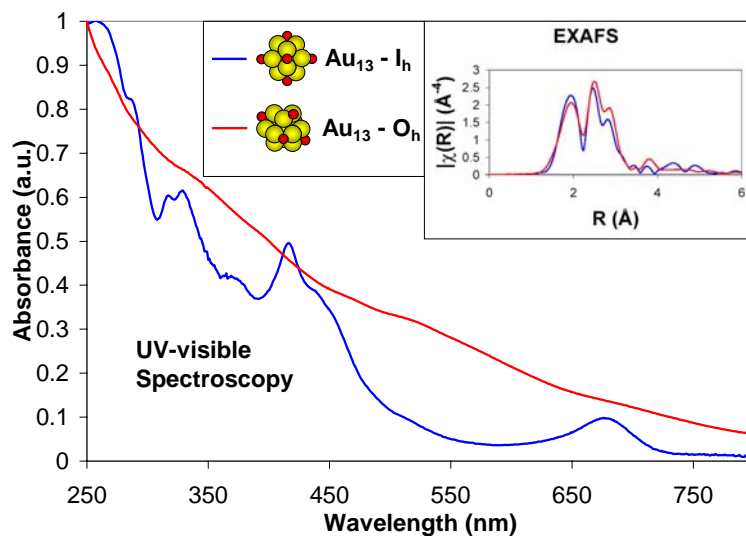


Figure 1

spectrum.

Extended x-ray absorption fine structure (EXAFS) measurements of these two materials (Figure 1, inset) were fit using Au-S and the first nearest neighbor Au-Au scattering paths and found to exhibit two different structures of a Au₁₃ cluster core with a ligand shell of six alkanethiols. The cluster exhibiting a molecule-like UV-visible spectrum (blue curves, Fig.1) was found to have a local structure consistent with an icosahedral core while the cluster with a smoothly varying UV-visible absorption spectrum (red curves, Fig. 1) was determined to be a cuboctahedral Au₁₃ core. This system embeds considerable structural fluxionality as shown by the data given in Figure 2. The EXAFS analysis reveals

that all three samples are icosahedral Au₁₃ clusters, albeit ones exhibiting differences in the average gold-gold bond lengths that

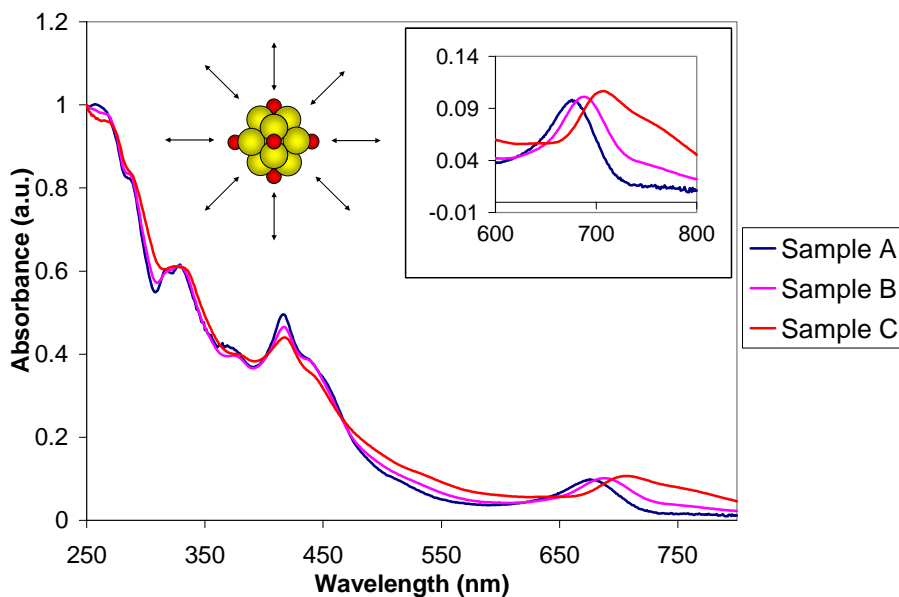


Figure 2

decrease from Sample A to Sample C. The noted differences in the UV-visible spectroscopy are correlated with a progression of structural relaxations of the gold core bonding driven by ligand exchange. The replacement of a thiol ligand with a phosphine (or vice-versa) drives these effects. For example, by replacing a thiol with a phosphine

on the cluster, additional electron density is made available for Au core bonding and a decrease in Au-Au bond lengths is the expected and observed result. Current efforts are focused on using high-resolution electron microscopy techniques to study nanoparticle structures of this sort and compare these data to that obtained at the level of the ensemble using x-ray spectroscopies.

Initial studies by transmission electron microscopy identified both fractions as sub-nanometer, highly monodisperse nanoparticles. Figure 3 is a representative Scanning transmission electron microscopy (STEM) high-angle annular dark-field (HAADF) image of Au clusters. The inset right below is a histogram of the particle size distribution of Au nanoparticles measured from HAADF images taken in different sample regions, where 1025 Au nanoparticles were counted.

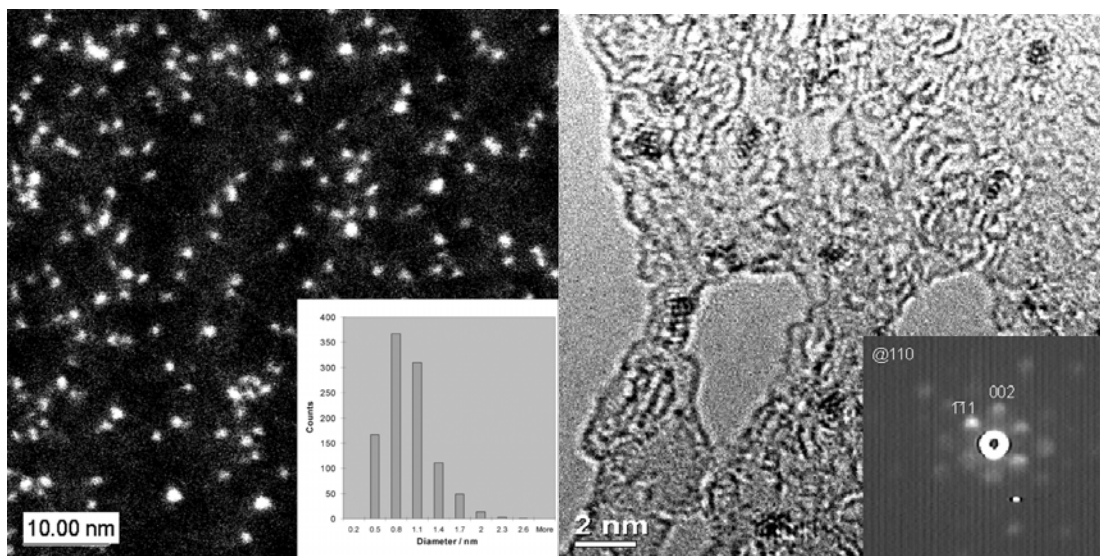


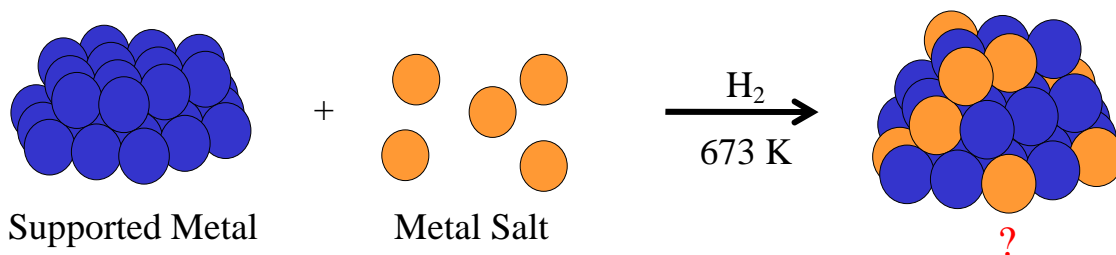
Figure 3

Figure 4

As indicated in the particle size histogram (Figure 3, inset), Au clusters have an average diameter of 0.82 ± 0.34 nm, with a very narrow size distribution, i.e., from 0.5 to 2.0 nm.. The size of the particles seen in this image suggests that the typical particle of gold

contains 13-55 atoms. Quantitative mass spectroscopic analysis is being developed. to provide more details about atoms per cluster.

The nanoparticles microstructure was further studied by electron microdiffraction and high resolution electron microscopy (HREM). Figure 4 is a HREM image of Au clusters in the same sample as scanned by STEM and strong diffraction pattern is seen for these particles with the size larger than 1nm (figure 4, inset). The pattern shown in the figure 4 (and others recorded at the several locations of the sample) is best indexed to an FCC structure with zone axis of 110. The values from the ratios of distances calculated for the FCC Au alloy (where $a=0.407\text{nm}$, $c/a=1.155$, $\theta= 54.74^\circ$) agree closely with those measured from the microdiffractions of a variety of nanoparticles residing in different regions of the samples ($c/a=1.1\pm 0.1$, $\theta = 56\pm 1^\circ$). For smaller particles with the size less than 1nm, the crystal structure can be deduced from HREM images. Figure 4 displays lattice fringes of those ultra small gold clusters with size less than 1nm; the average lattice parameter can be measured as 0.40 ± 0.02 nm, which is in good agreement with the Au-Au bond distance determined by EXAFS techniques. In addition to this, icosahedra Au_{13} clusters can be identified through the analysis of the structure of icosahedrons projected in the zone axis direction as well as HREM image simulation.



Scheme 2

The model system described above has the advantages of being both well-defined and easily characterizable by a variety of physical and spectroscopic techniques, while embedding many of the structural and electronic properties relevant to catalytic systems. Nanoscale catalysts, though, are generally used in complex supported forms and are, as a result, harder to characterize at the same level of detail. To address this deficiency we have begun to explore systems of supported nanoparticles of direct interest to energy technologies. Carbon supported bimetallic nanoparticles (Pt/Ru) are prepared via the high temperature reductive condensation of various metal salt precursors ((CH₃)₂Pt(COD), H₂PtCl₆, and RuCl₃) onto carbon black substrates. The initial goals of the project involve the use of presupported monometallic nanoparticles to template the reduction of the counter metal according to Scheme 2. Using a battery of analytical surface techniques, the composition, atomic structure, and size of these particles were mapped to give a size-correlated binary phase diagram. These nanoscale (2-3 nm) bimetallic alloys show atomic structures not ordinarily seen in the bulk binary phase diagram. Particles with high Ru compositions were seen with FCC structures and particles with high Pt compositions were seen with HCP structures, a phenomenon impacted by the nature of the nascent cluster used. When Pt particles were used as seeds for Ru deposition, the resulting particles tended towards FCC structures at all compositions. The use of Ru seed particles provided some examples of metastable HCP

structures although, as before, the FCC habits were a predominate structural form. The existence of metastable phases in the nanoparticles is suggestive of a complicated energy landscape that contains a number of different atomic environments and correlated chemical natures.

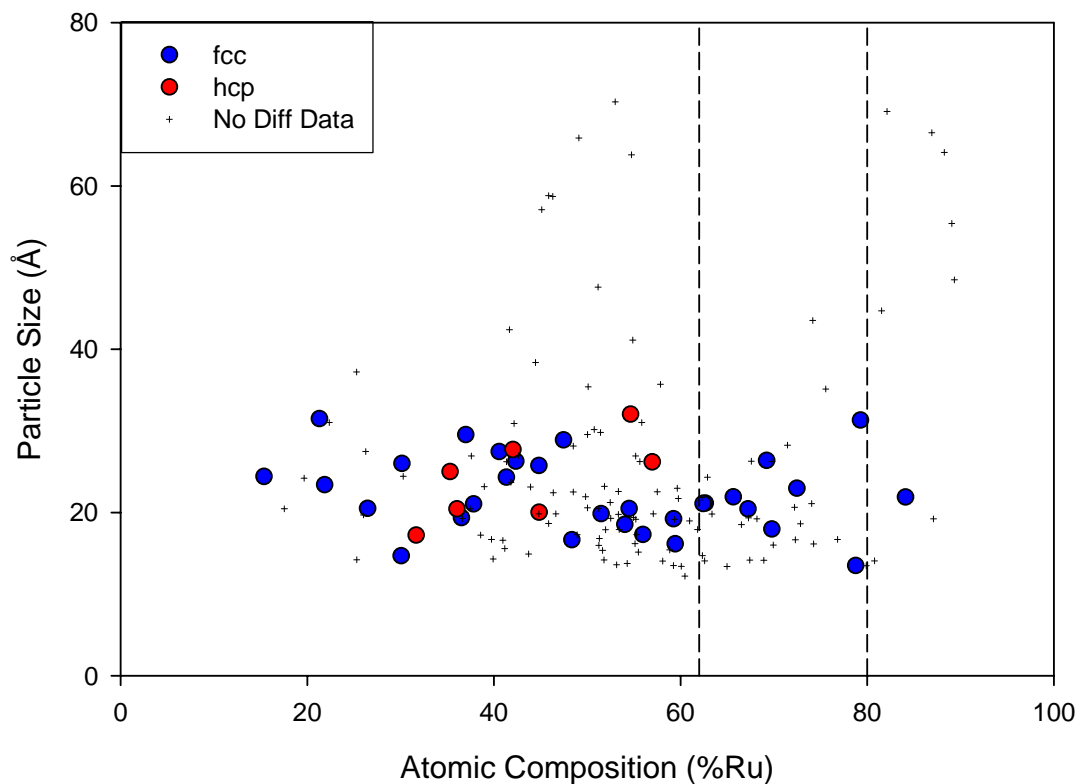


Figure 5. Phase diagram of bimetallic particles formed from the co-reduction of Carbon black + RuCl_3 + H_2PtCl_6 at 673K.

We have carried out direct density-functional-based simulations of Ru-Pt clusters on carbon-based supports. We have identified [3] that the structural properties, including bond lengths and distributions, are dictated by the cluster-substrate interface interactions, even starting with the dimers. In fact, the dimers experience ~25% increase in bond length when in equilibrium on support at zero Kelvin. Figure 4 shows the first-principles calculated bond-lengths relative to bulk Ru-Ru and Pt-Pt bonds for various sized clusters. Note that with and without substrate the dimer bond-length is dramatically affected. Furthermore, magnetism is eliminated as a possible effect that ameliorates the impact on structure.

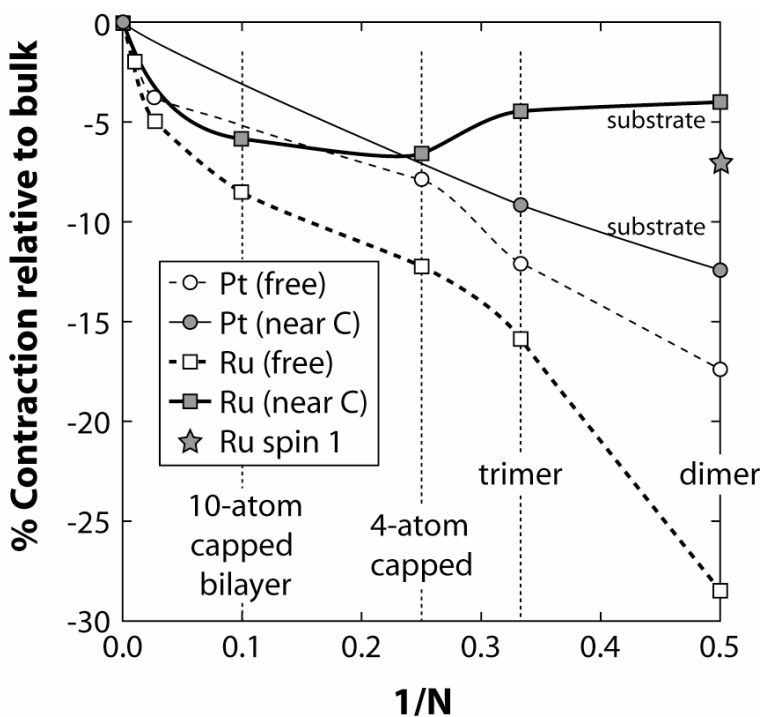


Figure 6. Calculated bond-lengths relative to bulk Ru-Ru and Pt-Pt bonds for various sized clusters with N atoms. The lower-energy spin-polarized Ru-dimer (star) has similar bond-length to non-spin-polarized dimer. Magnetism is not relevant for Ru clusters of ~27 atoms, but does have electronic effects for smaller clusters.

Suggested Reference Publications:

- 1) Hills, C.W.; Mack, N.H.; Nuzzo, R.G. “The Size-Dependent Structural Phase Behaviors of Supported Bimetallic (Pt-Ru) Nanoparticles” *J. Phys. Chem. B.* **2003**, *107*, 2626.
- 2) Frenkel, A.I.; Hills, C.W.; Nuzzo, R.G. “A View From the Inside: Complexity in the Atomic Scale Ordering of Supported Metal Nanoparticles” *J. Phys. Chem. B.* **2001**, *105*, 12689.
- 3) Sanjay Khare, D.D. Johnson, A. Rockett, Todd Martinez, Anatoly Frenkel and Ralph Nuzzo, to be published

This page intentionally left blank.

Columbia University: Controlling Structural Electronic and Energy Flow Dynamics of Catalytic Processes Through Tailored Nanostructures.

Collaborators: Adzic, Bartels, Feibelman, Heinz, Murray, O'Brien, Rahman

Applied Physics and Applied Mathematics, 200 SW Mudd, 500 West 120th St., New York.

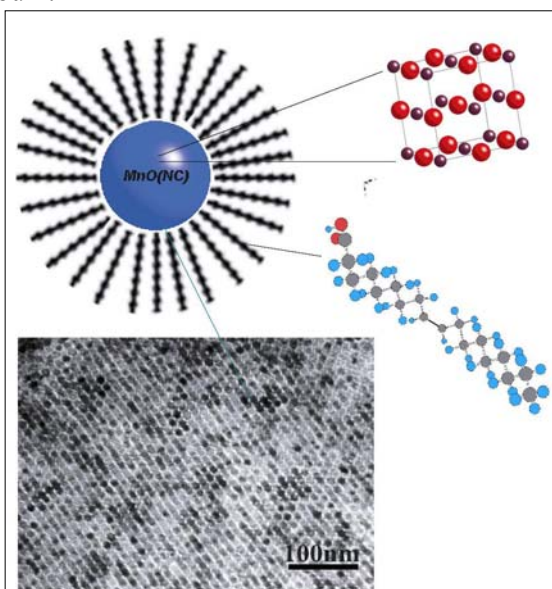
Synthetic Methodologies for Preparing Nanocrystal and Nanocrystal Assemblies with Applications in Catalyzed Oxidation Reactions

1. Transition metal oxide (TMO) nanocrystals

Transition Metal Oxide (TMO) Nanocrystals are nanometer dimension crystals composed of one or more metals from the *d* block of the periodic table and oxygen. The nanocrystals have capping groups which render them discrete, stable, and enable them to be manipulated in a variety of media such as solvents or polymers. The nanocrystals are ideally monodisperse, uniform in composition, crystalline, and can be prepared over a range of sizes from 1-100 nm. The selection of composition for the transition metal oxide (TMO) nanocrystals is based on materials with known catalytic properties in the bulk.

Metal and metal oxide nanocrystals have been prepared by new methods invented in the O'Brien group. Careful attention to purity, the concentrations of the reagents, the rate and order of their addition, and temperature is the minimum requirement for the reproducible formation of nanoparticles in desired composition and size distribution.

We have developed new procedures for the synthesis of new TMO nanocrystals grounded in the use of these techniques. The methods are distinct from sol-gel chemistry and other more traditional methods of producing colloids as discerned by the nature of the product. The capping groups (also called ligands because they bind to the surface of the nanocrystal) are typically long chain alkyl surfactants with heteroatom or polar head groups that react with and bind to the nanocrystal surface via covalent, electrostatic or coordination bonds (or some combination of all three), generally to the metal atoms. The lability of the surface ligand (ease with which it can be exchanged) depends upon the strength of the binding interaction. An extremely important part of the procedure is the ability to control initial conditions of nucleation, with separation from growth. The nanocrystals that result from a successful procedure of this kind can be highly uniform, phase pure, come in high yields with no tendency toward aggregation, and be relatively monodisperse. The absence of water and oxygen



is necessary at the start, and the solvents and ligands have to be dry and pure. In the development of experiments for a particular transition metal oxide, each system will have its own unique set of parameters in need of optimization, and then through a careful survey of several syntheses, we can develop a procedure for obtaining highly uniform particles over a range of sizes.

2. Results

In accordance with our original proposal we are working towards the “ultimate scenario,” in which one can envisage controlling many features through tailoring the nanostructure: control of photophysical properties of the semiconductor by tunability of the band gap by the size of the nanocrystal, control of the nanocrystal architecture by deposition of the materials on substrates.

2.1 Wide band gap semiconductor nanostructures: semiconductor tunability

We report a new synthesis of ZnO nanorods (submitted to J. Am. Chem. Soc.) by thermal decomposition of zinc acetate in organic solvents in the presence of oleic acid, which produces relatively monodisperse ZnO nanorods (ZnO quantum rods) with diameters of 2 nm and lengths in the range 40-50 nm (Figure 1). The diameter is an order of magnitude smaller than previously reported ZnO nanorods prepared by a variety of other methods and near UV absorption and PL measurements were able to determine that quantum confinement effects are present in these rods, with an excitonic ground state of 3.55 eV. We have also prepared nanocrystals of BaTiO₃ and TiO₂. The nanocrystals are prepared via a two step method involving the preparation of a precursor that yield monodisperse 10 nm nanoparticles that can be annealed to make highly crystalline samples on substrates.

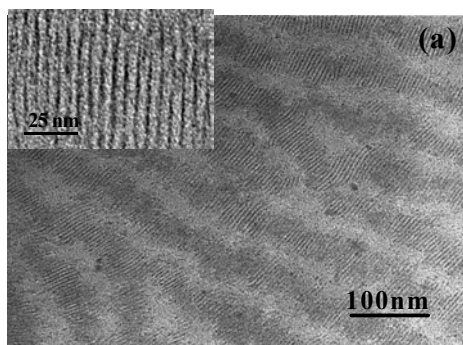


Figure 1. Transmission Electron Microscope Images of Zinc Oxide Nanorods.

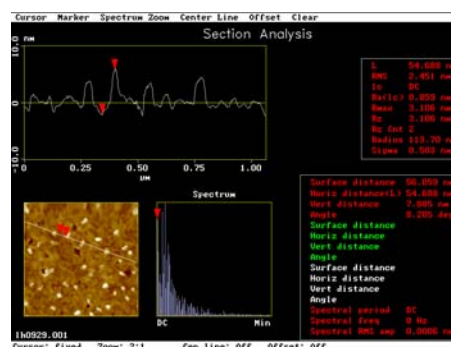


Figure 2. AFM Characterization Nanocrystals of the titanates on n-type silicon.

2.2. Copper oxide nanocrystals in CO oxidation: influence of size dependence at the nanoscale

Carbon monoxide oxidation activities over the Cu-Cu₂O-CuO system have revealed that copper may be a useful potential substitute metal in CO oxidation reactions (includes among others the work of G. A. Somorjai) And there is some discussion in the literature as to the role of the surface lattice oxygen of species non-stoichiometric copper oxides during the course of the reaction. Preparation of nanocrystals using our methods, has demonstrated the ability to control the oxidation state of the metal oxide and/or we have observed the stabilization at the nanoscale of non-stoichiometric oxides which are not normally stable under ambient conditions. We have recently prepared highly uniform nanocrystals of Cu₂O. We believe (although this is to be confirmed) the mechanism for the reaction proceeds via Cu nanocrystals which are subsequently oxidized and therefore we are presented with the opportunity of obtaining copper and copper oxide nanocrystals in different oxidation states. In collaboration with the Heinz and Bartels groups, we plan to try to observe the movement of CO molecules on these nanocrystal surfaces.

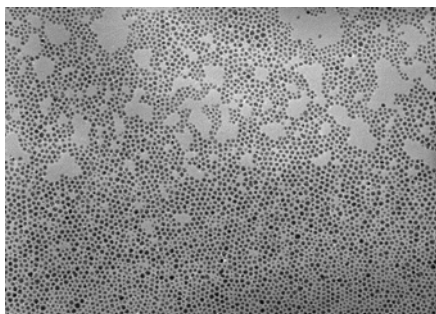


Figure 3. TEM of Cu₂O 5 nm nanocrystals

2.3. Nanocrystal Assemblies of CoPt₃-Iron oxides: Control of the nanocrystal architecture (Collaboration with Murray at IBM Watson)

We have been working to prepare multicomponent binary superlattices of nanocrystals, one of which would be small nanocrystals of metals. We have observed the affinity of small articles to attach themselves to larger ones (Figure 4), thus providing a possible route for making isolated units of catalyst cluster-on-semiconductor-nanocrystal.

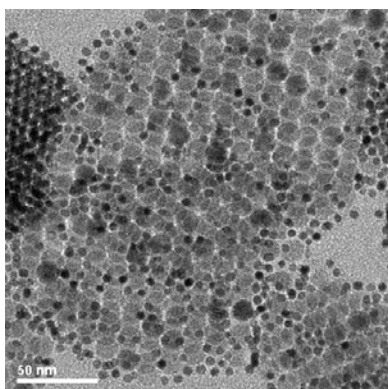


Figure 4. Fe₂O₃-CoPt₃ nanocrystal assemblies. The CoPt₃ are the small darker particles.

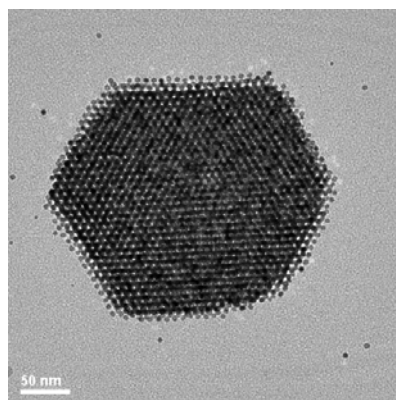


Figure 5. A self-assembled superlattice of CoPt₃ Nanocrystals

References/Publications

1. "Synthesis of Monodisperse Nanocrystals of Manganese Oxides", Yin, M. and O'Brien* S., *J. Am Chem. Soc.*, 2003, 10180 – 10181.
2. "Zinc Oxide Quantum rods" *submitted to JACS*, Ming Yin, Yi Gu, Igor L. Kuskovsky, Tamar Andelman, Yimei Zhu,† G. F. Neumark, and Stephen O'Brien.*
3. "Structural and Magnetic Characterization of Non-stoichiometric Iron Oxides", Redl, F. X., Yin, M., Black, C.T., Murray, C.B.M., O'Brien, S.*, 2004, In preparation.
4. "CO Oxidation behavior of copper and copper oxides," *Catal. Lett.*, Huang, T.-J., D.-H. Tsai, 2003, 87, 173-178.
5. "Carbon Monoxide Oxidation over Three Different Oxidation States of Copper", *J. Catal.*, Jernigan G. G., Somorjai, G. A., 1994, 147, 567-577.
6. "SEM and RHEED-REM Study of Au Particles Deposited on Rutile TiO₂" Akita, T., Okumura, M., Tanaka, K., Haruta, M., *J. Catal.*, 2002, 212, 119-123.

Studies of Active Oxygen Species for Hydrocarbon Conversion

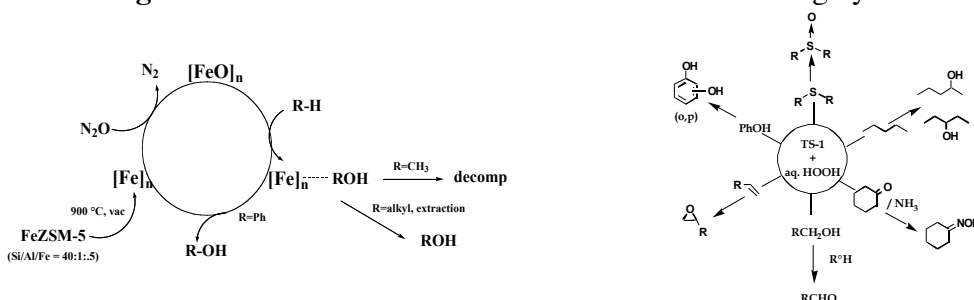
Current postdoctoral researcher: Monika Hartl

Collaborators: Michael Janicke, Juergen Eckert, Thomas Proffen, Neil Henson (all LANL); Prof. Alex Bell, Ben Wood (UC Berkeley); Prof. Tanja Pietrass and Mirka Mecerova (New Mexico Tech).

Chemistry Division, Los Alamos National Laboratory, MS J514, Los Alamos NM 87545; kcott@lanl.gov

Research Goal: Develop an understanding of the local structure at the Fe and Ti sites of the zeolite-based selective oxidation catalysts TS-1 and Panov's catalyst derived from FeS-1, and the closely related, if not identical Fe zeolite catalyst responsible for highly efficient reduction of nitrogen oxides.

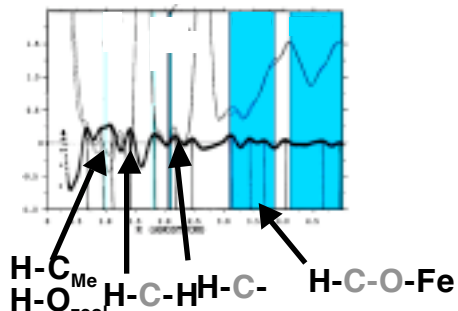
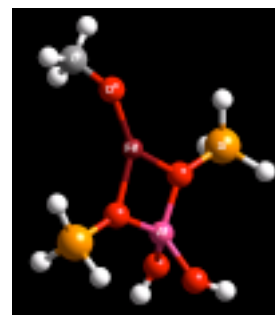
Recent Progress: Ti or Fe sites in or on zeolite frameworks are highly active and selective catalysts



for selective oxidation of hydrocarbon substrates. In both catalysts, the concentration of metal cation is very low, and has made direct spectroscopic and structural studies to report on the local structure of the metal cation sites difficult.

Our previously published work was the first direct determination that Ti and Fe substitute into specific sites within the zeolite framework. Our recent work has been focused on 1). Defining the nuclearity at the iron site (monomer vs. dimer), 2). Determine the interactions of bound intermediates with the iron site (e.g. $MeO-Fe$), and 3). Correlate this structural information with other catalytic and spectroscopic information to report on details of the highly reactive iron oxo responsible for the insertion into C-H bonds. We have used isotope difference pair distribution function analysis of neutron scattering data to obtain a preliminary description of the putative iron oxo site that has undergone insertion into a C-H bond of methane.

We have prepared several sets of the iron catalyst in which the putative iron oxo has been reacted with either CD_4 or CD_3H at low temperatures to form the zeolite-bound methoxy intermediates. Using total neutron scattering techniques coupled with isotope differences, we have extracted the hydrogen pair distribution function that indicates distances that may be assigned to the C-H, H-C-H, and H-C-O (and possibly H-O-zeol) distances in the bound methoxy intermediate. There are also peaks in the PDF in the region where the H-C-O-Fe distances are expected. Analysis of EXAFS data at the iron edge obtained on these same samples indicates it is unlikely that there is a Fe-O-Fe linkage. We have recently obtained total neutron scattering data on an analogous set of ^{57}Fe labeled samples for



comparison with natural abundance Fe samples in an attempt to obtain more specific information in the vicinity of the iron site. This data is currently being analyzed.

DOE Interest: Selective oxidation catalysts are crucial to the production and utilization of fuels. Our study of the local structure of model oxidation catalysts will lead to a better understanding of the electronic and structural requirements to generate high activity catalysts.

Future Plans: Our research will continue to focus on developing the best representation possible of the active site structure of Panov's catalyst and the Ti sites in TS-1.

In the near term, we have a substantial amount of neutron and EXAFS data to interpret from recent neutron scattering and synchrotron X-ray experiments on additional samples of Panov's catalyst, and its precursors. From the ^{57}Fe data sets, we hope to obtain more definitive information regarding the near-neighborhood of the Fe site. We have also just collected EXAFS data on a set of iron zeolite samples where a higher concentration of iron is introduced by sublimation of FeCl_3 . These samples will provide calibration data sets with which to compare our results against published reports that report the iron site is dimeric. Prof. Bell's group has also studied some of our samples that contain Al in the framework, and correlating FT-IR data with different Fe/Al concentrations, they suggest that iron interacts with anionic framework aluminum sites. This would be consistent with the absence of dimeric iron sites in these catalysts that are very dilute in iron.

Electronic structure calculations using small cluster models of the iron site will be performed to guide the interpretation of the PDF data, with the goal of providing a self-consistent model of the reactive iron-oxo site that leads to C-H insertion to form the bound iron methoxy.

In the process of obtaining this data, we will also determine the iron siting that results from different synthetic pathways. We have data which suggests that the iron siting varies with synthetic conditions (high pH, OH^- - vs. near-neutral, F^- - mediated syntheses); this may point to differences in ion pairing arrangements in the zeolite gel state between anionic metasilicate precursors and the cationic structure directing agent. Analogously, with our previous results that describe the Ti siting in TS-1, we will re-examine the siting of Ti as a function of synthetic route. The results of these studies, depending on the outcome, may have implications on the siting of Al and other cations in zeolite frameworks that form the basis of important catalytic processes.

Publications (2002-3):

"Nitrous Oxide Decomposition and Surface Oxygen Formation on Fe-ZSM-5", B. R. Wood, J. A. Reimer, A. T. Bell, M. Janicke, and K. C. Ott, *J. Catalysis* (submitted 9/2003).

"Studies of Methoxy Species Formed on Fe/Al MFI by Direct Oxidation of Methane by Nitrous Oxide", B. R. Wood, J. A. Reimer, M. T. Janicke, and K. C. Ott, *J. Catalysis* (submitted 11/2003).

"NMR Investigations of ^{15}NO and $^{15}\text{NH}_3$ of Gallium-Substituted Zeolites", M. Mearova, N. A. Miller, N. C. Clark, T. Pietrass, and K. C. Ott, *Appl. Cat. B*, (submitted 3/2004).

"Synthesis of dealuminated zeolites NaY and MOR and characterization by diverse methodologies: Al-27 and Si-29 MAS NMR, XRD, and temperature dependent Xe-129 NMR", J. M. Kneller, T. Pietrass, K. C. Ott, and A. Labouriau, *Microporous and Mesoporous Materials* **62**, 121-131, (2003).

"Nanoclusters in nanocages: Platinum clusters and platinum complexes in zeolite LTL probed by Xe-129 NMR spectroscopy", Enderle, BA; Labouriau, A; Ott, KC; Gates, BC, *Nano Letters* **2**, 1269 (2002).

"Hydrothermal Synthesis of Molecular Sieve Fibers: Using Microemulsions to Control Crystal Morphology", M. Z. Yates, K. C. Ott, E. Birnbaum, and T. M. McCleskey, *Angewandte Chemie Intl Ed. Engl.* **41**, 476 (2002).

"Osmium Carbonyls in Zeolite NaX: Size Differentiation by 129 Xe NMR Spectroscopy" B. Enderle, A. Labouriau, K. C. Ott, B. C. Gates, *J. Phys. Chem. B* **106**, 2109 (2002).

Nanocatalysts: Synthesis, Properties, and Mechanisms

Co-PI: Sheng Dai

Collaborators: D. R. Mullins, V. Schwartz, E.W. Hagaman, Jun Xu, S. J. Pennycook, S. Spooner, M. A. Amiridis, Sokrates Pantelides, Craig Barnes

Postdocs: Bei Chen, Wenfu Yan, Haoguo Zhu, Shannon Mahurin, Michelle Kidder, Andrew Lupini, Alberto Franceschetti.

Graduate Students: Lorna Ortiz-Soto

Chemical Sciences Division , Oak Ridge National Laboratory, Oak Ridge, TN 37831-6201
overburysh@ornl.gov

Goal

Explore and exploit novel synthetic techniques to prepare nanostructured catalysts with high selectivity and activity.

Recent Progress

Synthesis of nanostructured supports and catalysts: We have explored several methodologies to synthesize Au, Pt, and Pd nanoparticles and oxide nanoparticles inside oxide hosts. Stabilization of Au particles in silica supports has been a key challenge. A method was used in which Au precursor is co-assembled along with a template-surfactant and a functional ligand introduced on a siloxy precursor. By this co-assembly method, mesoporous silica networks similar to MCM-41, HMS, and MSU have been prepared with ethylenediamine or diethylenetriamine ligands attached to the pore walls of the mesoporous silica which in turn stabilize highly dispersed Au precursor. Carefully chosen methods of post-treatment to remove the surfactant and reduce the Au are critical to prevent loss of Au or excessive growth of Au particles. In addition to silica supports, a combination of hydrothermal and ultrasonic techniques have been used to prepare titania supports in five different forms (mesoporous, anatase, brookite, rutile) for preparation of Au catalysts by deposition-precipitation (D-P). Mixed mesoporous titania-silica supports with variable ratios of TiO_2 - SiO_2 have been prepared using a templated co-synthesis technique which inhibits rapid selective hydrolysis and precipitation of TiO_2 . These supports contain highly dispersed titanium cations some in tetrahedral sites, which are resistant to crystallization and provide a novel support for Au. A particularly interesting methodology permits layer-by-layer growth of an oxide onto silica supports using two-step non-aqueous chemisorption followed by hydrolysis. This method has been used to prepare single layers of titania, alumina or germania on silica supports, which couple with D-P of Au leads in some cases to extremely active Au catalysts. Co-synthesis techniques have been used to prepare mixed urania-titania and urania-silica nanoparticles inside mesoporous SiO_2 which even without Au or other precious metal are active for oxidation reactions. In addition to oxide supports, Au catalysts have also been prepared in microporous Al phosphate zeolite.

Support and particles size effects in Au catalysts: Five different forms of titania (mesoporous titania and nanocrystalline anatase, brookite, rutile forms and commercial P-25) were used as supports for identically prepared Au catalysts (by deposition-precipitation) to study the effect of crystallite atomic structure upon catalytic activity for CO oxidation. It is found that activities of the as-prepared catalysts are comparable, but brookite exhibits a greater stability towards sintering effects. Using the co-assembly with functional ligand methodology, silica supported Au catalysts were prepared with very small mean size Au particles. Comparison of these catalysts with titania supported catalyst demonstrated much higher activity for the titania supported catalysts indicating that optimal Au particle size is not the only important factor leading to high activity. Au catalysts supported in a microporous aluminum phosphate was found also to be

active for CO oxidation in spite of the fact that no reducible oxide is available for oxygen transfer to Au surfaces. On this catalyst CO oxidation in air deactivates rapidly, but high CO conversion is stabilized if hydrogen is added to the reactant mixture. By this addition, stable and essentially complete conversion of CO is achieved at 298 K while hydrogen conversion is very small.

Characterization of Au catalysts: Au catalysts prepared by the methods described above were characterized by a variety of means. A major emphasis was placed on the determination of particles size and so a XANES/EXAFS was used as well as small angle scattering of both x-rays (SAXS) and neutrons (SANS). XANES proved to be useful for its ability to distinguish the oxidation state of Au and studies of the reduction of the as-synthesized Au precursor catalysts were carried out on a variety of supports. In the active state, the Au on titania support is fully reduced to Au⁰. The activity in this state is comparable to that of the most active titania supported Au catalysts reported in the literature. EXAFS was used to obtain mean coordination numbers, and therefore mean particle size. Comparison with activity data indicates that activity is not clearly linked to particle size, at least over the 0.5 to 5 nm particle range accessible by EXAFS. SANS was also explored as a means of extracting particle size for a Au catalyst supported in mesoporous silica. Using contrast matching, it was possible to remove scattering from silica mesopores thereby permitting analysis of Au particles sizes. Contrast matching in mesoporous titania was less successful. The ORNL aberration corrected microscope has been used to examine several catalysts of interest. For the first time, images with atomically resolved Au atoms have been obtained. The most active state of Au / anatase titania catalysts is associated with thin Au rafts while aggregation of Au rafts into 3-d nanocrystals generally results in a decrease in activity. ¹³C NMR characterization of functionalized MCM-41s at various stages of their synthesis and surfactant removal has illuminated specific reaction paths that occur in the pores of these silicas in the course of forming gold nanoparticles. Polydentate amine functionality tethered in the MCM-41 pores is effective at retaining gold nanoparticles in the silica mesopores. Extensive Hoffmann elimination of retained surfactant is observed during the elevated temperature reduction of chloroauric acid to gold.

Theoretical studies of Au catalysts: Computational studies using density functional techniques have been carried out on free Au clusters and on Au cluster supported on anatase TiO₂. It is found that an oxygen vacancy on the titania stabilizes the adsorption of a Au atom, anchoring small Au rafts. Oxygen adsorption does not occur on single, stable Au adsorbate atoms, but anchored clusters of Au atoms (Au₇ or Au₁₀) do stabilize adsorption of both CO and O₂. Computed adsorption energetics now explain why activity is possible on small clusters but not on large bulk-like crystallites.

DOE interest

New catalysts are needed to achieve incremental or revolutionary improvements in technologies related to emission control, fuel cells and hydrogen utilization. This work provides a research basis for preparing, testing and understanding catalysts with potential application in these technologies.

Future Plans

Layer-by-layer growth of catalysts for control of activity: This synthesis methodology will be investigated extensively and will constitute a major portion of our effort. Layer-by-layer deposition onto nanostructured silica will be applied and the effect of several design factors will be exploited to prepare new Au catalysts. By this methodology and systematic variation, it should be possible to learn how to 1) control morphology using available silica support morphologies, 2) control support chemical activity by depositing different active overlayers such as TiO_x, AlO_x, ZrO_x, VO_x and GeO_x, 3) control placement of metal particles by exploiting capping and functionalization of external vs pore wall surfaces, 4) control pore sizes by sequential layer deposition onto pore walls and 5) control metal particle sizes by confined growth into pores of variable sizes. Layered structures of this type may be expected to exhibit variations in electronic properties (e.g. bandgap, localized electrons, valency) which could modulate catalytic or

photocatalytic behavior. Besides use as a support for Au catalysts, work will shift to include these oxides which themselves may be active catalysts.

Mechanistic studies and characterization of surface chemistry and catalytic performance:

A pulsed reactor with in situ FTIR will be completed and used to study mechanistic aspects of the CO oxidation reaction. It should be possible to simultaneously monitor the chemical nature of surface adsorbates and their time response to changes in the reactant concentration. Work will expand beyond CO oxidation to incorporate extensive studies of selective CO oxidation in the presence of H₂. This process is of high technological importance for fuel cells and the hydrogen economy. This selectivity will be examined on Au catalysts prepared by deposition on a wide variety of supports. Activity and mechanisms for water gas shift and propylene epoxidation reactions will also be examined. In addition to traditional techniques and those mentioned above, positron porosimetry will be developed and applied to the porous catalysts. High resolution Z-STEM will continue to be an important method to provide direct atomic detail of the structure of features on supported catalysts. Emphasis will be placed on using *in situ* and *operando* conditions.

Publications

Lee, B., H. Zhu, S. H. Overbury and S. Dai, *Preparation of Mesoporous Silica with Gold Nanoparticles by Co-synthesis Method*, Mesoporous Materials, in press (2004),

Overbury, S. H., L. Ortiz-Soto, H. Zhu, B. Lee, M. D. Amiridis and S. Dai, *Comparison of Au catalysts supported on mesoporous titania and silica: Investigation of Au particle size effects and metal-support interactions*, Catalysis Letters, in press (2004),

Yan, W., B. Chen, S. Mahurin, E. W. Hagaman, S. Dai and S. H. Overbury, *Surface Sol-Gel Modification of Mesoporous Silicas with TiO₂ for the Assembly of Ultrasmall Au particles*, J. Phys. Chem. , in press (2004),

Franceschetti, A., S. J. Pennycook and S. T. Pantelides, *Oxygen chemisorption on Au nanoparticles*, Chemical Physics Letters, 374 (5-6), (2003), 471-475.

Zhu, H. G., B. Lee, S. Dai and S. H. Overbury, *Coassembly synthesis of ordered mesoporous silica materials containing Au nanoparticles*, Langmuir, 19 (9), (2003), 3974-3980.

Zhang, Z. T., M. Konduru, S. Dai and S. H. Overbury, *Uniform formation of uranium oxide nanocrystals inside ordered mesoporous hosts and their potential applications as oxidative catalysts*, Chemical Communications, (20), (2002), 2406-2407.

This page intentionally left blank.

Surface Processes in Metal Phosphide Hydrotreating Catalysts

Postdocs: Shu, Y., Chun, W.-J.

Students: Lee, Y.-K., Wang, X., Clark, P., Gott, T.

Collaborators: Requejo, F., Yoshimura, Y., Bando, K., Asakura, K., Song, C.

Department of Chemical Engineering, Virginia Tech, Blacksburg, VA 24061
oyama@vt.edu

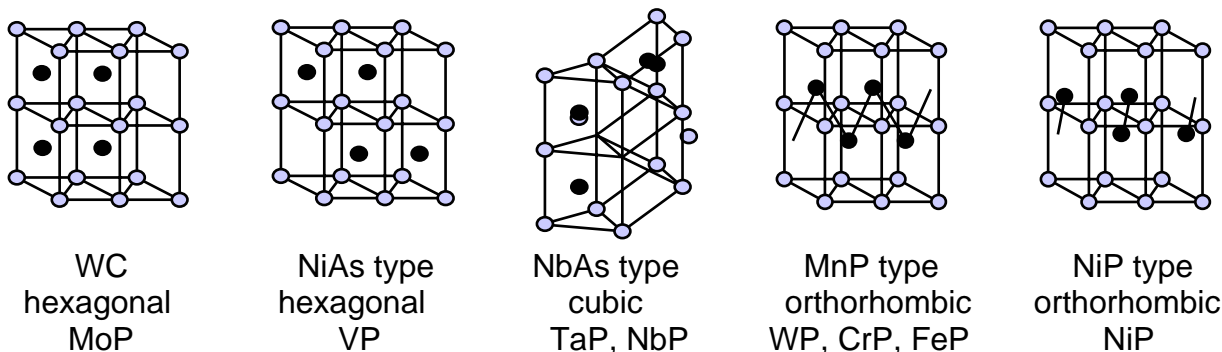
Goal

Study the reactivity of new phosphide catalysts for hydrotreating, and examine the mechanism of hydrodesulfurization (HDS) and hydrodenitrogenation (HDN).

Recent Progress

The high activity of phosphide catalysts continues to attract attention throughout the world, with many groups starting to investigate the activity of this interesting class of new materials. We have identified Ni_2P as the most active of the phosphides and are carrying out extensive studies of its properties.

Preparation of Metal Phosphides: The metal-rich transition metal phosphides are a broad class of compounds which combine metallic properties such as conductivity with refractory properties such as hardness. They adopt many types of structure, but in general are not layered so are completely different from standard sulfide catalysts. They offer the possibility of more accessible sites than sulfides, where the basal planes are largely inactive. The phosphides can be prepared readily by the temperature-programmed reduction in H_2 of phosphate precursors

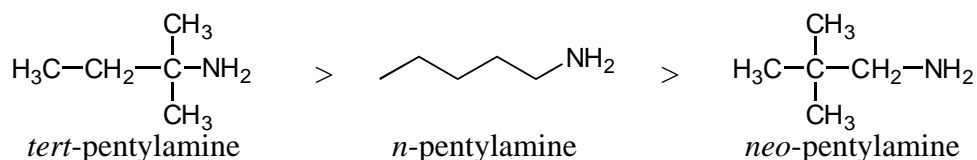


Ni_2P Supported on K-USY: Ultra stable Y-zeolites have a dual pore structure consisting of standard faujasite cages and a mesoporous system created by the steaming process in the synthesis of the materials. We have found that the USY zeolites with their acidity neutralized by K are effective supports for Ni_2P , giving highly active catalysts. At 30 atm and 613 K the conversion of 4,6-dimethyldibenzothiophene (DMDBT) was 98% compared with 85% for a conventional Ni-Mo-

S/Al₂O₃. The comparison was on the basis of equal number of sites as measured by CO uptake at room temperature for the phosphide and O₂ uptake at dry-ice/acetone temperature for the sulfide.

Studies with Real Feeds: Results with model compounds often do not correlate with those obtained with real feeds because the interactions between the components are complex, so most catalyst development is carried out with actual feeds. In order to evaluate the potential of the new catalyst it was subjected to a test with a hydrotreated gas oil of low sulfur (440 ppm) and nitrogen (8 ppm) contents and moderate aromatics content (27 wt%), which mimics that which would be used in a second-stage hydrotreating process. The measurements were made at realistic conditions (593 K and 3.9 MPa) using a stainless steel reactor of 9.5 mm O.D. (3/8 inch). Comparison was made with a current commercial Co-Mo-S/Al₂O₃ catalyst (Ketjenfine 756) of surface area 218 m²g⁻¹ and containing 11.2 wt.% Mo and 3.1 wt.% Co. For the Ni₂P/SiO₂ the HDS conversion was 85 % (± 2 %) with sulfur content reduced from 440 to 66 ppm. This compares favorably with the results obtained with the commercial Co-Mo-S/Al₂O₃ catalyst, which gives a conversion of 80 % and sulfur content of 86 ppm.

Mechanism of HDN of Pentylamines: The operative mechanism of N-elimination on the phosphide catalysts was investigated on a series of pentylamines of different structure. The following order of reactivity was found



There was no correlation of this order of reactivity with steric hindrance, suggesting that an S_N2 pathway was not involved. Similarly, there was no correlation with the stability of carbocation or carbanion species, suggesting that prior scission of the amine group as in an S_N1 or E1 mechanism was not occurring. However, there was a direct relationship between the order of reactivity and the number of β-hydrogens, and this suggested C-N bond scission by an E2 mechanism on the catalysts.

Calculated adsorbate structure: The mode of binding of alkylamines on Ni₂P surfaces was studied using ethylamine as a probe molecule. Ethylamine is the simplest alkylamine capable of undergoing a β-elimination. Its mode of adsorption was studied by Fourier transform infrared (FTIR) spectroscopy and theoretical molecular orbital calculations. Calculation of the structure of adsorbed ethylamine was performed using the Gaussian 98 program using the HF / 6-31g* basis set. The calculated vibrational frequencies were in excellent agreement with the experimental values.

In Situ EXAFS Studies: We have carried out measurements of the structure of the catalyst in its working state. Our work is unique in that the studies are carried out at high pressure and temperature in the liquid phase. We have verified that the Ni₂P catalyst is stable at reaction conditions.

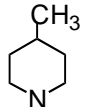
DOE Interest

Commercial hydrotreating catalysts are molybdenum or tungsten sulfides promoted by cobalt or nickel, and supported on alumina. The phosphide catalysts are a completely different class of material and represent a novel direction in hydroprocessing catalysis research.

Future Plans

Mechanism of HDS: A fundamental question in the deep HDS of substituted dibenzothiophenes is the manner in which the reaction proceeds. Two main pathways dominate: a) a direct desulfurization route (DDS) and b) a hydrogenation route (HYD). The mechanism operating on the phosphides will be probed using initial selectivity measurements in a batch reactor.

Mechanism of HDN of Piperidines: The NH₃ elimination step is usually the last step in a sequence of denitrogenation and is relatively facile. A more difficult step is the internal C-N bond hydrogenolysis (CNH) that occurs in heterocycles. A good probe of this reaction is piperidine (C₅H₁₁N) and its derivatives

Molecule						
Number of α-H's	4	4	3	4	2	4
Number of β-H's	4	4	7	3	10	2

The various compounds contain different numbers of α and β hydrogens, so are good substrates for identifying the reaction pathways.

Publications (2003-4)

1. S. T. Oyama, Y.-K. Lee, Transition Metal Phosphides: New Catalysts for Hydroprocessing, *ACS Fuel Chem. Div. Prep.* **2003**, 48, 173-174.
2. J. H. Kim, X. Ma, C. Song, S. T. Oyama, Y.-K. Lee, Kinetic Study of 4,6-Dimethyldibenzothiophene Hydrodesulfurization over Ni Phosphide, NiMo and CoMo Sulfide Catalysts, *ACS Fuel Chem. Div. Prep.* **2003**, 48, 40-41.
3. S. T. Oyama, X. Wang, R. Radhakrishnan, Adsorption of Ethylamine on Silica-Supported Nickel Phosphide, *Stud. Surf. Sci. Catal.* **2003**, 145, 347-350.
4. P. A. Clark, S. T. Oyama, Alumina-Supported Molybdenum Phosphide Hydroprocessing Catalysts, *J. Catal.* **2003**, 218, 78-87.
5. S. T. Oyama, Novel Catalysts for Advanced Hydroprocessing: Transition Metal Phosphides, *J. Catal.* **2003**, 216, 343-352.
6. T. Kawai, S. Sato, W.-J. Chun, K. Asakura, K. K. Bando, T. Matsui, Y. Yoshimura, T. Kubota, Y. Okamoto, Y.-K. Lee, S. T. Oyama, In Situ X-Ray Absorption Fine Structure Studies on the Structure of Ni₂P Supported on SiO₂, *Chem. Lett.* **2003**, 32, 956-957.
7. S. T. Oyama, X. Wang, Y.-K. Lee, W.-J. Chun, Active Phase of Ni₂P/SiO₂ in Hydroprocessing Reactions, *J. Catal.* **2004**, 221, 263-273.
8. S. T. Oyama, X. Wang, Mechanism of Hydrodenitrogenation in Phosphides and Sulfides, *J. Phys. Chem.* **2004**, Submitted.
9. J. H. Kim, X. Ma, C. Song, Y.-K. Lee, S. T. Oyama, Hydrodesulfurization of 4,6-Dimethyldibenzothiophene over NiMo, CoMo Sulfide and Ni Phosphide Catalysts: A Kinetic Study on Individual Reaction Pathways, *J. Catal.* **2004**, Submitted.

This page intentionally left blank.

Hydrogen Containing Functional Groups and the Structure of Coal

Postdoc: Opaprakasit, P.
Students: Berg, L.

Materials Science and Engineering, Penn State University, University Park, Pa 16802.
painter@matse.psu.edu

Goal

Obtain a fundamental understanding of the structure of coal.

Recent Progress

Recent work has focused on the nature of secondary interactions (e.g., hydrogen bonding, ionic interactions) in coal and the detection of thermal transitions. It has been shown that the amount of pyridine soluble material obtained from many coals is significantly enhanced by washing with weak acids (papers 2 and 3, listed below). This has important implications for the nature of interactions and the structure of these materials. For low rank coals, we have proposed that carboxylate ions and their metallic counter-ions phase separate from the organic component of coal to form micro-domains or clusters, in a similar fashion to synthetic ionomers such as Surlyn. This is important, because randomly dispersed $-\text{COO}^- \text{M}^+$ groups would not affect the swelling and solubility characteristics of a coal, as they do not provide the connectivity necessary to act as some sort of cross-link. In higher rank coals, our results indicated that π -cation interactions are important. These types of interactions have not previously been considered as a significant component of coal structure. As a result of this work, we have proposed that cross-linking in coal should be thought of in a different way and classified into two types; first, "permanent" covalent linkages that cleave only at elevated temperatures or through chemical reaction; second, "reversible" cross-links, largely associated with ionic structures such as carboxylate salts and π -cation complexes.

There is an important school of thought that regards coal as largely an associated structure, rather than a covalent network. However, most of the research supporting this view is based on results obtained from just one or two coals, whose behavior may be anomalous. The most widely studied of these is the APCS Upper Freeport coal, which has a significantly enhanced solubility in the mixed solvent system *N*-methyl-2-pyrrolidinone/carbon disulfide (NMP/CS₂), relative to the individual solvents and "good" solvents like pyridine. The solutions and solvent swollen residues obtained from this coal also display a rich range of complex behavior, forming gels and exhibiting viscoelasticity. The nature of the interactions in this mixed solvent system and the mechanism by which small amounts of certain additional additives further enhance coal solubility remains largely unknown. We recently examined interactions in the NMP/CS₂

mixed solvent system (paper 9, listed below). We demonstrated that this solvent system is capable of forming specific complexes with alkaline earth cations and this leads to color changes and absorptions in the UV/visible spectrum as a result of perturbations to the π -bonds of these molecules. Furthermore, solid complexes that precipitate out of solution are formed at certain solvent/cation molar ratios. We also demonstrated in a separate study that the (1:1) NMP/CS₂ mixed solvent system extracts cations from clays, again forming complexes that turn the supernatant solvent in contact with the clays black (paper 10, listed below). The individual solvents show no color change. It seems likely that the ability of this mixed solvent system to mobilize and complex with cations plays a crucial role in its ability to solubilize certain coals to a greater extent than other solvents.

Finally, it has been claimed that a transition observed near 110°C in Differential Scanning Calorimetric studies of certain coals is a glass transition temperature. This is significant, because many properties and processes (e.g., diffusion) change dramatically if a material is in the rubbery as opposed to the glassy state. However, we are suspicious of any thermal event observed near this temperature in materials that have adsorbed water and therefore decided to use a different technique to study this reported transition. Thermo-mechanical measurements are particularly sensitive to the T_g, as the modulus of a material will change by several orders of magnitude as a material is heated through this transition. The results we obtained by applying this technique demonstrated that there is no T_g near 110°C, but there is a presently undefined small structural rearrangement at 180°C (paper 4, listed below). Coal extraction yields in solvents at temperatures near 200°C (or more) are often enhanced and this transition may be important in these processes.

DOE Interest

A fundamental knowledge of the nature of the interactions in coal and coal/solvent systems is central to an understanding of physical structure, properties and the extent to which soluble material can be obtained from coal by the action of simple solvents.

Future Plans

We believe that our experiments demonstrating that the 1:1 NMP/CS₂ mixed solvent system is capable of forming complexes with certain cations is important and holds the key to not only understanding how the solubility of certain coals is enhanced in this mixture relative to other solvents, but also the nature of strong interactions in coal itself. The nature of the cations present in Upper Freeport (and presumably other coals), which could be organic, inorganic, or perhaps both, remains unknown and needs further investigation.

The nature of certain thermal transitions in coal will also be studied. In recent work a presently undefined transition or structural rearrangement near 180°C has been observed. Solvent extraction yields are considerably enhanced if performed just above this temperature and establishing the nature and significance of this transition is important.

Publications (2001-4)

1. *Intramolecular Hydrogen Bonding and Calixarene-Like Structures in p-Cresol Formaldehyde Resins*. Opaprakasit, P., Scaroni, A. and Painter, P.C. *J. Molecular Structure*, 570, 25 – 35 (2001).
2. *Ionomer-like Structures and their role in the pyridine-extractability of Argonne Premium Coals*. Opaprakasit, P.; Painter, P. C.; Coleman, M. M.; Scaroni, A.; Div. Of Fuel Chem. Preprints, American Chemical Society, 46(1), 331 – 333 (2001).
3. *Ionomer-Like Structures and π -Cation Interactions in Argonne Premium Coals*. Opaprakasit, P., Painter, P.C. and Scaroni, A. *Energy and Fuels*, 16, 543 – 551 (2002).
4. *Concerning the Glass Transition Temperature of Coal*. P. Opaprakasit, P. C. Painter, *Energy and Fuels*, 17, 354 – 358, (2003).
5. *Intramolecular Screening Effects in Non-dilute Polymer Solutions – an Equation of State Approach*. Berg, L.; Painter, P. C. *J. Polymer Science, Polymer Phys Ed.*, 41, 2911-2922 (2003)
6. *Concerning the Composition Dependence of the SANS χ Parameter in Isotope Blends*. Berg, L.; Painter, P. C. *J. Polymer Science, Polymer Phys.*, 41, 2923-2927 (2003).
7. *The Application of Generalized Two-Dimensional Infrared Correlation Spectroscopy to the Study of Hydrogen Bonded PVPh/PMMA Blends*. Huang, H.; Malkov, H.; Coleman, M. M.; Painter, P. C.; *Applied Spectroscopy* (submitted for publication).
8. *Concerning the Nature of Coal Solutions and Suspensions*. Painter, P.C.; Sobkowiak, M; Mathews, J.; Scaroni, M. *Energy and Fuels* (submitted for publication).
9. *Complex Formation in NMP/CS₂ Mixed Solvents*. Opaprakasit, P.; Painter, P.C. *Energy and Fuels* (submitted for publication).
10. *The Swelling of Clays in NMP/CS₂ Mixed Solvents*. Opaprakasit, P.; Painter, P.C. *Energy and Fuels* (submitted for publication).

This page intentionally left blank.

Fundamental Studies of Metal Centered Transformations Relevant to Catalysis

Graduate Students: David Churchill, Guang Zhu, Cary Zachmanoglou

Postdoctoral Associates: Jun Ho Shin, Kevin Janak and Joseph Tanski

Department of Chemistry, Columbia University, New York, NY 10027; parkin@chem.columbia.edu.

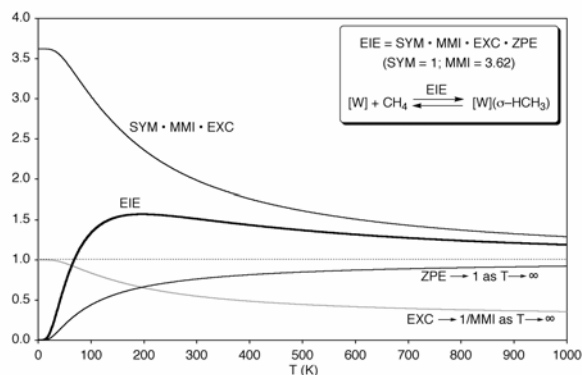
Goals

The specific objectives and research goals of the research performed during the previous grant period have been to obtain information that is relevant to transition metal mediated transformations of organic substrates. Such studies are of importance due to the fact that vast quantities of organic materials are available from natural resources but their full potential is yet to be realized because of synthetic difficulties. Specific issues that were addressed during the course of this research included studies designed to understand (i) the role of molybdenum in hydrodesulfurization and hydrodenitrogenation chemistry, (ii) the factors that influence the kinetics and thermodynamics of the diastereoselective oxidative addition of H₂ to a metal center, (iii) the details of the mechanism of C–H bond activation by molybdenocene and tungstenocene complexes, and (iv) equilibrium isotope effects pertaining to the interaction of H–H and C–H bonds with transition metal centers.

Recent Progress

(1) Transformations of Molybdenum Compounds Relevant to Hydrodesulfurization and Hydrodenitrogenation. With the advent of increasingly stringent regulations pertaining to acceptable levels for the sulfur-containing impurities in gasoline, hydrodesulfurization (HDS) and hydrodenitrogenation (HDN) continue to be the largest volume and most important industrial catalytic application of transition metals. Molybdenum is the most essential transition metal component of a typical HDS/HDN catalyst and for this reason we have started to investigate the reactivity of various molybdenum complexes towards heterocyclic sulfur and nitrogen compounds. Hydrodenitrogenation of polycyclic organonitrogen compounds, such as quinoline, may involve hydrogenation of both the heterocyclic and carbocyclic rings. It has, however, been noted that a considerable saving of hydrogen and a more useful ultimate product (namely propylbenzene) would be obtained if the heterocyclic ring of quinoline were to be selectively hydrogenated. Therefore, it is of relevance that $[\eta^6-(C_5N)\text{-quinoline}]\text{Mo}(\text{PMe}_3)_3$ reacts with H₂ to give $\text{Mo}(\text{PMe}_3)_4\text{H}_4$ and release 1,2,3,4-tetrahydroquinoline, the product of selectively hydrogenating the heterocyclic ring. In contrast, the isomer with quinoline coordinated by the carbocyclic ring, *i.e.* $[\eta^6-(C_6)\text{-quinoline}]\text{Mo}(\text{PMe}_3)_3$, is stable to H₂ under comparable conditions, thereby demonstrating that coordination by the heterocyclic ring facilitates reduction of quinoline.

(2) Equilibrium Isotope Effects (EIEs) Pertaining to the Coordination and Oxidative Addition of C–H and H–H Bonds. We have used a combination of experimental and computational methods to evaluate the isotope effects pertaining to the coordination and oxidative addition of C–H and H–H



bonds. An interesting aspect of these studies is the demonstration that the EIEs do not necessarily exhibit simple van't Hoff behavior by varying in a simple monotonic manner. Rather, the temperature dependence of the EIE may exhibit a maximum as illustrated for coordination of methane. Thus, depending upon the temperature, both normal and inverse EIEs may be obtained for coordination of a C–H bond in the same system.

Potential Impact of Research in Science and Technologies of Relevance to DOE

Our research focuses on several issues pertaining to catalysis that belong to the mission of the DOE. For example, fundamental studies on the reactions of sulfur and nitrogen heterocyclic with molybdenum complexes are directly relevant to HDS and HDN, the catalytic processes that are indispensable for processing and manufacturing fuels.

Future Plans

Future research will be concerned with: (i) The synthesis and structural characterization of well-defined mononuclear molybdenum and polynuclear molybdenum/cobalt compounds which feature the metals in sulfur-rich coordination environments that emulate the catalytic sites of HDS and HDN catalysts, and an investigation of their reactivity towards aromatic heterocyclic sulfur and nitrogen compounds such as thiophene, pyrrole, and pyridine derivatives, and (ii) the application of metallation-resistant *ansa* ligands to an investigation of investigation of intermolecular C–H bond activation reactions.

Publications Citing DOE Support

1. “Carbonyl Abstraction Reactions of $\text{Cp}^*\text{Mo}(\text{PMe}_3)_3\text{H}$ with CO_2 , $(\text{CH}_2\text{O})_n$, HCO_2H , and MeOH : The Synthesis of $\text{Cp}^*\text{Mo}(\text{PMe}_3)_2(\text{CO})\text{H}$ and the Catalytic Decarboxylation of Formic Acid” by Jun Ho Shin and Gerard Parkin, *J. Organomet. Chem.* **2002**, 642, 9-15.
2. “Synthesis and Structures of Zirconium–Pyrrolyl Complexes: A Computational Analysis of the Factors that Influence the Coordination Modes of Pyrrolyl Ligands” by Joseph M. Tanski and Gerard Parkin, *Organometallics* **2002**, 21, 587-589.
3. “Thiophene and Butadiene-Thiolate Complexes of Molybdenum: Observations Relevant to the Mechanism of Hydrodesulfurization” by Kevin E. Janak, Joseph M. Tanski, David G. Churchill, and Gerard Parkin, *J. Am. Chem. Soc.* **2002**, 124, 4182-4183.
4. “Kinetic and Thermodynamic Preferences For the Diastereoselective Oxidative Addition of H_2 to *trans*- $\text{Ir}(\text{P}^*\text{R}_3)_2(\text{CO})\text{Cl}$: Monodentate Chiral Phosphines may Impart Exceptional Degrees of Diastereoselectivity” by Jun Ho Shin and Gerard Parkin, *J. Am. Chem. Soc.* **2002**, 124, 7652-7653.
5. “The Electronic Influence of Ring Substituents and *Ansa* Bridges in Zirconocene Complexes as Probed by Infrared Spectroscopic, Electrochemical, and Computational Studies” by Cary E. Zachmanoglou, Arefa Docrat, Brian M. Bridgewater, Gerard Parkin, Christopher G. Brandow,

- John E. Bercaw, Christian N. Jardine, Mark Lyall, Jennifer C. Green, and Jerome B. Keister *J. Am. Chem. Soc.* **2002**, *124*, 9525-9546.
6. “The Syntheses and Structures of Coordinatively Unsaturated Aryloxy–Hydride Complexes of Molybdenum, Mo(PMe₃)₄(OAr)H: Reversible C–H Bond Activation and Comparison with their Tungsten Analogues” by Tony Hascall, Vincent J. Murphy, Kevin E. Janak and Gerard Parkin *J. Organomet. Chem.* **2002**, *652*, 37-49.
 7. “The Reactivity of Mo(PMe₃)₆ towards Heterocyclic Nitrogen Compounds: Transformations Relevant to Hydrodenitrogenation” by Guang Zhu, Joseph M. Tanski, David G. Churchill, Kevin E. Janak and Gerard Parkin *J. Am. Chem. Soc.* **2002**, *124*, 13658-13659.
 8. “A Non–Classical Hydrogen Bond in the Molybdenum Arene Complex [η⁶-C₆H₅C₆H₃(Ph)OH]Mo(PMe₃)₃: Evidence that Hydrogen Bonding Facilitates Oxidative Addition of the O–H Bond by Tony Hascall, Mu-Hyun Baik, Brian M. Bridgewater, Jun Ho Shin, David G. Churchill, Richard A. Friesner and Gerard Parkin, *J. Chem. Soc., Chem. Commun.* **2002**, 2644-2645.
 9. “Computational Evidence that the Inverse Kinetic Isotope Effect for Reductive Elimination of Methane from a Tungstenocene Methyl–Hydride Complex is associated with the Inverse Equilibrium Isotope Effect for formation of a σ–Complex Intermediate” by Kevin E. Janak, David G. Churchill, and Gerard Parkin *Chem. Commun.* **2003**, 22-23.
 10. “Normal and Inverse Primary Kinetic Deuterium Isotope Effects for C–H Bond Reductive Elimination and Oxidative Addition Reactions of Molybdenocene and Tungstenocene Complexes: Evidence for Benzene σ–Complex Intermediates” by David G. Churchill, Kevin E. Janak, Joshua S. Wittenberg and Gerard Parkin, *J. Am. Chem. Soc.* **2003**, *125*, 1403-1420.
 11. “Synthesis and Structure of [pz^{Bu^t2}]₂Mo(PMe₃)₄H, a d⁴ Molybdenum Complex that Exhibits η²–Coordination of the 3,5-Di-*t*-butylpyrazolyl Ligand” by Guang Zhu, Joseph M. Tanski and Gerard Parkin, *Polyhedron* **2003**, *22*, 199-203.
 12. “Tantalum Amido and Imido Complexes Supported by *Tris*[(2-indolyl)methyl]amine, a Tetradentate Trianionic Ligand with Reduced π–Donor Character” by Joseph M. Tanski and Gerard Parkin, *Inorg. Chem.* **2003**, *42*, 264-366.
 13. “The Photochemical Reactivity of Bis(*tert*-Butylcyclopentadienyl)molybdenum Dihydride: Synthesis and Structure of Dinuclear *trans*–[(Cp^{Bu^t})Mo(μ–σ,η⁵–C₅H₃Bu^t)H]₂” by David G. Churchill, Jun Ho Shin, and Gerard Parkin, *J. Chem. Crystallogr.* **2003**, *33*, 297-302.
 14. “Temperature Dependent Transitions between Normal and Inverse Equilibrium Isotope Effects For Coordination and Oxidative Addition of C–H and H–H Bonds to a Transition Metal Center” by Kevin E. Janak and Gerard Parkin, *J. Am. Chem. Soc.* **2003**, *125*, 6889-6891.
 15. “Deuterium and Tritium Equilibrium Isotope Effects for Coordination and Oxidative Addition of Dihydrogen to [W(CO)₅] and for the Interconversion of W(CO)₅(η²–H₂) and W(CO)₅H₂” by Kevin E. Janak and Gerard Parkin, *Organometallics* **2003**, *22*, 4378-4380.
 16. “Experimental Evidence for a Temperature Dependent Transition between Normal and Inverse Equilibrium Isotope Effects For Oxidative Addition of H₂ to Ir(PMe₂Ph)₂(CO)Cl”, Kevin E. Janak and Gerard Parkin, *J. Am. Chem. Soc.* **2003**, *125*, 13219-13224.

This page intentionally left blank.

Early Transition Metal Oxides as Catalysts: Crossing Scales from Clusters to Single Crystals to Functioning Materials

Dr. David. A. Dixon¹, Co-Principal Investigator (Co-PI), Dr. Zdenek Dohnalek², Investigator, Dr. Maciej Gutowski², Investigator, Dr. Jianzhi Hu², Investigator, Dr. Enrique Iglesia³, Co-PI, Dr. Bruce D. Kay², Co-PI, Dr. Jun Liu⁴, Co-PI, Dr. Charles H. F. Peden², Co-PI and Project Director, Dr. Lai-Sheng Wang⁵, Co-PI, Dr. Yong Wang², Investigator, Dr. John M. White⁶, Co-PI.

Postdocs: ⁶O.A. Bondarchuk, ²J.E. Herrera, ²J. Kim., ²J.-H. Kwak, ³T. Stuchinskaya, ⁵H.J. Zhai, (others TBA).

Students: ¹C. Chisolm, ³J. Macht, (others TBA).

¹University of Alabama, ²Pacific Northwest National Laboratory, ³University of California, Berkeley, ⁴Sandia National Laboratory, ⁵Washington State University, ⁶University of Texas at Austin

Contact information: C.H.F. Peden, P.O. Box 999, MS K8-93, Pacific Northwest National Laboratory, Richland, WA 99352 chuck.peden@pnl.gov

Goal

We are employing an integrated experimental/theoretical approach to advance our current ability to understand, design, and control the catalytic and surface chemistry of transition metal oxides, specifically for redox and acid-base chemistries. The approach combines novel solid-state inorganic synthesis, surface science, experimental and theoretical/computational chemical physics, and mechanistic organic chemistry to address this complex and important challenge.

Recent Progress

Materials synthesis and characterization

Ordered mesoporous silica, initially developed in 1992,ⁱ can be synthesized by using a self-assembly approach: surfactant molecules co-assemble with the inorganic materials into sophisticated nanoscale structures through favorable molecular interactions. The resultant nanoscale materials have extremely high surface area (>1000 m²/g), and highly uniform ordered nanoporosity with tightly controlled pore size and shape. These unique characteristics make the self-assembled nanoporous material an attractive candidate for catalytic applications. Previous work at UC-Berkeley (Iglesia and coworkers) and elsewhere demonstrated that WO_x exhibits unique chemical properties for acid-catalyzed reactions. Such catalytic properties are strongly affected by domain size, reducibility, and accessibility of the WO_x clusters when supported on conventional refractory metal oxide supports. However, a systematic investigation between the structural and functional relationship in this catalytic system has not been conducted, primarily due to the difficulties in material synthesis with atomic level control, advanced characterization to understand detailed physical and chemical properties, and interpretation and suggestion of mechanisms guided by advanced theory. Mesoporous silica, particularly SBA-15 type silica, provides a chemically inert and thermally stable scaffold for designing WO_x type model catalysts with controlled cluster size and spatial dispersion.

Our initial work in FY2004 has successfully demonstrated a solution based synthesis approach to highly disperse WO_x on SBA-15 mesoporous silica with excellent thermal stability (Figure 1a). High resolution magic angle spinning ¹H NMR methods are being developed to probe the surface structure and domain size of WO_x clusters supported on SBA-15. With ¹H NMR we have identified the chemical shift which is likely related to the hydroxyl groups associated with the WO_x clusters (Figure 1b), and have also initiated experiments that will potentially provide insight on proton mobility and Brønsted acid strength of WO_x.

We have also been preparing non-silica based mesoporous materials as catalyst supports for WO_x and other acid catalysts, in particular ZrO₂ based mesoporous materials. We are employing two approaches to synthesize ZrO₂-based mesoporous materials. The first approach involves direct synthesis of mesoporous ZrO₂. We are using high molecular weight block copolymer surfactants as the templates following the procedures initially developed by Stucky and coworkers.ⁱⁱ The high molecular weight of block copolymers makes their liquid crystalline structures more stable in the presence of ceramic precursors, so structural control is easier for complex compositions. The large molecules also expand the pore dimensions beyond 10 nanometers. The second approach involves coating mesoporous silica with ZrO₂. This approach may be more flexible because mesoporous silica is easy to make, and the coating can be tightly controlled. Thus, we are developing inorganically functionalized mesoporous structures using both solution based and gas phase based reactions. Once developed, this method can be used to deposit complex active catalytic groups on the pore surfaces as well.

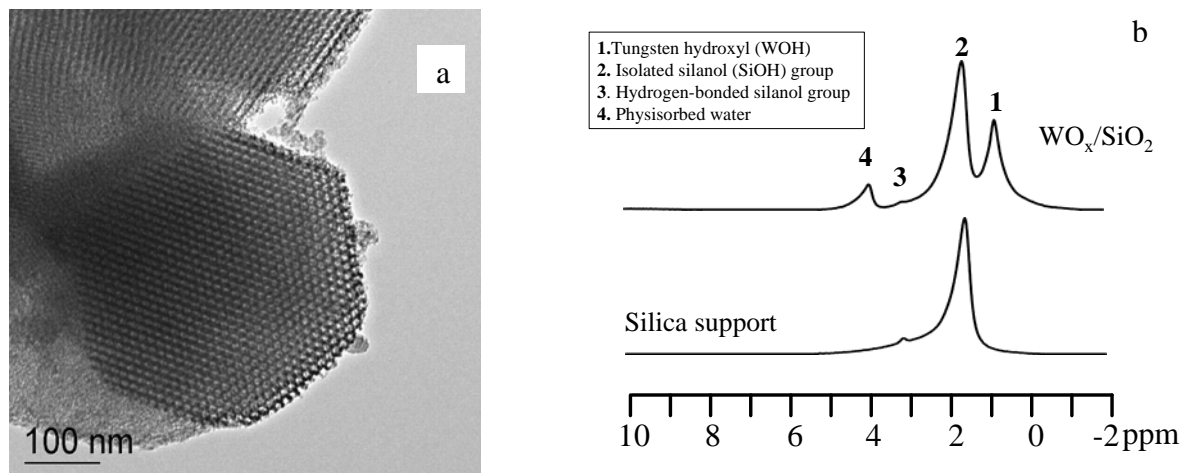


Figure 1: a) High resolution TEM image of 30wt% WO_x/SBA-15 SiO₂ after calcination at 500°C. b) High resolution ¹H MAS spectra obtained at a sample spinning rate of 5kHz.

UHV studies of model TMO catalysts

The initial focus of our UHV studies of model TMO catalysts is aimed at determining the optimum source for the deposition of tungsten oxides films and clusters. Direct evaporation of WO₃ in a molecular beam was found to provide a reliable, carbon-free source, of oxidized tungsten. To test the efficacy of this deposition method, a number of tungsten oxide films (thickness ~1μm) were deposited at various substrate temperatures and deposition angles on optically polished polycrystalline Ta substrates. The oxidation state of tungsten in the films was determined using XPS and was shown to be predominantly the (6+) oxidation state. At high substrate temperatures (> 600K), the films are crystalline and exhibit a cubic crystallographic structure as show by X-Ray Diffraction (XRD). At low substrate temperatures (< 300K) the WO₃ films are amorphous. Films deposited at low temperatures (20 – 300 K) and high deposition angles (> 70°) grow via diffusion limited ballistic deposition and exhibit a filamentous-like structure as shown in Figure 2. The surface area of such films is extremely high, approaching 1000m²/g. Current studies focus on detailed surface area, and binding site distribution measurements of the nanoporous WO₃ films as a function of synthesis and post-growth processing conditions. Parallel studies of WO₃ cluster formation on a TiO₂(110) substrate have just been initiated. These substrates will be used in the molecular beam scattering studies of the proposed research.

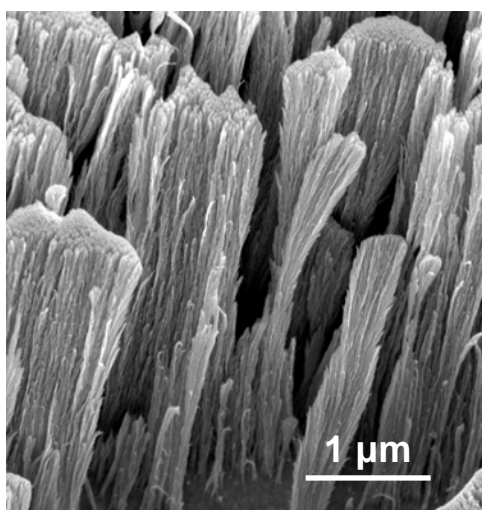


Figure 2: SEM micrograph of amorphous nanoporous WO₃ film deposited at glancing deposition angle of 85° on a Ta substrate at 20K.

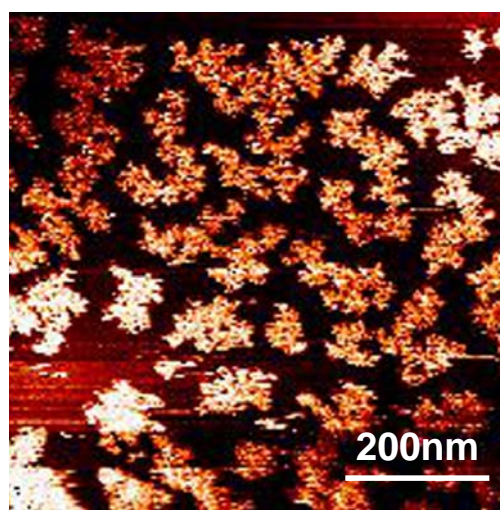


Figure 3: STM image of WO₃ clusters deposited on HOPG at room temperature.

Our initial scanning tunneling microscopy (STM) studies examined the deposition of sub-monolayer quantities of WO_3 on highly-oriented pyrolytic graphite (HOPG). The HOPG substrate provides large terraces with low defect densities and can be imaged relatively easily with atomic resolution. A STM image of WO_3 clusters formed from submonolayer WO_3 deposition at room temperature is shown in Figure 3. The fractal like shape of the clusters suggests that a diffusion-limited aggregation mechanism governs cluster growth. Scanning tunneling spectroscopy indicates that the WO_3 clusters are semiconducting in nature. Current efforts are aimed at understanding how the WO_3 cluster size and morphology depend on initial coverage and substrate temperature. STM studies of WO_3 cluster formation on $\text{TiO}_2(110)$ will begin in May 2004.

Photoelectron spectroscopy of W_xO_y^- clusters

We have been using photoelectron spectroscopy to study small tungsten oxide clusters of the form W_xO_y^- , with $x = 1-4$ and $y = 1-12$. Data have been obtained for WO_y^- ($y = 1-5$) and W_2O_y^- ($y = 1-6$). Theoretical calculations at the density functional theory (B3LYP) and molecular orbital theory (CCSD(T) with large basis sets of aug-cc-pVTZ quality have also been initiated for the WO_y^- series of clusters. Experimental data for the WO_y^- series of clusters showed that the electron binding energies increase with the oxygen content up to WO_4^- and level off beyond that, suggesting a behavior of sequential oxidation, i.e. electron transfer from W to O upon sequential addition of oxygen (see Figure 4: $d - \text{W } 5d$ features; $p - \text{O } 2p$ features). This observation is consistent with the theoretical calculations, which also revealed that WO_4 has a triplet ground state, i.e., a di-radical structure, whereas WO_5 contains a superoxide unit. These results are being prepared for publication.

Computational studies of catalyst systems

We have been using density functional theory to calculate the Brønsted basicities and acidities and Lewis acidities of model V_xO_y , Cr_xO_y , Mo_xO_y , and W_xO_y clusters and bonded to each other and to Si_xO_y or Zr_xO_y clusters. The oxygens are terminated with hydrogen atoms as appropriate to complete the valency. For the Group VIB oxides, we have studied the “+6” state of the metal atom with tetra-coordination (e.g., $(-\text{O})_2\text{W}(=\text{O})_2$), penta-coordination, (e.g., $(-\text{O})_4\text{W}(=\text{O})$), and hexa-coordination (e.g., $(-\text{O})_6\text{W}$). This allows us to explore the role of various surface defect sites. The addition of CH_3OH to the clusters leading to the formation of $\text{CH}_3\text{O}-$ and $\text{H}-$ and then to $\text{CH}_2\text{O}-$ and additional $\text{H}-$ has been studied to determine potential intermediates. In some cases, we find that transfer of the various groups can lead to cleavage of a metal-oxygen bridge bond. Calculations of nmr chemical shifts and of uv-vis absorption spectra at the DFT level for direct comparison to experiment have been initiated. The overall DOE effort in computational catalyst has received a large allocation (1 million node hours) on the new HP Linux cluster with 1980 nodes and 11.7+ peak Tflops in the MSCF in the EMSL at PNNL with M. Gutowski as PI.

DFT calculations with ultrasoft and projector augmented-wave pseudopotentials and gradient-corrected exchange-correlation functionals were done for various oxides, including the catalytic systems WO_3 , MoO_3 , and V_2O_5 , and the supports, TiO_2 , SiO_2 , Al_2O_3 , and MgO . The lattice constants, bulk modulus, and structure of the valence band and semi-core levels for these oxides were calculated in good agreement with experiment but the band gaps are systematically underestimated. The relaxation and corrugation of the (100) surface of WO_3 has been characterized.

NMR

We have measured the solid state ^{183}W magic angle spinning (MAS) NMR Spectra of phosphotungstic acid hydrate $\text{H}_3\text{PO}_4 \cdot 12\text{WO}_3 \cdot x\text{H}_2\text{O}$. Although this technique is a sensitive probe of structure, it has two shortcomings: (1) Inherent low NMR sensitivity (S/N) combined with long relaxation time \Rightarrow long measuring time and (2) Low $\gamma \Rightarrow$ meaning low resonant frequency. The dead time associated with probe ring down is a big problem. We are developing techniques to improve the signal to noise and to reduce the probe ring down by separating the chip capacitors from the receiver coil.

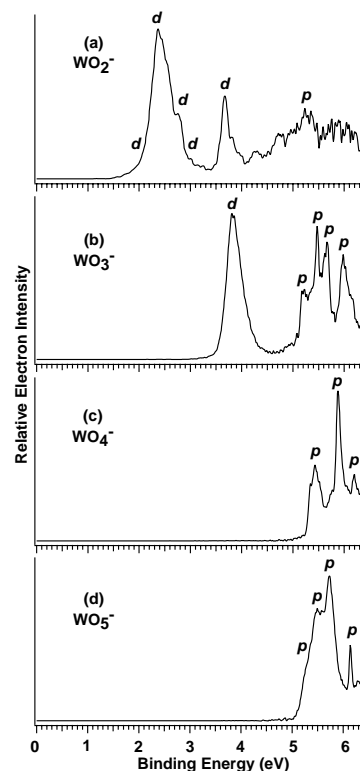


Figure 4:

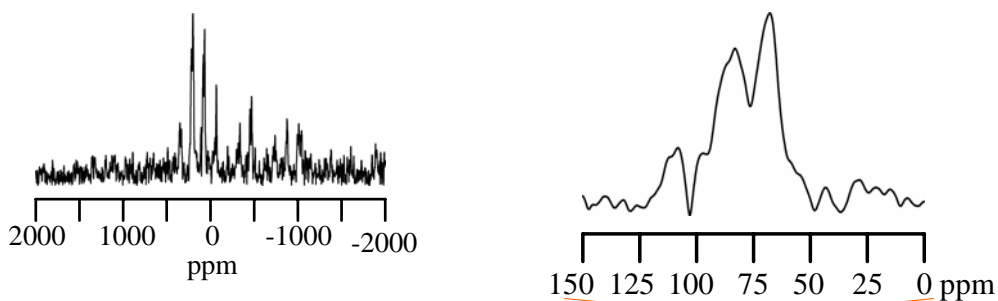


Figure 5: Preliminary Solid State ^{183}W (MAS) NMR Spectra of $\text{H}_3\text{PO}_4 \cdot 12\text{WO}_3 \cdot x\text{H}_2\text{O}$.

We have demonstrated that we can measure ^{51}V and ^{95}Mo solid state NMR at an 11.7T field strength to probe mixed vanadyl/molybdenyl catalysts. We are in the process of setting-up the ^{51}V - ^{95}Mo MAS distance measurement experiment after demonstrating that we can make good solid state measurements without spinning in the solid state.

DOE Interest

The proportion of chemical industry processes using catalysts exceeds 80%. Current commercial heterogeneous catalysts are structurally and chemically complex and data gathered from them can seldom be interpreted with atomic-level precision. We seek to reduce the complexity of TMO catalysts to levels addressable and controllable at the atomic level, while maintaining intimate linkages with practical catalysis and catalytic materials. The focus of the proposed work is to gain a fundamental understanding of chemical transformations in order to design and construct new catalysts with more precise control of specific chemical reactions. This will enable us to help DOE reach its goals of doing fundamental science to address the energy needs of the country by (1) improving energy conservation by new means of energy conversion and storage; (2) enable direct chemical conversions previously economically unfeasible and produce new routes to novel materials while at the same time minimizing by-products and environmental impact; and (3) protecting the environment

Future Plans

A number of tasks are being planned for the next year. 1) We will continue the PES studies of metal oxide clusters, extending to W_2O_y^- and W_3O_y^- series and substituting Mo and Cr for W and working on the $\text{PW}_{12}\text{O}_{40}^{3-}$, $\text{PMo}_{12}\text{O}_{40}^{3-}$, and $\text{SMo}_{12}\text{O}_{40}^{2-}$ Keggin anions. We will perform high level calculations on these ions and neutrals for method benchmark purposes. We will continue to study larger clusters of the metal oxides interacting with CH_3OH and the oxidative dehydrogenation reaction as well as the reductive dehydrogenation of 2-butanol to form butanes and H_2O . We will identify the thermodynamics of the pathways and find transition states to correlate with experimental measurements.

We will link theory, spectroscopic characterizations, and activity studies to calibrate the acid/base chemistry on WO_x catalysts. The methodology established on WO_x will be extended to VO_x and MoO_x catalytic systems for redox induced chemistries. We will also develop synthesis protocols to disperse metal oxides with controlled atomic connectivity and spatial dispersions such as Keggin structured anions on mesoporous silica, and to elucidate their structural and functional relationships for acid/base and redox chemistries. We will use solid state ^{51}V and ^{95}Mo NMR to investigate VO_x and MoO_x catalytic systems. We will continue the development of in-situ NMR capabilities and evaluate the feasibilities of solid state ^{183}W NMR at high and ultra-high magnetic fields available at PNNL.

References

- i. (a) Beck, J. S.; Vartuli, J. C.; Roth, W. J.; Leonowicz, M. E.; Kresge, C. T.; Schmitt, K. D.; Chu, C. T.-W.; Olson, D. H.; Sheppard, E. W.; McCullen, S. B.; Higgins, J. B.; Schlenker, J. L. *J. Am. Chem. Soc.* **1992**, *114*, 10834. (b) Kresge, C. T.; Leonowicz, M. E.; Roth, W. J.; Vartuli, J. C.; Beck, J. S. *Nature* **1992**, *359*, 710.
- ii. Zhao, D.; Feng, J.; Huo, Q.; Melosh, N.; Fredrickson, G. H.; Chmelka, B. F.; Stucky, G. D. *Science* **1998**, *279*, 548.

Fundamental Studies of Selectivity and Mechanisms of Oxide-Catalyzed Nitrogen Oxide Chemistry

PNNL Staff (2002-04): Peden, C.H.F., Szanyi, J., Henderson, M.A., Chambers, S.A.

Postdocs (2002-04): Ozensoy, E., Azad, S.

Collaborators (2002-04): Rodriguez, J., Graham, G.W.

Pacific Northwest National Laboratory, Richland, WA 99352

chuck.peden@pnl.gov

Goal

Develop a fundamental understanding of catalytic nitrogen oxide (NO_x) reactions on oxide surfaces, with special emphasis on identifying new and unique chemistry associated with molecules containing unpaired electrons in their ground state.

Recent Progress

We completed studies aimed at the identification of optimum parameters for the epitaxial growth of the mixed-oxides films, Ce_{1-x}Zr_xO₂ with x = 0.1, 0.2 and 0.3, by oxygen-plasma-assisted MBE on single crystal Y-stabilized ZrO₂ (YSZ) substrates. The resulting films were characterized by RHEED, LEED, XPS/XPD, XRD, and RBS/C in order to determine their bulk and surface structures and compositions. Pure-phase, epitaxial Ce_{1-x}Zr_xO₂ films readily grew on YSZ(111) without showing any contamination of yttria from the substrate. The resulting epitaxial film surfaces are unreconstructed and exhibit the structure of bulk CeO₂(111). XPS data indicate that both Ce and Zr cations are formally in the +4 oxidation state for all films prepared here. Small differences in the photoemission results for Zr-doped ceria films as compared to those obtained for pure ZrO₂ may be explained by changes in electronic structure when Zr is added to ceria that, in turn, results from longer Zr-O bond distances in the mixed oxides. The minimum yields obtained from the random and channeling spectra of these films also provide evidence that high quality single crystal CeO₂ and Ce_{0.7}Zr_{0.3}O₂ materials were grown. For the Zr-doped films, Zr atoms are shown to occupy the lattice sites of Ce in the bulk structure of CeO₂(111). Indeed, based on minimum yield values, the fraction of Zr substitution for Ce cations in the film was estimated to be 88%.

The interaction of N₂O with TiO₂(110) was studied in an effort to better understand the conversion of NO_x species to N₂ over TiO₂-based catalysts. The TiO₂(110) surface was used as a model system because this material is commonly used as a support and because oxygen vacancies on this surface are perhaps the best available models for the role of electronic defects in catalysis. Annealing TiO₂(110) in vacuum at high temperature (above about 800 K) generates oxygen vacancy sites that are associated with reduced surface cations (Ti⁺³ sites) and that are easily quantified using temperature programmed desorption (TPD) of water. Using TPD, x-ray photoelectron spectroscopy (XPS) and electron energy loss spectroscopy (EELS), we found that the majority of N₂O molecules adsorbed at 90 K on TiO₂(110) are weakly held, and desorb from the surface at 130 K. However, a small fraction of the N₂O molecules exposed to TiO₂(110) at 90 K decompose to N₂ via one of two channels, both of which are vacancy-mediated. One channel occurs at 90 K, and results in N₂ ejection from the surface and vacancy oxidation. We propose that this channel involves N₂O molecules bound at vacancies with the O-end of the molecule. The second channel results from an adsorbed state of N₂O that decomposes at 170 K to liberate N₂ in the gas phase and deposit oxygen adatoms at non-defect Ti⁺⁴ sites. The presence of these O adatoms is clearly evident in subsequent water TPD measurements. We propose that this channel involves N₂O molecules that are bound at vacancies with the N-end of the molecule, which permits the O-end of the molecule to interact with an adjacent Ti⁺⁴ site. The partitioning between these two channels is roughly 1:1 for adsorption at 90 K, but neither is observed to occur for moderate N₂O exposures at temperatures above 200 K. EELS data indicate that vacancies readily transfer charge to N₂O at 90 K, and this charge transfer facilitates N₂O decomposition. Based on this result, it appears that the decomposition of N₂O to N₂ requires trapping of the molecule at vacancies and that the lifetime of the N₂O-vacancy interaction may be key to the conversion of N₂O to N₂.

We performed x-ray photoelectron spectroscopy (XPS) and temperature programmed desorption (TPD) studies probing the surface chemistry of water on the oxidized and reduced surfaces of a 500 Å epitaxial CeO₂(111) film grown on yttria-stabilized ZrO₂(111). Oxidation with O₂ at 773 K under UHV conditions was sufficient to generate XPS spectra reflective of fully oxidized CeO₂(111). Surface reduction was carried out by annealing in UHV between 773 and 973 K, and the level of reduction was quantified using changes in the Ce3d_{3/2} 4f⁰ photoemission peak at 917 eV. As expected, the level of surface reduction increased with increasing temperature. Annealing at 773 K led to a surface with approximately 1/3rd of its surface Ce⁴⁺ sites reduced to Ce³⁺. The resulting Ce³⁺ sites were primarily in the first layer based on the fact that RT exposure of the film to O₂ resulted in nearly complete conversion of Ce³⁺ to Ce⁴⁺. Annealing at higher temperatures led to complete or nearly complete reduction of the first layer along with substantial levels of subsurface reduction that was not reoxidized by RT exposure to O₂. Comparisons with results in the literature for surface reduction of single crystal CeO₂(111) suggest that the volume of thick (~ mm) ceria crystals, which acts as a reservoir for oxygen vacancies, dictates the severity of reductive conditions required in order to observe significant levels of surface Ce³⁺ sites. In other words, the particular annealing temperatures and times required for a specific extent of surface reduction scales with the thickness of the crystal. Water TPD results indicate strong coverage dependence on the oxidized CeO₂(111) that destabilizes high coverages of water relative to low coverages. The presence of surface reduction (near a full ML of Ce³⁺ based on XPS data) removes much of the coverage dependent behavior. TPD uptake measurements, H₂ TPD spectra and XPS spectra in the Ce3d core level and Ce4f valence band (VB) regions all indicate that little or no irreversible water adsorption or Ce³⁺ oxidation was observed for this reduced surface. In contrast, exposure of water at 650 K promoted reduction of the surface above the level observed from annealing at 650 K in the absence of water, suggesting that water/OH groups may promote removal of lattice oxygen under certain conditions. Because water oxidation of Ce³⁺ surface sites has been observed for reduced ceria powders, but was not observed on the reduced CeO₂(111) surfaces studied here, we propose that the reduced (111) surface is more resistant than non-(111) terminations to being oxidized by water. An explanation based on theoretical arguments in the literature is offered for the resistance of Ce³⁺ sites to being oxidized by water.

We prepared a cubic CeO₂(001) film of thickness equal to ~58 nm was epitaxially grown on Y₂O₃-stabilized cubic ZrO₂ by oxygen plasma assisted molecular beam epitaxy (OPA-MBE). The interface was characterized using high resolution transmission electron microscopy (HRTEM). The interface exhibited coherent regions separated by equally-spaced misfit dislocations. When imaged from the [100] direction, the dislocation spacing is 3.3 ± 0.5 nm, which is slightly shorter than the expected value of 4.9 nm calculated from the differences in lattice constants given in the literature, but is fairly consistent with the 3.9 nm lattice mismatch measured by electron diffraction. Thus, the results indicated that the lattice mismatch between the film and the substrate is accommodated mainly by interface misfit dislocations above some critical thickness.

We have used x-ray photoelectron spectroscopy (XPS) and temperature programmed desorption (TPD) to probe the surface chemistry of water on the oxidized and reduced surfaces of a 500 Å epitaxial CeO₂(111) film grown on yttria-stabilized ZrO₂(111). Oxidation with O₂ at 773 K under UHV conditions was sufficient to generate XPS spectra reflective of fully oxidized CeO₂(111). Surface reduction was carried out by annealing in UHV between 773 and 973 K, and the level of reduction was quantified using changes in the Ce3d_{3/2} 4f⁰ photoemission peak at 917 eV. As expected, the level of surface reduction increased with increasing temperature. Annealing at 773 K led to a surface with approximately 1/3rd of its surface Ce⁴⁺ sites reduced to Ce³⁺. The resulting Ce³⁺ sites were primarily in the first layer based on the fact that RT exposure of the film to O₂ resulted in nearly complete conversion of Ce³⁺ to Ce⁴⁺. after. Annealing at higher temperatures led to complete or nearly complete reduction of the first layer along with substantial levels of subsurface reduction that was not reoxidized by RT exposure to O₂. Comparisons with results in the literature for surface reduction of single crystal CeO₂(111) suggest that the volume of thick (~ mm) ceria crystals, which acts as a reservoir for oxygen vacancies, dictates the severity of reductive conditions required in order to observe significant levels of surface Ce³⁺ sites. In other words, the particular annealing temperatures and times required for a specific extent of surface reduction scales with the thickness of the crystal. Water TPD results indicate strong coverage dependence on the oxidized CeO₂(111) that destabilizes high coverages of water relative to low coverages. The presence of surface reduction (near a full ML of Ce³⁺ based on XPS data) removes much of the coverage dependent behavior. TPD uptake measurements, H₂ TPD spectra and XPS spectra in the Ce3d core level and Ce4f valence band (VB) regions all indicate that little or no irreversible water adsorption or Ce³⁺ oxidation was observed for this reduced surface. In contrast, exposure of water at 650 K promoted reduction of the surface above the level observed from annealing at 650 K in the absence of water, suggesting that water/OH groups may promote removal of lattice oxygen under certain conditions. Because water oxidation of Ce³⁺ surface sites has been observed for reduced ceria powders, but was not observed on the reduced CeO₂(111) surfaces studied here, we propose that the reduced (111) surface is more resistant than non-(111)

terminations to being oxidized by water. An explanation based on theoretical arguments in the literature is offered for the resistance of Ce^{3+} sites to being oxidized by water.

Multi-layer hetero-structured thin films have been found to possess superior structural and functional properties, especially with respect to ion conductivities. One of the best examples is the dramatically enhanced ionic conductivity in the system of CaF_2 and BaF_2 when they are deposited alternating in thin layers. It is believed that the enhanced ionic conductivity in this type of structure is attributed to the interface defect structures. More recently, researchers have also observed that the ionic conductivity of yttria stabilized zirconia (YSZ) can be enhanced by increased dislocation density. This prompted us to develop pure and doped ZrO_2 and CeO_2 hetero-junction multi-layer thin films for enhanced ionic conductivity. Microstructural features of hetero-multi-layer $\text{ZrO}_2/\text{CeO}_2$ films, with thicknesses of several nanometer for each layer and grown on YSZ substrates, have been studied using TEM, HRTEM, EELS, EDX, and XRD in order to characterize phase, Ce valence state, interface structure, and the nature and number of internal defects. Our results demonstrate that the pure ZrO_2 layers are stabilized as a cubic phase when they are deposited alternating with thin layers of CeO_2 . Electron diffraction combined with dynamical electron diffraction calculations indicates that the oxygens in the pure cubic- ZrO_2 layer of several nanometers in thickness are displaced along the $\langle 111 \rangle$ directions.

Adsorption and reaction of NO on oxidized and reduced $\text{SrTiO}_3(100)$ surfaces have been studied using temperature programmed desorption (TPD). Major desorption peaks for NO from the fully oxidized surface are found at 140 and 260 K, along with a long tail that continues up to 500 K. The desorption features at 140 and 260 K correspond to activation energies of 36 and 66 kJ/mol, respectively, using a simple Redhead analysis. NO reacts non-dissociatively on the fully oxidized surface. Reactivity of reduced $\text{SrTiO}_3(100)$ is relatively higher than that of the fully oxidized surface and is influenced by the adsorption temperature of the NO molecules on the surface. NO and N_2O are the major desorption products following adsorption of NO on the reduced surface at 110 K. Desorption of N_2O from significantly reduced $\text{SrTiO}_3(100)$ indicates that the oxygen atoms of the adsorbed NO molecules are preferentially extracted by the surface oxygen vacancy sites whereas the surface gets oxidized as a result of the de-oxygenation of the adsorbates. Adsorption of NO on the reduced surface at 297 K is followed by breakage of the N-O bond producing adsorbed N and O atoms and recombination of these ad-species results in desorption of NO and N_2 from this surface. Adsorption of NO on the significantly reduced surface at 200 K is followed by desorption of NO, N_2 and N_2O as TPD products and the reactivity of this surface at 200 K presumably is a composite of the behavior observed for NO adsorption at 110 and 297 K.

DOE Interest

Catalysis continues to be vital to the chemical and petroleum industries, and to the development of pollution abatement technologies. The economic impact of catalysis has been estimated to be over 10 trillion dollars per year worldwide. Besides these practical reasons, the U.S. Department of Energy (DOE) has had a longstanding interest in catalysis also for advancing the fundamental understanding for the control of chemical transformations. In all catalyst research, a fundamental understanding of the chemical reaction mechanism(s) that occur on the catalyst surface, including an identification of the catalytic site(s) directly involved in the rate-limiting elementary process(es), is critically important to an effort to rationally develop improved catalysts and catalytic processes.

Future Plans

We will be completing studies of NOx adsorption and reaction on well-characterized $\text{TiO}_2(110)$ and $\text{CeO}_2(111)$ surfaces. These studies will include low-temperature STM measurements that provide a real space view of this chemistry as it occurs. The STM and surface reaction studies on TiO_2 will also focus on the effects of specific oxygen vacancy defects as well as the modification of this chemistry by co-adsorbed atomic and molecular oxygen, water, and hydroxyl groups. We will be initiating experiments that probe the adsorption and reaction of NOx on other important oxide surfaces and will begin to address the effects of support oxides on the observed chemistry of a catalytically active oxide material.

Publications (2002-4)

- 1) Kim, Y.J.; Herman, G.S.; Thevuthasan, S.; Shutthanandan, S.; McCready, D.E.; Gao, Y.; Peden, C.H.F. "Growth and Structure of Epitaxial $\text{Ce}_{1-x}\text{Zr}_x\text{O}_2$ Thin Films on Yttria-Stabilized Zirconia(111)." *J. Electron. Spectrosc. Rel. Phenom.* **126** (2002) 177-190.

- 2) Henderson, M.A.; Epling, W.S.; Peden, C.H.F.; Perkins, C.L. "Insights into Photoexcited Electron Scavenging Processes on TiO₂ Obtained from Studies of the Reaction of O₂ with OH Groups Adsorbed at Electronic Defects on TiO₂(110)." *J. Phys. Chem. B* **107** (2003) 534-545.
- 3) Wang, C.-M.; Thevuthasan, S.; Peden, C.H.F. "Interface Misfit Dislocations for an Epitaxial Cubic CeO₂ Film on Cubic ZrO₂." *J. Amer. Cer. Soc.* **86** (2003) 363-365.
- 4) Wang, C.-M.; Thevuthasan, S.; Gao, F.; Shutthanandan, V.; McCready, D.E.; Chambers, S.A.; Peden, C.H.F. "Interface Characteristics of Iso-Structural Thin Film and Substrate Pairs." *Nucl. Instr. and Meth. B* **207** (2003) 1-9.
- 5) Henderson, M.A.; Perkins, C.L.; Engelhard, M.H.; Thevuthasan, S.; Peden, C.H.F. "Redox Properties of Water on the Oxidized and Reduced Surfaces of CeO₂(111)." *Surf. Sci.* **526** (2003) 1-18.
- 6) Azad, S.; Szanyi, J.; Wang, L.-Q.; Peden, C.H.F. "Adsorption and Reaction of NO on Oxidized and Reduced SrTiO₃(100) Surfaces." *J. Vac. Sci. Technol. A* **21** (2003) 1307-1311.
- 7) Henderson, M.A.; Szanyi, S.; Peden, C.H.F. "Conversion of N₂O to N₂ on TiO₂(110)." *Catal. Today* **85** (2003) 251-266.
- 8) Rodriguez, J.A.; Azad, S.; Wang, L.-Q.; García, J.; Etxeberria, A.; González, L. "Electronic and chemical properties of mixed-metal oxides: Adsorption and reaction of NO on SrTiO₃(100)." *J. Chem. Phys.* **118** (2003) 6562-6571.
- 9) Thevuthasan, S.; Azad, S.; Marina, O.A.; Shutthanandan, V.; McCready, D.E.; Saraf, L.; Wang, C.M.; Lyubintsev, I.; Peden, C.H.F.; Petrovsky, V. "Influence of Multiple Interfaces on Oxygen Ionic Conductivity in Gadolinia-Doped Single Crystal Oxide Electrolyte Multi-Layer Nano Films." In Proceedings of the Third IEEE Conference on Nanotechnology, 2003, 550-552.
- 10) Wang, L.-Q.; Ferris, K.F.; Azad, S.; Engelhard, M.H.; Peden, C.H.F. "Adsorption and Reaction of Acetaldehyde on Stoichiometric and Defective SrTiO₃(100) Surfaces." *J. Phys. Chem. B* **108** (2004) 1646-1652.
- 11) Liu, G.; Rodriguez, J.A.; Chang, Z.; Hrbek, J.; Peden, C.H.F. "Adsorption and reaction of SO₂ on model Ce_{1-x}Zr_xO₂(111) catalysts." *J. Phys. Chem. B* **108** (2004) 2931-2938.
- 12) Azad, S.; Thevuthasan, S.; Shutthanandan, V.; Wang, C.M.; McCready, D.E.; Saraf, L.; Marina, O.A.; Peden, C.H.F. "Growth and Characterization of Single Crystal Multi Layer Nano Structures for Fast Ion Conduction." In Nanotechnology and the Environment, Masciangioli, T.M., Ed.; American Chemical Society (Washington, D.C.) 2004, in press.
- 13) Wang, C.-M.; Azad, S.; Thevuthasan, S.; Shutthanandan, V.; McCready, D.E.; Peden, C.H.F. "Distortion of the Oxygen Sub-Lattice in Pure Cubic-ZrO₂." *J. Matls. Res.* (2004) in press.
- 14) Sun H.P.; Graham, G.W.; Jen, H.W.; McCabe, R.W.; Thevuthasan, S.; Peden, C.H.F.; Pan, X.Q. "High Resolution Transmission Electron Microscopy Study of a Strong Metal-Support Interaction in a Model Planar Catalyst: Pd on Ceria-Zirconia." *J. Catal.*, submitted for publication.
- 15) Wang, C.-M.; Azad, S.; Thevuthasan, S.; Shutthanandan, V.; McCready, D.E.; Peden, C.H.F. "Microstructure of ZrO₂-CeO₂ Hetero-Multi-Layer Films Grown on YSZ Substrate." *Acta Materialia*, submitted for publication.

Microscopy with Single Atom Sensitivity for Solving Catalysis Problems

Postdocs: Albina Y. Borisevich, Andrew R. Lupini, Alberto Franceschetti, Bei Chen, Wenfu Yan

Collaborators: David R. Mullins, Viviane Schwartz, Sheng Dai, Steven H. Overbury, Sokrates T. Pantelides

Condensed Matter Sciences Division, Oak Ridge National Lab, Oak Ridge, TN 37831
pennycooks@ornl.gov

Goal

Address fundamental problems in catalytic systems using a combination of Z-contrast STEM with single-atom sensitivity and density functional theory calculations.

Recent Progress

High Catalytic Activity from 1 nm Au clusters on TiO₂: The 0.7 Å diameter beam of the aberration-corrected, 300 kV scanning transmission electron microscope (STEM) at ORNL provides the highest sensitivity for imaging individual atoms. Nanometer-sized gold particles were deposited on a variety of supports (mesoporous titania, anatase, brookite, rutile) in order to investigate the activity for the oxidation of CO. Previous work had associated the activity with ~3 nm sized Au particles and the presence of oxidized Au. However, we found that high activity at low temperatures corresponds to the presence of smaller, ~1 nm, Au particles that are only one or two monolayers thick and fully reduced. Larger (>5 nm) gold particles were far less active. Also, mono-dispersed, single Au atoms were not associated with high activity. First-principles density-functional calculations showed that Au nanoparticles bond only weakly to the stoichiometric anatase (001) surface. Oxygen vacancies in the substrate act as anchors to bond the nanoparticles in place, although at sufficiently high temperatures, the particles can diffuse and coalesce. Using the Au nanoparticle structures seen in the Z-contrast STEM as a starting point, we were able to investigate the catalytic properties. Unlike bulk gold, these nanometer-sized particles are able to adsorb both CO and O₂ molecules. The CO

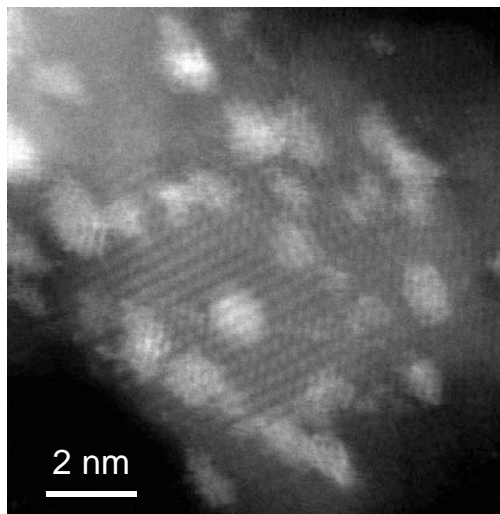


Fig. 3 STEM micrographs of highly active Au / TiO₂ (anatase). Bright patches are Au particles ~ 1nm diameter and mostly one monolayer thick.

adsorbs in an end-on configuration, while the O_2 adsorbs preferentially at the perimeters of the nanoparticles, bonding to both the nanoparticle and the substrate. This suggests that the active sites for O_2 absorption may be at the perimeter of the nanoparticles, explaining the decrease in activity with increasing particle size. In agreement with experiment, single Au atoms adsorbed at vacancies do not bond CO or O_2 . (Submitted to Science)

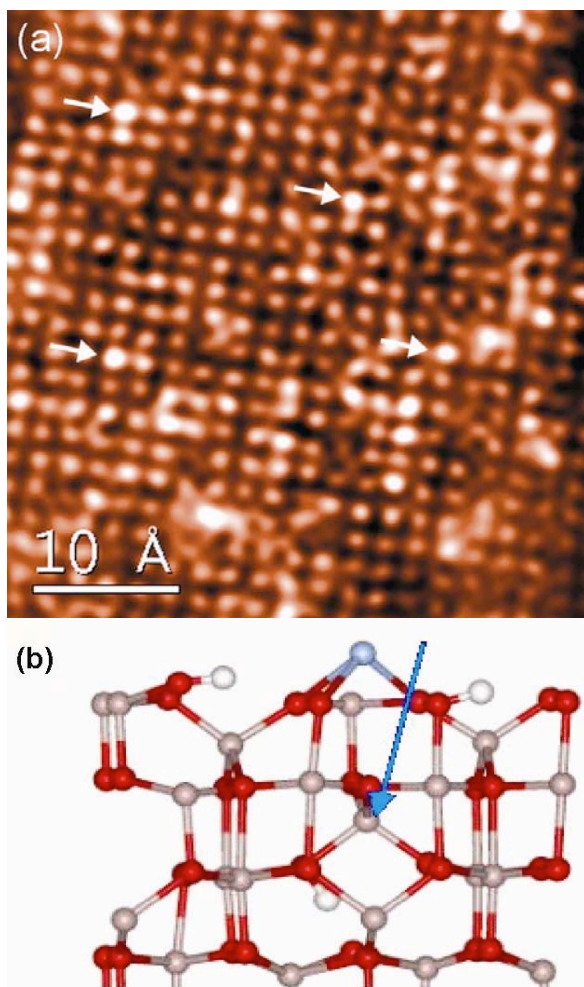


Fig. 2. (a) Z-contrast STEM image of the $\langle 100 \rangle$ surface of $g\text{-Al}_2\text{O}_3$; bright spots correspond to La atoms on the surface; several examples of preferred sites are arrowed. (b) calculated lowest-energy configuration of La atom (blue) on the $\langle 100 \rangle$ surface of $g\text{-Al}_2\text{O}_3$ above an Al-O column; the Al atom displaced by La is arrowed.

Al_2O_3 observed by STEM was shown to correspond to the lowest energy configuration (Fig. 2(b)).

The combination of sub-Ångstrom resolution imaging and theory clearly demonstrates that the stabilization is caused by isolated La atoms that bind strongly to

Mechanism of thermal stabilization of $g\text{-Al}_2\text{O}_3$ catalyst supports by La addition: $g\text{-Al}_2\text{O}_3$, a widely used catalytic support material, undergoes an undesirable phase transition to $\alpha\text{-Al}_2\text{O}_3$ at 1000°C with loss of surface area. Addition of La dopants was previously shown to extend the stability range to 1250°C , but the mechanism of the stabilization was never determined and was speculated to result from the formation of La_2O_3 or LaAlO_3 monolayers on the surface or substitution of Al by La in the bulk. To examine La distribution, samples of La-doped $g\text{-Al}_2\text{O}_3$ were investigated by Z-contrast STEM. It was found that La atoms are distributed on the surface of $g\text{-Al}_2\text{O}_3$ in an uncorrelated fashion; no clusters or ordered monolayers were observed (Fig. 2(a)). On the $\langle 100 \rangle$ surface of $g\text{-Al}_2\text{O}_3$ La atoms were found to occupy predominantly the positions directly above Al-O columns (examples arrowed).

Density functional theory calculations, conducted in parallel, have demonstrated that La atoms have overwhelming preference for the surface positions and are very strongly bound to the surface. In full agreement with the microscopic observations, no tendency towards cluster formation was found. The La site on the $\langle 100 \rangle$ surface of $g\text{-Al}_2\text{O}_3$

the surface of $g\text{-Al}_2\text{O}_3$, thus pinning it and preventing sintering and phase transformation. (Nature Materials, **3**, 143 (2004)).

DOE Interest

Catalysts are now used at some point in a vast number of modern manufacturing processes, from drug or fuel production to catalytic converters in cars, and will be of increasing importance to the worldwide economy. Understanding how and why they act is greatly assisted by the ability to determine individual cluster configurations.

Future Plans

The newly aberration-corrected STEM provides unique sensitivity for imaging the atomic configurations of supported cluster catalysts, and when combined with reaction rate measurements and density-functional calculations promises significant new insight into many previously unresolved issues, including:

The origin of the synergistic effect of bimetallic catalysts: We presently have the ability to distinguish individual second row transition metals from third row metals, eg. Pt/Ru and Au/Pd. We will investigate the preferred configurations of bimetallic clusters with measured reactivities in collaboration with Profs. M. Amiridis and R. Adams, University of S. Carolina.

Examination of different support materials: In collaboration with other groups we will investigate the role of different support materials, both experimentally, where the single atom-resolved Z-contrast microscopy provides unique insight, and theoretically using DFT calculations.

Three-dimensional imaging: We presently have about a 1 nm depth of view which allows us to image individual atoms with sub-Ångstrom lateral resolution and sub-nm depth resolution. We will investigate techniques for 3D visualization of supported catalyst clusters.

In-situ imaging with 3D atomic resolution: A next generation, aberration-corrected STEM with expected 0.4 Ångstrom lateral and 4 Ångstrom depth resolution has been approved by BES Division of Materials Sciences. This microscope will incorporate an in-situ capability for temperatures up to $\sim 800^\circ\text{C}$ under reaction conditions.

Publications (2003-4)

1. N. Shibata, S. J. Pennycook, T. R. Gosnell, G. S. Painter, W. A. Shelton, and P. F. Becher, "Observation of rare-earth segregation in silicon nitride ceramics at subnanometre dimensions," *Nature* **428**, 730 (2004).
2. S. W. Wang, A. Y. Borisevich, S. N. Rashkeev, M. V. Glazoff, K. Sohlberg, S. J.

- Pennycook, and S. T. Pantelides, "Dopants adsorbed as single atoms prevent degradation of catalysts," *Nature Materials* **3**, 274 (2004).
3. Varela, M., S. D. Findlay, et al. "Spectroscopic imaging of single atoms within a bulk solid." *Physical Review Letters* **92** art. no. 095502 (2004).
 4. M. Varela, A. R. Lupini, S. J. Pennycook, Z. Sefrioui, and J. Santamaria, "Nanoscale Analysis of $\text{YBa}_2\text{Cu}_3\text{O}_{7-x}/\text{La}_{0.67}\text{Ca}_{0.33}\text{MnO}_3$ Interfaces," *Solid State Electron.* **47**, 2245 (2003).
 5. A. C. Diebold, B. Foran, C. Kisielowski, D. Muller, S. J. Pennycook, E. Principe, and S. Stemmer, "Thin Dielectric Film Thickness Determination by Advanced Transmission Electron Microscopy," *Microsc. Microanal.* **9**, 493 (2003).
 6. C. Cantoni, D. K. Christen, M. Varela, J. R. Thompson, S. J. Pennycook, E. D. Specht, and A. Goyal, "Deposition and Characterization of $\text{YBa}_2\text{Cu}_3\text{O}_{7-d}/\text{LaMnO}_3/\text{MgO}/\text{TiN}$ Heterostructures on Cu Metal Substrates for Development of Coated Conductors," *J. Mater. Res.* **18**, 2387 (2003).
 7. L. J. Allen, S. D. Findlay, A. R. Lupini, M. P. Oxley, and S. J. Pennycook, "Atomic Resolution Electron Energy Loss Spectroscopy Imaging in Aberration Corrected Scanning Transmission Electron Microscopy," *Phys. Rev. Lett.* **91**, 105503/1 (2003).
 8. A. R. Lupini and S. J. Pennycook, "Localization in Elastic and Inelastic Scattering," *Ultramicroscopy* **96**, 313 (2003).
 9. S. J. Pennycook, A. R. Lupini, A. Kadavanich, J. R. McBride, S. J. Rosenthal, R. C. Puetter, A. Yahil, O. L. Krivanek, N. Dellby, P. D. Nellist, G. Duscher, L. G. Wang, and S. T. Pantelides, "Aberration-Corrected Scanning Transmission Electron Microscopy: The Potential for Nano- and Interface Science," *Zeitschrift fur Metallkunde* **94**, 350 (2003).
 10. A. Franceschetti, S. J. Pennycook, and S. T. Pantelides, "Oxygen Chemisorption on Au Nanoparticles," *Chem. Phys. Lett.* **374**, 471 (2003).
 11. M. F. Chisholm, Y. H. Wang, A. R. Lupini, G. Eres, A. A. Puretzky, B. Brinson, A. V. Melechko, D. B. Geohegan, H. T. Cui, M. P. Johnson, S. J. Pennycook, D. H. Lowndes, S. Arepalli, C. Kittrell, S. Sivaram, M. Kim, G. Lavin, J. Kono, R. Hauge, and R. E. Smalley, "Comment on 'Single Crystals of Single-Walled Carbon Nanotubes Formed by Self-Assembly'," *Science* **300**, U2 (2003).
 12. D. Kumar, S. J. Pennycook, J. Narayan, H. Wang, and A. Tiwari, "Role of Silver Addition in the Synthesis of High Critical Current Density MgB_2 Bulk Superconductors," *Supercond. Sci. Tech.* **16**, 455 (2003).
 13. X. Fan, R. Buczko, A. A. Puretzky, D. B. Geohegan, J. Y. Howe, S. T. Pantelides, and S. J. Pennycook, "Nucleation of Single-Walled Carbon Nanotubes," *Phys. Rev. Lett.* **90**, 145501/1 (2003).
 14. S. N. Rashkeev, K. Sohlberg, M. V. Glazoff, J. Novak, S. J. Pennycook, and S. T. Pantelides, "Transition Metal Atoms on Different Alumina Phases: The Role of Subsurface Sites on Catalytic Activity," *Phys. Rev. B* **67**, 115414/1 (2003).
 15. W. I. Park, G.-C. Yi, M. Kim, and S. J. Pennycook, "Quantum Confinement Observed in ZnO/ZnMgO Nanorod Heterostructures," *Adv. Mater.* **15**, 526 (2003).
 16. E. Abe, S. J. Pennycook, and A. P. Tsai, "Direct Observation of a Local Thermal Vibration Anomaly in a Quasicrystal," *Nature* **421**, 347 (2003).

High-resolution homo- and heteronuclear correlation NMR spectroscopy in solid state; applications to heterogeneous catalysis

Coworker: J. W. Wiench; Postdoc: J. Trebosc; Collaborators: V.S.-Y. Lin, R.J. Angelici, J.-P. Amoureux; Graduate student: S. Huh

Ames Laboratory, 230 Spedding Hall, Ames, IA 50011, mpruski@iastate.edu

Goal

Solid state NMR is used to investigate the materials and chemical reactions involved in heterogeneous catalysis and materials science.^{1-3,9-16,18-20} Development of new NMR techniques is the second major research area.^{4-8,17,21,22} An overview of selected results involving internuclear correlation methods is given below.

Recent Progress

MQMAS-J-HETCOR NMR. We have recently demonstrated a new solid state NMR method that provides high-resolution two-dimensional (2D) heteronuclear correlation (HETCOR) spectra between quadrupolar and spins-1/2 nuclei.²¹ The technique uses multiple-quantum magic angle spinning (MQMAS) NMR to achieve high resolution and *through-bond* (*J*) coupling for polarization transfer. As shown in Figure 1, this method affords a dramatically improved resolution when compared with the standard MAS-based approach. High selectivity, lack of orientational dependence and insensitivity to molecular motion proved useful in exploiting of this method for studying the bond topology and local order in catalysts.

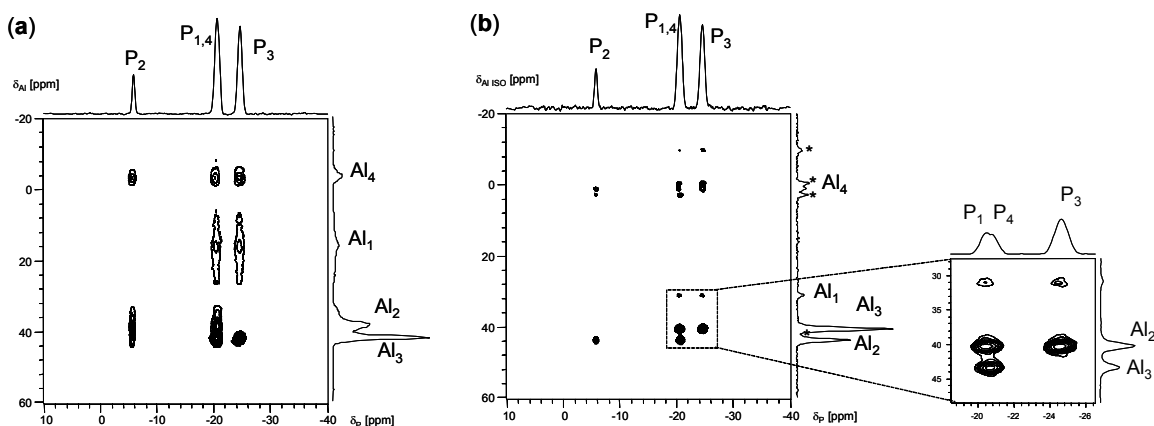


Figure 1. $^{27}\text{Al} \rightarrow ^{31}\text{P}$ spectrum of $\text{AlPO}_4\text{-14}$ catalyst obtained with MAS- (a) and MQMAS-J-HETCOR (b) methods at 14.1 T. All Al and P sites are resolved in spectrum (b), which provides isotropic resolution in both dimensions.

FS-J-RES NMR. We demonstrated the frequency-selective measurements of internuclear *distances* and *J coupling constants* in a multispin system SI_n , where S spin is a quadrupolar (observed) nucleus and I 's represent spin-1/2 nuclei.^{17,22} This method can also be used under high-resolution provided by MQMAS, which offers the possibility of measuring a *complete set of internuclear distances and J couplings in complex systems.*

Heterogeneous catalysts supported on silica materials. We demonstrated the applicability of several hetero- and homonuclear NMR methods to characterize the silica supports before and after tethering with various metal complexes and other functional groups (i.e. ‘gatekeepers’). An example of ^1H - ^{13}C HETCOR spectrum of an MCM-41 silica functionalized with allyltrimethoxysilane (ALTMS) is shown in Figure 2a. A double-quantum ^1H - ^1H correlation spectrum, which emphasizes two-spin correlations in this sample, is shown in Figure 2b.

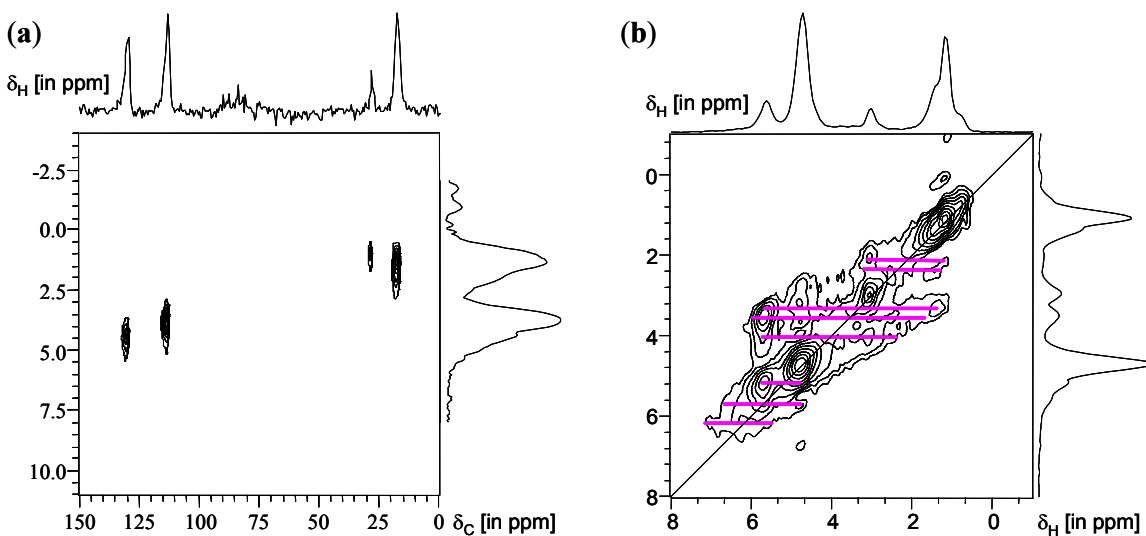


Figure 2. (a) ^1H - ^{13}C CP HETCOR spectrum of MCM-41 functionalized with ALTMS recorded at 9.4 T under 10 kHz MAS, using frequency switched Lee-Goldburg irradiation during ^1H evolution. (b) ^1H DQ MAS NMR spectrum of this sample recorded under 40 kHz MAS at 9.4 T.

DOE Interest

These fundamental studies will result in better understanding of the mechanisms of homogeneous and heterogeneous catalytic reactions, which include the removal or addition of heteroatoms (S, N, O, and Cl) by oxidation or hydrogenation, using primarily transition metal complexes and oxides as catalysts.

Of particular importance to the catalysis program will be the application of multidimensional NMR techniques to determine the structure, concentration, spatial distribution and mobility of various functional groups and reactants on the catalyst surface in 2-D and 3-D controlled environments, e.g., in multifunctional mesoporous materials. Development of state-of-the-art techniques in solid state NMR spectroscopy will provide new tools for these investigations.

Future Plans

Characterization of functionalized silica materials by solid state NMR spectroscopy. Our studies demonstrated that solid state NMR spectroscopy of mesoporous materials yields precise information about the nature of unfunctionalized silica surfaces as well as the structure and distribution of various groups that are anchored on the walls. We will use a suite of 1D and 2D NMR methods, mostly in the solid state, to (a) characterize the silica supports before and after tethering with metal complexes, (b) study the concentration, the conformational details and the mobility of adsorbed (tethered) and reacting species, and (c) monitor the catalytic reactions and the catalysts' stability under various reaction conditions. Some of the studies performed on the solid-liquid interfaces may involve liquid state NMR methodology.

Development of improved NMR methods. We plan to continue the development of improved NMR methods for studying the spin-1/2 and half-integer quadrupolar nuclei. We will explore the experimental strategies for enhancing the efficiency of homo- and heteronuclear correlation NMR spectroscopy in solids via improved methods of polarization transfer and high resolution techniques. Further increase in sensitivity will be achieved by using a higher magnetic field.

Publications (since 2002)

1. C.J. Fontenot, J.W. Wiench, G.L. Schrader and M. Pruski, "¹⁷O MAS and 3QMAS NMR Investigation of Crystalline V₂O₅ and Layered V₂O₅·nH₂O Gels", *J. Am. Chem. Soc.*, **2002**, 124, 8435-8444.
2. V. S.-Y. Lin, M.-K. Han, W. Deng, S. Kuroki, D. Radu, B. H. Shanks and M. Pruski, "Oxidative Polymerization of 1,4-Diethynylbenzene into Highly Conjugated Oligo(phenylene butadiynylene) Polymer Within the Channels of Surface-functionalized Mesoporous Silica and Alumina Materials", *J. Am. Chem. Soc.*, **2002**, 124, 9040-9041.
3. N. Savargaonkar, D.O. Uner, M. Pruski and T.S. King, "Determination of Hydrogen Adsorption and Desorption Kinetics on Silica Supported Pt, Rh and Ru Catalysts via Selective Excitation NMR Spectroscopy", *Langmuir*, **2002**, 18, 4005-4009.
4. R. Lefort, J.-P. Amoureux, J.W. Wiench and M. Pruski, "Optimization of Data Acquisition and Processing in Carr-Purcell-Meiboom-Gill MQMAS NMR", *J. Chem. Phys.*, **2002**, 116, 2493-2501.
5. J.-P. Amoureux and M. Pruski, "Advances in MQMAS NMR", *Encyclopedia of Nuclear Magnetic Resonance*, Ed. D. M. Grant and R. K. Harris, Volume 9: *Advances in NMR*, 226-251, John Wiley & Sons Ltd., Chichester, **2002**.
6. C. Fernandez, C. Morais, J. Rocha and M. Pruski, "High-resolution Heteronuclear Correlation Spectra between ³¹P and ²⁷Al in Microporous Aluminophosphates", *Solid State NMR*, **2002**, 21, 61-70.

7. J.-P. Amoureux and M. Pruski, "Theoretical and Experimental Assessment of Single- and Multiple-Quantum Cross Polarization in Solid-State NMR", *Mol. Phys.*, **2002**, 100, 1595-1613.
8. M. Pruski, J.-P. Amoureux and C. Fernandez, "Progress in High Resolution Solid State NMR of Quadrupolar Nuclei: Applications to Porous Materials and Catalysts", *NATO Series, Mathematics, Physics and Chemistry*, **2002**, 76, 107-114.
9. V.P. Balema, J.W. Wiench, M. Pruski and V.K. Pecharsky, "Solvent-free Mechanochemical Synthesis of Phosphonium Salts", *Chem. Commun.*, **2002**, 724-725.
10. J.W. Wiench, B. Tischendorf, J.U. Otaigbe and M. Pruski, "Structure of zinc polyphosphate glasses studied by two-dimensional solid and liquid state NMR", *J. Mol. Struct.*, **2002**, 602-603, 145-158.
11. W. Deng, P. Bodart, M. Pruski and B.H. Shanks, "Characterization of Mesoporous Alumina Molecular Sieves Synthesized by Nonionic Templating", *Microporous Materials*, **2002**, 52, 169-177.
12. V.P. Balema, J.W. Wiench, M. Pruski and V.K. Pecharsky, "Solvent-free Mechanochemical Transformations of Pt(II) Complexes", *Chem. Commun.*, **2002**, 1606-1607.
13. V.P. Balema, J.W. Wiench, M. Pruski, and V.K. Pecharsky, "Mechanically Induced Solid-state Generation of Phosphorus Ylides and the Solvent-free Wittig Reaction", *J. Am. Chem. Soc.*, **2002**, 124, 6244-6245.
14. K.J. Stranger, J.W. Wiench, M. Pruski and R.J. Angelici, "³¹P NMR and IR Characterization of Enantioselective Olefin and Arene Hydrogenation Catalysts Containing a Rhodium-Chiral Phosphine Complex Tethered on Silica", *J. Mol. Catal.*, **2003**, 195, 63-82.
15. S. Huh, J.W. Wiench, B.G. Trewyn, S. Song, M. Pruski and V.S.-Y. Lin, "Tuning of Particle Morphology and Pore Properties in Mesoporous Silicas with Multiple Organic Functional Groups", *Chem. Comm.*, **2003**, 2364-2365.
16. S. Huh, J.W. Wiench, J.-C. Yoo, M. Pruski and V.S.-Y. Lin, "Organic Functionalization and Morphology Control of Mesoporous Silicas via a Co-condensation Synthesis Method", *Chem. Mater.*, **2003**, 15, 4247-4256.
17. J. Trebosc, J.-P. Amoureux, J.W. Wiench and M. Pruski, "Simultaneous Frequency-Selective Solid-State NMR Analysis of Internuclear Distances and Through-Bond Connectivities in the Presence of Quadrupolar Nuclei", *Chem. Phys. Lett.*, **2003**, 374, 432-438.
18. S. Huh, H.-T. Chen, J.W. Wiench, M. Pruski and V.S.-Y. Lin, "Controlling the Selectivity of Competitive Nitroaldol Condensation by Using a Bifunctionalized Mesoporous silica Nanosphere-Based Catalytic System", *J. Am. Chem. Soc.*, **2004**, 126, 1011-1012.

19. D.R. Radu, C.-Y. Lai, J.W. Wiench, M. Pruski and V.S.-Y. Lin, "Gatekeeping Layer Effect: A Poly(lactic acid)-Coated Mesoporous Silica Nanosphere-Based Fluorescence Probe for Detection of Amino-Containing Neurotransmitters", *J. Am. Chem. Soc.*, **2004**, 126, 1640-1641.
20. J.W. Wiench, V.P. Balema, V.K. Pecharsky and M. Pruski, "Solid State ^{27}Al NMR Investigation of Thermal Decomposition of LiAlH_4 ", *J. Solid State Chem.*, **2004**, 177, 648-653.
21. J.W. Wiench and M. Pruski, "Probing Through Bond Connectivities with MQMAS NMR", *Solid State NMR*, in press.
22. J. Trebosc, J.-P. Amoureux, L. Delevoye, J. Wiench and M. Pruski, "Frequency Selective Measurement of Heteronuclear Scalar Couplings in Solid-State NMR", *Solid State Sci.* submitted.

This page intentionally left blank.

Carbon-13 NMR of Solid State Hydrocarbons and Related Substances

Senior Staff: Alderman, D. W., Facelli, J. C., Orendt, A. M., Mayne, C. L., Solum, M. S., Arif, A. M.

Postdocs: Strohmeier, M., Steuber, D., Hu, J. Z., Barich, D. H., Gunneau, F. N., Veranth, J. M., Jiang, Y.

Students: Clawson, J., Bai, S., Iuliucci, R. J., Steuber, D.

Collaborators: Scott, L. T., Taylor, C. M. V., Ye, C., Parry, R. W., Boerio-Goates, J., Asay, B., Hiskey, M. A., Harris, R. K., Winans, R. E., Tomczyk, Hunt, J. E., Anderson, K. L., Fletcher, T. H., Miller, J. S., Sarofim, A. F., Wind, R. A., Ellis, P. D.

Department of Chemistry, University of Utah, Salt Lake City, UT 84112

grant@chemistry.utah.edu

pug@vpres.adm.utah.edu

Goal

Development and exploitation of new solid state carbon-13 experimental techniques to obtain the chemical shift tensors in hydrocarbons and related substances including correlation of these data with advance theoretical constructs. These data are then employed to characterize complex structures and systems that evolve from simple hydrocarbons.

Recent Progress

Spectroscopic developments in our laboratory include a new solid-state **INADEQUATE** method and a new **FIREMAT** variant of a single crystal experiment that has high promise for smaller single crystals. We have also been pleased to note very promising synergism of x-ray powder experiments which, with **REITVELD** analysis, complements our NMR efforts. The extension of our ^{13}C NMR efforts into the ^{15}N NMR field is evolutionary in character and fits nicely into our overall strategy of characterizing molecular structures.

The importance of the chemical shift tensor in modeling molecular structure continues to enjoy success. This is made possible in part by improved theoretical methods for intermolecular lattice effects that become significant whenever the molecule exhibits high charge polarization effects. We therefore are focusing on new experimental methods that provide this information with better reliability and convenience.

Collaborations with personnel at both ANL and LANL on **REITVELD** analysis of powder x-ray data, has demonstrated the power of our **FIREMAT** experiment for estimating the initial structural features of polymorphs of solid organic materials which significantly improves the convergence of the **REITVELD** software. This approach is especially fruitful in powder samples when complete crystallographic data are not presently available from single crystals. The appearance of impurities, mixed crystals, polymorphs, and multiple

molecules per asymmetric unit are readily characterized by solid-state NMR, whereas it is difficult to determine this information directly from micro-crystalline powder diffraction data, especially on materials of unknown structure. Furthermore, chemical shift tensors provide reasonably good estimates of an initial set of vicinal angles that speeds up the data reduction of powder diffraction histograms from several months to merely hours in relatively large molecules that presently are too large to do the analysis without good initial estimates of the conformational angles. There is also some evidence that the chemical shift tensors give a more sensitive estimate of bond distances between directly bonded atoms. The mutual verification of the solid state NMR and diffraction data from the Sector 1 beam line at the Advanced Photon Source (APS) at Argonne exhibits the synergism between the two techniques, and exhibits the success one can have on molecules in the 500 to 2000 Dalton range.

The **INADEQUATE** experiment alluded to above is very useful when more than one molecular isomer is obtained due to mixed crystals and/or multiple molecules per asymmetric unit. The different isomeric molecular structures exhibit closely paired lines at corresponding atomic positions and their assignment into molecular sets is greatly enhanced by the **INADEQUATE** connectivities that link directly bonded atoms. These data are valuable in assigning sets of lines when two or more unique molecular structures are present in the sample.

DOE Interest

Some of our most recent results, not yet in published form, are still exploratory and are woven into our future work. These results document, in large measure, the continuation of present efforts with major emphasis placed on recently developed theoretical and experimental techniques. Synergism with applied efforts is established by our participation in the DOE/ASCI alliance program that continues to employ theory and experimental methods developed largely with DOE/BES support. We will continue to collaborate with staff at: (a) the ANL/APS sector 1 beam line who assist in acquiring powder diffraction data on structures containing more than one molecule per asymmetric unit; (b) we plan to acquire low angle neutron scattering data on the GLAD facility on the ANL reactor to study the structure of amorphous PAH materials and correlate these data with NMR data on the same samples; (c) continue our collaboration with Dr. Randy Winans (Chemistry Division, ANL) on soot samples collected from various pyrolysis/combustion sources in order to maximize the structural information provided by combining NMR and mass spectroscopy data.

Future Plans

Our future plans are focused in three areas. (1) Refinement of the work on single crystal FIREMAT experiments (taken at the icosahedral angle) on small crystals that provide the data needed to determine full chemical shift tensors. (2) Continue to explore the synergism between solid state NMR and X-ray powder diffraction data with special emphasis on molecules which crystallize with more than one molecule per asymmetric unit. (3) Expand the data base on chemical shift tensors to include the effects of ring strain and curvature with an emphasis of cyclopentafused polycyclic aromatic hydrocarbons. Such structures are usually highly toxic and are always found in pyrolysis/combustion environments.

Publications (2000-2004)

1. Carbon-13 Shift Tensors in Polycyclic Aromatic Compounds. 8. A Low Temperature NMR Study of Coronene and Corannulene, Orendt, A. M.; Facelli, J. C.; Bai, Shi; Rai, A.; Gossett, M.; Scott, L.T.; Boerio-Goates, J.; Pugmire, R.J.; and Grant, D.M. *J.Phys.Chem.*, **2000**, *104*, 149-155.
2. Modified Spectral Editing Methods for ^{13}C CP/MAS Experiments in Solids, Hu, J. Z., Harper, J. K., Taylor, C., Pugmire, R. J., and Grant, D. M., *J. Mag. Res.*, **2000**, *142*, 326-330.
3. ^1H Dynamic Nuclear Polarization in Supercritical Ethylene at 1.4 T, Wind, R.A.; Bai, S.; Hu, J. Z.; Solum, M.S.; Ellis, P.D.; Grant, D.M.; Pugmire, R.J.; Taylor, C.M.V.; and Yonker, C.R., *J. Mag. Res.*, **2000**, *143*, 233-239.
4. Investigation of Polyethylene by Means of Magic Angle Turning and Separated-Local-Field Experiments, by Hu, J.Z.; Want, W.; Bai, S.; Alderman, D.W.; Pugmire, R.J.; Taylor, C.M.V., and Grant, D.M., *Macromolecules*, **2000**, *33*, 3359-3367.
5. ^1H and ^{15}N Dynamic Nuclear Polarization Studies of Carbazole. Hu, J.Z.; Solum, M.S.; Wind, R.A.; Nilsson, B.L.; Peterson, M.A.; Pugmire, R.J.; and Grant, D.M., *J.Phys.Chem.*, **2000**, *104*, 4413-4420.
6. A High Resolution ^{13}C 3D CSA-CSA-CSA Correlation Experiment by Means of Magic Angle Turning, Hu, Z. Z.; Ye, C.; Pugmire, R. J.; and Grant, D. M. *J.Mag.Res.*, **2000**, *145*, 230-236.
7. Carbon-13 Chemical-Shift Tensors in Polycyclic Aromatic Compounds, 9. $^1\text{Biphenylene}$, Barich, D. H.; Orendt, A. M.; Pugmire, R. J.; and Grant, D. M, *J.Phys.Chem.A*, **2000**, *104*, 8290-8295.
8. Structural Determination in Carbonaceous Solids Using Advanced Solid State NMR Techniques, Hu, J. Z.; Solum, M. S.; Taylor, C. M. V.; Pugmire, R. J. and Grant, D. M., *Energy & Fuels*, **2001**, *15*, 14-22.
9. ^{13}C Chemical shift tensors in an analogous series of heterosubstituted polycyclic aromatic compounds, Barich, D. H.; Facelli, J. C.; Hu, J. Z.; Alderman, D. W.; Want, W.; Pugmire, R. J.; and Grant, D. M., *Magn. Reson. Chem.* **2001**, *39*, 115-121.
10. Investigation of Polymorphs of Dimethyl-3, 6-Dichloro-2, 5-Dihydroxyterephthalate by ^{13}C Solid State NMR, Strohmeier, M.; Orendt, A. M.; Alderman, D. W.; and Grant, D. M. *J. Am. Chem. Soc.*, **2001**, *123*, 1713-1722.
11. Carbonates, Thiocarbonates, and the Corresponding Monoalkyl Derivatives: I. Their Preparation and Isotopic ^{13}C NMR Chemical Shifts, Stueber, D.; Patterson, D.; Mayne, C. L.; Orendt, A. M.; Grant, D. M. and Parry, R. W, *Inorganic Chem.* **2001**, *40*, 1902-1911.
12. Carbonates, Thiocarbonates, and the Corresponding Monoalkyl Derivatives: II. The X-Ray Crystal Structure of Potassium Methyl-Trithiocarbonate ($\text{KS}_2\text{CSC}_2\text{H}_3$), Stueber, D.; Arif, A. M.; Grant, D. M.; and Parry, R. W. , *Inorganic Chem.* **2001**, *40*, 1912-1914.
13. The Calculation of ^{13}C Chemical Shift Tensors in Ionic Compounds Utilizing Point Charge Arrays Obtained from Ewald Lattice Sums, Stueber, D.; Guenneau, F. N.; and Grant, D. M., *J. Chem. Phys.*, **2001**, *114*, 9236-9243.
14. Investigation of the Structural Conformation of Biphenyl by Solid State ^{13}C NMR, and Quantum Chemical NMR Shift Calculations, Barich, D. H.; Grant, D. M.; Pugmire, R. J.; and Iulicucci, R. J., *J.Phys.Chem. A*, **2001**, *105*, 6780-6784.
15. A Novel Dipolar-Dephasing Method for Slow Magic Angle Turning (MAT) Experiment, Hu, J. Z.; Taylor, C. M. V.; Pugmire, R. J.; and Grant, D. M., *J. Mag. Res.* **2001**, *152*, 7-13.
16. Carbonates, Thiocarbonates, and the Corresponding Monoalkyl Derivatives: III. The ^{13}C Chemical Shift Tensors in Potassium Carbonate, Bicarbonate, and Related Monomethyl Derivatives, Sueber, D.; Oredt, A. M.; Facelli, J. C.; Parry, R. W.; and Grant, D. M.; *Solid State NMR*, **2002**, *22*, 29-49.
17. The ^{13}C Chemical Shift Tensor Principal Values and Orientatins in Dialkyl Carbonates and Trithiocarbonates, Stueber, D. and Grant, D. M., *Solid State NMR*, **2002**, *22*, 439-457.
18. Obtaining Molecular and Structural Information from ^{13}C - ^{14}N Systems with ^{13}C FIREMAT Experiments, Strohmeier, M.; Alderman, D. W.; and Grant, D. M.; *J. Magn. Reson.* **2002**, *155*, 263-277.

19. ^{15}N Chemical Shift Tensors of β -HMX, Clawson, J. S.; Strohmeier, M.; Stueber, D., Orendt, A. M.; Barich, D. H.; Asay, B.; Hiskey, M. A.; Pugmire, R. J.; and Grant, D. M.; *J Phys. Chem. A* **2002**, *106*, 6352-6357.
20. Carbon-13 Chemical-Shift Tensors in Polycyclic Aromatic Compounds; Fluoranthene and Decacyclene, Barich, D.H.; Hu, J. Z.; Pugmire, R. J.; and Grant, D. M.; *J. Phys. Chem.* **2002**, *106*, 6477-6482.
21. ^{13}C and ^{15}N Chemical Shift Tensors in adenosine, Guanosine Dihydrate, 2'-Deoxythymidine, and Cytidine, Stueber, D.; and Grant, D. M.; *J. Am. Chem. Soc.* **2002**, *124*, 10539-10551.
22. Five- π Pulse Magic-Angle Turning Spectra of Solids, Grant, D. M.; *Encyc. of NMR* (D. M. Grant and R. K. Harris, Eds.), Wiley, Chichester, England, **2002**, *2* (Supplemental Volume) 73-90.
23. Nitrogen-15 Chemical Shift Tensors and Organic Structure, Pugmire, R. J.; 2002, *Encyc. of NMR*. (D. M. Grant and R. K. Harris, Eds.) Wiley, Chichester, England, **2002**, *2* (Supplemental Volume) 298-306.
24. The Study of Anthracene Aerosols by Solid State NMR and ESR, Solum, M. S.; Veranth, J. M.; Jiang, Y. J.; Orendt, A. M.; Sarofim, Adel F.; and Pugmire, R. J.; *Energy Fuels*, **2003**, *17*, 738-743.
25. ^{15}N Chemical Shift Tensors of Substituted Hexaazaisowurtzitanes: The Intermediates and By-products in the Synthesis of CL20, Clawson, J. S.; Anderson, K. L.; Pugmire, R. J. and Grant, D. M., *J. Phys. Chem.* **2004**, (in press).
26. A New Sensitive Isotropic-Anisotropic Separation Experiment—SPEED MAS. Strohmeier, M.; Grant, D. M., *J. Magn. Reson.* **2004**, (in press).

Bio-inspired Iron Catalysts for Hydrocarbon Oxidations

Project initiated September 1, 2003; 2003-04 budget: \$143,000 total costs

Postdoctoral associate: Megumi Fujita

Graduate student: Paul Oldenburg

Department of Chemistry and Center for Metals in Biocatalysis, University of Minnesota, Minneapolis, Minnesota 55455

Phone: 612 625 0389; fax: 612 624 7029; e-mail: que@chem.umn.edu

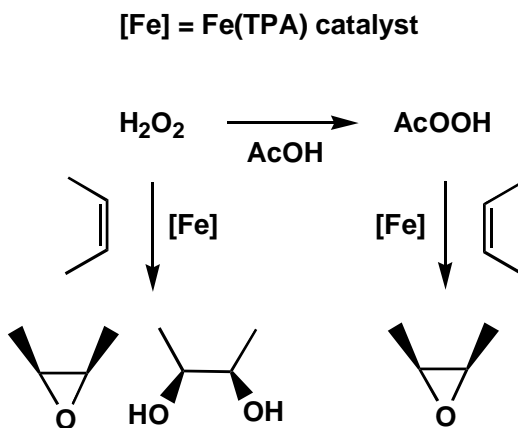
Goal

Develop iron catalysts for hydrocarbon oxidations inspired by nonheme iron oxygenases and to understand their mechanism of action

Recent progress

In situ formation of peracetic acid from H_2O_2 and acetic acid catalyzed by $Fe(TPA)$:

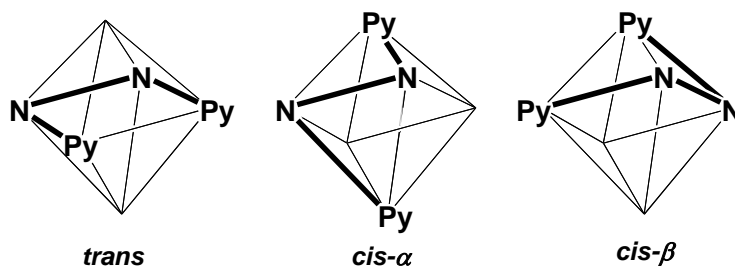
We have previously demonstrated that $Fe^{II}(TPA)$, the iron(II) complex with tris(2-pyridylmethyl)amine, serves as an efficient catalyst for the H_2O_2 -mediated oxidation of olefins to epoxides and cis-diols. In the case of cyclooctene, the oxidations in CH_3CN are stereospecific and an epoxide-to-diol ratio of 1:1.2 is observed. Interestingly, we have found that the addition of increasing amounts of acetic acid results in a shift of the ratio to 16:1 in favor of epoxide with a 7-fold excess of acetic acid over H_2O_2 . The same results are obtained with the use of peracetic acid. We thus conclude that $Fe(TPA)$ catalyzes *in situ* formation of peracetic acid. This method may provide a new route to this important oxidant from its readily available and cheap precursors.



Topological control of the epoxide-to-diol ratio in iron-catalyzed olefin oxidation:

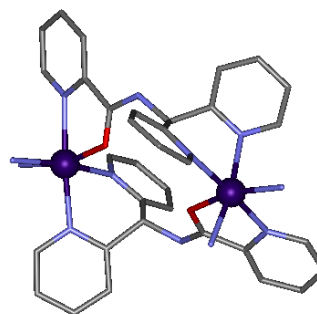
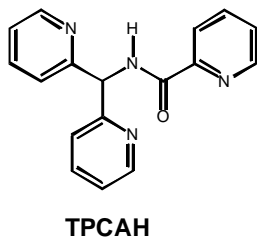
In exploring ligands related to TPA for the catalysis of olefin oxidation, we previously found that the tetradentate BPMCN ligand (BPMCN = *N,N'*-dimethyl-*N,N'*-bis(2-pyridylmethyl)-*trans*-1,2-diaminocyclohexane) forms iron(II) complexes in both the *cis*- α and the *cis*- β topology. Both isomers catalyzed olefin oxidation efficiently but with significantly different epoxide-to-diol ratios. The *cis*- α isomer afforded almost all

epoxide (8:1), while the *cis*- β isomer afforded predominantly diol (1:4). Although both isomers were characterized by X-ray crystallography, the possible participation of a third ligand topology related to the *cis*- α isomer, the so-called *trans* isomer with all four ligating nitrogen atoms occupying the equatorial plane, could not be excluded from consideration. A ligand enforcing such a planar geometry, *N,N'*-dimethyl-*N,N'*-bis(2-pyridylmethyl)-1,5-diazacyclooctane, was thus synthesized, and its iron complex made and characterized. As hoped for, this complex catalyzed olefin oxidation and afforded an epoxide-to-diol ratio of 10. This result confirms the importance of ligand topology in determining the course of olefin oxidation by this family of iron catalysts.



New ligand frameworks:

We have initiated a study on the iron complex of TPCAH, a ligand related to TPA in which a benzylic methylene group is converted to a carbonyl moiety. This ligand would be expected to have a weaker ligand field than TPA and may thus favor a high-spin state without the introduction of sterically hindering 6-methyl substituents as in the case of 6-Me₃-TPA. The X-ray crystal structure of the iron(II) perchlorate complex [Fe(TPCAH)N(NCCN₃)₂]₂(ClO₄)₄ reveals that TPCAH acts as a tetradentate ligand but to two metal centers and the complex has a dimeric structure in the solid state. Perhaps surprisingly, the complex nevertheless catalyzes olefin oxidation with H₂O₂ as oxidant with an epoxide-to-diol ratio of 36:1. Isotope labeling studies using H₂¹⁸O₂ and H₂¹⁸O (cyclooctene as a substrate)



displayed a labeling pattern that indicates an epoxidation mechanism resembling that of TPA (Class A low-spin catalyst). Furthermore the use of *cis*- and *trans*-2-heptenes reveals significant retention of configuration in the epoxide, also consistent with Fe(TPA) behavior. However a high-spin iron(III)-alkylperoxo intermediate can be observed upon addition of tert-butyl hydroperoxide at -40°C in acetonitrile, which is typical of a Class B high-spin catalyst. When the minority diol product was examined in isotope labeling experiments, both oxygen atoms derive from H₂O₂, a pattern typical of Class B catalysts. This case thus raises questions with respect to the correlation between the spin-state and

the type of reaction that we have elaborated upon earlier and emphasizes the point that much remains to be learned about the role the iron center plays in these reactions.

Synthesis of chiral ligands:

Efforts to synthesize polydentate ligands containing optically active centers have been initiated but it is premature to report results from these rather recent efforts.

Interest to DOE

Learning to control the activation of dioxygen and its derivatives by biomimetic iron centers to afford oxidants capable of stereospecific hydrocarbon oxidation is an area of potentially enormous environmental and energy-saving impact. Our initial results suggest that this is an avenue worth further exploration.

Future plans

Continued detailed mechanistic studies of the reactions of peroxides with nonheme iron(II) complexes to understand the molecular basis for the observed branching between olefin epoxidation and cis-dihydroxylation.

Investigation of both structural and electronic factors to affect this branching ratio.

Synthesis of chiral ligands for asymmetric olefin oxidation

Publications (2004)

Fujita, M.; Que, L., Jr. "In situ Formation of Peracetic Acid in Iron-Catalyzed Epoxidations by Hydrogen Peroxide in the Presence of Acetic Acid" *Adv. Synth. Catal.* **2004**, *346*, 190-194.

This page intentionally left blank.

Polynuclear Aromatic Hydrocarbons with Curved Surfaces: Buckybowls

Postdocs: Wang, L. (funded by university)

Students: Bachavala, P.

Collaborators: Sygula, R. (Angelici, R. J., Ames Laboratory/Iowa State)

Department of Chemistry, Mississippi State University, MS State, MS 39762

prabideau@provost.msstate.edu; as338@ra.msstate.edu

Goal

The gram-scale synthesis of polynuclear aromatic hydrocarbons (PAHs) with carbon frameworks that can be identified on the buckminsterfullerene C_{60} surface (buckybowls), and the use of these bowl-shaped structures as precursors for larger and more complex curved-surface systems.

Recent Progress

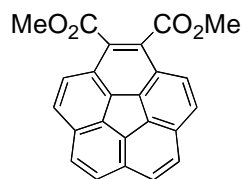
Early work under the DOE sponsored program produced the first "locked" buckybowl by incorporation of an additional five-membered ring onto corannulene, and the first two semibuckminsterfullerenes ($C_{30}H_{12}$'s) representing half of the C_{60} surface. While these and other buckybowls were made by our program and others on mg levels, we have more recently developed new methods for the gram-scale synthesis of tetrabromocorannulene (**1**), corannulene (**2**), and corannulene-dicarboxylate (**3**).



1



2



3

DOE Interest

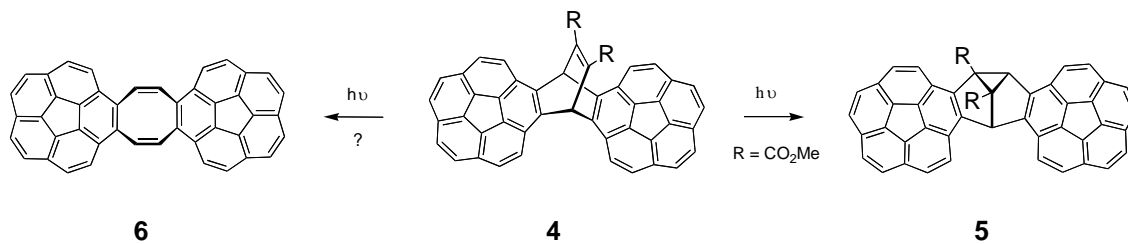
These novel, bowl-shaped structures may be involved in host-guest relationships that have potential in the area of catalysis; they represent the end-caps of closed nanotubes and, as such, could serve as precursors for controlled nanotube synthesis; and they could become an environmental concern if the wide-scale use of fullerenes is ever realized due to potential fragmentation processes of the latter.

Future Plans

Future plans for the program will involve the production of novel, curved PAH systems by (a) applications of the newly developed synthetic methodology, and (b) exploitation of the availability of **1-3** as synthons for further elaboration. Due to space limitations, only a few examples are shown below. However, the availability of new synthetic methodology to produce curved-surface PAHs on gram-scale levels will afford a wide variety of opportunities for the generation of unusual systems. And, while the structural features of these systems are quite interesting, there has been little done to date with the exploration of their chemistry.

Twin Corannulenes

A recent example of the new methodology is the synthesis of twin corannulene **4**. This system is of interest for potential host-guest chemistry (see model below for possible interaction with C₆₀); it also undergoes an extraordinarily facile di- π methane

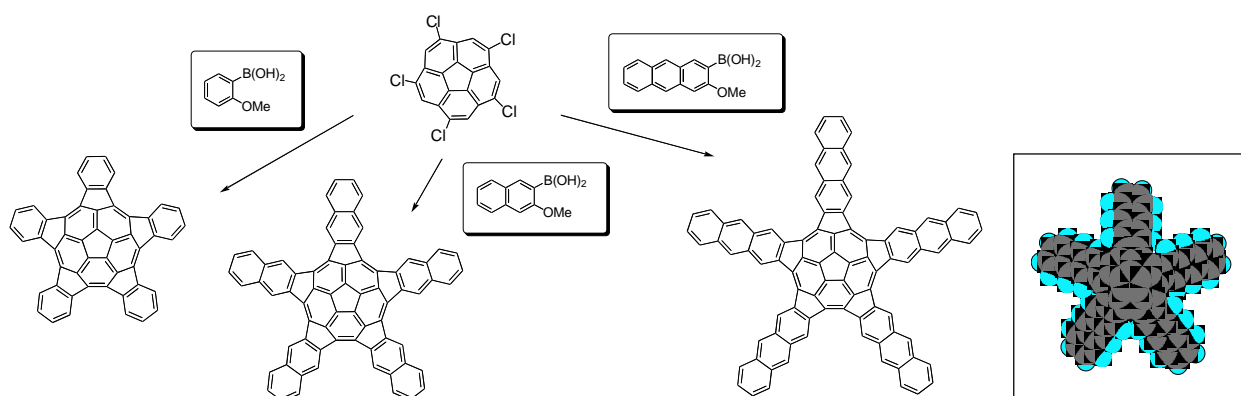


rearrangement to semibullvalene **5**. We plan to convert the R groups to hydrogen or methyl to explore the non-sensitized photochemical conversion, presumably to **6** which has added host-guest possibilities due to the tub-shaped COT ring. It also should have tremendous potential for acceptance of lithium since corannulene readily accepts four electrons and COT forms an aromatic dianion.

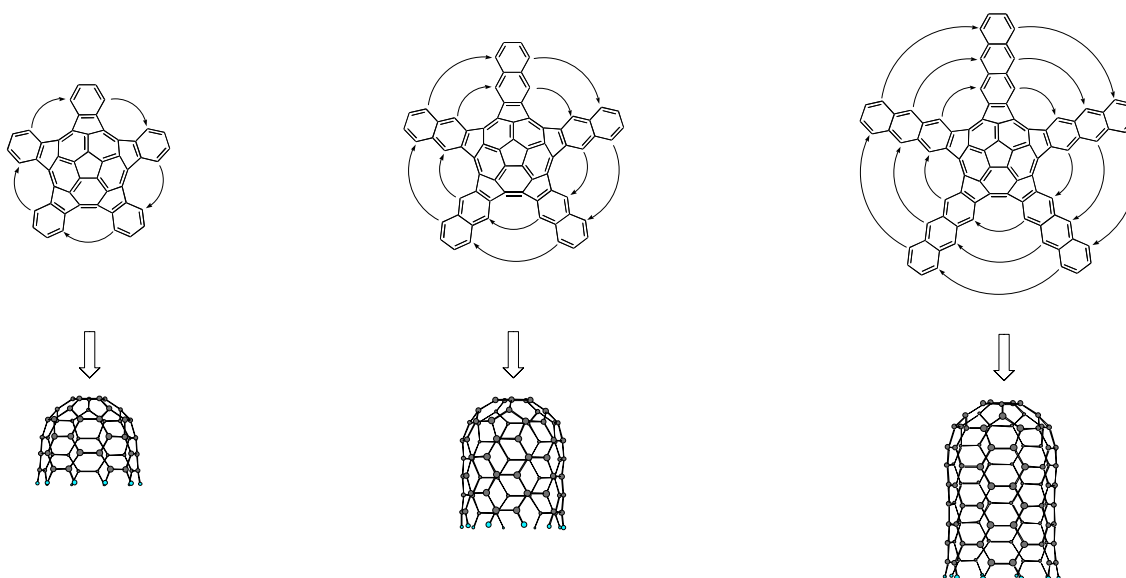


Pentasubstituted Corannulenes as Synthons

The availability of gram quantities of corannulene provides an opportunity to use the easily produced pentachlorocorannulene as a synthon. We have successfully used Suzuki coupling routes with monobromocorannulene to incorporate a single fluoranthene unit. If this can be done at all five sites from a pentasubstituted corannulene, it will produce some remarkable structures as illustrated below for one, two, and three PAH additions. Of course these structures are not planar due to the bowl-shaped inner corannulene core. Moreover, the addition of five-membered rings around the periphery of corannulene will have the effect of "tightening" the core ring system providing an even greater level of curvature (at least to the point where "peri" type interactions may become possible).



Perhaps the most exciting aspect of this project is the possibility that if these “starburst” type PAHs can be formed, they might be induced to “zip up” to form closed-end nanotubes. Of course an organic synthesis of model nanotubes would open the door for a number of studies relating to their properties and behavior.



Publications, 2002-03:

1. Z. Marcinow, D. Groves, and P. W. Rabideau, “A New $C_{32}H_{12}$ Buckybowl,” *The Journal of Organic Chemistry*, 67, 3537 (2002).
2. Z. Marcinow, A. Sygula, P. W. Rabideau, “Improved Synthesis of Benz[a]acephenanthrene,” *Synlett*, 1839 (2002).

3. A. Sygula, R. Sygula, F. R. Fronczek and P. W. Rabideau, "The Addition of Organolithium Reagents to Corannulene and Conformational Preferences in 1-Alkyl-1,2-Dihydro-corannulenes," *The Journal of Organic Chemistry*, 67, 6487 (2002).
4. A. Sygula, S. Karlen, R. Sygula, and P. W. Rabideau, "Formation of the Corannulene Core by Nickel-Mediated Intramolecular Coupling of Benzyl and Benzylidene Bromides: A Versatile Synthesis of Dimethyl 1,2-Corannulene Dicarboxylate," *Organic Letters*, 4, 3135 (2002).
5. A. M. Alvarez, R. J. Angelici, A. Sygula, R. Sygula, P. W. Rabideau, "Hexahapto Corannulene Buckybowl Complexes of Iridium, Including Ring-to-Ring Migration," *Organometallics*, 22, 624 (2003).
6. A. Sygula, R. Sygula, A. Ellern and P. W. Rabideau, "A Novel Twin Corannulene: Synthesis and Crystal Structure Determination of a Dicolorannulenobarrelele dicarboxylate," *Organic Letters*, 2003, 5, 2595.

Kansas State University Contribution: Controlling Structural Electronic and Energy Flow Dynamics of Catalytic Processes Through Tailored Nanostructures.

Postdoc: S. Stolbov

Students: S. Hong and F. Mehmood

Collaborators: Heinz, O'Brien, Bartels

Department of Physics, Cardwell Hall, Kansas State University, Manhattan, KS 66506

email: rahman@phys.ksu.edu**Goal**

The overall goal of the project is to pursue the development of new catalysts which may exploit the selective support of specific surface reactions by applying steric and entropic control over the diffusion motion and reaction energy, respectively. Towards this end, Rahman's group has the preliminary goal of understanding the binding, activation energies and diffusion pathways of atoms, molecules and clusters on inhomogeneous (stepped, kinked, with co-adsorbates, etc.) surfaces through theoretical calculations and computer simulations.

Progress during the first 6 Month of the Funding Period:

During the first six month of the project, theoretical work has progressed on several fronts. The first of these is the implementation of a powerful code for the calculation of the electronic structure of adsorbates on surfaces and on nanostructures from first principles using the full potential LAPW (linear augmented plane wave) method. This code, together with the one based on pseudopotentials in the plane wave representation, is now being used in Rahman's group to examine the energetics, changes in electronic structure, diffusion, and reactivity of several systems in conjunction with the work of experimental collaborators on this grant.

Diffusion of CO molecules on Cu(111): Heinz and Bartels groups find interesting changes in the diffusion of CO molecules on Cu(111) as a function of adsorbate coverage. It is conceivable that both activation energy barriers and prefactors are affected. We have obtained preliminary results for the adsorption of CO on Cu(111) which show that for low coverage the strong bond between the CO molecule and Cu atom impacts the local surface structure, as indicated in Fig.1. Our calculational super cell is large enough to allow the examination of changes in the diffusion characteristics as CO coverage is increased.

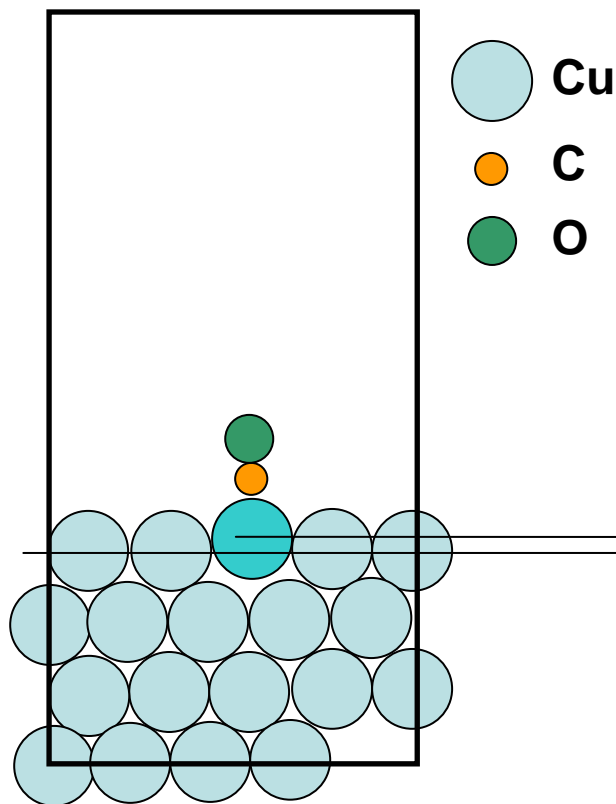


Fig. 1. Side view of the supercell containing 3x5 Cu atoms per layer and a CO molecule (CO coverage of 1/15). We find that the minimum of the total energy corresponds to the adsorption of CO molecule on the top of Cu atom. The adsorption causes a strong atom relaxation, namely the Cu atom located below the molecule undergoes upward shift of about 0.28 Å with respect to the other topmost Cu atoms. The equilibrium C-O bond length is found to be equal to 1.16Å, whereas the C-Cu bond is equal to 1.86Å

Adsorption of ThioPhenol on Cu(111): Motivated by the beautiful experimental observations from Bartels' laboratory, we are carrying out calculations of the nature of the binding of thiophenol molecules on Cu(111). Preliminary results indicate that the adsorption geometry is non-trivial. We are in the process of carrying out similar calculations of thiophenols on Au(111) to understand the rationale for the complex behavior on Cu(111).

Alkali Adsorption on Cu(111) and Pd(111): Complementary work in Rahman's group on S and C adsorption on several types of stepped Pd surfaces have led us to examine the effect of alkali metal adsorption on transition metal surface. Alkali metals are well-known as promoters in heterogeneous catalysis. On adsorption at prototype catalyst surfaces, like that of a transition or noble metal, they substantially increase the rates of various chemical reactions. It is also reported that when alkali adsorb on Cu surfaces they form so-called quantum wells with quasi-two-dimensional electronic states localized along the surface. The ensuing novel properties of the system find many applications, including those in photochemistry and nanotechnology, however, the mechanism responsible for the enhanced reactivity is as yet not understood. We have carried out extensive comparative studies of the adsorption of Na and K on Cu and Pd surfaces. We find that of the several theoretical measures of catalytic activity that have been proposed, the isoelectronic reactivity index $w^N(r)$ is the most reflective of dramatic changes in behavior. For both Cu and Pd surfaces, which are by themselves of varied electronic structure, we find a huge increase and delocalization of $w^N(r)$ on alkali metal adsorption (see Fig. 2). We trace this phenomenon to an unusual feature in the surface potential formed by the adsorbate (see Fig. 3) which may ultimately be the driving force for the "promotion effect" of alkalis. We also find a relationship between the characteristics of the surface potential and the observed unusual optical properties of the quantum wells on these systems. We hope our experimental colleagues can substantiate our predictions through related measurements on these interesting systems.

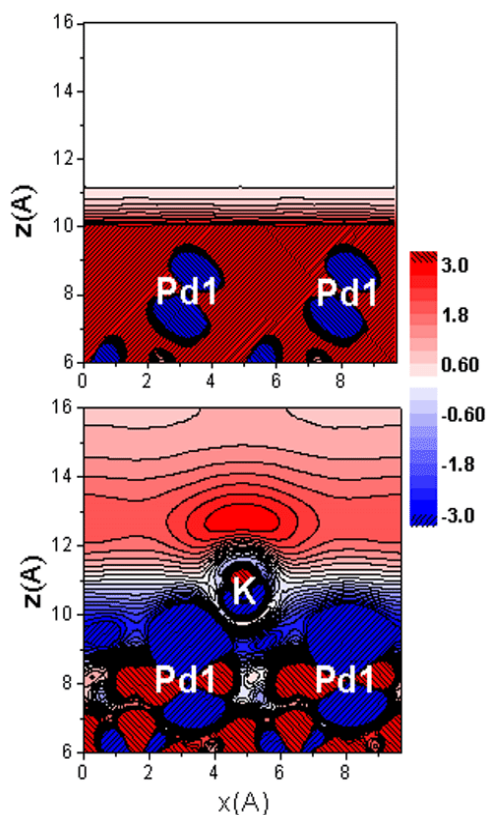


Fig. 2. Plot of $w^N(r)$ for clean Pd(111) (upper panel) and for a 0.25 coverage of K on it ($K_{0.25}/Pd(111)$) (lower panel) along the plane perpendicular to the surface. Pd1 mark the positions of the topmost Pd atoms and K that of potassium atoms. A drastic decrease in $w^N(r)$ is seen for the clean surface (the white area corresponds to $w^N(r) = 0$), while adsorption of K induces a huge increase and delocalization of $w^N(r)$ even at points far from the adsorbate.

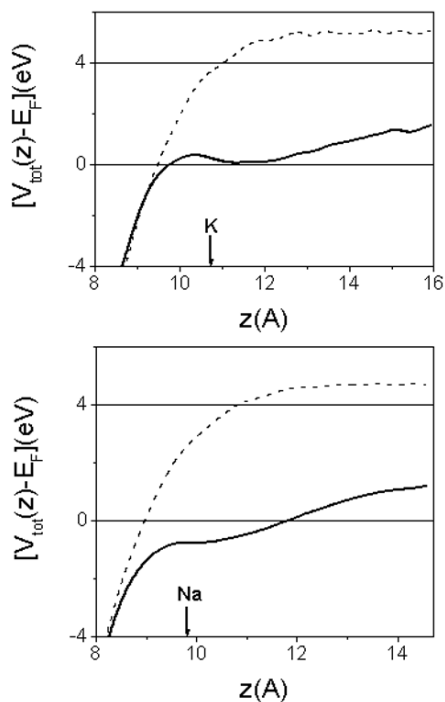


Fig. 3. Self consistent total potential plotted along the surface normal. The upper panel displays the potential for Pd(111) (dashed line) and for a 0.25 K overlayer on Pd(111) (solid line). The lower panel provides the same for Cu(111) (dashed line) and $Na_{0.25}/Cu(111)$ (solid line). Arrows indicate the positions of the alkali atoms. Instead of an expected simple reduction of the surface barrier, the alkali adsorbates form a **groove-like or plateau-like** region of further reduced potential in the vicinity of the surfaces.

DOE Interest

Catalytic reactions have great importance for a broad range of industrial and environmental processes ranging from catalytic CO oxidation in exhaust systems to catalytic hydro-desulfurization of gasoline. This project aims at understanding catalytic processes on the

atomic scale by development and applications of methods that can follow molecular dynamics at high excitation level.

Future Plans

Continuation of the above projects: The two collaborative projects described above require extensive systematic studies in close collaboration with experimentalists. We intend to pursue them. In the case of CO diffusion on Cu(111), we will be examining the influence of increasing CO coverage on the activation energy barriers and diffusion paths. More importantly, we will pay attention to calculations of the diffusion prefactors which are expected to play an important role and cannot be taken to have the same value for all intervening diffusion events. By understanding the most optimal diffusion paths we will be in a position to predict energy-saving reaction pathways. In the case of the structure, adsorption and dynamics of thiophenol molecules on Cu(111), we need to get better insights from adsorption on a substrate like Au(111) on which the energetics is already known from experiments. Such calculations need to be carried out for the Au(111) to gain insights on the nature of the anchoring of the S molecule on the surface.

Transition Metal Oxide Nanocrystals: We are very encouraged by the recent developments in O'Brien's group on the synthesis and characterization of transition metal oxide nanocrystals. We find ourselves well equipped with the tools to carry out theoretical calculations and computer modeling of these useful materials. We will begin by examination of the geometric and electronic structure of small Cu₂O nanocrystals. Some work in this direction has already begun. We will be most interested in investigating the reactivity of these nanoparticles along the lines discussed above for transition metal surfaces.

Kinetic Monte Carlo Simulations: Some members of Rahman's group are engaged in developing a methodology for kinetic Monte Carlo simulations which does not suffer from a priori biasing of the system's temporal and spatial evolution through a set of input energetics. Instead, a data base of the energetics of relevant events and diffusion processes is developed by the system as it evolves. Efforts are underway to generate mapping functions capable of generating the energetics through "self teaching". We plan to implement this novel approach in calculations of the diffusion of CO molecules on Cu surfaces, in collaboration with the experimental work of Heinz and Bartel groups..

Publications Relevant to the Project(2003-4)

1. F. Baumberger, Th. Herrman, A. Kara, S. Stolbov, N. Esser, T. S. Rahman, J. Osterwalder, W. Richter, and T. Greber, "Optical recognition of atomic steps on surfaces," *Phys. Rev. Lett.* **90**, 177402 (2003).
2. I. Makkonen, P. Salo, M. Alatalo, and T. S. Rahman, "*Ab initio* studies of stepped Pd surfaces with and without S," *Phys. Rev. B*, **67**, 165415 (2003).
3. R. Nunthel, T. Gleitsmann, P. Pouloupoulos, A. Scherz, J. Linder, E. Kosubek, Ch. Litwinski, Z. Li, H. Wende, K. Baberschke, S. Stolbov, and T. S. Rahman, "Impact of surfactant-assisted epitaxial growth of Ni on Cu(001) on magnetic properties," *Surf. Sci.* **531**, 53 (2003).

4. S. Durukanoglu and T. S. Rahman, "Structure of Ag(410) and Cu(320)," *Phys Rev. B* **67**, 205406 (2003).
5. S. Durukanoglu, A. Kara, and T.S. Rahman, "Excess and Local Thermodynamic Properties of Stepped Metal Surfaces," *Phys. Rev. B* **67**, 235405 (2003).
6. I. Makkonen, P. Salo, M. Alatalo, and T. S. Rahman, "Characteristics of adsorption of S on Pd vicinal surfaces," *Surf. Sci.* **532-535**, 154 (2003).
7. M. Tringides, Z. Chvoj, C. Ghosh, and T. S. Rahman, "Prefactors for interlayer diffusion: Ag/Ag(111)," *J. Phys.: Condensed Matter* **15**, 5223 (2003).
8. T. S. Rahman, A. Kara, and S. Durukanoglu, "Structural relaxations, vibrational dynamics and thermodynamics of vicinal surfaces," *J. Phys. Condensed Matter*, **15**, S3197 (2003).
9. A. Karim, M. Rusanen, I. T. Koponen, T. Ala-Nissila, and T. S. Rahman, "Fluctuation of Surface Steps in Thermal Equilibrium: a kinetic Monte Carlo study," *Surf. Sci.*, to appear
10. O. Trushin, A. Kara, T. S. Rahman, "Self-teaching kinetic Monte Carlo technique for simulation of surface phenomena," *Phys. Rev. B*, to be published
11. S. Stolbov and T. S. Rahman, "Giant increase in isoelectronic reactivity of transition and noble metal surfaces upon alkali metal adsorption," submitted to *Nature*.
12. S. Stolbov, F. Mehmood, T. S. Rahman, I. Makkonen, P. Salo, and M. Alatalo, "Site selectivity in chemisorption of C on Pd(211)," submitted to *Phys. Rev B*.
13. A. Al-Rawi, A. Kara, and T. S. Rahman, "Vibrational dynamics and excess entropy of multi-grain nanoparticles," *J. Comp. and Theo. Nanosci.*, to appear.

This page intentionally left blank.

Homogeneous CO Hydrogenation Revisited

Jerome W. Rathke, Robert J. Klingler, Michael J. Chen, and Rex E. Gerald II
Chemical Engineering Division, Argonne National Laboratory, Argonne, Illinois 60439

Contact: Jerry Rathke
Phone: 630-252-4549
Fax: 630-252-9373
E-Mail: rathke@cmt.anl.gov
Web Site: <http://www.cmt.anl.gov/toroid-cavity/>

Research Goals and Objectives

The Fluid Catalysis Program explores catalysis mechanisms, new catalytic species, and new catalytic reaction chemistry using an array of in situ spectroscopic and kinetic techniques at the high pressures and temperatures that are frequently used in industrial chemical processes. The Fluid Catalysis Program's research in the area of catalytic chemistry in supercritical media stems from the interesting and favorable physical properties of these media that allow increased scrutiny of catalytic mechanisms by powerful NMR techniques that operate most effectively in low viscosity gas or supercritical-fluid phases. Also, because bond energies are defined in terms of gas-phase chemistry, thermochemical measurements in the gas-like supercritical media are more easily interpretable in terms of the bond dissociation energies of the various bonds in organometallic catalysts. Experimental thermochemical and kinetic data from supercritical fluids is highly amenable to theoretical calculation. We have recently conducted supercritical homogenous CO hydrogenation for the first time and, in related research, uncovered the first cobalt catalyst for the supercritical phosphine-modified hydroformylation of olefins and measured the thermodynamics of the key hydrogen addition step for these catalysts. In research on high-pressure in situ spectroscopic devices, we have developed the toroid-pressure probe, the R&D 100 Award winning toroid-cavity imager, and most recently, a magic-angle-spinning toroid-cavity probe that imparts the high sensitivity and imaging capability of toroids to high-resolution solid-state NMR spectroscopy. In other research, reverse micelles are utilized as nano-sized minireactors to allow catalytic reactions that normally require highly polar solvents to be conducted in the supercritical phase. In this endeavor, the first high-pressure NMR characterization of reverse micelles in supercritical carbon dioxide has recently been achieved.

This abstract describes the Fluid Catalysis Program's recent in situ spectroscopic and kinetic investigations of homogeneous catalytic carbon monoxide hydrogenation in supercritical media.

Recent Progress

Considerable research on homogeneous catalysts for the hydrogenation of CO was undertaken in several laboratories in the late 1970's and early 1980's. The most studied of homogeneous CO hydrogenation catalysis systems is the cobalt carbonyl catalyzed reaction which has been shown to follow a rate law that is first order in both $\text{HCo}(\text{CO})_4$ and H_2 pressure. The reaction is believed to proceed through an early coordinated

formaldehyde intermediate that produces, dependent upon the reaction conditions and solvent, variable amounts of methanol, methyl formate, and ethylene glycol as initial reaction products. In the proposed mechanism, higher alcohols and higher formate esters are produced by secondary homologation and transesterification reactions associated mainly with the initially produced methanol and methyl formate.

Since most of the early kinetic studies on these systems were accomplished using high-pressure autoclaves, it seems possible that recent advances in high-pressure spectroscopic techniques that would allow in situ scrutiny of these systems might provide more information on them, today. We recently tested the use of a high-pressure toroid NMR probe on the cobalt carbonyl catalyzed CO hydrogenation in supercritical carbon monoxide medium for the first time. Use of a single-phase homogeneous supercritical system containing catalyst and reactant gases was utilized to avoid gas-liquid mixing problems that might otherwise interfere with kinetic studies in an unstirred NMR pressure vessel using conventional liquid media.

The reaction rate and products and the cobalt containing species associated with the catalytic reaction were measured in situ at 180 and 200 °C and at total pressures of hydrogen and carbon monoxide near 260 atm. The second order rate constant at 200 °C, $12 \times 10^{-8} \text{ s}^{-1} \text{ atm}^{-1}$, measured in supercritical carbon monoxide is close to the reported value for the nonpolar solvent, benzene ($15 \times 10^{-8} \text{ s}^{-1} \text{ atm}^{-1}$) and considerably smaller than that reported in the more polar solvent, 2,2,2-trifluoroethanol ($84 \times 10^{-8} \text{ s}^{-1} \text{ atm}^{-1}$). The products of the reaction including methanol and methyl formate were quantified by in situ ^1H NMR, while in situ ^{59}Co NMR revealed cobalt carbonyl hydride and dicobalt octacarbonyl as the only detectable cobalt species. Preliminary measurements yielded an approximate activation barrier of 34 kcal/mole. Separate experiments established that the homologation of methanol, the pathway for production of higher alcohols under CO hydrogenation conditions in polar solvents, did not occur to a measurable extent in the nonpolar supercritical CO medium used here.

DOE Interest

In earlier high-pressure kinetic studies, the Fluid Catalysis Program demonstrated the first mononuclear catalyst for homogeneous carbon monoxide hydrogenation and determined the rate law and the currently accepted mechanism for the $\text{HCo}(\text{CO})_4$ catalyzed reaction (see F. A. Cotton and G. Wilkinson, *Advanced Inorganic Chemistry*, Sixth Edition, 1999, p. 1253). In the past year, in research aimed at experimental and theoretical parameterization of the reaction coordinates of this mechanistically important reaction, it conducted kinetic measurements on homogeneous catalytic carbon monoxide hydrogenation, in situ, in an NMR probe for the first time. Also, supercritical carbon monoxide was used as a gas-like reaction medium (to aid in the theoretical calculations) for the first time in homogeneous CO hydrogenation.

This program pioneered the use of homogeneous catalysts in supercritical fluids and invented supercritical hydroformylation catalysis. To conduct in situ spectroscopic studies of supercritical and other high-pressure industrial process chemistry, it developed the toroid-pressure probe, the R&D 100 Award winning toroid-cavity imager, and most recently, a magic-angle-spinning toroid-cavity probe that imparts the high sensitivity and

imaging capability of toroids to high-resolution solid-state NMR spectroscopy. This program recently reported the first high-pressure NMR characterization of reverse micelles in supercritical carbon dioxide.

Future Research

In future work on homogeneous CO hydrogenation, accurate determinations of such parameters as activation barriers and kinetic isotope effects, afforded by high-pressure NMR in a gas-like medium that is highly amenable to theoretical (density functional) calculations will allow scrutiny of the early steps in this important reaction. The earlier work with autoclaves had established a strong temperature coefficient and a significant isotope effect on this system, but the uncertainties and complexities associated with sampling from autoclaves discouraged attempts to accurately determine these parameters with the high-pressure techniques available at that time. Evaporation of the volatile $\text{HCo}(\text{CO})_4$ into the autoclave headspace increased by removal of liquid samples, and uncertain quenching of samples containing this unstable species are problems associated with autoclave sampling methods that are alleviated by the high-pressure NMR technique used here.

Publications 2003-2004

Cobalt(I) Salt Formation in Hydroformylation Catalysis

J. W. Rathke, R. J. Klingler, M. J. Chen, R. E. Gerald II, and K. W. Kramarz
The Chemist **80(1)**, 9-12, 2003

Ionic Species in Cobalt-Catalyzed Hydroformylation

J. W. Rathke, R. J. Klingler, M. J. Chen, and R. E. Gerald II
In *Chemical Engineering Division Annual Technical Report 2002*, ANL-03/13,
pp. 77-78, 2003

Two Dimensional B1-Gradient NMR Imager

Rex E. Gerald II, Rafael L. Greenblatt, and Jerome W. Rathke
U. S. Patent 6,538,444 Issued March 25, 2003

Nuclear Magnetic Resonance Imaging Apparatus

Rex E. Gerald II, Robert J. Klingler, and Jerome W. Rathke
U. S. Patent 6,674,283 Issued January 6, 2004

In Situ High Pressure NMR Studies of $\text{Co}_2(\text{CO})_6[\text{P}(\text{p-CF}_3\text{C}_6\text{H}_4)_3]_2$ in Supercritical Carbon Dioxide: Ligand Substitution, Hydrogenation, and Hydroformylation Reactions, M. J. Chen, R. J. Klingler, J. W. Rathke, and K. W. Kramarz, *Organometallics*, accepted for publication.

Supercritical Catalytic CO Hydrogenation

J. W. Rathke, R. J. Klingler, and M. J. Chen, *The Chemist*, accepted for publication.

This page intentionally left blank.

Organometallic Cyano-Cages as Scaffolds, Ligands, and Sequestrants

Postdocs: Yao, H.; Ramamoorthy, B.; Ramesh, M.; Hsu, S. C. N.

Ph.D. students: Kuhlman, M. L.; Boyer, J.; Contakes, S. M.

Collaborators: Espenson, J. H. (Ames); Nuzzo, R. G. (UIUC); Frenkel, A. I. (Yeshiva); Vairavamurthy, A. (Brookhaven)

Department of Chemistry, University of Illinois at Urbana-Champaign, Urbana, IL 61801

rauchfuz@uiuc.edu

Goal:

Develop new metal-rich ensembles for applications in catalysis and in separations.

Background:

In 1998 we discovered an efficient route to organometallic cages with box-like structures. Specifically tricyanides $fac\text{-}L_nM(\text{CN})_3$ were found to condense with facial tritopic Lewis acids to give $M_8(\text{CN})_{12}$ species, e.g. $\{[\text{CpCo}(\text{CN})_3]_4[\text{Cp}^*\text{Rh}]_4\}^{4+}$. Such species were the first cyanometallate cages ever described after literally hundreds years of research on cyanide coordination chemistry. Related reactions afforded “incomplete” or “defect” boxes consisting of $M_7(\text{CN})_9$ frameworks such as $\{[\text{Cp}^*\text{Rh}(\text{CN})_3]_4[\text{Cp}^*\text{Rh}]_3\}^{2+}$. $[\text{Cp}^*\text{Rh}(\text{CN})_3]$ was subsequently found to condense with $\text{Mo}(\text{CO})_3$ sources to give inclusion complexes $\{M\text{-}[\text{Cp}^*\text{Rh}(\text{CN})_3]_4[(\text{CO})_3\text{Mo}]_4\}^{3-}$ ($M = \text{Cs}^+, \text{K}^+$). The presence of alkali metal cations M^+ is required for cage stability. Competition studies showed that Cs^+ binds more tightly than K^+ by $>10^4$. The incorporation of alkali metal centers into organometallic frameworks is an unusual supramolecular motif. This research also demonstrated the versatility of the cage-building process, i.e. vertices can range from $M(\text{CO})_3$ to $(\text{C}_5\text{R}_5)\text{M}^{2+}$. The specific finding that Cs^+ binds more tightly than K^+ points to fundamental concepts related to Cs^+/K^+ separations. The work also highlights the considerable advantage to the organometallic approach to cage-forming processes, because the versatility of organometallic reagents allows greater control over the charge on the cage.

These architecturally novel species represent the starting point for development of fundamental but still application-oriented studies described in a stepwise manner below.

Recent Developments

Non-labile M-CN linkages are critical to cage formation

Findings: We examined condensations where the M-CN bonds are labile: box-like structures do *not* form, rather one obtains smaller trigonal bipyramidal or tetrahedral cages. These condensations formally involve $[\text{Mo}(\text{CN})_3(\text{CO})_3]^{3-}$, but in this species the Mo-CN bonds are labile. With K^+ and Cs^+ one obtains trigonal prismatic $\{\text{Cs}\text{-}[(\text{CO})_3\text{Mo}]_6(\text{CN})_9\}^{8-}$ whereas with smaller alkali metal cations one obtains smaller tetrahedranes such as $\{\text{Na}\text{-}[(\text{CO})_3\text{Mo}]_4(\text{CN})_6\}^{5-}$.

Implications: It was unknown if the box and defect box motifs would spontaneously form when metal electrophiles were presented with 1.5 equiv of cyanides. Clearly the use of preformed $[L_nM(CN)_3]^{n-}$ building blocks is critical. This study also demonstrated that the size of the alkali metal cation strongly influences the cage architecture - small ions give smaller cages. This work strongly suggests that the ability of the boxes to discriminate between Cs^+ vs. K^+ is due to the poor fit of the latter in the cage. The overarching implication is that rigid, 3-dimensional architectures display higher selectivity for ion complexation than do flexible ligands. Most ligands in use are flexible, hydrocarbon-based species, thus a considerable opportunity exists for the design of rigid inorganic frameworks.

Charge-neutral organometallic boxes display high affinities for alkali metal cations

Finding: Charge-neutral cages bind cations very well. This result came from our discovery of a templated synthesis of $[CpCo(CN)_3]_4[Cp^*Ru]_4$, which binds Cs^+ , Rb^+ , NH_4^+ , K^+ , Tl^+ , $N_2H_5^+$, and $MeNH_3^+$. The affinity for Cs^+ vs. K^+ remains high, and K_{Cs} is estimated $>10^{10}$. Neither Na^+ nor any dication binds to these cages. Ion exchange kinetics are first order in the filled box, i.e. rate-determining loss of the cation followed by rapid uptake of the new cation. Ion-binding to empty cages follow first order kinetics in terms of the concentrations of both box and the alkali metal cation. K^+ inserts into the box more quickly than does Cs^+ .

Implications: The fact that anionic cages bind alkali metal cations at their interiors is unsurprising given the electrostatic forces involved and the 3-dimensional enclosure provided. Particularly encouraging and somewhat unexpected is the fact that *charge-neutral* cages display high affinities for cations. In fact, it is increasingly clear that *cationic* cages also bind cations, which is unprecedented.

Encapsulated guests display modified reactivity

Finding: The 1H NMR spectrum of $\{MeNH_3[CpCo(CN)_3]_4[Cp^*Ru]_4\}^+$ displays the full complement of 1H - ^{13}C , ^{13}C - ^{14}N , and 1H - ^{14}N couplings, which indicates that the cation is shielded from solution, thereby suppressing intermolecular exchange processes. Further evidence of the ability of the box to protect guests is the absence of H-D exchange of the encapsulated NH_4^+ with D_2O . Finally, the ammonium ions are immune to attack by strong base.

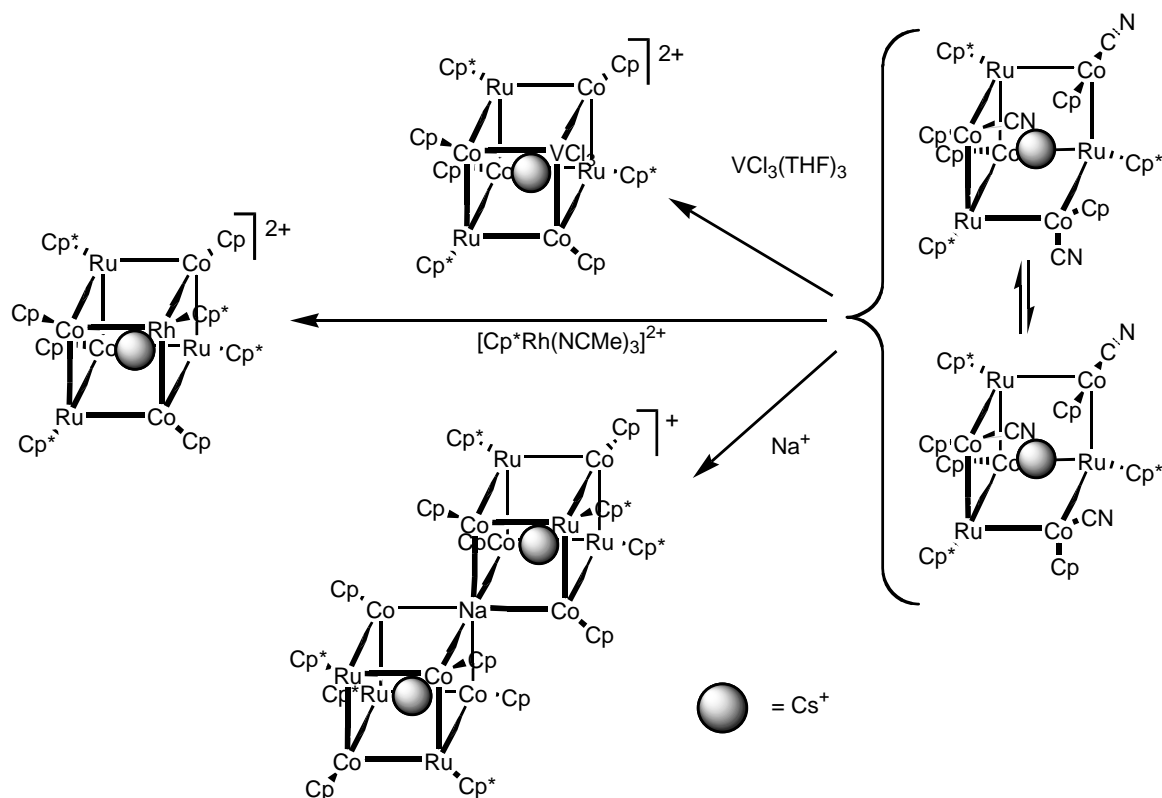
Implications: The unusual environment provided by the box suggests that unusual chemistry could be performed inside such containers. Many host-guest species are known, but it is rare to see slow in-out exchange of the guest molecules in solution.

Incomplete boxes are excellent ligands

Finding: Parallel with the preparation of $\{Cs[CpCo(CN)_3]_4[Cp^*Ru]_4\}^+$, routes were developed to the defect box $\{Cs[CpCo(CN)_3]_4[Cp^*Ru]_3\}$, which is missing one metal vertex (Ru_3 vs. Ru_4). This species possesses three terminal cyanides suitable for further complexation. Indeed the defect box binds a range of metal electrophiles to give boxes. Using this "box-completion" reaction, one can generate boxes containing terminally bound reactive ligands, e.g. $\{Cs[CpCo(CN)_3]_4[Cp^*Ru]_3VCl_3\}$. One can also construct nano-scale cages such as the double boxes, e.g., $\{Cs[CpCo(CN)_3]_4[Cp^*Ru]_3\}_2Fe^{2+}$, and the cluster-fused boxes, e.g., $\{Cs[CpCo(CN)_3]_4[Cp^*Ru]_3Ru_3S_2(arene)_2\}^{2+}$.

Implications: The box completion process (see Scheme) establishes that the defect boxes perform like Tp^- , Cp^- , and other tridentate ligands. Insofar as facially binding tridentate

ligands are central to many catalytic reactions, this new family of multimetallic ligands is a promising source of novel ligands for catalytic applications.



Scheme: Box-completion reactions demonstrating the tridentate character of the “defect” boxes.

Tetrahedral $L_nM(CN)_3$ vertices give larger cages

Finding: This subproject began with the synthesis of the new ligands $[RB(CN)_3]^-$, where R = alkyl, aryl. Condensation of these anions with Cp^*Rh^{++} sources affords the hexagonal prismatic cage $\{[PhB(CN)_3]_6[Cp^*Rh]_6\}^{6+}$.

Implications: At issue in any synthetic advance, i.e. the development of cyanometallate boxes, is the scope for expanding the concept to broader range of products. The $B_6Rh_6(CN)_{12}$ cage has greater internal volume vs. the aforementioned boxes, as demonstrated by the inclusion of THF at the cage interior. Furthermore the solubility of these species allows thorough characterization.

DOE Interest

The new cages demonstrate unparalleled selectivity for Cs^+ vs. K^+ , relevant to DOE-specific separations issues. The boxes and incomplete boxes present revolutionary or at least very novel designs. The work demonstrates new classes of ligands that incorporate supramolecular interactions. These efforts are relevant to the development of new supports, ligands, and scaffolds for catalysis.

Future Plans

- 1) Electro-active boxes, i.e. cages that undergo redox changes at mild potentials, allowing electrochemically switchable behavior. By changing the charge on the cluster, one could switch an ion-binding cage to a container that is no-longer ion binding. This approach could underpin ion-specific sensors as well as recyclable sequestrants for guest ions of interest to DOE nuclear research, e.g. $^{137}\text{Cs}^+$. Key to progress in this area are redox-active vertices, and promising advances are being made.
- 2) New, inexpensive vertices. To enable broader applications of the cage chemistry, we are interested in new kinds of vertices that might be more readily (easily, cheaply) prepared than say $[\text{CpM}(\text{CN})_3]^-$. The species $[\text{PhB}(\text{CN})_3]^-$ and analogues are being examined to this end.
- 3) Proton-box interactions. Organometallic cages, such as $\{[\text{CpCo}(\text{CN})_3]_4[\text{Cp}^*\text{Ru}]_4\}$ can apparently undergo reversible tetraprotonation. Furthermore the boxes interact in an outer-sphere manner with alkyl ammonium ions ($R > \text{Me}$), without incorporation. Such interactions may open the way for the binding of boxes to ammonium-rich environments. The outer-sphere interaction of organic substrates and organometallics is an area of both fundamental and topical interest.
- 4) Catalytically active boxes. Species of the type $\{\text{Cs}_c[\text{CpCo}(\text{CN})_3]_4[\text{Cp}^*\text{Ru}]_3\text{ML}_n\text{Cl}/\text{H}/\text{R}\}$ ($M = \text{Ti}, \text{V}, \text{Ru}, \text{etc.}$), derived from box-completion reactions, are potential catalysts.

Selected publications

1. "Structural and Mechanistic Studies on Ion Insertion into the Molecular Box $[\text{CpCo}(\text{CN})_3]_4[\text{Cp}^*\text{Ru}]_4$ " Ramesh, M.; Rauchfuss, T. B. *J. Organometal. Chem.* **2004**, in press.
2. "Synthesis and Characterization of the Hexagonal Prismatic Cage $\{\text{THF}_c[\text{PhB}(\text{CN})_3]_6[\text{Cp}^*\text{Rh}]_6\}^{6+}$ " Kuhlman, M. L.; Yao, H.; Rauchfuss, T. B. submitted 2004.
3. "Hybrid Cluster-Cages Formed via Cyanometallate Condensation: $\text{CsCo}_4\text{Ru}_6\text{S}_2(\text{CN})_{12}$, $\text{Co}_4\text{Ru}_9\text{S}_6(\text{CN})_9$, and $\text{Rh}_4\text{Ru}_9\text{S}_6(\text{CN})_9$ Frameworks" Kuhlman, M. L.; Rauchfuss, T. B. *Inorg. Chem.* **2004**, *43*, 430-435.
4. "Tricyanometallate Building Blocks and Organometallic Cyanide Cages" Contakes, S. M.; Klausmeyer, K. K.; Rauchfuss, T. B. *Inorg. Synth.* **2004**, *34*, 00.
5. "Structural Chemistry of "Defect" Cyanometallate Boxes $\{\text{Cs}_c[(\text{C}_5\text{R}_5)\text{M}(\text{CN})_3]_4[\text{Cp}^*\text{Ru}]_3\}$ ($M = \text{Co}, \text{R} = \text{H}; M = \text{Rh}, \text{R} = \text{Me}$)" Kuhlman, M. L.; Rauchfuss, T. B.; Wilson, S. R. *J. Am. Chem. Soc.* **2003**, *124*, 10084-92.
6. "Membership Rules for a Molecular Box: the Admission Process and Protection Provided to Guest Molecules", Hsu, S. C. N.; Ramesh, M.; Espenson, J. H.; Rauchfuss, T. B., *Angew. Chem. Int. Ed.* **2003**, *42*, 2663-6.
7. Systematic Assembly of the Double Molecular Boxes: $\{\text{Cs}_c[\text{CpCo}(\text{CN})_3]_4[\text{Cp}^*\text{Ru}]_3\}$ as a Tridentate Ligand", Contakes, S. M.; Kuhlman, M. L.; Ramesh, M.; Wilson, S. R.; Rauchfuss, T. B., *Proc. Nat. Acad. Sci.* **2002**, 4889-4893.

Controlling Structural Characteristics of Single-Walled Carbon Nanotubes (SWNT) by Tailoring Catalyst Composition and Synthesis Conditions

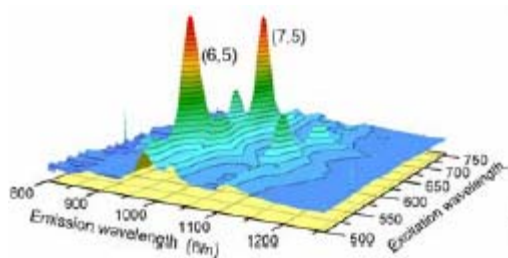
Students: Olga Rueda, Jose E. Herrera, Liang Zhang
 Collaborators: R. B. Weisman (Rice), L. Balzano (SWeNT), O. Matarredona (SWeNT), C. Lieber (Harvard), M. Strano (Illinois), P. Balbuena (South Carolina), Ming Zheng (Dupont)
 Contact: D. Resasco, 100 E. Boyd St, Norman OK 73019;
 phone: (405) 325-4370; Email: resasco@ou.edu
 web page: www.ou.edu/engineering/nanotube

Goal

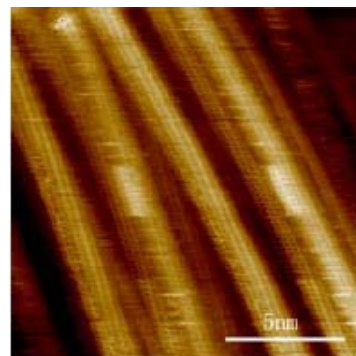
Advance the knowledge of the mechanisms responsible for the formation of single-walled carbon nanotubes to get control over their structural parameters (diameter and chirality). Through a detailed knowledge of the growth mechanism it will be possible to produce SWNT with tailored properties that are directly related to the structural parameters.

Recent Progress

Controlled Synthesis of SWNT: We have produced single-walled carbon nanotube samples with very narrow distribution of diameters and chiralities (n,m). By controlling the rate of metal agglomeration, it was possible to keep the nanotube diameter at $0.8 \text{ nm} \pm 0.05 \text{ nm}$. The narrowness of the diameter distribution of our samples was corroborated at Rice University. Spectrofluorimetric measurements that can be used to identify the (n,m) structure of all the semiconducting nanotubes present in the sample revealed that this sample comprised mostly the (6,5) and (7,5) nanotubes. This is the narrowest distribution of nanotube types ever produced. The diameter of these tubes is 0.75 and 0.83 nm, respectively. Noteworthy, not only the diameter distribution but the distribution of chiral angles is remarkably sharp. The angles of these two nanotubes are 27 and 24.5°, respectively; close to the chiral angle of the arm-chair nanotubes (30°). These conclusions were further confirmed by studies at Illinois (Raman) and Harvard (STM). The characteristics of the SWNT are illustrated below.



Spectrofluorimetric analysis of SWeNT (Left) and competing (Right) SWNT samples. Courtesy of Dr. Bruce Weisman at Rice



STM Image of SWNT produced by SWeNT™'s low temperature method. Courtesy of Dr. Charles Lieber at Harvard University

Incorporation of SWNT in matrices and study of their properties: With these high-quality, well-characterized SWNT materials we have expanded our studies to explore the interactions of nanotubes of narrow-diameter-distribution with surfactants, polymers, DNA and other organic molecules. We have investigated the electrical, mechanical, and thermal properties, as well as their field emission characteristics to determine relationships between the diameter and chirality of the nanotubes and their physical properties. In addition, we are investigating the use of these tailored SWNT as unique catalyst supports with high thermal and electrical conductivities for applications as fuel-cell electrodes.

(n,m) Speciation of SWNT: One of the most sought after capabilities that will open many opportunities for SWNT in nanoelectronics is to separate monodispersed samples of specific (n,m) characteristics. Only those SWNT for which n-m is a multiple of 3 are metallic and within the semiconducting, each (n,m) pair has a characteristic band gap and electronic response. To produce nanodevices it is important to be able to use specific (n,m) nanotubes. We have recently collaborated with researchers at Dupont who have been able to obtain from our SWNT monodispersed (6,5) nanotubes by selective interaction with DNA molecules of specific sequence (i.e. d(C,G)_q with q=16-40).

DOE Interest

Single-wall carbon nanotubes (SWNT) can be considered as one of the building blocks for nanoscale science and nanotechnology. They exhibit exceptional chemical and physical properties. Among the various synthesis methods investigated, the catalytic decomposition of carbon-containing molecules over solid catalysts appears as a promising technique since it has the potential to be scaled-up at a relatively low cost. A number of researchers have investigated different catalyst formulations and operating conditions. Yet, obtaining high quality SWNT has not been possible with this method. By focusing on tailoring the catalyst formulation and operating conditions, we have obtained high yields and selectivities to SWNT, and what is most remarkable, a high degree of control on nanotube diameter and chirality. Such control may open a vast number of opportunities for research on specific nanotubes structures. It may also generate technological applications in diverse fields such as nanoelectronics, nanosensors, field emission, fuel cell electrodes, tailored catalyst supports, etc.

Future Plans

We plan to continue improving our ability to control of producing nanotubes with specific (and varying) (n,m) structure by manipulating catalyst composition and reaction conditions. At the same time, we will continue investigating the reaction mechanisms responsible for the SWNT growth. To help us in this task, we are collaborating with a theorist who is conducting molecular dynamics and Monte Carlo simulations of the growth process. Our plan is provide her with detailed experimental kinetic parameters to compare with the theoretical calculations. At the same time, we plan to continue working on the dispersion, functionalization, and separation of SWNT with the ultimate goal of separating metallic from semiconducting nanotubes, and even further produce different monodispersed samples of individual (n,m) characteristics.

Publications 2002-2003

- Qin, S; Qin, D.; Ford, W. T.; Resasco, D. E.; Herrera, J. E. “Functionalization of Single-Walled Carbon Nanotubes with Polystyrene via Grafting to and Grafting from Methods.” *Macromolecules* (2004), 37(3), 752-757.
- “Polymer Brushes on Single-Walled Carbon Nanotubes by Atom Transfer Radical Polymerization of n-Butyl Methacrylate” Shuhui Qin, Dongqi Qin, Warren T. Ford, Daniel E. Resasco, and Jose E. Herrera, *Journal of the American Chemical Society* (2004), 126(1), 170-176.
- “Loss of single-walled carbon nanotubes selectivity by disruption of the Co-Mo interaction in the catalyst”, J. E. Herrera and D. E. Resasco, *Journal of Catalysis* 221, (2004) 354-364
- Dispersion of Single-Walled Carbon Nanotubes in Aqueous Solutions of the Anionic Surfactant NaDDBS’ Olga Matarredona, Heather Rhoads, Zhongrui Li, Jeffrey H. Harwell, Leandro Balzano, and Daniel E. Resasco *Journal of Physical Chemistry B* (2003), 107(48), 13357-13367.
- “Narrow (n,m)-Distribution of Single-Walled Carbon Nanotubes Grown using a Solid Supported Catalyst”, Sergei M. Bachilo, Leandro Balzano, Jose E. Herrera, Francisco Pompeo, Daniel E. Resasco, and R. Bruce Weisman, *Journal American Chem. Soc.* (2003), 125, 11186
- “Structural Characterization of Single-Walled Carbon Nanotubes” Daniel E. Resasco and Jose E. Herrera. *Encyclopedia of Nanoscience and Nanotechnology*, (2003) American Scientific Publishers (H. S. Nalwa Ed.), Vol. 10, pp 1-23.
- “Temperature dependence of the quality of silicon nanowires produced over a titania-supported gold catalyst” Nataphan Sakulchaicharoen and Daniel E. Resasco *Chemical Physics Letters* 377 (2003) 377-383
- “In-Situ TPO/Raman to Characterize Single-Walled Carbon Nanotubes” Jose E. Herrera and Daniel E. Resasco. *Chemical Physics Letters* 376 (2003) 302–309
- “Raman Characterization of SWNT of Various Diameters Obtained by Catalytic Disproportionation of CO” J. E. Herrera, L. Balzano, F. Pompeo, and D.E. Resasco. *Journal of Nanoscience and Nanotechnology* (2003), 3, 133-138
- “Role of Co-W Interaction in the Selective Growth of Single-Walled Carbon Nanotubes from CO Disproportionation” Herrera, Jose E.; Resasco, Daniel E. *Journal of Physical Chemistry B* (2003), 107, 3738-3746.
- “Catalytic Production Of Single-Walled Carbon Nanotubes, Functionalization, and Incorporation In Polymer Matrices” D. Resasco, L. Balzano, F. Pompeo, H. Barraza and J. Herrera, *NanoTech 2002 AIAA Journal* 2002-5762 (2003)
- “Nucleation of Polypropylene Crystallization by Single-Walled Carbon Nanotubes” Brian P. Grady, Francisco Pompeo, Robert L. Shambaugh, and Daniel E. Resasco, *Journal of Physical Chemistry B* 106 (2002) 5852-5858.
- “Water-solubilization of single-walled carbon nanotubes by functionalization with glucosamine” F. Pompeo and Daniel E. Resasco. *Nano Letters* 2 (2002) 369-373
- “Characterization of single-walled carbon nanotubes (SWNT) produced by CO disproportionation on Co-Mo catalysts” W. E. Alvarez, F. Pompeo, J. E. Herrera, L. Balzano, and D. E. Resasco. *Chemistry of Materials* 14 (2002) 1853-1858
- "SWNT-filled thermoplastic and elastomeric composites prepared by miniemulsion polymerization" H. Barraza, F. Pompeo, E. O’Rear, D. E. Resasco, *Nano Letters* 2 (2002) 797-802

This page intentionally left blank.

Fundamental Studies on the High Temperature Kinetics for the Catalytic Combustion of Methane

Students: Zhu, Guanghui; Han, Jinyi; Figaro, Patrick
Collaborators: Zemlyanov, D.

School of Chemical Engineering, Purdue University, West Lafayette, IN 47907
Fabio@purdue.edu

Goal

Understand the catalytic chemistry for the reaction of combustion of methane on palladium catalysts.

Recent Progress

We have completed most of the work using foils and single crystals of Pd. We have established the kinetics of methane combustion on the metal and oxide phases of Pd. The next step is to study the effect of the support. We have studied water-gas shift reactions also.

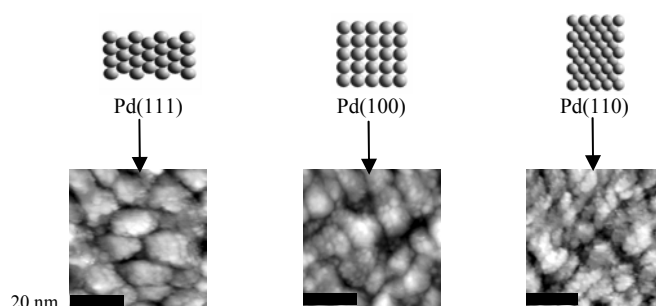
*Studies of water gas shift reactions*¹ The kinetic parameters for water-gas shift reaction on Cu based catalysts were measured under fuel reformer conditions for fuel cell applications (7% CO, 8.5% CO₂, 22 % H₂O, 37 % H₂, and 25% Ar) at 1 atm total pressure and temperature in the range of 200 °C. The rate per unit of Cu surface area at the stated concentrations was $0.8 \times 10^{-6} \text{ mol m}^{-2} \text{ s}^{-1}$ at 200 °C. The overall reaction rate as a function of the forward rate (r_f) is $r = r_f(1-\beta)$, where $r_f = k_f[\text{CO}]^{0.8} \cdot [\text{H}_2\text{O}]^{0.8} \cdot [\text{CO}_2]^{-0.7} \cdot [\text{H}_2]^{-0.8}$, k_f is the forward rate constant, $\beta = ([\text{CO}_2] \cdot [\text{H}_2]) / (K \cdot [\text{CO}] \cdot [\text{H}_2\text{O}])$ is the approach to equilibrium, and K is the equilibrium constant for the water-gas shift reaction. This expression indicates a strong inhibition on the forward rate by H₂ and CO₂. When ceria was added to the catalyst, it decreased the Cu surface area and did not increase the rate per unit of Cu surface area, suggesting that ceria is not a promoter. The addition of ZnO did not increase the rate per unit of Cu surface area either. Thus, Cu is the active site for catalysis. It was proposed that the kinetics can be explained based on the “Redox” mechanism with $\text{CO}^* + \text{O}^* \rightarrow \text{CO}_2^* + *$ as the rate-determining step.

*Increase of Pd surface area by O₂ oxidation*² By a combination of supported and model catalyst studies, surface science and TEM (in collaboration with Professor A.K. Datye) measurements we observed an increase in the Pd surface area by oxidation of Pd. This result is important in rationalizing the data in supported catalysts for the combustion of methane.

*Coverage of Palladium by Silicon Oxide during Reduction in H₂ and Complete Oxidation of Methane*³ The interaction between silica and palladium following complete

oxidation of methane or following reduction in H_2 was investigated on a polycrystalline palladium foil and on supported Pd/SiO₂ catalysts. During methane oxidation, oxidized silicon covered the palladium oxide surface as observed by TEM on Pd/SiO₂ catalysts and by XPS on palladium foil. On the Pd foil, the source of silica was a silicon impurity, common on bulk metal samples. The migration of oxidized silicon onto PdO deactivated the catalysts by blocking the active sites for methane oxidation. Silicon oxide overlayers were also observed covering the Pd surface after reduction of Pd/SiO₂ by H_2 at 923 K.

*The rate of methane combustion is not sensitive to the structure of the catalyst*⁴ We have measured the rates and kinetics on Pd(111), Pd(100), Pd(110), and Pd foil. Based on the constancy of rates and the similar structure of the catalysts after reaction, we concluded that the kinetics is not sensitive to the structure of the catalyst.



STM pictures of single crystals after combustion reaction

*Rates of reaction at high temperatures*⁵ We measured the kinetics at high temperatures using non-porous model catalysts. These data will be benchmark values for catalytic combustion at high temperature. Under the reaction conditions used, supported porous catalysts would have been limited by heat and mass transport limitations. The high temperature conditions are important in practical applications. We have found that the turnover rate for oxidation on PdO is 10 times higher than on Pd at 907 K. Water inhibition is not present at the higher temperatures.

DOE Interest

Catalytic combustion can generate energy with minimum production of NO_x. Palladium is the most active metal for the catalytic combustion of methane. The understanding of the catalytic chemistry for this process will help in the design of commercial systems.

Future Plans

Preparation of flat oxide supports For the preparation of model catalyst we will need flat alumina and zirconia supports. We are constructing an atomic layer epitaxy device to prepare thin (50 layers) of alumina and zirconia over Si(100). It is imperative that the oxide be atomically flat so we can distinguish the metal clusters by AFM.

Preparation of metal clusters We will prepare metal clusters by spin coating and by evaporation. The aim is to prepare clusters in the range 1-10 nm with a size distribution of 1 nm.

Specific studies of metal clusters on oxides:

- Does the PdO interact strongly with the support (alumina or zirconia) causing it to lose activity?
- What is the cause for deactivation of catalysts?
- How does the support (ZrO_2 and Al_2O_3) affect the shape and morphology of metal particles? How do structural defects on the support affect particle uniformity, dispersion?
- How does the support (ZrO_2 and Al_2O_3) affect the thermal stability of Pd particles? How does the rate of sintering change depending on environment: vacuum, O_2 , steam, CO_2 , and reaction conditions?
- How do the shape and morphology of metal particles change under reaction conditions depending on the nature of the support? How do these changes correlate with catalytic activity?

Publications (2003-4)

1. N. Koryabkina, A. A. Phatak, W.F. Ruettinger, R. J. Farrauto, and F. H. Ribeiro, "Determination of kinetic parameters for the water-gas shift reaction on copper catalysts under realistic conditions for fuel cell applications", *Journal of Catalysis*, **217**, 233-239, 2003.
2. J. Han, G. Zhu, D. Zemlyanov, and F.H. Ribeiro, "Increase of Pd Surface Area by Treatment in Dioxygen", Submitted to the *Journal Catalysis*, November 2003.
3. Guanghui Zhu, Ken-ichiro Fujimoto, Dmitri Yu. Zemlyanov, Abhaya K. Datye, Fabio H. Ribeiro, "Coverage of Palladium by Silicon Oxide during Reduction in H_2 and Complete Oxidation of Methane", Submitted to the *Journal of Catalysis*, December 2003.
4. Guanghui Zhu, Jinyi Han, Dmitri Y. Zemlyanov, Fabio H. Ribeiro, "The Turnover Rate for the Catalytic Combustion of Methane over Palladium is not Sensitive to the Structure of the Catalyst", Submitted to the *Journal of the American Chemical Society*, February 2004.
5. Guanghui Zhu, Dmitri Yu. Zemlyanov, Fabio H. Ribeiro, "Temperature Dependence of the Reaction Kinetics for the Complete Oxidation of Methane on Palladium and Palladium Oxide", Submitted to the *Journal of Physical Chemistry B*, March 2004.

This page intentionally left blank.

DeNOx and DeSOx Reactions on Oxide and Carbide Surfaces: Experimental and Theoretical Studies

José A. Rodriguez, J. Hrbek, J. Hanson, G. Liu, P. Liu, and X. Wang
Department of Chemistry, Brookhaven National Laboratory

Abstract

In this talk examples will be presented that illustrate the use of synchrotron-based photoemission, x-ray absorption spectroscopy, and time-resolved x-ray diffraction in the characterization of catalytic systems that involve metal oxides and metal carbides [1-5]. Density-functional calculations were used to help in the interpretation of experimental results and the prediction of chemical behavior [6]. Nowadays a major effort in environmental catalysis is focused on reducing the content of sulfur and nitrogen oxides in the atmosphere. NOx and SOx species are common air pollutants produced during the combustion of fuels in automotive engines, factories and power plants. Sulfur dioxide results from the burning of S-containing impurities present in all oil and coal derived fuels. On the other hand, nitrogen oxides are produced by the thermal fixation and oxidation of nitrogen in combustion operations that use air as an oxidant. In our industrial society, there is a clear need to develop methods with a high efficiency for the removal or destruction of SOx (DeSOx processes) and NOx (DeNOx processes) compounds. Studies have been carried out to investigate the fundamental chemistry of sulfur and nitrogen dioxides on single-crystal surfaces and bulk powders of several oxides and carbides. We have found that metal-doped MgO and carbides of titanium and molybdenum are very useful for the control of environmental pollution. These studies reveal several aspects that can be useful for facilitating the breaking of S-O and N-O bonds and enhancing the efficiency of DeSOx and DeNOx catalysts [1-6].

- 1) J.A. Rodriguez, G. Liu, T. Jirsak, J. Hrbek, Z. Chang, J. Dvorak and A. Maiti, *J. Am. Chem. Soc.* **124**, 5242 (2002).
- 2) J.A. Rodriguez, P. Liu, J. Dvorak and T. Jirsak, J. Gomes, Y. Takahashi and K. Nakamura, *Phys. Rev. B*, **69**, 115414 (2004).
- 3) J.A. Rodriguez, J.C. Hanson, A.I. Frenkel, J.Y. Kim, and M. Perez, *J. Am. Chem. Soc.* **124**, 346 (2002).
- 4) J.A. Rodriguez, T. Jirsak, L. González, J. Evans, M. Pérez, and A. Maiti, *J. Chem. Phys.* **115**, 10914 (2001).
- 5) J.A. Rodriguez, X. Wang, J.C. Hanson, G. Liu, A. Iglesias-Juez and M. Fernandez-Garcia, *J. Chem. Phys.* **119**, 5659 (2003).
- 6) J.A. Rodriguez, *Theor. Chem. Acc.* **107**, 117 (2002).

This page intentionally left blank.

Project : Chemical Interactions in Multimetal/Zeolite Catalysts

Project Code: DE FG02-87ERA 13654

Principal Investigators: Wolfgang M.H. Sachtler,

Abstract

This two-year project has led to a significant improvement in the fundamental understanding of the catalytic action of zeolite-supported redox catalysts. Fe/MFI catalysts have been studied for two prototype reactions:

- (1) One step oxidation of benzene to phenol with N_2O as the oxidant
- (2) Reduction of nitrogen oxides to N_2 with hydrocarbons.

The mechanism has been studied for both prototypes and the crucial active sites have been identified by EXAFS, TPR, FTIR and isotopic labeling.

Chemical vapor deposition has been used to obtain catalysts with high Fe content

Hydrothermal synthesis followed by dealumination was used to obtain catalysts with very low Fe content in accessible positions.. To discern the catalytic action of Fe sites from those of acid sites, selective poisoning of Fe by H_2S was used

The most important conclusion of this research is that Fe-oxo ions are the active sites in both prototype reactions.

For benzene oxidation to phenol highest activity is achieved with **mono-nuclear** Fe-oxo-ions ;

For NO_x reduction to N_2 , **dinuclear ions**, such as $[HO-Fe-OH]^{2+}$ are active sites.

References

1. "Identification of Highly Active Iron Sites in N_2O -Activated Fe/MFI," J. Jia, Q. Sun, B. Wen, Lin X, Chen, W M.H. Sachtler, *Cat Lett* 82 (2002) 7-11.
2. "Chemical Anchoring of Palladium by Fe-oxo ions in Zeolite ZSM-5," Bin Wen, Jifei Jia, Wolfgang. M. H. Sachtler *J. Phys. Chem. B* 106 (2002) 7520-7523.
3. " Identification by Isotopic Exchange of Oxygen Deposited on Fe/MFI by Decomposing N_2O ," Jifei Jia, Bin Wen, and Wolfgang M.H. Sachtler, *J.Catal.* 210 (2002) 453-459.
- 4.. "One-step Oxidation of Benzene to Phenol with Nitrous Oxide over Fe/MFI Catalysts," Jifei Jia, Krishnan S. Pillai, and Wolfgang M. H. Sachtler, *J. Catal.*, 221 (2004) 119-126.

This page intentionally left blank.

**New instrumentation bridges the “pressure gap” in catalysis studies:
Fundamental studies of catalyst surfaces under relevant pressure conditions**

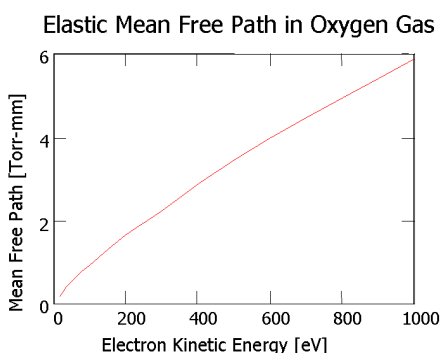
Miquel Salmeron, D. F. Ogletree, Hendrick Bluhm, Eleonora Hebenstreit, Felix Requejo,
Hongjian Wang and Guido Ketteler

Lawrence Berkeley National Laboratory. Berkeley, CA. USA

Catalytic phenomena require the investigation of surfaces in contact with gases under pressures ranging from millibars to several atmospheres. This applies also to fields such as environmental chemistry, electrochemistry, and biology. The investigation of those phenomena calls for experimental techniques that are not only surface sensitive, but also can operate under elevated pressures.

Several surface science methods fulfill these requirements and can provide information of the structure under equilibrium conditions with the gas phase. Chief among them are:

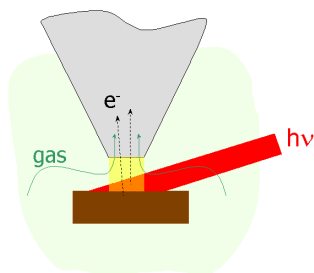
- 1) Scanning probe methods, which can reveal atomic scale topographic and spectroscopic details of a surface and can operate at gas-liquid and liquid-solid interfaces [1].
- 2) Optical methods like sum-frequency generation (SFG), which owe their surface sensitive to selection rules that requires the absence of inversion symmetry. For centro-symmetric media this happens precisely at interfaces. In this manner the gas phase does not contribute directly to the signal. [2,3].
- 3) Photoelectron spectroscopies (PES), including XPS (or ESCA), X-ray absorption and emission (XAS, XES), etc. are widely used for studies of the electronic structure of surfaces. They provide information about surface elemental composition and chemical bonding. Although traditionally PES has been used under high vacuum conditions, today, thanks to developments initiated at the Lawrence Berkeley Laboratory, it is



possible today to perform studies under high pressure⁴. Because of its novelty, high-pressure PES (HPPES) is the subject of the current presentation.

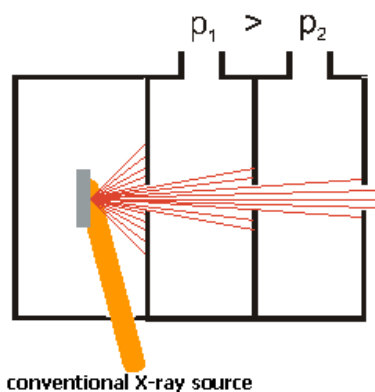
The main problem with PES is that electrons are strongly attenuated by collisions with the gas phase, to such an extent that the mean free path of 500 eV

Firs
ade:

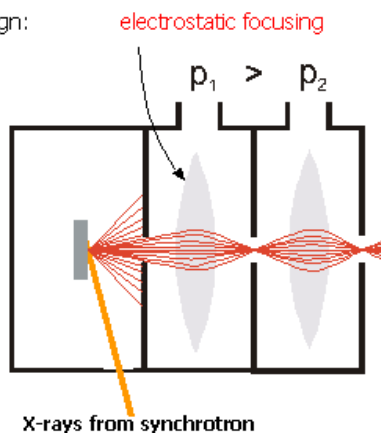


electrons in 4 torr of gas is about 1 mm. In our instrument the sample, in the reaction chamber, is located at a distance of the about 1 mm from an aperture (see diagram on the left) that communicates with another chamber pumped to a vacuum that is 2 to 3 orders of magnitude lower. For example if the pressure in the reaction chamber is 1 Torr, the pressure in the second chamber is about 10^{-2} torr. Traditional differential pumping schemes collect only electrons in a very small solid angle (line-of-site). In our method we used electrostatic focusing, such that the orifices separating the differentially pumped chambers are part of a lens system and are located at the focal points of several electrostatic lenses. Using this method we increased the

Previous designs:



New design:



collection efficiency by 3 orders of magnitude.

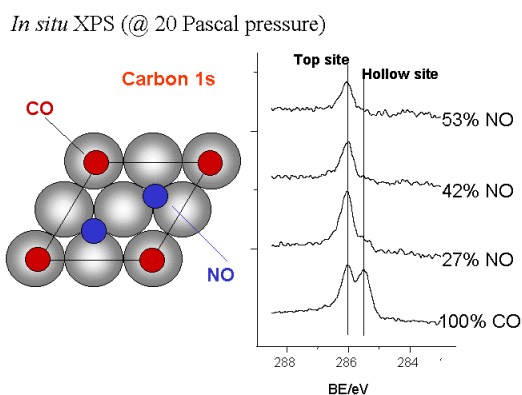
Several benefits derive from this novel instrument, among them:

- Possibility to perform PES studies at high pressures, of up to 10-20 Torr at present.
- Gas flow and variable sample temperature, from -100°C to 600°C (higher and lower values possible).
- Elimination of charging problems in insulators, due to neutralization by ions in the gas phase generated by the incoming X-ray beam.
- Spectra of gas molecules located between sample and aperture excited by the incoming X-ray beam are obtained, in addition to that of the surface species. This makes possible to detect reactant and products a few tenths of mm from the catalyst surface.
- Finally, there is an exciting and still an unexploited feature of this instrument. This is the possibility to detect hot gas species desorbing from the surface before they

collide with other molecules in the gas phase or with the walls. These “hot” molecules carry information of the energetics and dynamics of the reaction. They could be analyzed downstream of the molecular jet escaping through the first aperture by mass spectrometry and time of flight measurements. Crossed with a Laser beam, it should be possible to excite molecules through single or multiple photon absorptions for studies of the internal excited modes.

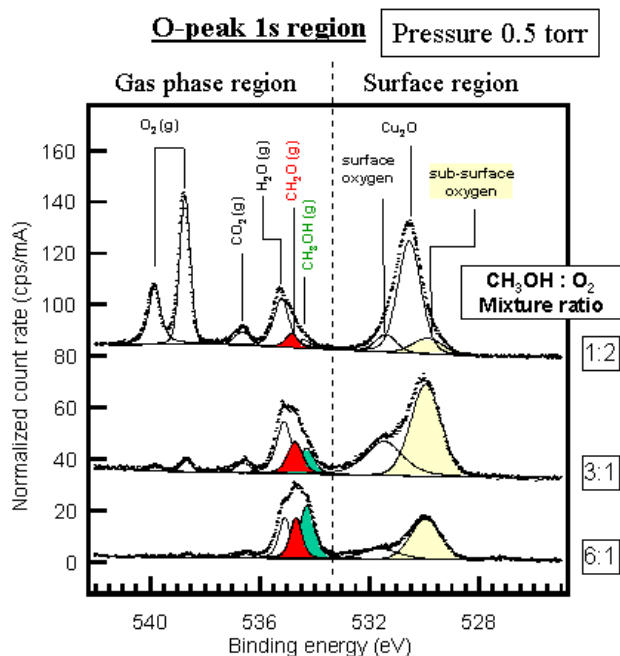
We give here examples of studies we carried out over the last 3 years:

- a) Determination of the structure of the ice surface through its melting transition. XAS was used to determine the amount of water molecules with unsaturated H-bonds. This can be detected by the increased X-ray absorption at energies near the absorption edge of oxygen (from the O1s to the H₂O 4a₁-derived orbitals) [5].
- b) CO+NO equilibrium structures over Rh(111). XPS of C, N and O was used to determine the adsorption site of CO and NO molecules in equilibrium with mixed gases in the torr pressure range. As the NO partial pressure increased it displaced CO from hollow sites first and from top sites at higher pressure [6].



- c) Partial oxidation reaction of methanol to formaldehyde on Cu catalyst. The intensity of the gas phase products (H₂O, CO₂ and CH₂O) was followed as a function of substrate temperature and reactant pressure. It was shown that there is a linear correlation between the catalytic activity of the sample and the presence of a sub-surface oxygen species that can only be observed *in situ* [7].
- d) Structure and equilibrium phase diagram of PdO formed over Pd(111) under high O₂ pressure.

Cu-catalyzed oxidation of methanol



At present there exist three HPPES instruments of this kind in the world, two at the Advanced Light Source in Berkeley, the third one at BESSY, Berlin. The first was built in 1999 in line 9.3.2 of the ALS. This was followed by an improved second generation of instruments built in a joint collaboration between Berkeley and the Fritz-Haber Institut in Berlin, Germany. The second Berkeley instrument is part of the Molecular Environmental Science beam line 11.0.2. At the ALS the HPPES instruments are receiving numerous user applications, both for

catalysis and for environmental studies projects. While at present only the prototype instrument is open to the general public, the new instrument is expected to be available in a few months.

References:

- [1] B. J. McIntyre, M. Salmeron, G.A. Somorjai, *Catal. Lett.* 14 (1992) 263
K.B. Rider, K. Hwang, M. Salmeron and G. Somorjai. *J. Am. Chem. So.* 124, (2002) 5588.
- [2] T. Dellwig, G. Rupprechter, H. Unterhalt, H.-J. Freund, *Phys. Rev. Lett.* 85 (2000) 776-779.
- [3] P.B. Miranda, L. Xu, Y.R. Shen, M. Salmeron, *Phys. Rev. Lett.* 81 (1998) 5876-5879.
- [4] D. F. Ogletree, H. Bluhm, G. Lebedev, C.S. Fadley, Z. Hussain, M. Salmeron, *Rev. Sci. Instrum.* 73, 3872 (2002).
- [5] H. Bluhm, D. F. Ogletree, C. S. Fadley, Z. Hussain, M. Salmeron, *J. Phys.: Condens. Matter* 14, L227 (2002).
- [6] Felix G. Requejo, Eleonore L.D. Hebenstreit, D. Frank Ogletree and Miquel Salmeron. *Catalysis Letters*. In press, 2004.
- [7] H. Bluhm, M. Hävecker, A. Knop-Gericke, D. Teschner, E. Kleimenov, V.I. Bukhtiyarov, D.F. Ogletree, M. Salmeron and R. Schlögl. *J. Phys. Chem.* In press, 2004.

Homogeneous-Heterogeneous Reactions: Thermal and Chemical Coupling

DE-FG02-88ER13878

Lanny Schmidt
Department of Chemical Engineering and Materials Science
University of Minnesota
Minneapolis MN 55455
612 625 9391
Schmidt@cems.umn.edu

Hydrogen from Ethanol

We show that ethanol can be converted directly into H₂ with >80% selectivity and >95% conversion by catalytic partial oxidation at contact times <5 milliseconds over Rh and Rh-Ce catalysts. This can be made to occur by rapid vaporization and mixing with air using an automotive fuel injector at temperatures sufficiently low and times sufficiently fast that homogeneous reactions producing acetaldehyde, ethylene, and total combustion products can be minimized. The reaction can also be run with or without added water to increase H₂ and optimize operating conditions. This process has great potential for low cost H₂ generation in fuel cells for small portable applications where liquid fuel storage is essential and where systems must be simple, robust, and capable of repeated startup and shutdown. We show that carbohydrates can be converted economically into hydrogen at efficiencies exceeding 80% by the combination of fermentation to produce ethanol and millisecond reactors to produce H₂. This provides a convenient, transportable, liquid fuel for efficient generation of electricity from biomass.

Olefins from Biodiesel

The methyl esters derived from soy oil can be converted into olefins with up to 80% yield at high conversions by partial oxidation with air on a Rh-Ce catalyst in an autothermal reactor at residence times of ~5 milliseconds. These results are compared to the corresponding reactions of *n*-hexadecane which is a related fossil fuel used in steam cracking of naphthas to produce olefins. At lower C/O ratios, biodiesel also produces up to 90% yield of H₂. Yields of both lower olefins and H₂ are nearly identical with both the ester and alkane, even though the former has double bonds that might be expected to lead to carbon formation.

The results suggest that the process is initiated by surface reactions near the front face of the catalyst which consumes all of the O₂. Olefins are formed primarily by homogeneous pyrolysis later in the catalyst, and rapid quenching within 20 milliseconds prevents secondary reactions that make many products. While hexadecane forms up to 80% *n*-olefins at even higher C/O, biodiesel forms comparable amounts of smaller olefinic esters and *n*-olefins containing 8 to 10 carbon atoms. Evidently the attack of the esters occurs preferentially near the double bond location on the long chain fatty acid producing these fragments.

This page intentionally left blank.

Catalysts for the Living Polymerization of Olefins

Recent Students: Mehrkhodavandi, P.; Adamchuk, J.; Pryor, L. L.; Gabert, A.; Tonzetich, Z. J.; Schrodi, Y.

Postdocs: Goodman, J. T.; Ruhland, K.

Department of Chemistry, Massachusetts Institute of Technology, Cambridge, MA 02139

rrs@mit.edu

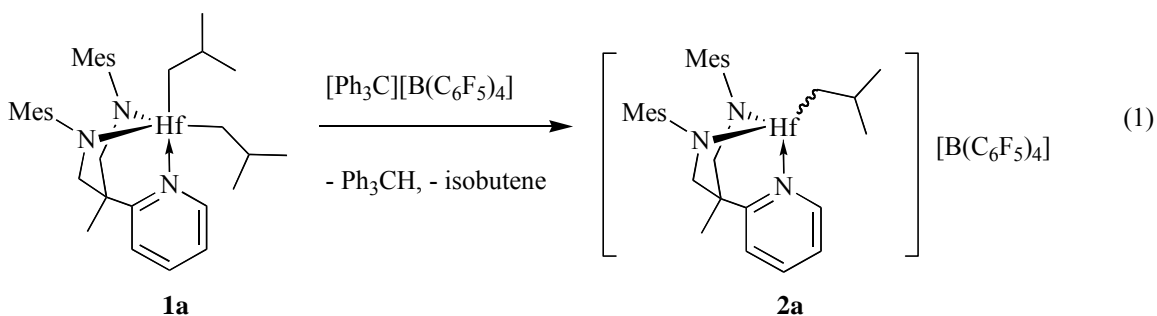
Goals

The overall research goals are to explore the chemistry of zirconium and hafnium complexes that contain diamido/donor ligands in order to develop new olefin polymerization catalysts, and in particular, living polymerization catalysts. Ultimately we also hope to control the structure of the polyolefins prepared by well-defined catalysts through the use of asymmetric ligands that would lead to isotactic structures, and to polymerize olefins that contain a protected functionality.

Recent Progress

Recently we have focussed on (i) kinetic and mechanistic studies of the polymerization of 1-hexene by zirconium and hafnium catalysts that contain a [(MesitylNCH₂)₂C(CH₃)(2-C₅H₄N)]²⁻ ([MesNpy]²⁻) ligand (see **1a** in eq 1); (ii) catalysts that contain related [(2,6-X₂C₆H₃NCH₂)₂C(CH₃)(2-C₅H₄N)]²⁻ (X = Cl or F) ligands; and (iii) zirconium and hafnium catalysts that contain an asymmetric diamido/donor ligand in an attempt to effect stereocontrol of 1-hexene polymerization.

We have found that {[MesNpy]Hf(isobutyl)}⁺ initiators (**2a**, equation 1) are essentially perfectly living catalysts for polymerization of up to 600 equivalents of 1-hexene



at 0 °C in bromobenzene or chlorobenzene, and that certain bulky bases (diisopropylether, tributylamine, and triethylamine) are well-behaved inhibitors of 1-hexene polymerization. Dimethylaniline and diphenylether are not well-behaved inhibitors as a consequence of deactivation of the cationic alkyl by CH activation in the phenyl ring adjacent to the basic functionality.

Related catalysts that contain [Ar_{X2}Npy]²⁻ ligands in which the aryl ring (Ar_{X2}) contains ortho halides (X = Cl or F) are progressively worse catalysts than the mesityl-substituted species; they react more slowly with 1-hexene and they are more prone to β hydride elimination processes. In general, ortho-fluorides were found to interact with the metal, even in five-

coordinate neutral dialkyl precursors (Figure 1). Attempts to prepare some $[\text{Ar}_{\text{F}_2}\text{Npy}]^{2-}$ complexes resulted in exchange of one or two dimethylamino groups with one or two ortho fluorides. Activation of dimethyl species with $[\text{Ph}_3\text{C}][\text{B}(\text{C}_6\text{F}_5)_4]$ in bromobenzene led initially to the formation of dimeric monocations such as $\{[\text{Ar}_{\text{X}_2}\text{Npy}]_2\text{M}_2\text{Me}_3\}[\text{B}(\text{C}_6\text{F}_5)_4]$, which are inactive for polymerization of 1-hexene. The $\{[\text{Ar}_{\text{X}_2}\text{Npy}]_2\text{M}_2\text{Me}_3\}[\text{B}(\text{C}_6\text{F}_5)_4]$ compounds react further with $[\text{Ph}_3\text{C}][\text{B}(\text{C}_6\text{F}_5)_4]$ to give $\{[\text{Ar}_{\text{X}_2}\text{Npy}]\text{MMe}\}[\text{B}(\text{C}_6\text{F}_5)_4]$ species, which are active for polymerization of 1-hexene. The living characteristics of the polymerization therefore are compromised to varying degrees when ortho halides are employed in the aryl ligands ($\text{F} > \text{Cl}$).

Similar studies have been completed with diamido/donor ligands of the type $[(2,6\text{-Cl}_2\text{C}_6\text{H}_3\text{NCH}_2\text{CH}_2)_2\text{NMe}]^{2-}$. We found that Zr systems of this type were well-behaved, but the Hf systems were plagued by relatively slow rates of initiation relative to propagation.

Most recently we have completed a study of Zr and Hf complexes that contain two new unsymmetric diamido-N-donor ligands, H_2A and H_2B . The Zr and Hf complexes that have

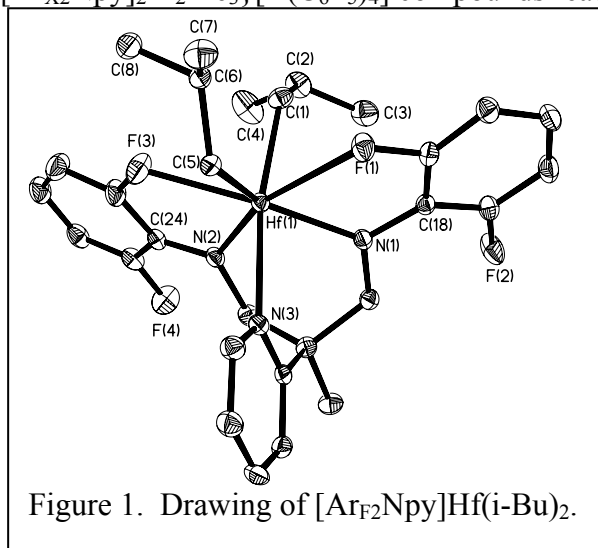
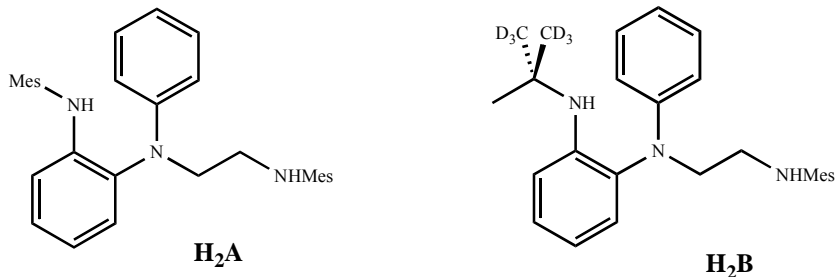


Figure 1. Drawing of $[\text{Ar}_{\text{F}_2}\text{Npy}]\text{Hf}(\text{i-Bu})_2$.



been isolated include $[\text{A}]\text{MX}_2$ ($\text{M} = \text{Zr}$ or Hf , $\text{X} = \text{NMe}_2$, Cl , or Me) and $[\text{B}]\text{MX}_2$ ($\text{M} = \text{Zr}$ or Hf , $\text{X} = \text{NMe}_2$, Cl , Me). Methyl abstraction in $[\text{A}]\text{MMe}_2$ ($\text{M} = \text{Zr}$ or Hf) with $[\text{Ph}_3\text{C}][\text{B}(\text{C}_6\text{F}_5)_4]$ gives rise to cationic complexes which are active initiators for the polymerization of 1-hexene. Similar activation of $[\text{B}]\text{MMe}_2$ ($\text{M} = \text{Zr}$ or Hf) species gives rise to dimeric monocations that eventually break-up and react further to yield cationic monomethyl species. Unfortunately, in all cases the poly[1-hexene] produced was found to be atactic. It is postulated that the central donor can dissociate from the metal, invert, and reassociate in order to produce the opposite enantiomer at a rate that is competitive with insertion into the metal-alkyl bond.

DOE Interest

The consequences of this work are expected to be the synthesis of sophisticated or "smart" new materials from ordinary and functionalized olefins in high yield in the form of diblock or triblock copolymers.

Future Plans

Future research will focus on C₁ ligands related to those we have investigated to date that contain a racemic chiral auxiliary and on new types of racemic C₂ symmetric diamido ligands.

Publications (2001-present)

1. "Cationic Zirconium Complexes that Contain Mesityl-substituted Diamido/Donor Ligands. Decomposition via CH Activation and Its Influence on 1-Hexene Polymerization" Schrodi, Y.; Schrock, R. R.; Bonitatebus, P. J. *J. Organometallics* **2001**, *20*, 3560.
2. "Cationic Hafnium Alkyl Complexes that are Stable Toward β Hydride Elimination Below 10 °C and Active as Initiators for the Living Polymerization of 1-Hexene" Mehrkhodavandi, P.; Schrock, R. R. *J. Am. Chem. Soc.* **2001**, *123*, 10746.
3. "A Kinetic Investigation of the Polymerization of 1-Hexene by the {[t-BuNON]ZrMe}[B(C₆F₅)₄] Initiator" Goodman, J. T.; Schrock, R. R. *Organometallics* **2001**, *20*, 5205.
4. "Synthesis and Structures of Zirconium and Hafnium Alkyl Complexes that Contain [H₃CC(2-C₅H₄N)(CH₂NAr)₂]²⁻ ([ArNpy]²⁻; Ar = Mesityl or Triisopropylphenyl) Ligands" Mehrkhodavandi, P.; Schrock, R. R.; Bonitatebus, P. J. Jr. *Organometallics* **2002**, *21*, 5785.
5. "Living Polymerization of 1-Hexene by Cationic Zirconium and Hafnium Complexes that Contain a Diamido/Donor Ligand of the Type [H₃CC(2-C₅H₄N)(CH₂NMesityl)₂]²⁻. A Comparison of Methyl and iso-Butyl Initiators." Mehrkhodavandi, P.; Schrock, R. R.; Pryor, L. L. *Organometallics* **2003**, *22*, 4569.
6. "Zirconium and Hafnium Complexes that Contain the Electron-Withdrawing Diamido/Donor Ligands, [(2,6-X₂C₆H₃NCH₂)₂C(2-C₅H₄N)(CH₃)]²⁻ (X = Cl or F). An Evaluation of the Role of ortho-Halides in 1-Hexene Polymerization." Schrock, R. R.; Adamchuk, J.; Ruhland, K.; Lopez, L. P. H. *Organometallics* **2003**, *22*, 5079.
7. "Synthesis, Characterization, and Polymerization Behavior of Zirconium and Hafnium Complexes that Contain Unsymmetric Diamido-N-Donor Ligands" Tonzetich, Z. J.; Lu, C. C.; Schrock, R. R.; Hock, A. S.; Bonitatebus, P. J., Jr. *Organometallics*, submitted.

This page intentionally left blank.

High Temperature Chemistry of Aromatic Hydrocarbons

Postdocs: Mack, J.

Students: Ansems, R.; Bancu, M.; Donovan, P.; Hill, T.; Jackson, E.; Peng, L.; Tsefrikas, V.; Xue, X.

Collaborators: de Meijere, A.; Diederich, F.; Guldi, D.; Hirsch, A.; Jenneskens, L. W.; Petrukhina, M. A.; Rabinovitz, M.; Schleyer, P. v. R.; Willner, I.; Wudl, F.

Department of Chemistry, Boston College, Chestnut Hill, MA 02467
lawrence.scott@bc.edu

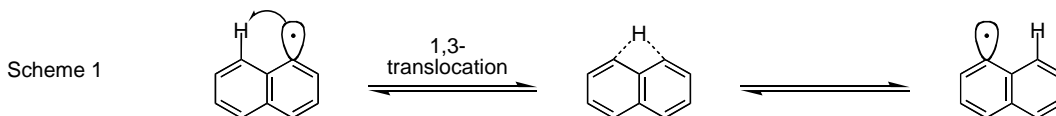
Goal

The primary goal of this research is to uncover all the principal reaction channels available to polycyclic aromatic hydrocarbons (PAHs) at high temperatures in the gas phase and to establish the factors that determine which channels will be followed in varying circumstances. New structure-property relationships for PAHs are also studied.

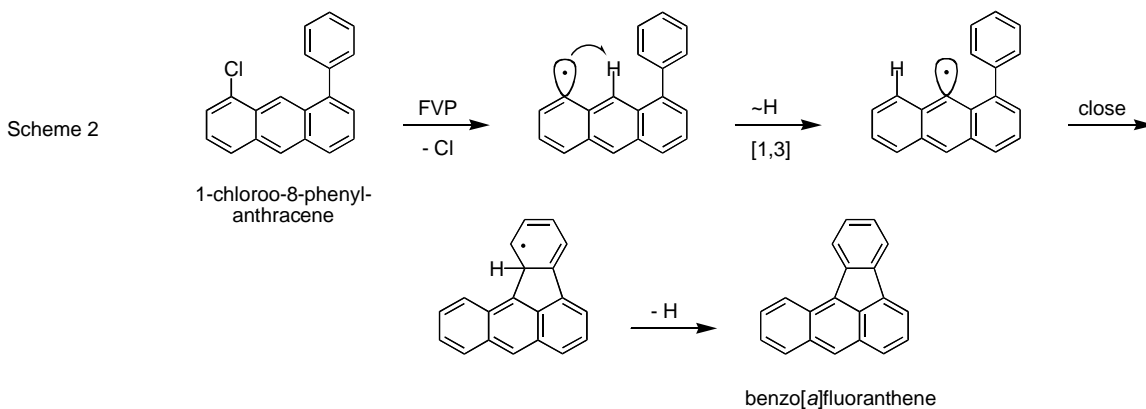
Recent Progress

The latest results from three representative projects are summarized here (all still unpublished).

1,3-Translocation of hydrogen atoms in aryl radicals. Earlier in this project, we predicted, demonstrated, and published the first unambiguous example of a hydrogen atom 1,2-shift in an aryl radical at high temperatures in the gas phase [*JACS* **1999**, *121*, 5444]. Our subsequent calculations have predicted that a hydrogen atom should also be able to “jump,” with comparable facility, from one ring to the next by a 1,3-translocation to a *peri*-radical center (Scheme 1).

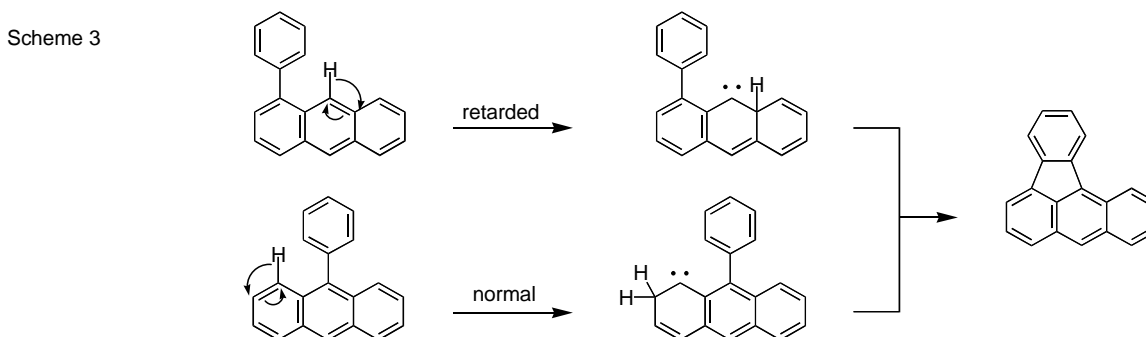


Since this process would be degenerate in the 1-naphthyl radical, we have examined a less symmetrical system. Structural features were incorporated to provide an opportunity for the rearranged radical (but not the starting radical) to close a new ring and aromatize to an easily identifiable product. As shown in Scheme 2, flash vacuum pyrolysis (FVP) of 1-chloro-8-phenylanthracene gives benzo[*a*]fluoranthene, presumably by the predicted 1,3-translocation of a *peri*-hydrogen atom to the radical center created by homolysis of the C–Cl bond.



Control experiments show that very little benzo[*a*]fluoranthene is formed by FVP of the corresponding unchlorinated hydrocarbon, 1-phenylanthracene. Deuterium labeling studies are now underway to prove that the hydrogen atom attached at the position vacated by the chlorine atom is the one that originated at C(9).

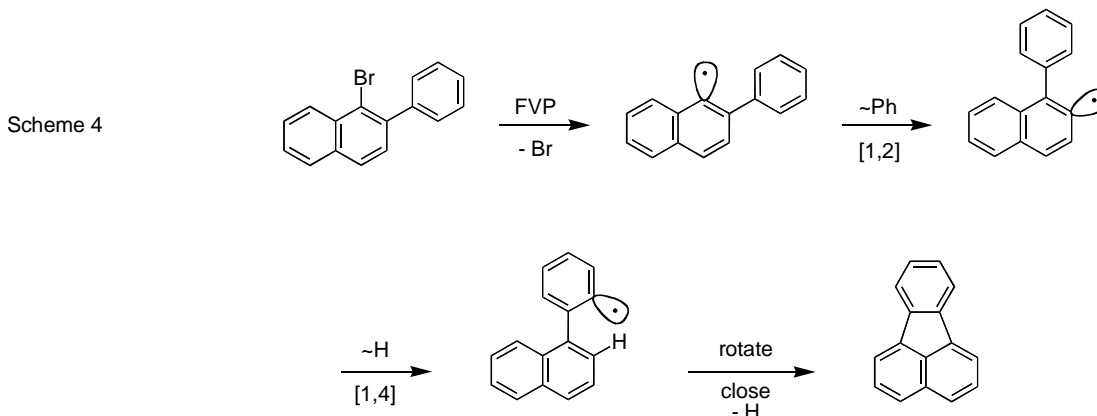
Cyclodehydrogenations to form 5-membered rings. At high temperatures in the gas phase, PAHs bearing peripheral phenyl groups commonly suffer cyclodehydrogenations to produce more highly condensed PAHs. The mechanism(s) by which these cyclizations occur and the hydrogens are lost, however, are not well established. We have previously shown that hydrogen atoms on the rims of intact PAHs can shift reversibly to *ortho*-positions, thereby generating transient carbenes [*JACS* **1991**, *113*, 9692], and it seems reasonable that such hydrogen shifts could trigger many cyclodehydrogenations. In agreement with this hypothesis, we have found that the thermal cyclodehydrogenation of 1-phenylanthracene to benzo[*a*]fluoranthene is significantly slower than formation of the same product by thermal cyclodehydrogenation of 9-phenylanthracene, under the same conditions (Scheme 3).



Generation of the proposed carbene intermediate by a hydrogen shift in the former case would simultaneously disrupt the aromaticity of two rings, whereas the same reaction in the latter case would disrupt the aromaticity of only one ring, which should be energetically less costly. The observed rate difference is difficult to explain by other mechanisms, *e.g.*, cyclization of an aryl radical that results from loss of a hydrogen atom.

Phenyl group 1,2-shifts in aryl radicals. To determine whether or not a phenyl group can migrate along the rim of a PAH radical, we have generated the 2-phenyl-1-naphthyl radical in the gas phase by FVP of 2-phenyl-1-bromonaphthalene (Scheme 4).

As predicted, a 1,2-shift moves the phenyl group over next to the ring junction where, following 1,4-translocation of a hydrogen atom, the radical cyclizes to form fluoranthene. The isolation of fluoranthene in this experiment constitutes the first good evidence that 1,2-shifts of phenyl groups are feasible in aryl radicals at high temperatures (Scheme 4).



DOE Interest

An understanding of the fundamental molecular transformations, rearrangements, and interconversions of PAHs at high temperatures in the gas phase, as revealed by careful studies on small, well-designed, molecular systems, provides insights into the underlying chemistry of many processes that are more complex and critically important to life in the twenty-first century, such as the generation of energy by the combustion of fossil fuels, the uncatalyzed gasification and liquefaction of coal, the production of fullerenes in fuel-rich flames, and the formation of soot and carcinogenic pollutants in smoke. The rational control of any of these processes, whether it be the optimization of a desirable process or the minimization of an undesirable one, requires a clear knowledge of the basic chemistry that governs the fate of the species involved.

Future Plans

We plan to repeat our experiments on the 1,3-translocation of hydrogen atoms in aryl radicals (Scheme 2) using a deuterated starting material, to demonstrate that the hydrogen originating on the central ring ends up at the site vacated by the chlorine atom. Further studies on thermal cyclodehydrogenations to form 5-membered rings are planned, and we also plan to test the generality of phenyl group 1,2-shifts in aryl radicals. New studies will be initiated on thermal cyclodehydrogenations to form 6-membered rings and on the mechanism by which phenyl groups are lost at high temperatures.

Publications (last 2 years)

- 1) "A Rational Chemical Synthesis of C₆₀," Scott, L. T.; Boorum, M. M.; McMahon, B. J.; Hagen, S.; Mack, J.; Blank, J.; Wegner, H.; de Meijere, A. *Science* **2002**, 295, 1500-1503.
- 2) "Stability and Aromaticity of the Cyclopenta-Fused Pyrene Congeners," Havenith, R. W. A.; Jiao, H.; Jenneskens, L. W.; van Lenthe, J. H.; Sarobe, M.; Schleyer, P. v. R.; Kataoka, M.; Nacula, A.; Scott, L. T. *J. Am. Chem. Soc.* **2002**, 124, 2363-2370.
- 3) "From Bifluorenylidine Dianion to Dibenzo[*g,p*]chrysene Dianion: Sensitivity of Anisotropy Changes to Bonding Structure," Shenhar, R.; Beust, R.; Hagen, S.; Bronstein, H. E.; Willner, I.; Scott, L. T.; Rabinovitz, M. *J. Chem. Soc., Perkin Trans. 2* **2002**, 449-454.
- 4) "An Insight into the Aromaticity of Fullerene Anions: Experimental Evidence for Diamagnetic Ring Currents in the Five-Membered Rings of C₆₀⁶⁻ and C₇₀⁶⁻." Sternfeld, T.; Thilgen, C.; Hoffman, R. E.; Heras, M. d. R. C.; Diederich, F.; Wudl, F.; Scott, L. T.; Mack, J.; Rabinovitz, M. *J. Am. Chem. Soc.* **2002**, 124, 5734-5738.
- 5) "A Four-Step, Alternating Reductive Dimerization/Bond-Cleavage of Indenocorannulene," Aprahamian, I.; Hoffman, R. E.; Sheradsky, T.; Preda, D. V.; Bancu, M.; Scott, L. T.; Rabinovitz, M. *Angew. Chem. Int. Ed. Engl.* **2002**, 41, 1712-1715.
- 6) "Transition Metal Complexes of an Open Geodesic Polyarene," Petrukhina, M. A.; Andreini, K. W.; Mack, J.; Scott, L. T. *Angew. Chem. Int. Ed. Engl.* **2003**, 42, 3375-3379 (highlighted on the cover).
- 7) "Conjugated Belts and Nanorings With Radially Oriented p-Orbitals," Scott, L. T. *Angew. Chem. Int. Ed. Engl.* **2003**, 42, 4133-4135 (invited *Highlight*).
- 8) "Molecular Satellite Dishes: Attaching Parabolic and Planar Arenes to Heterofullerenes," Hauke, F.; Atalick, S.; Guldi, D.; Mack, J.; Scott, L. T.; Hirsch, A. *Chem. Commun.* **2004**, web edition 23 Feb.
- 9) "Methods for the Chemical Synthesis of Fullerenes," Scott, L. T. *Angew. Chemie*, an extensive review submitted at the request of the editor.

Design of olefin metathesis catalysts for unfunctionalized and functionalized olefins

Co-PIs: Bradley Chmelka, Juergen Eckert

Graduate students: Anthony Moses, Heather Leifeste, Scott Roney

Collaborators: Robert Maughon (Dow Chemical), Dennis Hucul (Dow Chemical)

Department of Chemical Engineering, University of California, Santa Barbara CA 93106
sscott@engineering.ucsb.edu

Goal

Olefin metathesis is a powerful method for forming new C=C bonds. However, the full potential of heterogeneous metathesis catalysts has yet to be exploited, because supported metal oxides show low rates of activation and rapid deactivation. The goal of our project is to create fundamental knowledge about how carbene active sites are formed and how they are lost in supported metal oxide catalysts, in order to increase metathesis activity and impart functional group tolerance.

Recent Progress

A well-defined organometallic complex, methyltrioxorhenium (CH_3ReO_3 , MTO), generates metathesis activity without high temperature activation (calcination) when supported on certain inorganic oxides, although it is inactive in solution. The mechanisms by which MTO is grafted and activated and the nature of the MTO-support interaction are unknown, but may be directly relevant to the problems of inorganic metathesis catalysts.

Methyltrioxorhenium is unreactive towards the mildly acidic surface hydroxyls of silica. It does chemisorb onto the surfaces of niobia and silica-alumina powders, to give supported catalysts which are different in their electronic structure. Niobic acid, transformed to niobia by calcination at 450°C , turns purple at room temperature in the presence of white MTO. Grafting MTO onto silica-alumina (13 wt.% alumina, $500\text{ m}^2/\text{g}$) leads to a color change of the solid from white to orange when silica-alumina is not subjected to thermal treatment, or dark yellow-brown when the solid is pretreated under vacuum at 450°C . The color change may be associated with oxidation state or coordination sphere changes at Re.

The uptake of Re is self-limiting during gas phase grafting, yet stabilizes at values (ca. 15 wt.%) higher than might be expected for a deposition reaction limited by the availability of surface hydroxyl sites. Indeed, the hydroxyl sites appear not to be the point of attachment for MTO, since methane is not generated and the ^1H MAS NMR spectrum of MTO/silica-alumina shows a strong signal due to unreacted $\equiv\text{SiOH}$ at 1.7 ppm, in addition to signals for the methyl ligand (2.7 ppm) and adsorbed water (5.3 ppm), Figure 1a. The high loading of MTO suggests oxide-induced polymerization, similar to the formation of poly-MTO observed by Herrmann in acidic aqueous solution.

^{13}C CP/MAS NMR with natural abundance ^{13}C indicates the presence of multiple carbon sites for MTO grafted onto silica-alumina, Figure 2b. Our computational studies are aimed at understanding this complexity by developing models for the binding of MTO to oxide supports. We are simultaneously investigating the energy of the

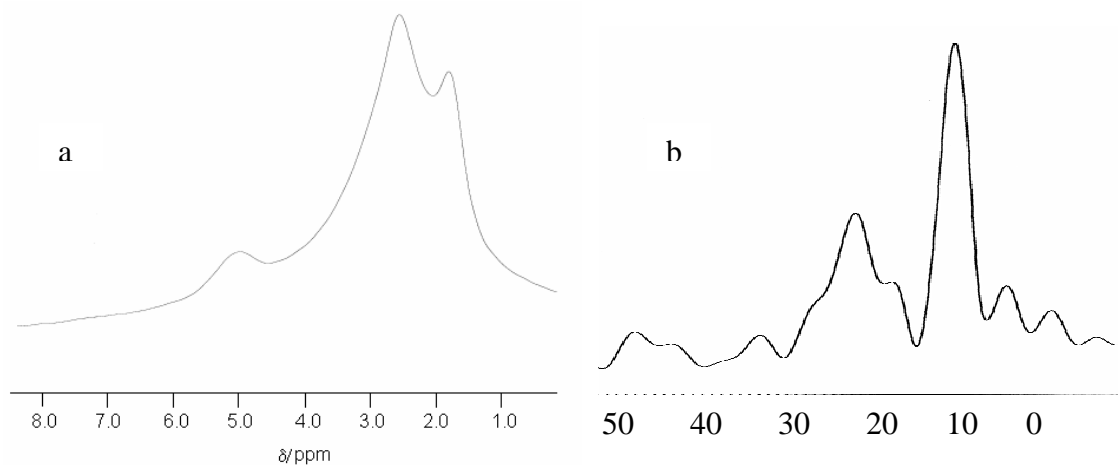


FIGURE 1. NMR of MTO on silica-alumina: (a) ^1H MAS NMR (hydroxyls partially D-exchanged); (b) ^{13}C CP/MAS NMR; 24 hour data acquisition with spinning at 10 kHz.

methylidene tautomer, a potential initiating site. Using clusters to represent silica, silica-alumina and niobia surfaces, energy minimizations have been carried out (Gaussian98) using DFT methods and various basis sets to investigate MTO and its tautomer interacting with the oxide surface via two O atoms, Figure 2. In our preliminary studies, we consistently find a significant lowering of the energy of the supported tautomer relative to adsorbed MTO, by comparison to the unsupported molecules. More sophisticated models for the silica-alumina and niobia surfaces are currently being developed.

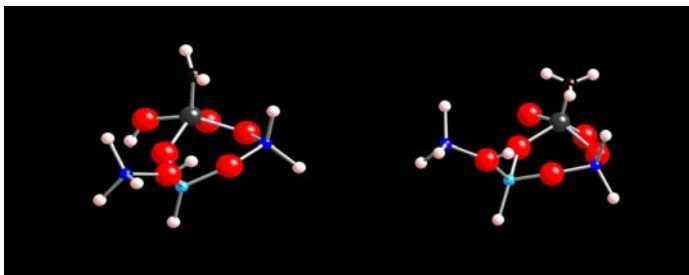


FIGURE 2. Cluster models of MTO (right) and the methylidene tautomer (left) on silica-alumina. The difference in energy between the two structures is 46 kJ/mol, compared with 108 kJ/mol for the isolated molecules.

Frequency calculations for MTO on all-silica and silica-alumina clusters show a dramatic decrease (by as much as 100 cm^{-1}) of the methyl torsional frequencies relative to the bulk solid. This result has been confirmed qualitatively by vibrational spectroscopy using Inelastic Neutron Scattering (INS), Figure 3. Note the large number of bands in the region below 250 cm^{-1} for surface-grafted MTO, which not only confirm the lowering of the methyl torsional frequency, but also suggest the existence of multiple MTO species on the surface. INS is particularly sensitive to low-frequency motions involving H atoms of adsorbed or bound species. Furthermore, such spectra can readily be calculated (Figure 3b) from the frequencies and amplitudes obtained for our models. We expect to be able to derive information on the binding of MTO by an iterative comparison of observed INS spectra and those calculated from different structural models.

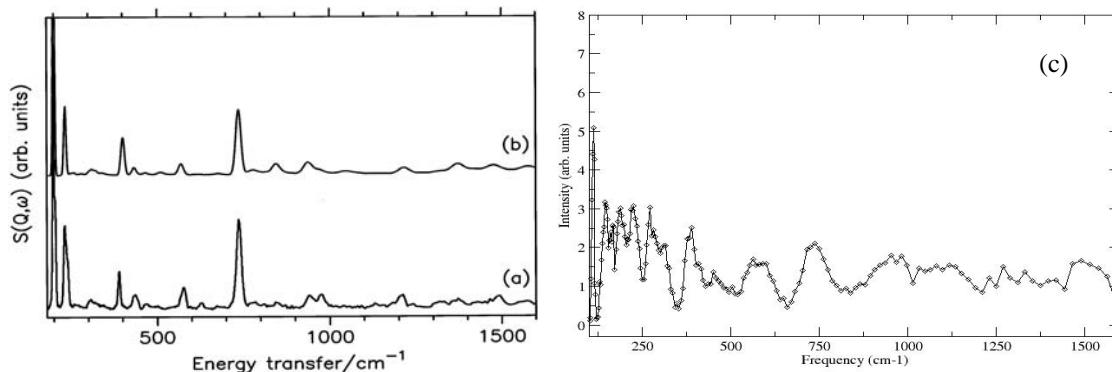


FIGURE 3. INS spectra of MTO (observed (a) and calculated (b)) and MTO grafted on silica-alumina. Spectrum (c) recorded at 20 K. (Left: S.F. Parker and H. Herman, *Spec Acta* A56 (2000) 1123)

We are also investigating the structure of grafted MTO using X-ray absorption spectroscopy, Figure 4. Analysis of the EXAFS is underway to provide information about the coordination environment of Re and bond distances, which will allow us to perform more definitive calculations.

DOE Interest

Supported perrhenate catalysts are of particular interest for olefin metathesis, because they are active at much lower temperatures and are more functional group-tolerant than either Mo- or W-based catalysts. These properties make them potentially useful in liquid phase reactions involving biorenewable feedstocks, such as seed oils.

Future Plans

We plan to mitigate deactivation by attaching rhenium to silica or silica/alumina via protolytically stable Re-C-Si linkages. This objective is being pursued via a co-condensation synthesis to produce vinyl-functionalized SBA-15, on which the surface organic groups will be used to anchor rhenium oxide. Characterization of grafted complexes will be undertaken using multidimensional solid-state NMR.

Inhibiting the adsorption of polar impurities or reaction by-products will be achieved with surface silylation. Sn incorporation into the oxide support is being pursued in order to promote functional group tolerance without enhancing deactivation or precluding reactivation of the active sites. This goal is particularly important as we work towards the design of metathesis catalysts for biorenewables.

Publications (2003 -). This project began 9/15/2003. No publications have appeared at this time (3/15/2004).

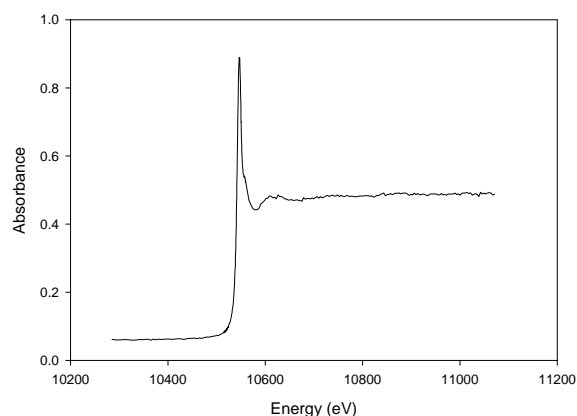


FIGURE 4. X-ray absorption at the Re L_{III} edge (10,535 keV) for MTO supported on silica-alumina pretreated at 450°C. This spectrum was acquired at CAMD (Baton Rouge, LA).

This page intentionally left blank.

Title: Transition Metal Mediated Transformations of Small Molecules

PI: Ayusman Sen
Department of Chemistry
The Pennsylvania State University, University Park, PA 16802
Phone: 814-863-2460; Fax: 814-863-8403
Email: asen@chem.psu.edu
<http://research.chem.psu.edu/axsgroup/>

Postdoctoral scholars: Shengsheng Liu, Sachin Borkar
Graduate students: Christine Elia, Shahid Murtuza, April Hennis, Gregory Long,
Sharon Elyashiv-Barad, Cecily Andes, Myeongsoon Kang, Jeffrey
Funk, Megan Majcher
Undergraduate students: Benjamin Snedeker, Kyle Bartosh, Michelle L. Werner, Jennifer
D. Polley, Seth B. Harkins, Karl Oyler, David Goldstein, Heather
Rowlands

Goals and Objectives

Catalytic polymer synthesis by metal compounds is of great scientific, as well as practical, importance because of the high efficiency, high specificity, and low energy demands often associated with such systems. The theme of the proposed research is the design of new metal-based systems for the synthesis of novel classes of polymers. In the process, we hope to address key questions concerning the steps involved in such polymerization reactions.

Significant Recent Achievements and Results

Below we briefly summarize some of our recent research achievements. Further details regarding our work can be found in the publications and patents listed at the end of this section.

A significant fraction of the work during the current grant period has been devoted to catalytic systems for the homo and copolymerizations of norbornene derivatives and acrylates. A new palladium-based catalyst was found for the vinyl addition polymerization of norbornene derivatives, including those with pendant oxygen functionalities. For norbornene, a polymerization rate of 1000 tons norbornene/mol Pd•hour was observed at 25°C. However, the polymerization rate was found to decrease for norbornene derivatives with pendant functionalities. *Endo*-substituted norbornenes are polymerized more slowly than their corresponding *exo* isomers. The size of the substituent plays a role. However, the coordinating ability of the functionality plays an even bigger role in attenuating polymerization than its size. The formation of chelates upon the coordination of the *endo*-functionalized norbornene is responsible, in part, for the observed decrease in polymerization rate. A further and, even greater, reason for the diminution of activity of *both* the *endo* and the *exo*-functionalized isomers is simply the coordination of the functionality to the metal center.

We have also investigated a novel acrylate copolymerization system. A neutral palladium complex was found to effect the polymerization of acrylates. Over 10 mol% incorporation of 1-hexene in the polymer was achieved when the latter was added together with methyl acrylate. The polymerization occurs by a free radical mechanism that is tied to a β -H elimination chain termination/transfer step.

Finally, a copper-mediated procedure for the synthesis of random copolymers of methyl acrylate with 1-alkenes, ranging from ethene to 1-decene, as well as norbornene derivatives, has been discovered. Copolymers with greater than 20 mol% incorporation of the 1-alkene are formed. The system is *living*, thereby allowing the synthesis of novel block terpolymers of methyl acrylate with 1-alkenes and/or norbornenes by the sequential addition of the latter monomers.

Future Plans

During the upcoming year we intend to follow, for the most part, the lines of research outlined in the most recent proposal. This will involve investigations of homogeneous metal-catalyzed processes for the synthesis of polymers and copolymers. The principal goal of the proposed research will be the design of new metal-catalyzed systems for the formation of polymers with interesting architectures. The research will focus on two specific areas: (A) metal-mediated homo and copolymerization of functionalized vinyl monomers and (B) metal-catalyzed polypeptide synthesis through alternating copolymerization of imines with carbon monoxide.

Impact on Science and Technologies of Relevance to DOE

Catalytic polymer synthesis by metal compounds is of great scientific, as well as practical, importance because of the high efficiency, high specificity, and low energy demands often associated with such systems. Indeed, several high-volume commercial polymers are only accessible through metal-mediated routes. Hence, the achievement of a fundamental understanding of all aspects of such catalysis is an important goal. The Technology Vision 2020 report also cites the importance of developing new catalysts for customizing polymer properties. The theme of our research is the design of new metal-based catalytic systems for the synthesis of novel classes of polymers. For example, the copolymerization of functionalized vinyl monomers with non-polar alkenes remains an area of great interest in synthetic polymer chemistry, because the addition of functionalities to a polymer which is otherwise non-polar can greatly enhance the range of attainable properties. One particular area of interest is the homopolymerization of norbornene derivatives and their copolymerization with acrylates to form materials suitable for deep UV photolithography. Polyacrylates show good adhesion and have been used extensively as photoresist materials, but suffer from poor dry etch resistance. On the other hand, polynorbornenes exhibit superior etch resistance and thermal stability. Thus, norbornene homo and copolymers may provide the optimum properties.

Refereed Publications and Patents Based on DOE Grant (2001-present)

1. “Grafting of Syndiotactic Polystyrene by Branched Oligoethene Using $[\text{Ni}(\pi\text{-methallyl})(\text{Br})]_2/\text{AlCl}_3$ Catalyst,” Shengsheng Liu and Ayusman Sen, *J. Polym. Sci., A: Polym. Chem.*, **2001**, 39, 446.

2. "Synthesis of Novel Linear Polyethene-Based Graft Copolymers by Atom Transfer Radical Polymerization," Shengsheng Liu and Ayusman Sen, *Macromolecules*, **2001**, *34*, 1529.
3. "New Olefin Polymerization and Copolymerization Catalysts. Effect of Coordinating Functionalities," Ayusman Sen, *Pure Appl. Chem.*, **2001**, *73*, 251.
4. "Transition Metal Phthalocyanine and Porphyrin Complexes as Catalysts for the Polymerization of Alkenes," Gregory S. Long, Benjamin Snedeker, Kyle Bartosh, Michelle L. Werner, and Ayusman Sen, *Can. J. Chem.*, **2001**, *79*, 1026.
5. "A Novel, Efficient, Palladium-Based System for the Polymerization of Norbornene Derivatives: Scope and Mechanism," April D. Hennis, Jennifer D. Polley, Gregory S. Long, Ayusman Sen, Dmitry Yandulov, John Lipian, George M. Benedikt, Larry F. Rhodes, and John Huffman, *Organometallics*, **2001**, *20*, 2802.
6. "New Tantalum-Based Catalyst System for the Selective Trimerization of Ethene to 1-Hexene," Cecily Andes, Seth B. Harkins, Shahid Murtuza, Karl Oyler, and Ayusman Sen, *J. Am. Chem. Soc.*, **2001**, *123*, 7423.
7. "Copper-Mediated Controlled Copolymerization of Methyl Acrylate with 1-Alkenes under Mild Conditions," Shengsheng Liu, Sharon Elyashiv, and Ayusman Sen, *J. Am. Chem. Soc.*, **2001**, *123*, 12738.
8. " Et_2Al^+ Aluminium Ion-like Chemistry. Synthesis and Reactivity toward Alkenes and Alkene Oxides," Kee-Chan Kim, Christopher A. Reed, Gregory S. Long, and Ayusman Sen, *J. Am. Chem. Soc.*, **2002**, *124*, 7662.
9. "Copolymerization of Methyl Acrylate with Norbornene Derivatives by Atom Transfer Radical Polymerization," Sharon Elyashiv-Barad, Nils Greinert, and Ayusman Sen, *Macromolecules*, **2002**, *35*, 7521.
10. "A Palladium-Based System for the Polymerization of Acrylates. Scope and Mechanism," Christine Elia, Sharon Elyashiv-Barad, Ayusman Sen, Raquel López-Fernández, Ana C. Albéniz, and Pablo Espinet, *Organometallics*, **2002**, *21*, 4249.
11. "Diametrically Opposite Trends in Alkene Insertion in Late and Early Transition Metal Compounds: Relevance to Transition Metal-Catalyzed Polymerization of Polar Vinyl Monomers," Myeongsoon Kang, Ayusman Sen, Lev Zakharov and Arnold L. Rheingold *J. Am. Chem. Soc.*, **2002**, *124*, 12080.
12. "Copolymerization of Ethene with Norbornene Derivatives Using Neutral Nickel Catalysts," George M. Benedikt, Ed Elce, Brian L. Goodall, Heather A. Kalamarides, Lester H. McIntosh, Larry F. Rhodes, K. T. Selvy, Robert A. Shick, Cecily Andes, Karl Oyler, and Ayusman Sen, *Macromolecules*, **2002**, *35*, 8978.

13. "Strategies for Catalytic Polymerization of Polar Monomers," Ayusman Sen and Myeongsoon Kang in "Late Transition Metal Polymerization Catalysis," Wiley-VCH, Weinheim, 2003, p. 307.
14. "Trends in Alkene Insertion in Late- and Early-Transition Metal Compounds: Relevance to Transition Metal-Catalyzed Polymerization of Polar Vinyl Monomers," Myeonsoon Kang, Ayusman Sen, Lev Zakharov, Arnold I. Rheingold, In "Beyond Metallocenes: Next-Generation Polymerization Catalysts," *ACS Symp. Ser.*, **2003**, 857, 143.
15. "The Addition Polymerization of Functionalized Norbornenes: The Effect of Size, Stereochemistry and Coordinating Ability of the Substituent," Jeffrey K. Funk, Cecily E. Andes, and Ayusman Sen, *Organometallics*, 2004, *in press*.

Patents

1. "Preparation of Highly Branched, Liquid Polymers of Ethylene and/or α -Olefins in the Presence of Aluminum-Based Catalyst Systems," Ayusman Sen, Louis M. Wojcinski, and Shahid Murtuza, *U. S. Patent*, 6,232,257 (2001).
2. "Transition Metal-Free Olefin Polymerization Catalyst," Ayusman Sen, Louis M. Wojcinski, and Shengsheng Liu, *U. S. Patent*, 6,291,387 (2001).
3. "Palladium(II) Catalyzed Polymerization of Norbornene and Acrylates," Ayusman Sen and April Hennis, *U. S. Patent*, 6,300,440 (2001).
4. "Metal Catalyzed Synthesis of Hyperbranched Ethylene and/or α -Olefin Polymers," Ayusman Sen, Jang Sub Kim, James H. Pawlow, Shahid Murtuza, Smita Kacker, and Louis M. Wojcinski, *U. S. Patent*, 6,303,717 (2001).
5. "Highly Selective Catalytic Process for Synthesizing 1-Hexene from Ethylene," Ayusman Sen, Shahid Murtuza, Seth B. Harkins, and Cecily Andes, *U. S. Patent*, 6,344,594 (2002).
6. "Alkyl Magnesium Catalyzed Synthesis of Ethylene and α -Olefin Polymers," Ayusman Sen and Jang Sub Kim, *U. S. Patent*, 6,407,299 (2002).
7. "Catalyst and Methods for Polymerizing Cycloolefins", John-Henry Lipian, Larry F. Rhodes, Brian L. Goodall, Andrew Bell, Richard A. Mimna, John C. Fondran, Jayaraman Saikumar, April D. Hennis, Christine N. Elia, Jennifer D. Polley, and Ayusman Sen, *U. S. Patent*, 6,455,650 (2002).
8. "Process for Synthesizing Linear Polymers of Ethylene and α -Olefins," Ayusman Sen, Louis M. Wojcinski, and Shengsheng Liu, *U. S. Patent*, 6,489,416 (2002).

9. "Preparation of Highly Branched, Liquid Polymers of Ethylene and/or α -Olefins in the Presence of Aluminum-Based Catalyst Systems," Ayusman Sen, Louis M. Wojcinski, and Shahid Murtuza, *U. S. Patent*, 6,518,384 (2003).
10. "Palladium(II) Catalyzed Polymerization of Norbornene and Acrylates," Ayusman Sen, Smita Kacker, April Hennis, and Jennifer D. Polley, *U. S. Patent*, 6,593,440 (2003).

This page intentionally left blank.

Alkene Oxidation with Platinum Oxo Complexes and Gold Cluster Complexes as Models for Supported Gold Cluster Catalysts

Postdocs: Anupam Singh, Anandhi Upendran
Students: Endre (Andy) Szuromi

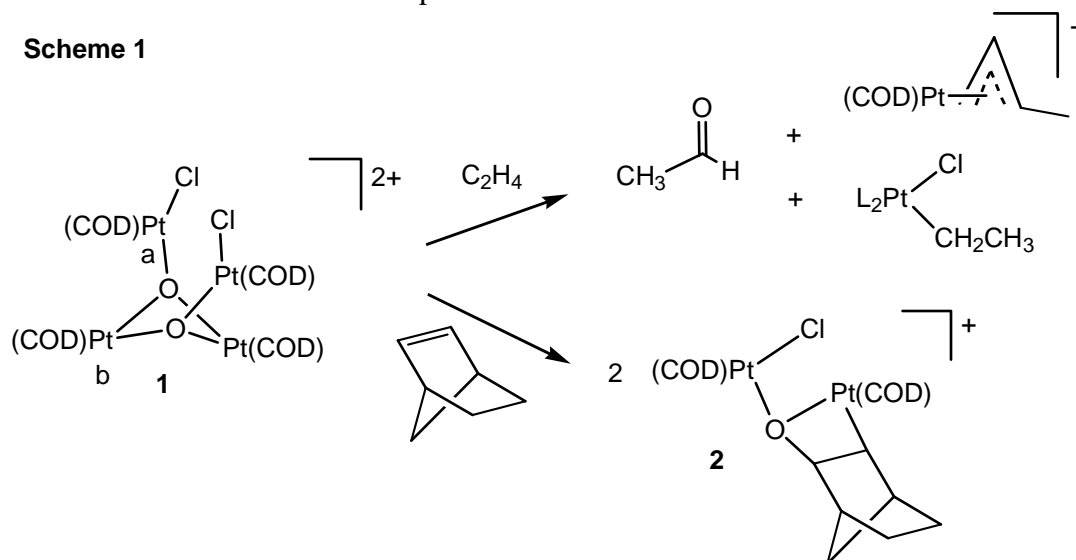
Department of Chemistry, University of Missouri, Columbia, MO 65211
sharpp@missouri.edu

Goals

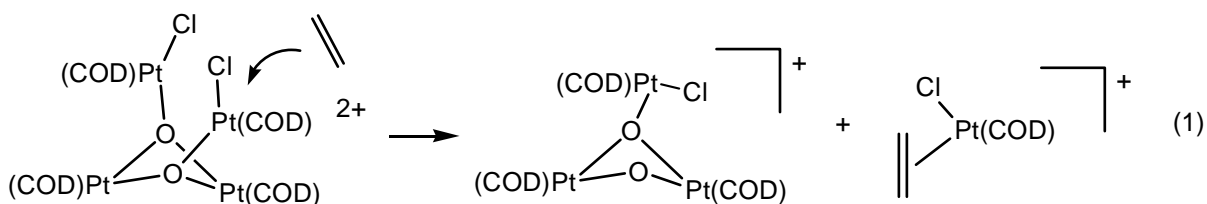
1) Understand the factors in late transition metal oxo complex reactions with alkenes and other unsaturated substrates and 2) improve understanding of supported gold cluster catalysts by the preparation and study of gold complexes and gold cluster complexes containing Au-M (M = Al, Ga, Si, Ge, Ti) and Au-O bonds.

Recent Progress

Alkene oxidation chemistry. Oxo complex $[(1,5\text{-COD})_2\text{Pt}_2(\mu^3\text{-O})_2\{(1,5\text{-COD})\text{PtCl}\}_2]^{2+}$ (**1**) oxidizes ethylene to acetaldehyde (Scheme 1). This is a complex reaction and we sought an alkene that would give a more clearly defined reaction. Norbornylene is such an alkene and gives, in quantitative yield, platinaoxetane **2** (Scheme 1), the first metallaoxetane to be formed from the reaction of an oxo complex with an alkene.

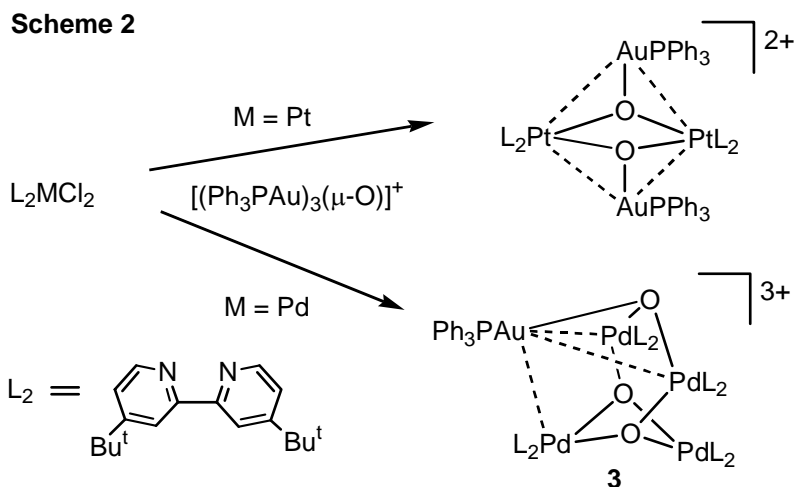


Mechanistic studies of the norbornylene reaction are in progress. Preliminary kinetic studies indicate that the reaction is first order in alkene. DFT calculations to determine the alkene attack site (Pt(a) or Pt(b) in Scheme 1) have begun. Charge distribution favors attack at Pt(b) but product stability strongly favors attack at Pt(a) with formation of $[(\text{COD})\text{PtCl}(\text{C}_2\text{H}_4)]^+$ and $[(1,5\text{-COD})_2\text{Pt}_2(\mu^3\text{-O})_2\{(1,5\text{-COD})\text{PtCl}\}]^+$ (**3**) (eq 1). These highly CPU intensive calculations are continuing and will help us understand the reactions of **1**.



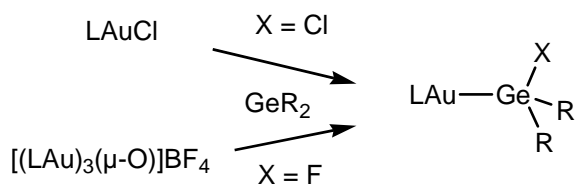
Modifications to **1** and reactions with other substrates have also been undertaken. We have successfully prepared the bromide analog of **1** and find that its reactions parallel those of **1**. Styrene, propene, cyclopentene, and diethylacetylene react readily with **1**. The propene reaction is analogous to the ethylene reaction and gives acetone, though in low yield. The platinum containing products have not yet been identified. The styrene reaction is complex and the major platinum-containing product is CODPtCl₂. The cyclopentene and diethylacetylene look very promising giving CODPtCl₂ and one other platinum-containing complex.

New oxo complexes. Parallel with the above studies on **1** we have been expanding our inventory of similar oxo complexes for possible alkene reactions. New complexes are given in Scheme 2 and include our first example of a Pd oxo complex **3**, which bears considerable resemblance to **1**. Unfortunately, the new complexes appear not to react with alkenes.

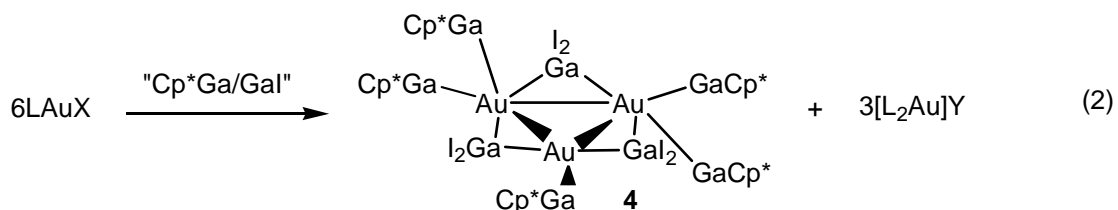


Gold-electropositive metal clusters. Work in this new area began with reactions of LAuCl (L = a phosphine) with GeR₂ (R = N(SiMe₃)₂) (Scheme 3). For all L examined, insertion of GeR₂ into the Au-Cl bond was observed giving the new complexes LAu-Ge(Cl)R₂. To obtain the more desirable chloride free analog ([LAu-GeR₂]⁺), [(LAu)₃(μ-O)]BF₄ was treated with GeR₂. LAu-Ge(F)R₂ was obtained, presumably by fluoride abstraction from BF₄⁻.

Scheme 3



The remarkable cluster **4** with gold bonded solely to Ga was formed in the reaction shown in eq 2. Isolation of this cluster bodes well for the synthesis of a new family of group 13 ligated gold cluster complexes. Preliminary DFT calculations on **4** indicate strong polarization of the Cp*Ga-Au bond and essentially neutral gold atoms.



DOE Interest

The improved understanding of the chemistry of metal oxo complexes and gold cluster complexes that will be gained by studying the reactivity and formation of the above complexes will increase our fundamental understanding of critical interactions in important catalytic processes. The benefits could be many, including increased efficiency, new processes, and less pollution.

Future Plans

We will continue our work on the platinum alkene oxidation chemistry. Our objectives are to complete the kinetic studies of the norbornylene reaction with [(1,5-COD)₂Pt₂(μ³-O)₂{(1,5-COD)PtCl₂}₂]²⁺ (**1**) and derivatives and to prepare new examples of oxo complexes which are capable of alkene oxidation. DFT studies will be continued to assist in our search. Our objectives in the gold cluster area are to prepare the aluminum analog of **4** and to elucidate the reactivity of the cluster complexes. The aluminum analog of **4** is expected to show even greater charge transfer from aluminum to gold giving negatively charged gold centers.

Publications (2002-present)

"Water Promoted Reaction of a Platinum (II) Oxo Complex with Ethylene" Flint, B.; Li, J. J.; Sharp, P. R. *Organometallics*, **2002**, *21*, 997-1000.

"Diphosphazane supported platinum(II) triflate, amine, and amido complexes: synthesis and X-ray crystal structures" Xia, A.; Sharp, P. R. *Polyhedron*, **2002**, *21(12-13)*, 1305-1310.

“Reactions of $[\text{L}_2\text{Pd}(\mu\text{-OH})_2]^{2+}$ (L = PPh_3)” Kannan, S.; James, A. J.; Sharp, P. R. *Inorg. Chim. Acta*, **2003**, 345, 8-14.

“Platinum and Palladium Imido and Oxo Complexes with Small Natural Bite Angle Diphosphine Ligands” Anandhi, U.; Holbert, T.; Lueng, D.; Sharp, P. R. *Inorg. Chem.* **2003**, 42(4), 1282-1295.

“Alkene Oxidation by a Platinum Oxo Complex and Isolation of a Platinoxane” Szuromi, E.; Hui, S.; Sharp, P. R. *J. Am. Chem. Soc.* **2003**, 124(35), 10522-10523.

“A Gold-Gallium Cluster Complex with Gold Bonded only to Gallium” Anandhi, U.; Sharp, P. R. *Inorg. Chem.* submitted.

Growth of Metal and Semiconductor Nanostructures Using Localized Photocatalysts

Postdocs: Zhongchun Wang

Students: Song, Y.

Collaborators: Medforth, C. J., Singh, A. K., Pereira, E., Brinker, C. J., Xu, H.

Department of Chemical and Nuclear Engineering, University of New Mexico, NM 87131
jasheln@unm.edu.

Goal

Develop photocatalytic synthesis methods for producing metallic nanostructures.

Recent Progress

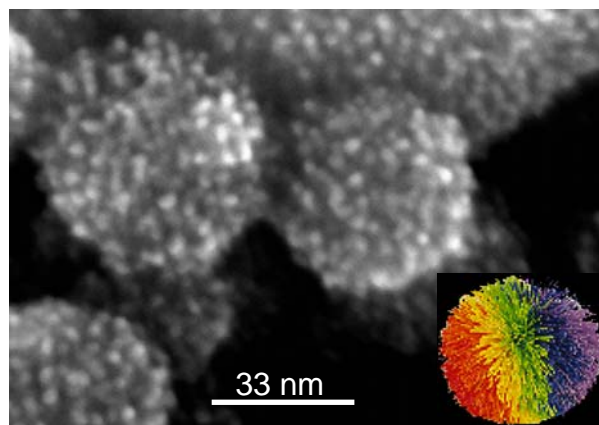
Our main objective is to understand and develop a new and novel light-driven approach to the controlled growth of unique metal and semiconductor nanostructures and nanomaterials. In this bio-inspired photochemical process, porphyrin photocatalysts provide metal nucleation and growth centers at which metal salts are reduced from aqueous solutions at ambient temperatures to produce desired metal nanostructures. Photocatalyst molecules are pre-positioned at the nanoscale to control the location and morphology of the metal nanostructures that are grown. Self-assembly, chemical confinement, and molecular templating are some of the methods used for nanoscale positioning of the photocatalyst molecules. When exposed to light, a photocatalyst molecule repeatedly reduces metal ions from solution, leading to deposition in the vicinity of the photocatalyst molecule and the formation of the nanostructure or nanomaterial.

This new synthetic approach has proven to be very successful for producing metal nanostructures and nanostructured materials, giving a number of amazing new and novel metal nanostructures. Of particular note are the platinum metal Koosh-ball like nanodendrites and the platinum-lace foams and foam balls (which were extensively reported in the scientific media) and, most recently, the gold- and platinum-decorated porphyrin nanotubes. In fact, the discovery of porphyrin nanotubes by our group was also an indirect outcome of the DOE research effort in photocatalytic growth of metal nanostructures. The nanomaterials resulting from these studies will have applications in nanoelectronics, photonics, sensors, catalysis, and microelectromechanical systems.

Another of our goals has been to elucidate the processes involved in the photocatalytic growth of metal nanomaterials and provide the scientific basis for controlled synthesis of a wide variety of nanomaterials, and we have made considerable progress in this effort as well. In this regard, we have fully elucidated the mechanisms associated with the growth of the platinum and palladium nanodendrites.

Surfactant-Templated Platinum and Palladium Nanostructures: We have discovered and extensively studied a porphyrin-based photocatalytic method for controlling the growth of

Figure 1. Globular platinum nanodendrites grown on Brij-35 micelles. The size distribution is very broad when porphyrin photocatalyst is absent. Nanodendrite size and uniformity is easily controlled by using a micelle-bound porphyrin (SnOEP) to photocatalytically grow a large initial population of platinum seed nanoparticles, which then grow autocatalytically by oxidation of ascorbic acid into the nano-Koosh balls.
Inset: A Koosh® ball.



novel platinum metal nanodendrites templated on surfactant assemblies containing the photocatalyst. When the porphyrin photocatalyst is localized in the micelles, three-dimensional globular dendrites of dimensions between 3-100 nm have been produced. A transmission electron microscopy (TEM) image of these platinum nano-Koosh-balls is shown in Figure 1. The size and uniformity of these nanodendrites can be controlled by altering the platinum-to-photocatalyst concentration ratio and/or the light exposure. Control is realized because the micelle-bound porphyrins (SnOEP) photocatalytically grow a large initial population of platinum seed nanoparticles, which then become catalytic at a certain size and grow into the nano-Koosh balls by Pt-catalyzed oxidation of ascorbic acid and reduction of Pt ions. These platinum nanodendrites were shown to be active catalysts for H₂ evolution from water.

In contrast with the micelles, localization of the porphyrin within the bilayers of unilamellar liposomes and exposure to white light initiates the growth of dendritic sheets of platinum. Depending on the illumination conditions and the concentrations of porphyrin and Pt, the growth of these Pt sheets leads to either thin (~2-nm) flat circular dendrites of 50-200-nm diameters or extended Pt foam-like materials. The morphology of the Pt foams is easily photocatalytically controlled to give individual Pt-coated liposomes, Pt foam balls, or monolithic Pt foams. The Pt foam balls and monolithic foams are shown in scanning electron microscopy (SEM) images in Figure 2(a) and (b), respectively.

Porphyrin-Nanotube-Templated Platinum and Gold Nanostructures: One of the most

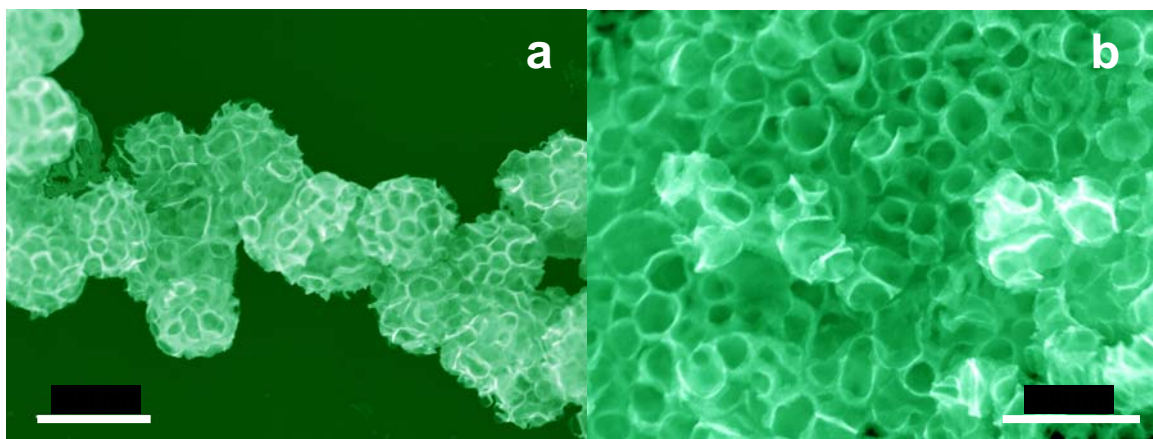


Figure 2. Platinum foam balls (a) and monolithic platinum foams (b) composed of 2-nm thick dendritic platinum sheets coating aggregated liposomes.

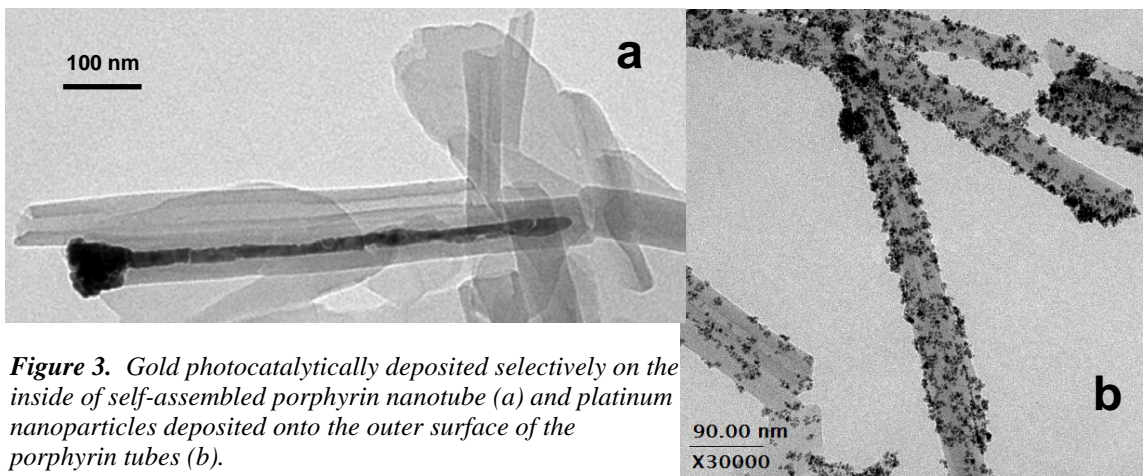


Figure 3. Gold photocatalytically deposited selectively on the inside of self-assembled porphyrin nanotube (a) and platinum nanoparticles deposited onto the outer surface of the porphyrin tubes (b).

exciting discoveries made during the course of the DOE work is that porphyrins can be self-assembled into well formed nanotubes. These nanotubes are composed of mixtures of two porphyrins—one anionic and the other cationic. The diameters of the porphyrin tubes are monodisperse and the tube diameter can be varied by altering the molecular structure of the porphyrins making up the tubes. Furthermore, one of these porphyrins can be made to be a photocatalytic metal derivative, making possible the use of the nanotubes as templates for the photocatalytic growth of metal-nanotube composite structures.

Figure 3 shows typical TEM images of two examples of the photocatalytic deposition of metals onto one type of the porphyrin nanotubes. We suspect the selectivity for gold deposition inside the tubes and platinum on the outside the tubes is based on the opposite charges of the metal ions—the Au(I) complex is positively charged and the Pt(II) complex is negatively charged. The porphyrins making up the tube walls are expected to be active in electron and energy transfer since the porphyrins are self-assembled as *J*-aggregates, which give interesting collective electronic properties such as intense resonance light scattering. The possibility of energy and light conductivity is supported by the lack of gaps in the gold nanowires.

Peptide Nanotube Templates: We have also been investigating the possibility of using peptide nanotubes as templates for photocatalytic metal deposition. Currently, we have synthesized these nanotubes and grown platinum nanoparticle inside the apparently porous walls of the tubes in a dense and homogeneously distributed fashion. Very recently, we have succeeded in making ‘pink’ tubes, which incorporate a photocatalytic porphyrin. We now plan to use the porphyrin-impregnated peptide nanotubes to grow various metal nanostructures.

DOE Interest

The research has led to highly nanoengineered materials for applications in catalysis, nanoelectronics, photonics, MEMS, and nanomagnetic systems. These nanomaterials are composed of platinum, palladium, and gold, and they may potentially be made from other useful metals and semiconductors. The development of a fundamental understanding of the uses and limitations of biomimetic photocatalysis as a means of producing metal and semiconductor nanostructures and nanomaterials is progressing and is expected to lead to further new applications of this new nanotechnology. The work has led to a relationship with InfraSUR LLC, a small business that is developing our photocatalytic metal reduction processes for

environmental remediation. We are also in discussions with a major automotive manufacturer concerning the potential use of the platinum nanodendrites in fuel cells.

Future Plans

Platinum Nanostructures and Nanostructured Materials: We need to further explore the synthetic possibilities of these types of materials and improve our understanding of the factors that control their morphology. Our main objectives will be to produce new nanomaterials for specific applications and gain additional expertise in controlling their nanostructure. Specifically, we will investigate additional templating materials (e.g., porphyrin nanotubes and fibers, polymers, and silicates), develop new alloyed metal nanostructures (Pt,Pd,Ni,Fe,Rh), formulate new composite nanostructures by sequential addition of different metals, determine the minimum size of nanoparticles that can be made, incorporate metal nanoparticles and nanosheets at specific locations in polymer electrolytes and other materials (for fuel cells), and determine the thermal and mechanical stability, porosity, and other materials properties relevant to these specific applications. Experimental techniques to be used include high-resolution electron microscopy (TEM,SEM), XRD, UV-visible, fluorescence and Raman spectroscopy.

Porphyrin-Nanotube Templated Nanostructures We will focus a large part of our work on making new metal-nanotube composite structures and investigating their catalytic, optical, and electronic properties. For example, we expect the platinized porphyrin nanotubes to be excellent nanostructures for evolving hydrogen, given that they may already incorporate light-harvesting and electron-transport functionality coupled with photosynthetic reaction centers and hydrogenase catalytic function (Pt nanoparticles) in optimal proportions. The plasmonic properties of metal nanostructure grown inside and/or outside of the tubes will be investigated.

Other Methods of Localizing Photocatalyst Molecules We will use the peptide nanotubes with incorporated photocatalytic porphyrins to grow metal nanostructures and investigate their structure and properties. We will investigate other ways of positioning porphyrins at the nanoscale for fabrication of metal and semiconductor nanostructures.

Other Metals and Semiconductors We will investigate the photocatalytic reduction of other metals and semiconductors for applications in waste treatment, nanoelectronics, nanotagging, nanophotonics, and nanomagnetism.

Publications (2003-4)

1. Song Y, Yang Y, Medforth C J, Pereira E, Singh A K, Xu H, Jiang Y, Brinker C J, van Swol F, Shelnett J A. Controlled Synthesis of 2-D and 3-D Dendritic Platinum Nanostructures *J. Am. Chem. Soc.* 2004, *126*, 635-645.
2. Song Y, Challa S R, Haddad R E, Qiu Y, Medforth C J, Watt R K, van Swol F, Shelnett J A, Synthesis of peptide-nanotube platinum-nanoparticle composites *Chem. Commun.* 2004, Submitted.
3. Song Y, Singh A K, Qiu Y, Shelnett J A, Photocatalytically Nanoengineered Foam-Like Platinum Materials Templated on Liposomes *Angew. Chem., Int. Ed.* In preparation.
4. Wang Z, Shelnett J A, Self-Assembled Porphyrin Nanotubes, *Nature*, In preparation.

Self-Assembly of Polyelectrolyte Structures in Solution:
From Atomic Interactions to Nanoscale Assemblies

Co-Investigators: P. F. Britt, A. Habenschuss, B. K. Annis, A. A. Chialvo, G. D. Wignall, Y. B. Melnichenko (ORNL); J. W. Mays (UT/ORNL); M. Muthukumar (U. Mass., Amherst), P. T. Cummings (Vanderbilt)

Postdocs: S. I. Yun, K. Hong

Collaborators: E. R. Zubarev, Iowa State University

Chemical Sciences Division, Oak Ridge National Laboratory, Oak Ridge, TN 37831-6197
simonsonjm@ornl.gov

Goal

Predict and control the nanoscale structures formed by polyelectrolytes in solution based on a fundamental understanding of extent and importance of the full range of interactions from atomic to nanoscale dimensions.

Recent Progress

Research is aligned along parallel, complementary efforts in synthesis of model polyelectrolytes, detailed characterization at the atomic and macromolecular length scales, and fundamental theoretical and computational models of structure and interactions in solution.

Polyelectrolyte synthesis. The goal of this task is to synthesize novel polyelectrolytes designed to highlight specific interactions in solution that lead to significant differences in the observed conformation, interactions with counterions, and self-assembly of nanoscale structures. Building on an extensive base of literature studies of polystyrene sulfonate (PSS), we have focused on the synthesis of poly(cyclohexadiene) sulfonate (PCHDS). For this material the stiffer chain will permit determination of the effect of this important variable on structure and interactions in solution.

Sulfonation of well-defined (molecular weight: ~8,000g/mol, PDI: ~1.06) poly(1,3-cyclohexadiene) polymers (PCHDS) was accomplished by using SO₃/dioxane, SO₃/triethyl phosphate complexes or acetyl sulfate (acetic anhydride in sulfuric acid) in various solvents. The degree of sulfonation can be controlled by varying the ratio of sulfonation agent to monomer units. Synthesis of deuterated PCHD, needed for small-angle neutron scattering studies of polymer conformation in solution, was found to depend strongly on the synthesis of the deuterated 1,3-CHD monomer. While proton exchange of 1,4- or 1,3-cyclohexadiene with DMSO-d₆ gave impure product material that could not be purified, an alternate synthetic approach starting from cyclohexanol was successful for the production of undeuterated 1,3-CHD in 60% yield (~99.8% purity). Using this approach, we have synthesized perdeuterated PCHDS of varying molecular weight for investigations of the effect of chain length on polyelectrolyte conformation and self-assembly. We have also synthesized short-chain (~2000 molecular weight before sulfonation) PSS samples for studies of local order of counterions near charged sites on the polyelectrolyte chain.

Structural studies in solution. Both short-range (atomic dimensions) and longer scale (macromolecular) interactions contribute to polyelectrolyte self-assembly. We are investigating the

interaction of polyelectrolytes with counterions and solvent molecules (water) through wide-angle neutron diffraction with isotopic substitution (NDIS) and laboratory-based X-ray scattering. Initial NDIS experiments on a ternary model system including polyethylene oxide (PEO), water (D₂O) and lithium iodide indicate that the ether oxygens of PEO do not compete effectively for solvation sites near the lithium ion in solution.¹ Total structure factors $G(r)$ were obtained using laboratory X-ray scattering techniques for ternary LiI-D₂O-PEO mixtures at the same concentrations as the wide-angle neutron studies. Preliminary assignments of the observed structural features from these experiments are consistent with the neutron scattering results, and include additional information on pair correlation distances (i.e., those not involving Li). Future studies will add to our understanding of this competitive solvation effect through investigation of water-poor ternary mixtures, where insufficient water is available to form complete solvation shells.

Small-angle neutron scattering (SANS) is being used to probe details of macromolecular conformation and the formation of self-assembled structures. Initial studies with PCHDS indicated only a poorly defined “polyelectrolyte peak” with a surprisingly weak dependence on ionic strength in solution. Parallel light-scattering studies of PCHDS indicated significantly stronger aggregation of PCHDS in solution as compared with PSS. This aggregation, extensive even at very low polyelectrolyte concentration, leads to the poor resolution of the polyelectrolyte peak in the SANS experiments. The newly synthesized perdeuterated PCHDS enables additional definitive SANS studies of this system through contrast matching.

In collaboration with Professor E. R. Zubarev, Iowa State University, SANS studies were carried out at Forschungszentrum Jülich (Germany) on amphiphilic heteroarm star polyelectrolytes. These polyelectrolytes included 12 arms (6 uncharged polystyrene, 6 polyacrylic acid), each incorporating an average of 25 monomer units. In a “nonselective” solvent (70% chloroform, 30% methanol) the observed dimensions ($R_g \sim 26\text{Å}$) reflect the size of the unimer, while in D₂O/dimethyl formamide, self-assembled core-shell micelles form at the lowest concentrations. In chloroform the radii of gyration indicate aggregation of about 3 unimers at infinite dilution, and larger self-assembled micelles at higher concentrations.

Theory, Modeling and Simulations. Both coarse-grained approaches and atomistically-detailed simulations are being applied to understand short-range interactions and their contributions to nanoscale conformation and assembly. Detailed molecular dynamics (MD) simulations are currently in progress on interactions of PSS and PEO with ions and solvent molecules. Detailed Brownian dynamics simulations showed that the counterions condense on the polymer backbone by an adsorption mechanism, yielding a degree of ionization of about 0.3 for a flexible polyelectrolyte. The simulations predict that the degree of ionization increases with increasing chain stiffness. Studies of stiff-chain polyelectrolytes show that either, or both, hydrophobic interactions between incompletely-sulfonated chain segments and hydrophilic (e.g., counterion sharing) interactions can contribute to self assembly in solution, and that the extent of aggregation is sensitive to chain stiffness.

DOE Interest

The fundamental knowledge gained from this research contributes to the scientific foundation required for tailoring the macromolecular structure and self-assembly of complex nanoscale polyelectrolyte structures. This ability to predict and control structure will enable a clearer understanding between the relationships between structure and function in ionic polymer systems.

Future Plans

Our capabilities for investigation of chain conformation and self-assembly will be significantly enhanced through the availability of the deuterated polyelectrolytes. In addition to synthetic progress within this program, we will collaborate with staff and users of the Center for Nanophase Materials Science through a recently-approved Partner User proposal, making available additional facilities and expertise for synthesis of deuterium-labeled and perdeuterated polyelectrolyte samples. We will focus near-term studies of macromolecular conformation and self-assembly on deuterated PCHDS with varying degrees of sulfonation, and with changing ionic strength and counterions. Understanding the structural results from these studies will depend on understanding and controlling the extent of aggregation as a function of polymer and salt concentrations. Theoretical and Brownian-dynamics simulation studies will focus on representing and predicting effects of changing backbone stiffness, degree of functionalization (e.g., sulfonation) and solution ionic strength on macromolecular conformation and the extent of self-assembly.

We will take advantage of the high solubility of LiCl to extend studies of competitive solvation in PEO-D₂O-LiCl ternary mixtures to systems with insufficient water (Li:D₂O ratio greater than 1:4) in order to gain further insight into the competitive solvation of counterions in solution. Our studies of short-range interactions in short-chain polysulfonate oligomers will focus on lithium salts, with further studies highlighting the effect of changing charge density (valency) of the counterion. Simulation studies of the binary and ternary mixtures will give insight into details of local structure, as well as indications of the nature (e.g., hydrated ion layers) of possible electrostatic bridges in self-assembled structures. The combination of the wide-angle neutron scattering with X-ray measurements will give insight into both the local environment around the counterion in solution and the effects of these counterions on local structural features of other interactions, such as chain charge-site solvation.

Publications for 2002-2004 (This program began at the end of FY 2002.)

1. Annis, B. K.; Badyal, Y. S.; Simonson, J. M. "Neutron-Scattering Determination of the Li⁺ Environment in an Aqueous Poly(Ethylene Oxide) Solution," *J. Phys. Chem. B* 108, 2554-2556 (2004).

This page intentionally left blank.

Ferrocene-Based Nanoelectronics

Postdoctoral Associates
Graduate Students
Collaborators

Denis A. Kissounko, Laura Picraux
Chaiwat Engtrakul, Lixin Wang, Jennifer Shaw
Michael Fuhrer, Stephanie Getty

Department of Chemistry and Biochemistry, University of Maryland, College Park, MD 20742
lsita@umd.edu

Goal

Synthesize and investigate the conduction physics of a variety of proposed ferrocene diode / transistor designs in order to address the fundamental question; can electron transport within nm-length scale molecular structures be modulated in a controlled and reversible fashion?

Recent Progress

Ferrocene-based molecular components for nanoelectronics offer a number of distinct advantages relative to all carbon frameworks, including lower and tunable redox properties. During the past year, substantial progress towards achieving the stated goal has been made by surmounting a number of scientific and technical obstacles. More specifically, a concise and general synthetic route to the requisite 2,5-diethynylpyridyl-linked diferrocene dithiols and monothiols has been achieved that now allows for the directed and controlled assembly of metal/organometallic/metal test structures and the fabrication of self-assembled monolayers (SAMs) on Au(111) that are amenable to quantitative electrochemical characterization of electron-transfer rates. Methods have also been developed for the construction of the key Au nanoparticle (Au NP)/ferrocene dithiol/Au(111) test structures shown in Figure 1 that will be used to acquire current / voltage (I/V) characteristics for the ferrocene molecular components. Complementing this approach, an alternative test structure based on the fabrication of a molecularly-bridged nanogap between two gold electrodes has also now been successfully fabricated. This test structure schematically shown in Figure 2 has the additional feature of possessing a novel aluminum oxide gate electrode, and in preliminary studies,

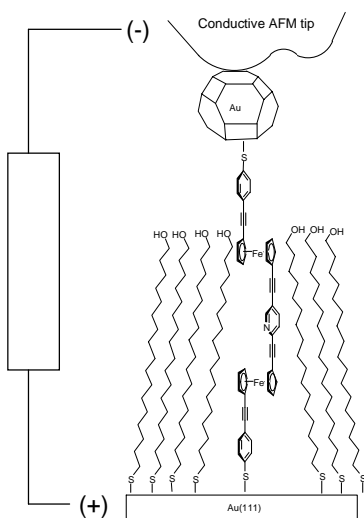


Figure 1. Schematic of experimental design for measuring I/V characteristics of ferrocene-based single molecules.

reproducible I/V data for one of the ferrocene dithiol molecules have been collected which exhibit surprisingly high conduction for a molecular species at a remarkably low bias of only 50 mV. Importantly, this conductance responds to application of a gate voltage in a predictable manner.

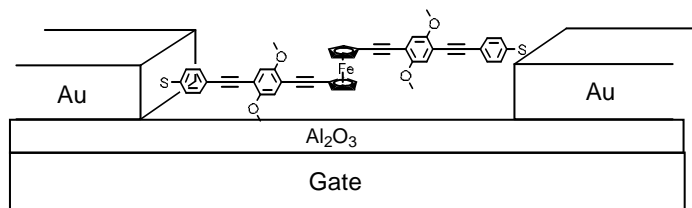


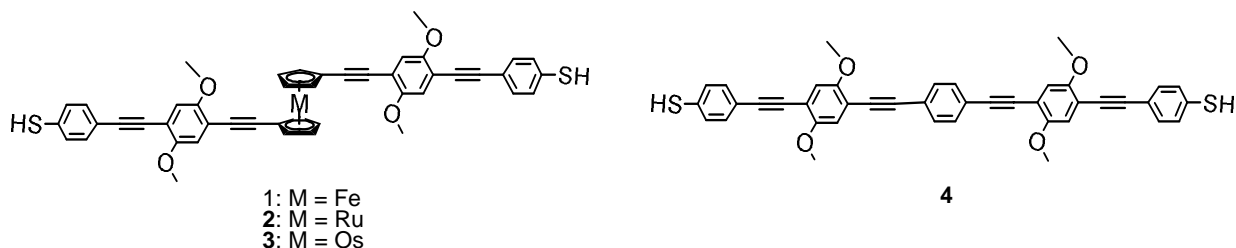
Figure 2. Schematic of a nanogap test structure to measure the I/V characteristics of ferrocene-based single molecules

DOE Interest

The successful realization of the goals of this project should play an important role in the continued evolution in design of molecular components for nanoelectronic devices, which in turn, will have a positive impact on the science and potential technologies associated with these systems.

Future Plans

The first credible, reproducible I/V data for one of the ferrocene molecules using a nanogap test structure, namely compound **1**, has been acquired, and these data have already provided exciting preliminary results in the form of remarkably high observed conductance. In the next year, one of the primary objectives will be to better understand the data that have obtained for **1** by placing it on a firm theoretical foundation. More specifically, it was originally thought that the ferrocene unit in the molecular construct would be electronically localized, i.e., conduction would occur through electron-hopping rather than via through-bond tunneling. The electrochemical studies that have been carried out now point to the opposite conclusion that the ferrocene unit in **1** is, in fact, well coupled electronically to the conjugated organic fragments, and overall, the organometallic framework provides a very low barrier to electron tunneling. The high observed conduction for **1** is further attributed to being due to the Fe center's d orbitals being in close proximity to the Fermi levels of the Au electrodes. To provide additional experimental and theoretical support for this hypothesis, two avenues of research will be pursued during the next year. First, compound **4** will be synthesized and its I/V characteristics compared with that of **1**. Second, Carlos Gonzalez, a theoretical chemist at NIST and Harold Baranger, a physicist at Duke, who both specialize on the theory of conduction through molecules, have been enlisted to computationally investigate the predicted properties of **1** and **4** at the theoretical level. By replacing the first row Fe center in **1** by the analogous second and third row group 8 metals, Ru and Os, i.e., compounds **2** and **3**, respectively, the relationship of the metal's d orbital energy levels on transmission efficiency will be investigated.



New Chemical Routes to Advanced Ceramic Materials: Metal Catalyzed Syntheses and Polymerization Reactions of Alkenylpolyborane Single Source Precursors

Graduate Students: Xiaolan Wei, Kersten Forsthoefel, Upal Kusari, Jude Clapper, Robert Butterick, Yugi Li, Chang Yoon

Department of Chemistry, University of Pennsylvania, Philadelphia, Pennsylvania 19104-6323, lsneddon@sas.upenn.edu

Goal

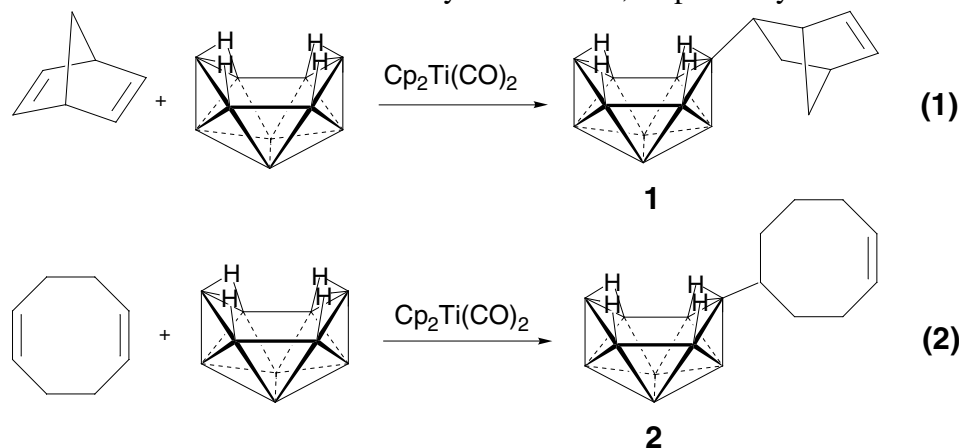
Develop new metal-catalyzed routes to single-source precursors to technologically important solid-state materials.

Recent Progress

New Routes to Organodecaborane Polymers via Ruthenium-Catalyzed Ring Opening Metathesis Polymerization

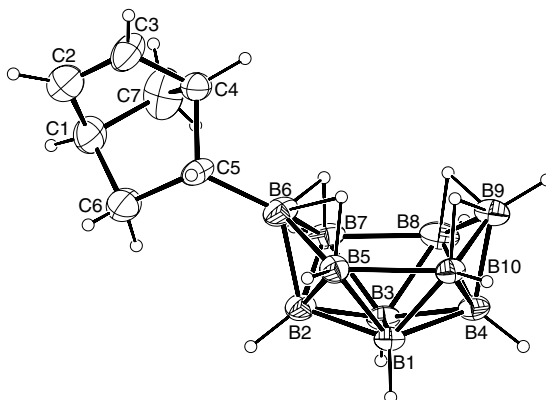
As a part of our interest in the design of new polymeric precursors to non-oxide ceramics, we have been investigating the development of new general metal-catalyzed methods for the synthesis of polyborane polymers. We have found during the last year that ruthenium-catalyzed ring opening metathesis polymerization (ROMP) of organodecaboranes containing cyclic-olefin substituents provides a new efficient route to poly(organodecaborane) polymers.

As shown in **Eqs. 1** and **2**, the high yield syntheses of the key decaboranyl-substituted norbornene and cyclooctene monomers were achieved by employing the titanium-catalyzed reaction of decaborane with norbornadiene and cyclooctadiene, respectively.

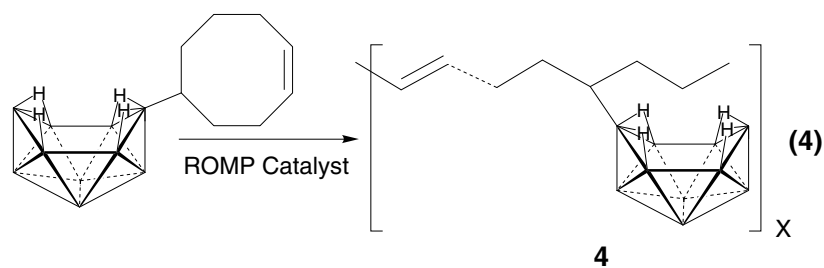
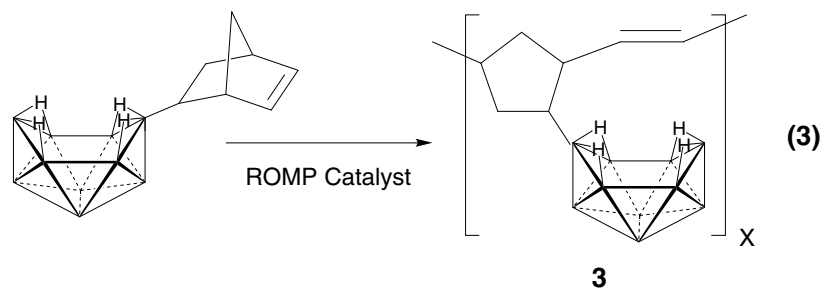


Typical conditions involved the reaction of a large excess of the olefin with decaborane in the presence of ~3 mol% catalyst at 90°C for 72 h. The products were easily isolated in pure form and excellent yields (**1**, 98% and **2**, 96%) from the metal catalyst by filtration through silica gel. As shown in the figure below, a single crystal X-ray determination of **1** confirmed a 6-

substituted norbornenyl-decaborane structure resulting from the titanium-catalyzed hydroboration of the norbornadiene C5-C6 double bond.



Because of their air stability and tolerance to various functional groups, “Grubbs-type” ROMP catalysts appeared to be ideal candidates for the syntheses of polyborane polymers. Indeed, ROMP of monomers **1** and **2** with either the first-generation (**I**) or second-generation (**II**) catalysts readily yielded the poly(organodecaborane) polymers shown in **Eqs. 3** and **4**.



Both the **I** and **II** catalysts polymerized **1** efficiently, giving ~90% conversions in the 1 h reaction time. Molecular weight studies by size exclusion chromatography employing both multi-angle light scattering and DRI detectors showed that molecular weights with Mn in excess of 30 KDa can be readily obtained with polydispersities (PDI's) between 1.1 and 1.8.

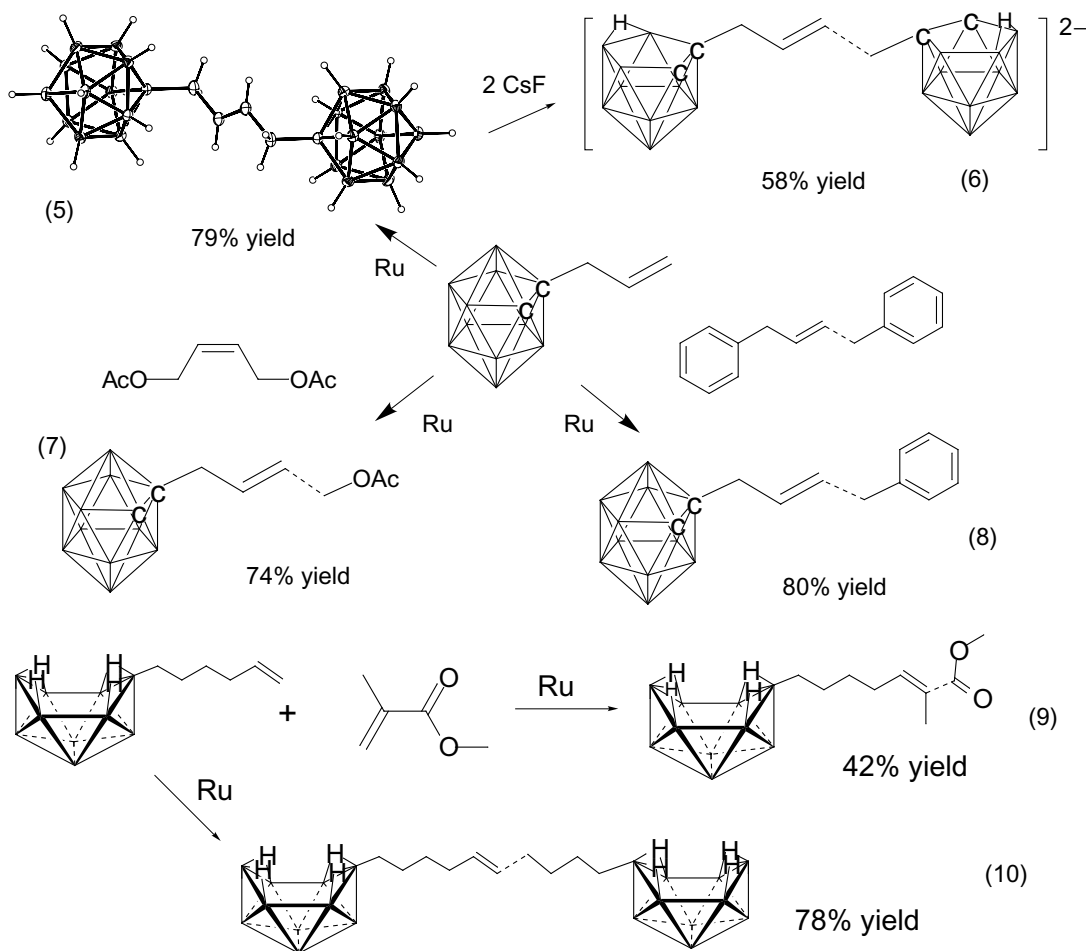
TGA studies of samples of **3** and **4** (each having Mn of ~32 KDa) indicated that for both polymers weight loss begins near 100°C and is essentially complete for **3** by 500°C and for **4** by 700°C to give final char yields of 72% and 70%, respectively. Given that DSC studies show that the Tg's of both polymers are in the 65-70°C range, these polymers have excellent potential for applications requiring molten processing. We are currently studying the ceramic conversions and the properties of the derived ceramics.

Future Studies

The results presented above clearly demonstrate that ruthenium-catalyzed ROMP reactions are important new methods for the systematic formation of polyborane polymers. Since ruthenium-based ROMP catalysts work with a wide variety of functionalized olefins, we will now explore the use of these reactions to produce more complex poly(organopolyborane) polymers and copolymers than possible with our previously developed methods.

Ruthenium Catalyzed Alkenylpolyborane Metathesis Reactions: New Routes to Functionalized Polyboranes.

Metal-catalyzed olefin metathesis has become a widely used synthetic tool for carbon-carbon bond formation. Recent studies in our laboratory of both the homometathesis and cross-metathesis of alkenylboranes catalyzed by Grubbs-type catalysts have now shown that ruthenium catalyzed metathesis reactions are efficient high yield methods for the synthesis of organopolyboranes. The scheme below presents some results from our initial studies of the reactions of allyl-*o*-carborane and 6-hexenyldecaborane. Both compounds readily undergo homometathesis (Eqs. 5 and 10) to produce olefin-bridged compounds. As shown at the upper left, an X-ray study of the linked carborane confirmed the central double bond (1.35(2)Å).



Our initial studies have also shown efficient cross-metathesis of both compounds with a variety of olefins, including allylbenzene, allylacetate, allyltrimethylsilane, methyl acrylate, styrene and stibene. Thus, the cross-metathesis reactions provide important new routes to functionalized decaborane and *o*-carborane compounds. As also depicted in the scheme, we have now converted the olefin-linked carborane to the bis(dicarbollide) compound by deboronation with fluoride anion.

Future Studies

We plan to explore the deboronation reactions of the cross-methasis products to develop general routes to functionalized dicarbollides and then investigate the coordination chemistry of these new anions. We will likewise explore the use of the functionalized decaboranes as starting materials for the synthesis of boron-substituted derivatives of other important cage systems, including for example, $3\text{-RC}_2\text{B}_{10}\text{H}_{11}$, $\text{RCB}_{11}\text{H}_{11}^-$, $\text{RB}_{10}\text{H}_9^{2-}$ and $\text{RB}_{12}\text{H}_{11}^{2-}$.

Impact on Science and Technologies of Relevance to DOE

The development of efficient methods for the production of complex structural and electronic materials in usable forms with controlled structures, orders and porosities ranging over different length scales is one of the most challenging and important problems of modern solid-state chemistry and materials science. This research program is focused on the design, syntheses and applications of new processible chemical precursors to non-oxide ceramics, including boron carbide, silicon carbide and boron-carbide/silicon-carbide composites, that will allow the formation of these technologically important materials in forms, such as films, fibers and nanostructures, that have been unattainable with conventional methods.

Recent DOE Sponsored Publications (2002-present)

1. Interrante, L. V.; Moraes, K.; Liu, Q.; Lu, N.; Puerta, A. R.; Sneddon, L. G. "Si-Based Ceramics from Polymer Precursors" *Pure and Applied Chem.* **2002**, *74*, 2111-2117.
2. Puerta, A. R.; Remsen, E. E.; Bradley, M. G.; Sherwood, W.; Sneddon, L. G. "Synthesis and Ceramic Conversion Reactions of 9-BBN-Modified Allylhydridopolycarbosilane: A New Single-Source Precursor to Boron-Modified Silicon Carbide" *Chem. Mater.* **2003**, *15*, 478-485.
3. Moraes, K.; Vosburg, J.; Wark, D.; Interrante, L. V.; Puerta, A. R.; Sneddon, L. G.; Narisawa, M. "The Microstructure and Indentation Fracture of SiC-BN Composites Derived from Blended Precursors of AHPCS and Polyborazylene" *Chem. Mater.* **2004**, *16*, 125-132.
4. Wei, X.; Carroll, P. J.; Sneddon, L. G. "New Routes to Organodecaborane Polymers via Ruthenium-Catalyzed Ring Opening Metathesis Polymerization" *Organometallics* **2004**, *23*, 163-165.
5. Pender, M. J.; Forsthoefel, K.; Kusari, U.; Sneddon, L. G. "Molecular and Polymeric Precursors to Boron Carbide" in preparation

Nanoscience and Nanoparticles for 100% Selective Catalytic Reactions

G.A. Somorjai, J.W. Ager III, H. Frei, M. Salmeron, T.D. Tilley

Lawrence Berkeley National Laboratory, Berkeley, CA 94720

GASomorjai@lbl.gov

Goal

The research conducted in the project is designed to develop new heterogeneous catalysts with 100% selectivity for the development of clean manufacturing processes that do not produce waste byproducts.

Recent Progress

Heterogeneous catalysts are nanoparticles. They are utilized in most industrial chemical processes in the form of metal clusters dispersed on high surface area oxide supports. Recent breakthroughs in nanotechnology have created the ability to control material structures on scales that are relevant for catalyst design (e.g. the diffusion length of molecular intermediates in a bifunctional catalyst, ca. 5 nm). Here we study the structure, composition and dynamic properties of catalysts to achieve 100% selectivity in multipath surface catalyzed reactions.

Synthesis and Characterization of High Surface Area Model Catalysts: Uniform shape and size Pt nanoparticles encapsulated in mesoporous silica (SBA-15) were prepared by a novel two-step method. It consists of the preparation of the metal nanoparticles by H₂ reduction of aqueous K₂PtCl₄, followed by addition of a tri-block copolymer and Si precursor which results in the development of a mesopore-structure of type SBA-15 around the nanoparticles. The studies indicate that the incorporation of small metal particles does not disrupt the hexagonal ordering of the SBA-15 channels. Coupled with TEM measurements, gas adsorption experiments confirm that the Pt nanoparticles are located in the internal structure (i.e. pores and walls) of the mesoporous silica. In parallel, Rh nanoparticles were synthesized using a reverse-micelle method. TEM and HRTEM revealed that the particles are close to monodisperse and highly crystalline. The Rh particles were supported on SBA-15 to form an active high surface catalyst that is currently being studied for catalytic ethylene hydrogenation and ethane hydrogenolysis.

An important aspect of the design of 3-D metal nanoparticle catalysts is variation and control of the chemical nature of the porous oxide support. We have explored modification of the SBA-15 silica pore surface by introducing a vanadium oxide layer. Structural aspects of the overlayer were elucidated by UV-Raman, UV-Vis DRS, XRD, TEM, and physisorption measurements. For these as well as all mesoporous materials with encapsulated metal particles, SAXS measurements at SSRL provide crucial

information on the pore diameter and the structural integrity of the material upon chemical processing.

Rh and Pt nanoparticles encapsulated into SBA-15 were synthesized by sonicating dispersed metal particles with the mesoporous silicate in solution (collaboration with Prof. Peidong Yang, UCB). Weight loadings of over 10% were obtained. The effect of sonication on mesoscale order, pore size distribution, and surface area was evaluated. FT-IR and UV-Raman were used to investigate changes in the silica framework caused by sonication and by sample preparation methods such as pellet pressing.

The study of a new class of metal/metal oxide core-shell structures for heterogeneous catalysis has been initiated (collaboration with Prof. Paul Alivisatos, UCB). Pt nanoparticles are used as the core, and Co_3S_4 or CoO as the shell. HRTEM indicates that the CoO shell is multicrystalline, furnishing access of gas molecules to the core by diffusion along grain boundaries as evidenced by the observation of C_2H_4 hydrogenation at low temperature.

Development of New and Sensitive Probes of Chemical Reactions on Metal and Metal Oxide Nanocluster Assemblies: XPS studies have revealed the first valence band photoemission spectra of Au nanoparticles as a function of size and separation. Quantum size effects are observed by a decrease of the density of states at the Fermi level when the particle size is below 1.7 nm. This reduction can have implications on the chemical activity and selectivity of nanoparticles that we are planning to explore. We also observed a metal-to-insulator transition when the small nanoparticles (< 1.7 nm) are separated by more than 10 Å. For Co nanoparticles, the first X-ray absorption and emission spectra have been obtained *in situ* in liquid suspension as function of particle size (measurements conducted at the ALS). Using resonant inelastic X-ray spectroscopy, the build-up of d-d electron transfer excitation was observed as function of size in the 3 to 9 nm diameter range. The purpose of these experiments is to determine the quantum size effects on electronic structure that may affect the catalytic properties of monodispersed nanoparticles.

In-Situ Reaction Studies of Nanoengineered Catalysts: Ethylene hydrogenation and ethane hydrogenolysis were studied on Pt/SBA-15. Low temperature (190-230 K) ethylene hydrogenation was investigated in a microreactor with plug-flow hydrodynamics. Kinetic measurements on Pt/SBA-15 materials with Pt particle size varying from 1.7–7 nm confirmed the structural insensitivity of this reaction. For ethane hydrogenolysis to proceed, both C-H and C-C bond activation must occur. The structure sensitivity of the reaction has previously been demonstrated on Ni catalysts. Detection of methane did not occur until temperatures > 573 K, indicative of the high activation of bond breaking that must occur. The activity of the Pt/SBA-15 materials was found to be insensitive to Pt particle size. The severe conditions (> 573 K, high pressures of ethane and hydrogen) employed in this study demonstrated that our model catalysts are robust.

Monitoring of heterogeneous catalysis by time-resolved vibrational spectroscopy is essential for the elucidation of the detailed mechanisms under reaction conditions. We have developed a method based on time-resolved FT-IR spectroscopy that affords observation of the lifetime of intermediates of hydrocarbon conversions over supported metal catalysts for the first time. The approach builds on a reactor design in which a

continuous gas flow of one reactant merges with a short (> 300 microsec) pulse of a second reactant, synchronized with the FT-IR spectrometer, in close proximity to the catalyst. Using ethylene hydrogenation over a supported Pt catalyst as a first example, two intermediates were detected: One is the well-established spectator surface ethylidyne ($1339, 2880\text{ cm}^{-1}$) showing a decay time of 300 msec (473 K). A transient absorption at 1200 cm^{-1} revealed the presence of a second surface species with a lifetime shorter than 100 msec. Based on these observations and the detection of accompanying CH stretching absorption at 2875 and 2860 cm^{-1} known from steady-state spectroscopy, we attribute the transient to surface ethyl species. $\text{CH}_3\text{CH}_2\text{Pt}$ has been proposed as the kinetically relevant reaction intermediate of ethylene hydrogenation. This is the first observation of the lifetime of $\text{CH}_3\text{CH}_2\text{Pt}$ under reaction conditions.

DOE Interest

The development of heterogeneous catalysts with 100% selectivity is a high priority goal for energy-efficient and environmentally friendly chemicals manufacturing.

Future Plans

New synthetic methods will be developed with the goal of generating monodisperse Rh and other metal or metal oxide particles with well-defined geometry and surface structure, including routes to 'naked' nanoparticles that obviate the need for stabilizing ligands. Comparison of catalytic activities versus surface structure could lead to the development of highly selective catalysts. We will expand microporous oxide supports for nanoparticles to include titania, alumina and zirconia. Research on our core/shell structures will be extended to different core materials such as Al_2O_3 , SiO_2 , or TiO_2 , with focus on improving the thermal stability.

The development of new and sensitive probes of chemical reactions on nanocluster assemblies will, along one direction, build on X-ray photoelectron spectroscopies at the ALS for measuring the size effects on the electronic structure of nanoclusters. Moreover, a high-pressure reaction cell will be built for the study of gas chemisorption on the nanoclusters. *In-situ* Raman and IR reflectance spectroscopy will be employed for the study of mesoporous silica-supported metal particles in a reactor cell. Time-resolved FT-IR spectroscopy for hydrocarbon conversions under reaction conditions will be expanded to the microsecond and nanosecond time range by employing the step-scan technique. Methods will be developed for the triggering of catalysis with sub-microsecond reactant pulses.

Future *in-situ* studies of nanoengineered catalysts will focus on the effect of particle size on reaction selectivity, in addition to activity. The hydrogenation/dehydrogenation of cyclohexene is a multi-path reaction currently under study. A fully automated reactor system for investigating the particle size effect on n-hexane reforming is in progress. Time-resolved FT-IR experiments on the same systems will be conducted for identifying and determining the lifetime of transient surface intermediates. Sum frequency generation measurement of metal nanoparticle catalysts will be pursued based on a total internal reflection cell.

Publications (2002-2004)

- Konya, Z., Puentes, V.F., Kiricsi, I., Alivisatos, A.P., Somorjai, G.A., "Nanocrystal Templating of Silica Mesopores with Tunable Pore Sizes," *Nano Lett.* **2**, 907 (2002). LBNL-50171
- Konya, Z., Puentes, V.F., Kiricsi, I., Zhu, J., Alivisatos, A.P., Somorjai, G.A., "Novel Two-Step Synthesis of Controlled Size and Shape Platinum Nanoparticles Encapsulated in Mesoporous Silica," *Catal. Lett.* **81**, 137 (2002). LBNL-49393
- McCrea, K.R., Zhu, J., Somorjai, G.A., "Active Sites of Heterogeneous Catalysis: Development of Molecular Concepts and Future Challenges", *Top. Catal.* **18**, 157 (2002). LBNL-46884
- Grunes, J., J. Zhu, J., and G. A. Somorjai, "Focus Article: Catalysis and Nanoscience," *Chem. Commun.* 2257 (2003). LBNL-52668
- Ko, M. K., and H. Frei, "Millisecond FT-IR Spectroscopy of Surface Intermediates of C₂H₄ Hydrogenation over Pt/Al₂O₃ Catalyst under Reaction Conditions," *J. Phys. Chem. B* **108**, 1805 (2004). LBNL-53310
- Konya, Z., V. F. Puentes, I. Kiricsi, J. Zhu, J. W. Ager III, M. K. Ko, H. Frei, A. P. Alivisatos, and G. A. Somorjai., "Synthetic Insertion of Gold Nanoparticles into Mesoporous Silica," *Chem. Mat.* **15**, 1242 (2003). LBNL-51329
- Konya, Z., J. Zhu, A. Szegedi, I. Kiricsi, A. P. Alivisatos, and G. A. Somorjai, "Synthesis and Characterization of Hyperbranched Mesoporous Silica SBA-15," *Chem. Commun.* 314 (2003). LBNL-51646
- Rose, M. K., A. Borg, J. C. Dunphy, T. Mitsui, D. F. Ogletree, and M. Salmeron., "Chemisorption and dissociation of O₂ on Pd(111) studied by STM," *Surf. Sci.* **547**, 162 (2003). LBNL-53563
- Zhu, J., Z. Konya, V. F. Puentes, I. Kiricsi, C. X. Miao, J. W. Ager III, A. P. Alivisatos, and G. A. Somorjai, "Encapsulation of Metal (Au, Ag, Pt) Nanoparticles into the Mesoporous SBA-15 Structure," *Langmuir* **19**, 4396 (2003). LBNL-51370

In-situ and Time-Resolved Characterization of Working Catalysts by Ultraviolet Resonance Raman Spectroscopy

Postdocs: Hack-Sung Kim, Raymond Ho
Students: Yek-Tann Chua, Chao Zhang, Li Zhang
Collaborators: James Haw, John Nicholas

Department of Chemistry, Northwestern University, Evanston, IL 60208
Chemistry Division, Argonne National Laboratory
pstair@northwestern.edu

Goal

Characterize and understand heterogeneous catalysts and catalytic chemistry using in-situ and time-resolved Raman spectroscopy

Recent Progress

Ultraviolet Raman spectroscopy continues to develop as a powerful tool for the in-situ study of catalysts and catalytic chemistry. Experiments have shed light on the nature and mechanism of coke formation during acid-catalyzed reactions in zeolites. The effects of resonance enhancement have been used to detect and discriminate catalytic sites and subtle changes in molecular structure induced by adsorption in catalyst pores.

Mechanism and Topology of Coke Formation:
UV Raman spectroscopy is useful for monitoring the chemical intermediates in coke formation, and distinguishing polyolefin from polyaromatic coke. Moreover, the observed intensity pattern in the UV Raman spectra of coke is diagnostic for whether aromatic coke has a 1-Dimensional, chain-like or 2-Dimensional sheet-like topology. Coke formed during the methanol-to-hydrocarbons reaction (MTH) catalyzed by zeolite H-MFI has the 1-D topology characteristic of fused aromatic chains; coke formed on alumina-supported chromia has the 2-D topology (Fig. 1).

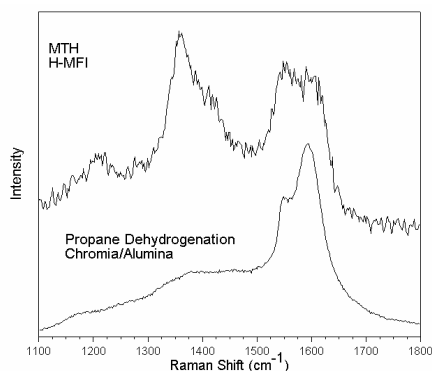


Figure 1 UV Raman spectra of coke.

Chemical Behavior of Catalytic Peroxides and Superoxides: Resonance enhancement makes it possible to detect and study chemically active peroxide and superoxide species adsorbed on iron clusters in zeolite H-MFI using UV Raman spectroscopy. The thermal and chemical stability of these species were found to be strongly dependent on the hydroxyl

content of the iron clusters. In particular, on highly dehydroxylated Fe/MFI samples peroxide and superoxide species are stable to at least 250°C where catalytic reactions occur.

Nature of Adsorbed Benzene from Resonance Raman Spectroscopy: Normal Raman spectroscopy involves transitions that occur on the ground electronic potential energy surface. Resonance Raman spectroscopy involves electronically excited states in the Raman scattering process. Consequently, resonance Raman spectroscopy is a sensitive tool for probing electronic excited states. The UV resonance Raman spectrum of benzene adsorbed in MFI silicalite is dramatically different than the spectrum of the free molecule (Fig. 2).

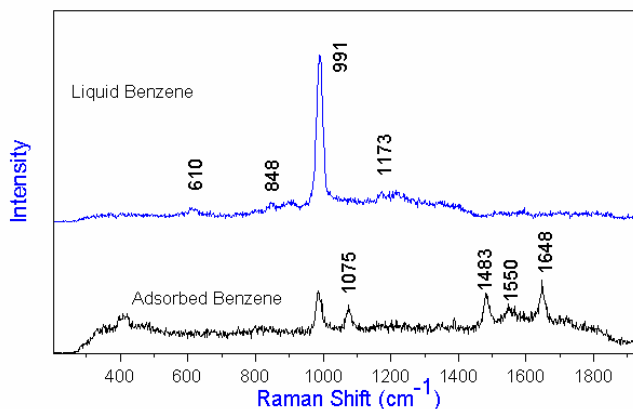


Figure 2 UV Raman spectra of benzene.

The spectrum reveals that the point group of benzene changes in the excited electronic state to either D_{2h} (planar elongated) or D_{3d} (chair) due to steric interactions with the channel walls.

DOE Interest

These new UV resonance Raman spectroscopy measurements provide a view of molecular adsorption, active sites, and catalytic chemistry within zeolites, one of the most important catalytic materials for energy production and utilization.

Future Plans

Quantitative Raman Spectroscopy: Due to variations in scattering volume, Raman spectroscopy is not generally a quantitative analysis technique. With zeolites, however, the TOT bending vibration provides an internal standard that can be used to adjust for scattering volume changes. Measurements on a series of adsorbed hydrocarbons will be used to develop a quantitative calibration of Raman intensity vs. adsorbate loading.

Time-Resolved Raman Spectroscopy: Using a pulsed infrared laser, it is possible to rapidly activate and quench catalytic reactions within zeolites. Since diffusion is slow on the timescale of the heating and quenching, the zeolite pores behave like a constant volume reactor during these experiments. We plan to use this method to follow hydrocarbon reaction pathways with unprecedented time resolution.

Simultaneous Spectroscopy/Performance Experiments: By interfacing a gas chromatograph to the fluidized bed reactor used for in-situ Raman spectroscopy

measurements, it will be possible to monitor the performance of a catalyst during reaction while measuring the Raman spectrum at the same time.

Multi-Wavelength Raman Spectroscopy: From a comparison of visible and ultraviolet laser excited Raman spectra it is apparent that resonance enhancement is operative for many molecule and materials systems of interest in catalysis. In a mixture the species that are resonance enhanced are selectively displayed in the measured Raman spectrum. In order to obtain a more comprehensive view of the species present in catalytic mixtures, Raman spectra will be recorded at a series of excitation wavelengths in the visible and ultraviolet wavelength regions.

Recent Publications

1. UV-Raman characterization of Iron peroxo adsorbates on Fe/MFI catalyst with high activity for NO_x reduction, Z. X. Gao, H. S. Kim, Q. Sun, P. C. Stair and W. M. H. Sachtler, *J. Phys. Chem. B.* **105**, 6186-6190 (2001).
2. A Comparison of Ultraviolet and Visible Raman Spectra of Supported Metal Oxide Catalysts, Y. T. Chua, P. C. Stair, I. E. Wachs, *J. Phys. Chem. B* **105**, 8600-8606 (2001).
3. Advances in Raman Spectroscopy for Catalysis Research, P. C. Stair, *Current Opinion in Solid State & Materials Science* **5**, 365-369 (2001).
4. In Situ Ultraviolet Raman Spectroscopy, P. C. Stair, in *In-Situ Spectroscopy in Heterogeneous Catalysis*. Ed. James F. Haw, Wiley-VCH, Weinheim, p. 121 (2002).
5. A UV Raman Spectroscopic Study of Coke Formation in the Methanol to Gasoline Conversion over Zeolite H-ZSM-5, Y. T. Chua and P. C. Stair, *J. Catal.* **213**, 39-46 (2003).
6. UV Raman Spectrum of 1,3-Dimethylcyclopentenyl Cation Adsorbed in Zeolite H-MFI, Y. T. Chua, P. C. Stair, J. B. Nicholas, W. Song and J. F. Haw, *J. Am. Chem. Soc. Comm.* **125**, 866-867 (2003).
7. Nanocrystalline Todorokite-Like Manganese Oxide Produced by Bacterial Catalysis, Kim, H.-S.; Pasten, P. A.; Gaillard, J.-F.; Stair, P. C.; *J. Am. Chem. Soc.* **125**, 14284-14285 (2003).
8. In-situ ultraviolet Raman spectroscopy of supported chromia/alumina catalysts for propane dehydrogenation, V. S. Sullivan; P. C. Stair, S. D. Jackson, *Catalysis in Application, [Papers presented at the International Symposium on Applied Catalysis], Glasgow, United Kingdom, July 16-18, 2003*, 32-38 (2003).
9. Catalytic Oxidative Dehydrogenation of Propane over Mg-V/Mo Oxides, Pless, J. D., Bardin, B. B., H.-S. Kim, D. Ko, M. T. Smith, R. R. Hammond, P. C. Stair, and K. R. Peoppelmeier, *J. Catal.* Accepted.
10. Vibrational Spectra of Alumina- and Silica-Supported Vanadia Revisited: An Experimental and Theoretical Model Catalyst Study, N. Magg, B. Immaraporn, J. B. Giorgi, T. Schroeder, M. Bäumer, J. Döbler, Z. Wu, E. Kondratenko, M. Cherian, M. Baerns, P. C. Stair, J. Sauer, H.-J. Freund, *J. Catal.* Submitted.

This page intentionally left blank.

Institute for Environmental Catalysis

Faculty: Mark Asta, Michael Bedzyk, Linda Broadbelt, Vinayak Dravid, Donald Ellis, Jean-Francois Gaillard, Franz Geiger, Kimberly Gray, Mark Hersam, Joseph Hupp, Harold Kung, Mayfair Kung, Laurence Marks, SonBinh Nguyen, Ken Poepelmeier, Wolfgang Sachtler, Randall Snurr, Peter Stair, Richard Van Duyne, Eric Weitz

Postdocs: Deanna Hurum, Chang-Yong Kim, Oliver Warschkow, Guang Xiong, Wenmei Xue, Qui Zhou,

Students: Le Chen, Steven Christensen, Tendai Gadzikwa, Juan Henao-Lopez, Brian Quezada, Ashi Savara, Chun-Yi Sung, Simon Albo, Hao Feng, Christopher Konek, Courtney Lanier, Xiaoyan Ma, Feng Qu, Ian Saratovsky, Catherine Schmidt, Jared Smit, Alyson Whitney, So-Hye Cho, Hiu-Ying Law, Ann Chiaramonti, Maria Curet-Arana, Yingmin Wang, Xinjiang Zhu, Smita Edulji, Chen Huang, Li Liu

Argonne Staff: Li Chen, Larry Curtiss, Michael Pellin, Hau Wang, Marion Thurnauer

Department of Chemistry, Center for Catalysis and Surface Science, Northwestern University, Evanston, IL 60208

Chemistry Division, Argonne National Laboratory

pstair@northwestern.edu

Goal

Advance the molecular level understanding of catalytic chemistry designed to reduce human impact on the environment.

Highlights

The Institute for Environmental Catalysis supports six (6) research projects that address, broadly, topics in catalytic oxidation.

The Surface Structure – Chemistry Relationship: This surface science project includes the synthesis of metal oxide and mixed-metal oxide single crystals, surface structure determination of oxide surfaces using diffraction (x-ray & electron) and microscopy techniques, and associated surface chemistry studies. Recent accomplishments include the synthesis of large magnesium orthovanadate and hematite single crystals suitable for surface structure analysis, the structure determination of several SrTiO₃ surfaces, and studies of the structure and composition dependence in methyl group chemistry on hematite surfaces.

Novel Selective Oxidation Catalysis: The selective oxidation of CO by supported gold nanoparticles and the novel synthesis of supported gold catalysts by Jet Enhanced Nanoparticle Deposition (JEND) have been studied. Focusing on gold supported on alumina, a combination of catalytic, in-situ spectroscopic, and electron microscopy results indicate that

surface hydroxyl groups play an important role in the active site for CO oxidation. At the same time XANES measurements show mostly metallic gold. These results can be reconciled by postulating an active site consisting of a hydroxyl group bonded to a gold cation that is embedded in an otherwise metallic gold cluster. The first samples for catalytic studies were synthesized by the JEND method. This method involves a gas phase condensation and reaction between atomic gold, aluminum and oxygen to produce highly uniform, alumina supported gold nanoparticles.

Nano-structured Membrane Oxidation Catalysts: Novel selective oxidation catalysts have been synthesized using nano-structured organic and alumina membranes as the catalyst host. These catalysts have been studied both experimentally and computationally. Manganese-based catalysts, active for the enantioselective epoxidation of olefins, have been shown to be exceptionally robust against deactivation when incorporated into molecular square frameworks. Vanadium oxide supported in alumina membranes made by anodic aluminum oxidation demonstrates remarkable selectivity for the oxidative dehydrogenation of cyclohexane to cyclohexene. On conventional Vanadia/alumina catalysts only small amounts of cyclohexene are produced compared to the deeper oxidation products benzene, CO, and CO₂.

Low Temperature NO_x Reduction for Diesel Engine Exhaust Abatement: The reaction mechanism for NO₂ reduction by acetaldehyde catalyzed BaNa-Y zeolite has been studied by FTIR and isotopic labeling. A key intermediate in this reaction is proposed to be O₂NCH₂NO₂⁻, which is formed by a sequence of reactions starting with the formation of acetate ions and subsequently the aci-anion of nitromethane. Further reaction with NO₂ forms the O₂NCH₂NO₂⁻, which is stabilized by ionic environment in the zeolite. This intermediate leads to ammonia via reaction with water, and N₂ is formed by well-known reactions between ammonia and NO₂.

Gas Phase Photocatalysis: The mechanism of photocatalytic oxidation of volatile organic compounds and chlorinated hydrocarbons by TiO₂ is under investigation. From a combination of spectroscopic evidence localized “hot spots” in the photocatalytic activity have been attributed to the interface region of rutile and anatase crystals of TiO₂.

Metal Oxides in Aquatic Systems: In aquatic systems manganese oxides (MnO_x) are formed primarily by biological processes and have been shown to have unique chemical properties. However, their structures are often difficult to determine owing to intimate association with a complex nucleation medium, small particle size, lack of long-range order, and diversity of structure types. Syntheses of well-characterized MnO_x model compounds are underway in order to provide standards for establishing spectroscopic and x-ray scattering signatures.

DOE Interest

These projects represent a broad attack on the development and fundamental understanding of catalytic systems for selective oxidation. Success in this area is expected to impact energy technology in diverse ways, ranging from the clean-up of hydrogen for fuel cell applications to the more efficient and cleaner use of energy in chemical manufacturing.

2003 Publications

1. Agrios, A. G., Gray, K. A. & Weitz, E. Photocatalytic Transformation of 2,4,5-Trichlorophenol on TiO₂ under Sub-Band-Gap Illumination [Erratum for Langmuir 2003, 19, 1402-1409]. *Langmuir* **19**, 5178 (2003).
2. Agrios, A. G., Gray, K. A. & Weitz, E. Photocatalytic Transformation of 2,4,5-Trichlorophenol on TiO₂ under Sub-Band-Gap Illumination. *Langmuir* **19**, 1402-1409 (2003).
3. Boechat, C. B., Terra, J., Eon, J.-G., Ellis, D. E. & Rossi, A. M. Reduction by hydrogen of vanadium in vanadate apatite solid solutions. *Physical Chemistry Chemical Physics* **5**, 4290-4298 (2003).
4. Bonifacic, M., Asmus, K.-D. & Gray, K. A. On the Reaction of 2,4,5-Trichlorophenol with Hydroxyl Radicals: New Information on Transients and Their Properties. *Journal of Physical Chemistry A* **107**, 1307-1312 (2003).
5. Cheng, L., Fenter, P., Bedzyk, M. J. & Sturchio, N. C. Fourier-Expansion Solution of Atom Distributions in a Crystal Using x-Ray Standing Waves. *Physical Review Letters* **90**, 255503/1-255503/4 (2003).
6. Costello, C. K. et al. On the potential role of hydroxyl groups in CO oxidation over Au/Al₂O₃. *Applied Catalysis, A: General* **243**, 15-24 (2003).
7. Czaplewski, K. F., Li, J., Hupp, J. T. & Snurr, R. Q. Vapor permeation studies of membranes made from molecular squares. *Journal of Membrane Science* **221**, 103-111 (2003).
8. De Meyer, K. M. A. et al. Packing Effects in the Liquid-Phase Adsorption of C₅-C₂₂ n-Alkanes on ZSM-5. *Journal of Physical Chemistry B* **107**, 10760-10766 (2003).
9. Ellis, D. E. & Warschkow, O. Evolution of classical/quantum methodologies: applications to oxide surfaces and interfaces. *Coordination Chemistry Reviews* **238-239**, 31-53 (2003).
10. Ellis, D. E. & Warschkow, O. Toward structure-function relations - a hybrid quantum/classical approach. *Advances in Quantum Chemistry* **42**, 35-66 (2003).
11. Erdman, N. et al. Surface Structures of SrTiO₃ (001): A TiO₂-rich Reconstruction with a c(4 × 2) Unit Cell. *Journal of the American Chemical Society* **125**, 10050-10056 (2003).
12. Erdman, N. & Marks, L. D. SrTiO₃(0 0 1) surface structures under oxidizing conditions. *Surface Science* **526**, 107-114 (2003).

13. Fu, L., Johnson, D. L., Zheng, J. G. & Dravid, V. P. Microwave plasma synthesis of nanostructured g-Al₂O₃ powders. *Journal of the American Ceramic Society* **86**, 1635-1637 (2003).
14. Goodner, D. M. et al. X-ray standing wave study of the Sr/Si(0 0 1)-(2 * 3) surface. *Surface Science* **547**, 19-26 (2003).
15. Hurum, D. C., Agrios, A. G., Gray, K. A., Rajh, T. & Thurnauer, M. C. Explaining the Enhanced Photocatalytic Activity of Degussa P25 Mixed-Phase TiO₂ Using EPR. *Journal of Physical Chemistry B* **107**, 4545-4549 (2003).
16. Keefe, M. H., O'Donnell, J. L., Bailey, R. C., Nguyen, S. T. & Hupp, J. T. Permeable, microporous polymeric membrane materials constructed from discrete molecular squares. *Advanced Materials (Weinheim, Germany)* **15**, 1936-1939 (2003).
17. Kim, H.-S., Pasten, P. A., Gaillard, J.-F. & Stair, P. C. Nanocrystalline todorokite-Like manganese oxide produced by bacterial catalysis. *Journal of the American Chemical Society* **125**, 14284-14285 (2003).
18. Kung, H. H. & Kung, M. C. Heterogeneous catalysis: what lies ahead in nanotechnology. *Applied Catalysis, A: General* **246**, 193-196 (2003).
19. Kung, H. H., Kung, M. C. & Costello, C. K. Supported Au catalysts for low temperature CO oxidation. *Journal of Catalysis* **216**, 425-432 (2003).
20. Marks, L. D. & Sinkler, W. Sufficient conditions for direct methods with swift electrons. *Microscopy and Microanalysis* **9**, 399-410 (2003).
21. McMillan, S. A., Snurr, R. Q. & Broadbelt, L. J. Origin and Characteristics of Preferential Adsorption on Different Sites in Cobalt-Exchanged Ferrierite. *Journal of Physical Chemistry B* **107**, 13329-13335 (2003).
22. McMillan, S. A., Haubein, N. C., Snurr, R. Q. & Broadbelt, L. J. Ab Initio Stochastic Optimization of Conformational and Many-Body Degrees of Freedom. *Journal of Chemical Information and Computer Sciences* **43**, 1820-1828 (2003).
23. McMillan, S. A., Broadbelt, L. J. & Snurr, R. Q. Effect of local framework heterogeneity on NO adsorption in cobalt-ferrierite. *Journal of Catalysis* **219**, 117-125 (2003).
24. Pless, J. D. et al. Single-Crystal Growth of Magnesium Orthovanadate, Mg₃(VO₄)₂, by the Optical Floating Zone Technique. *Crystal Growth & Design* **3**, 615-619 (2003).
25. Sun, Q. & Sachtler, W. M. H. Mn/MFI catalyzed reduction of NO_x with alkanes. *Applied Catalysis, B: Environmental* **42**, 393-401 (2003).

26. Warschkow, O., Ellis, D. E., Gonzalez, G. B. & Mason, T. O. Defect cluster aggregation and nonreducibility in tin-doped indium oxide. *Journal of the American Ceramic Society* **86**, 1707-1711 (2003).
27. Warschkow, O., Ellis, D. E., Gonzalez, G. B. & Mason, T. O. Defect structures of tin-doped indium oxide. *Journal of the American Ceramic Society* **86**, 1700-1706 (2003).
28. Wen, B. & Sachtler, W. M. H. Enhanced Catalytic Performance of Co/MFI by Hydrothermal Treatment. *Catalysis Letters* **86**, 39-42 (2003).
29. Xue, W. M., Kung, M. C., Kozlov, A. I., Popp, K. E. & Kung, H. H. Catalytic aminolysis of epoxide by alumina prepared from amine-protected Al precursor. *Catalysis Today* **85**, 219-224 (2003).

This page intentionally left blank.

MICROPOROUS AND MESOPOROUS NANO-SIZE TRANSITION METAL OXIDES: PREPARATION, CHARACTERIZATION, AND APPLICATIONS

Postdocs: Laubernds, K. Polverejan, M.; Willis, W. S.; Zerger, R. P.; Gao, Q.

Students: Gomez, S.; Espinal, L.; Liu, J.; Cai, J.; Giraldo, O.; Hoz deVila, N.; Calvert, C.; Couttenye, R.; Ghosh, R.; Kumar, R.; Makwana, V.; Son, Y. C.; Villegas, J.; Yuan, J.; Zhang, Q.; Cao, L.; Garces, J. G.; Hincapie, B.; Xia, G. G.; Tong, W.; Chen, X.

Collaborators: Hanson, J.; Iton, L. E.; Navrotsky, A.; Tsapatsis, M.; Howell, A. R.; Aindow, M.; Marquez, M.; Ching, S.; Satyapal, S.; Rusling, J. F.; Malz, R.

Department of Chemistry, Unit 3060, University of Connecticut, Storrs, CT 06269-3060.

Suib@uconnvm.uconn.edu

Goal

To synthesize porous nano-wires, helices, lines, patterns, powders, and other morphologies for selective catalytic oxidations.

Recent Progress

Much of our research has concerned the synthesis of porous octahedral molecular sieves (OMS) and octahedral layered (OL) materials that are nano-size. Synthesis and characterization of nano-materials of porous manganese oxides in various surface areas and morphologies has been a major research effort. Applications of such systems in catalysis and as sensors have also been pursued.

A major focus of our research has been to produce nano-size porous manganese oxide materials. Tetraalkylammonium manganese oxide sols have been prepared using phase transfer techniques with mixed aqueous/organic solvents. Such sol-gel syntheses can also involve the sole use of organic solvents. These precursor sols are extremely stable and have been used to prepare a variety of novel materials with interesting morphologies, including helices,²⁻⁴ nano-lines, and nanopatterns.¹ Such colloidal sols can also be used to form thin films that have excellent ion-exchange properties with 100% of cations being exchanged in a 3 sec period.⁴ This fast exchange is likely due to the presence of interconnected micro-, meso-, and macropores. The nano-lines on glass surfaces have been characterized with a variety of methods including atomic force microscopy (AFM) and electron paramagnetic resonance (EPR).²

Novel porous inorganic helices have been synthesized by slow heating of these colloidal (~ 15 Å diameter hexagonal plates as determined by small angle neutron scattering) sols and high resolution transmission electron microscopy of the sol precursors. The helices are excellent semiconductors, and can be ion-exchanged and heated to produce new compositions and structures that retain their helical macrostructure. Mechanistic studies of formation of these helices via magnetic resonance imaging (MRI) methods suggest that buckling of the gel occurs via gravitational forces.¹ A patent has issued on these helical materials.^A

Nano-lines have been prepared by slow evaporation of the colloidal precursor TMAMnO₄ by dip coating procedures. The complicated nature of these lines shows that the lines are actually composed of a series of lines. Cross sections via X-ray fluorescence imaging of manganese concentrations show that the mid sections of the widths of the lines are thicker than the edges of the lines, leading to the formation of columns of semicircles.

Another synthesis effort has focused on the preparation of nano-size manganese oxide octahedral layered (OL) materials of birnessite, OL-1. These materials have been pillared with organic amine species.⁸ Synthesis and X-ray absorption studies of nanosize OL-1 materials having tetramethylammonium cations as templates have been a large focus of our recent efforts. Another thrust has been the incorporation of Fe³⁺ species in the framework of octahedral

molecular sieve (OMS) cryptomelane, known as OMS-2.^{5,22} Many natural manganese oxide nodule materials are composed of iron and manganese, however, it has been difficult to achieve framework substitution of iron due to instability problems until our recent studies.

A novel synthesis of bulk OMS materials with an asymmetric 2x4 tunnel structure having a pore size of dimensions 4.6 Å by 9.2 Å and having a tunnel diagonal as large as 10.3 Å has been prepared.¹⁰

Incorporation of manganese colloids into MCM-41⁸ and into layered double hydroxides (LDH)⁹ materials has also been done in order to produce manganese in specific locations in mesoporous and layered materials, respectively. These materials afford various coordination environments and potential unique physical and chemical properties not available in OMS and OL materials. Nanoparticles of mordenite zeolite materials have been made.¹⁰ All of these systems have an emphasis on preparation of nanomaterials.

Related synthetic efforts include the use of layer by layer films of alternating polymer, myoglobin (heme containing) proteins, and manganese oxides. Such films are prepared by using alternating layers of positively and negatively charged species and monitoring the thickness with an *in situ* quartz crystal microbalance. Multi-layer films made from tetralkylammonium permanganate are also readily exchangeable, show more reversible electrochemistry of intercalated dye molecules than corresponding bulk powders, and are uniform. Colloids, helices, and patterned films have been made as an extension of this work by incorporating myoglobin into manganese oxide precursors since the earlier work suggested an association between these systems.¹² Some recent work in this area of manganese oxide layer by layer films in the absence of myoglobin show excellent activity for the selective oxidation of styrene to styrene oxide.¹³ There is a clear interaction of H₂O₂ with the manganese oxide films, which leads to enhanced oxidation of styrene.

(1) Catalysis and Other Applications.

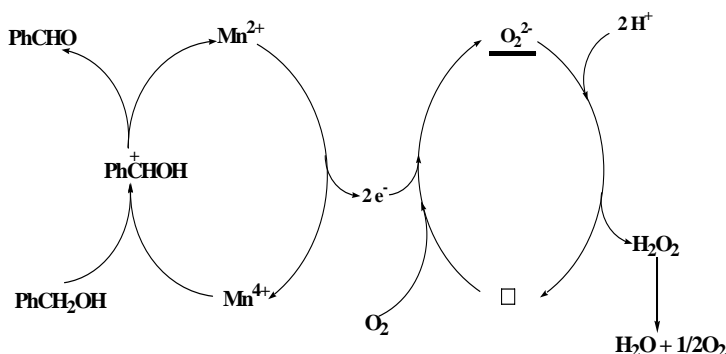
Our major efforts have focused on the use of several OMS and OL materials in the selective oxidation of alcohols.¹⁴ These catalysts are outstanding materials for the selective aerobic catalytic oxidation of alcohols. The selectivity in almost all cases is 100%. We believe that these materials and processes have commercial value and a patent application has been submitted in this area.^B A two-step Mars-van Krevelen model involving an exchange between gas phase oxygen and lattice oxygen of the OMS-2 catalyst was found to give a better fit. This was further corroborated by an oxygen isotope labeling study. The changes in the ¹⁶O and ¹⁸O content of the product water confirm this observation.

Kinetic isotope effects are used to ascertain if the oxidative attack on the alcohol molecule is at the secondary hydrogen atom or at the hydroxyl hydrogen atom. The fact that C-H and C-D bonds differ in their zero-point energies is used to make this distinction. The presence of an isotope effect greater than 1 implies that the benzyl alcohol substrate reacts much faster than its di-deuterated analogue. The presence of a large kinetic isotope effect implies that the removal of a secondary H atom is indeed the rate-controlling step. A mechanism in which the abstraction of the secondary H atom leads to the formation of a free radical is not feasible as shown by experiments using quinone as a radical trap. These results point to an electron-deficient carbon center in the intermediate formed in the rate-determining step.

Not many examples of oxidations are known to occur by the Mars van Krevelen pathway in the liquid phase due to competition from readily generated free radicals. Our proposed mechanism indicates a multi-electron redox event occurring in the liquid phase (See Fig. 1). This result coupled with the potential of shape-selectivity in the regularly ordered tunnels makes these OMS-2 materials an interesting new class of oxidation catalysts. Nano-ribbon porous manganese oxide materials are also useful in these selective oxidation reactions.¹⁵

Two key recent studies regarding selective oxidations have been done. First, hollow spheres of OMS-2 containing H⁺ ions lead to a doubling of the rate for selective oxidation of alcohols.¹⁶ These data clearly show that morphology is important as regards rate and that an interplay of

micro-, meso-, and macropores may be important in improving the rate of transport. The second study is an extension of the ^{18}O labeling experiments that clearly show that the rates of these reactions are related to the surface area of the catalyst, to the incorporation of H^+ via NH_4^+ exchange, and to the lability of surface oxygen in the manganese catalysts.¹⁷ A combination of labeling, mass spectrometry, temperature programmed desorption, and synthetic and microanalytical experiments were done to come to these conclusions. A review of the synthesis and applications of OMS and OL materials with an emphasis on catalysis has been prepared.¹⁸ Fig. 1, Proposed Mechanism for Aerobic Oxidation of Alcohols using OMS-2.



Manganese oxide nanoparticles can also be used for the degradation of nerve gas simulants. The Department of defense is currently exploring use of such systems for real chemical warfare agents. These systems have been patented in collaboration with United Technologies Research Center (UTRC).^D

A process for the synthesis of 2,2,6,6-tetra-methyl-4-oxopiperidine from acetone and ammonia-donor compounds in the presence of CaY zeolite catalysts has also recently been developed.¹⁹ This process is being licensed by Crompton. In related research we have used zeolite type materials for the alkylation of aniline.²⁰ A final application of porous manganese oxide nanomaterials (films) is their use as sensors in detection of halogenated hydrocarbons.²¹ This process is being used by Olin for applications in monitoring chlorinated species in swimming pools.

List of Publications of S. L. Suib, Acknowledging DOE Support

January 1, 2002 – February 5, 2004

1. Giraldo, O.; Durand, J.P.; Ramanan, H.; Laubernds, K.; Suib, S. L.; Tsapatsis, M.; Brock, S. L.; Marquez, M. Dynamic Organization of Inorganic Nanoparticles into Periodic Micrometer-Scale Patterns, *Ang. Chem., Int. Ed.*, 2003, **42**, 2905-2909.
2. Marquez, M.; Robinson, J.; Van Nostrand, V.; Schaefer, D.; Ryzhkov, L.; Lowe, W.; Suib, S. L. Atomic Force Microscopy, Electron Paramagnetic Resonance and X-ray Fluorescence Investigations of Self-Assembled Lines from Colloidal Solutions of Lamellar MnOx , *Chem. Mater.*, 2002, **14**, 1493-1499.
3. Veretennekov, I.; Indeikina, A.; Chang, H. C.; Marquez, M.; Suib, S. L.; Giraldo, O. Mechanism for Helical Gel Formation from Evaporation of Colloidal Solutions, *Langmuir*, 2002, **18**, 8792-8798.
4. Chen, X.; Shen Y. F.; Suib, S. L.; O'Young, C. L. Characterization of Manganese Oxide Octahedral Molecular Sieve (M-OMS-2) Materials with Different Cation Dopants, *Chem. Mater.*, 2002, **14**, 940-948.
5. Cai, J.; Liu, J.; Suib, S. L. Preparative Parameters and Framework Dopant Effects in the Synthesis of Layer-Structure Birnessite by Air Oxidation, *Chem. Mater.*, 2002, **14**, 2071-2077.
6. Ching, S.; Welch, E. J.; Hughes, S. M.; Bahadoor, A. B. F.; Suib, S. L.

- NonAqueous Sol-Gel Syntheses of Microporous Manganese Oxides, *Chem. Mater.*, 2002, **14**, 1292-1299.
7. Tong, Wei, Xia, G. G.; Tian, Z. R.; Liu, J.; Cai, J.; Suib, S. L.; Hanson, J. C. Hydrothermal Synthesis and Characterization of Sodium Manganese Oxo-Phosphate, *Chem. Mater.*, 2002, **14**, 615-620.
 8. Gomez, S.; Giraldo, O.; Suib, S. L. New Synthetic Route for the Incorporation of Manganese Species into the Pores of MCM-48, *Chem. Mater.*, 2003, submitted.
 9. Villegas, J.; Giraldo, O. Suib, S. L. Synthesis and Characterization of New Layered Double Hydroxides Containing Intercalated Manganese Oxide Species, *Inorg. Chem.*, 2003, in press.
 10. Hincapie, B. O.; Garces, L. J.; Zhang, Q.; Sacco, A.; Suib, S. L. Synthesis of Mordenite Nanocrystals, 2003, *Micropor. Mesopor. Mater.*, **67**, 19-26.
 11. Suib, S. L.; Brock, S. L. Eds., Synthesis of Nanoparticles and Nanostructured Materials, ACS Symposium Series, in process of editing, 2003, from ACS Meeting in New Orleans, March 22-27, 2003.
 12. Gao, Q.; Suib, S. L.; Rusling, J. F. Colloids, Helices, and Patterned Films Made From Heme Proteins and Manganese Oxide, *Chem. Comm.*, 2002, 2254-2255.
 13. Espinal, L.; Suib, S. L.; Rusling, J. F. Films of MnO₂ Nanoparticles for Epoxidation of Styrene, 2004, *J. Am. Chem. Soc.*, submitted.
 14. Makwana, V. D.; Son, Y. C.; Howell, A. R.; Suib, S. L. The Role of Lattice Oxygen in Selective Benzyl Alcohol Oxidation Using OMS-2 Catalyst: A Kinetic and Isotope-Labeling Study, *J. Catal.*, 2002, **210**, 46-52.
 15. Liu, J.; Cai, J.; Son, Y. C.; Gao, Q. Suib, S. L.; Aindow, M. Magnesium Manganese Oxide Nanoribbons: Synthesis, Characterization and Catalytic Application, *J. Phys. Chem.*, 2002, **106**, 9761-9768.
 16. Yuan, J.; Laubernds, K.; Zhang, Q.; Suib, S. L. Self-Assembly of Microporous Manganese Oxide Octahedral Molecular Sieve Hexagonal Flakes into Mesoporous Hollow Nanospheres, *J. Am Chem. Soc.*, 2003, **125**, 4966-4967.
 17. Makwana, V.; Garces, L. J.; Liu, J.; Son, Y. C.; Suib, S. L., *Catal Today.*, 2003, 2003, **85**, 225-233.
 18. Ghosh, R.; Son, Y. C.; Suib, S. L. Liquid Phase Epoxidation of Olefins by Manganese Octahedral Molecular Sieves, *J. Catal.*, 2004, in press.
 19. Son, Y., C.; Suib, S. L.; Malz, R. E. A Selective Process to Prepare Triacetone Amine, in Catalysis of Organic Reactions, Morrell, Ed., Marcel Dekker, NY, 2002, 559-564.
 20. Garces, J. Suib, S. L. Selective N,N-methylation of Aniline over co-crystallized Zeolites RHO and Zeolite X(FAU) and over Linde Type L(Sr,K-LTL), *J. Catal.*, 2003, **217**, 107-116.
 21. Liu, J.; Durand, J. P.; Espinal, L.; Garces, J.; Gomez, S.; Son, Y.; Villegas, J. Suib, S. L., Layered Manganese Oxides: Syntheses, Properties and Applications, in Handbook of Layered Materials for Catalytic Applications", S. M. Auerbach, K. A. Carrado, P. K. Dutta, Eds.; Marcel-Dekker: NY, 2003, in press.
 22. Liu, J.; Makwana, V.; Cai, J.; Suib, S. L.; Aindow, M. Effects of Alkali Metal and Ammonium Cation Templates on Nonfibrous Cryptomelane-type Manganese Oxide Octahedral Molecular Sieves (OMS-2), *J. Phys. Chem. B.*, 2003, *J. Phys. Chem.*, 2003, **107**; 9185-9194.

Patents.

- A. Suib, S. L.; Giraldo, O.; Marquez, M.; Brock, S. L. Manganese Oxide Helices, Rings, Strands, and Films and Methods of their Preparation, US Patent 6,503,476, January 7, 2003.

- B. Son, Y. C.; Suib, S. L.; Howell, A. R. Catalytic Oxidation of Alcohols Using Manganese Oxides, US Patent 6,486,357, November 26, 2002.
- C. Malz, R. E.; Son, Y. C.; Suib, S. L. Process for the Synthesis of 2,2,6,6-tetra-methyl-4-oxopiperidine from acetone and ammonia-donor compounds in the presence of CaY zeolite catalysts, PCT Int. Appl. 2002 28,833, April 11, 2002.

This page intentionally left blank.

Small Molecule Activation with Sterically Hindered Tris(pyrazolyl)borate Metal Complexes

Postdocs: Pariya, C.; Mukherjee, S.

Students: Thyagarajan, S.; Qin, K.; Shay, D. T.; Jove, F. A.; Schwarzwald, J. (undergrad)

Collaborators: Rheingold, A. L.; Yap, G. P. A.; Evans, D. H., Tolman, W. B.; Cramer, C. J.

Department of Chemistry and Biochemistry, Center for Catalytic Science and Technology,
University of Delaware, Newark, DE 19716

theopold@udel.edu

Goal

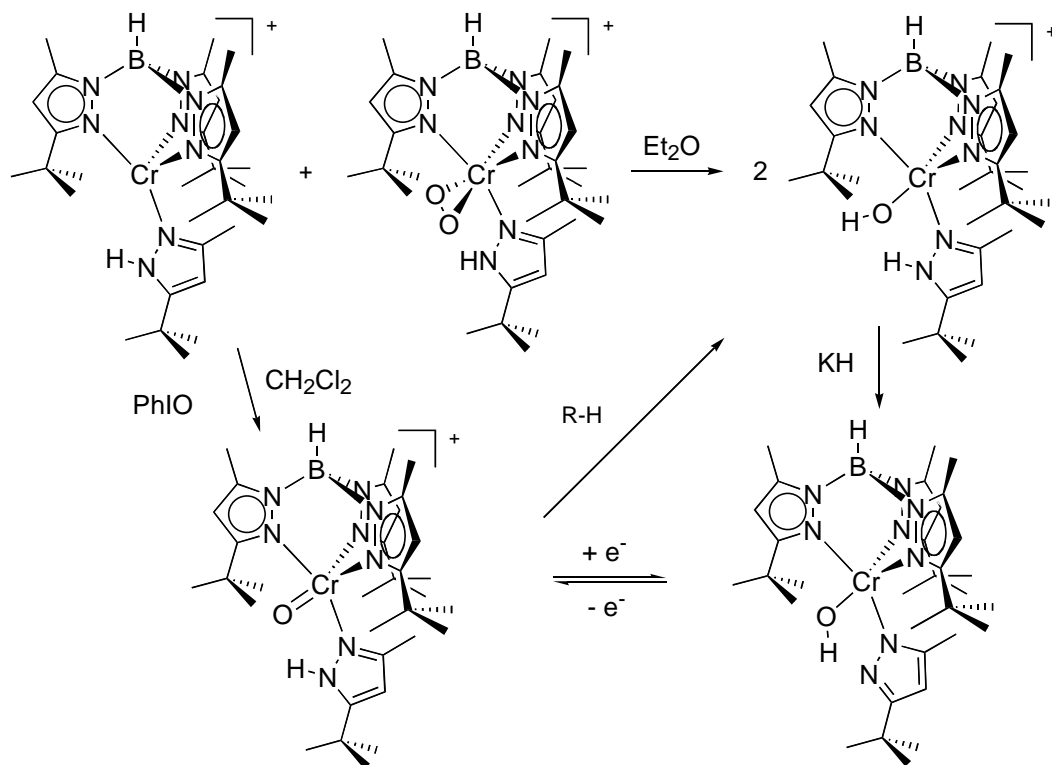
Develop catalysts for the activation of O₂ and its use as terminal oxidant in the functionalization of organic molecules.

Recent Progress

Chromium Dioxygen Complexes: We have prepared a series of chromium(III) superoxide complexes via binding of O₂ to coordinatively unsaturated chromium(II) precursors.¹ These complexes are the first structurally characterized representatives of their kind (i. e. chromium(III) superoxide complexes), and they all adopt the rare ‘side-on’ binding mode of superoxide that we first discovered in Tp^{tBu.Me}Co(O₂).

Dioxygen Activation: Reaction of the dioxygen complexes with their precursors results in splitting of the O-O bond and the formation of reactive chromium(IV) oxo intermediates. Avoiding all hydrogen atom donors in the reaction of [Tp^{tBu.Me}Cr(pz'H)]BARF with PhIO has allowed the isolation and full characterization of [Tp^{tBu.Me}Cr(O)(pz'H)]BARF.² The redox chemistry of the latter was investigated in collaboration with Prof. D. H. Evans, in order to estimate the affinity of the oxo complex for a hydrogen atom.⁶

Hydrocarbon Activation: [Tp^{tBu.Me}Cr(O)(pz'H)]BARF reacts with organic molecules containing weak C-H bonds ($D_{C-H} < 90$ kcal/mol) by hydrogen atom abstraction to yield the chromium(III) hydroxide [Tp^{tBu.Me}Cr(OH)(pz'H)]BARF. Activation parameters and isotope effects for several reactions have been determined. For example, the kinetic isotope effect for the hydrogen atom abstraction from 9,10-dihydroanthracene at 293 K is $k_H/k_D = 25.2$. Determination of the temperature dependencies of the H- and D-abstraction reactions revealed large differences ($\Delta\Delta H^\ddagger = 7.5(5)$ kcal/mol and $A_H/A_D = 10^{-4.3(1.1)}$). These values indicate a significant contribution of quantum mechanical tunneling to the hydrogen atom transfer. H-atom tunneling has been invoked for several oxidation enzymes, and this small molecule reaction provides a valuable model system for the study of H-atom tunneling.



Cobalt Imido Complexes: Our investigation of cobalt dioxygen chemistry has yielded evidence for the intermediacy of the terminal cobalt oxo species $\text{Tp}^{\text{tBu.Me}}\text{Co}=\text{O}$ in several reactions; however, This compound is apparently too reactive for even spectroscopic detection. We have thus pursued the chemistry of isoelectronic imido complexes, $\text{Tp}^{\text{tBu.Me}}\text{Co}=\text{NR}$, as chemical models. For example, reaction of $\text{Tp}^{\text{tBu.Me}}\text{Co}(\text{N}_2)$ with Me_3SiN_3 yielded a cobalt(III) amido species resulting from hydrogen atom abstraction from the ligand by the inferred imido complex $\text{Tp}^{\text{tBu.Me}}\text{Co}=\text{NSiMe}_3$.⁵

Stable Cobalt imido complexes: To our surprise, tertiary alkyl azides (e. g. $\text{R} = \text{}^t\text{Bu, Ad}$) have produced isolable cobalt(III) imido complexes. However, the thermal reactivity of these compounds also includes the functionalization of ligand C-H bonds. The mechanism of this C-H activation and the exact nature of the unusual products are currently under investigation.

Peroxynitrite chemistry: The recent interest in peroxynitrite led us to explore the synthesis of stable peroxynitrite complexes by the reactions of $\text{Tp}^{\text{tBu.Me}}\text{Co}(\text{O}_2)$ with NO and $\text{Tp}^{\text{tBu.Me}}\text{Co}(\text{NO})$ with O_2 . We have gathered spectroscopic evidence for an unstable intermediate, but could only isolate the nitrate isomer $\text{Tp}^{\text{tBu.Me}}\text{Co}(\text{O}_2\text{NO})$.³

Tris(pyrazolyl)borate Iron chemistry: The prevalence of iron in oxidation enzymes and the position of this element between chromium and cobalt has motivated some exploration of $\text{Tp}^{\text{tBu.Me}}\text{Fe}$ chemistry. Thus we have prepared $\text{Tp}^{\text{tBu.Me}}\text{Fe}(\text{CO})$ (from $\text{Tp}^{\text{tBu.Me}}\text{Fe}-\text{R}$) and we have strong evidence for the formation of $\text{Tp}^{\text{tBu.Me}}\text{Fe}(\text{N}_2)$. The latter compound should provide entry into dioxygen chemistry of the $\text{Tp}^{\text{tBu.Me}}\text{Fe}$ fragment.

DOE Interest

O₂ is a readily available and environmentally benign oxidant. Catalytic oxidations using O₂ (including those proceeding in fuel cells) are of critical importance to chemistry and electricity generation.

Future Plans

Generation and reactivity of metal oxo complexes: The coordination and cleavage of O₂ by metal (Cr, Co) complexes yields metal oxo species that can activate and functionalize C-H bonds (as do isoelectronic imido complexes). We plan to measure the hydrogen affinities of relevant compounds (D_{MO-H}), and to study the kinetics and mechanism of the hydrogen atom transfer. We hope to learn more about tunneling contributions to those reactions.

Oxidation resistant ligands: Some of the C-H bond activation we have seen has involved substituents of our ligand system (the tris(pyrazolyl)borates – ‘Tp^R’). We plan to explore the chemistry of Tp-ligands with amide groups in the 3-position, in the hope of preventing ligand destruction.

Iron chemistry: We are just beginning the exploration of iron complexes and hope to find informative parallels and differences to what we have learned with cobalt and chromium.

Publications (May 2002 – May 2004)

1. The First Structurally Characterized Chromium (III) Superoxide Complex Features ‘Side-on’ Bonding, K. Qin, C. D. Incarvito, A. L. Rheingold and K. H. Theopold, *Angew. Chem. Int. Ed.*, **2002**, *41*, 2333.
2. Hydrogen Atom Abstraction by a Chromium(IV) Oxo Complex Derived from O₂, K. Qin, C. D. Incarvito, A. L. Rheingold, and K. H. Theopold *J. Am. Chem. Soc.* **2002**, *124*, 14008.
3. In Pursuit of a Stable Peroxynitrite Complex – NO_x (x = 1-3) Derivatives of Tp^{t-Bu,Me}Co, S. Thyagarajan, C. D. Incarvito, A. L. Rheingold, and Klaus H. Theopold, *Inorganica Chimica Acta*, **2003**, *345*, 333.
4. Variable Character of O-O and M-O Bonding in Side-on (η²) 1:1 Metal Complexes of O₂, C. J. Cramer, W. B. Tolman, K. H. Theopold, A. L. Rheingold, *PNAS* **2003**, *100*, 3635.
5. Intramolecular C-H Activation by Inferred Terminal Cobalt Imido Intermediates, S. Thyagarajan, D. T. Shay, C. D. Incarvito, A. L. Rheingold, and Klaus H. Theopold *J. Am. Chem. Soc.* **2003**, *125*, 4440.
6. Studies of the Oxidation of a Hydroxochromium(III)-[hydrotrispyrazolylborate] pyrazolyl Complex, C. C. Van Kirk, K. Qin, K. H. Theopold, and D. H. Evans, *J. Electroanal. Chem.* **2004**, *565*, 185.
7. Preparation and Ligand Substitution Reactions of Tp^{Ms}Ru(COD)H Including Intramolecular Ligand Metalation, C. Pariya, C. D. Incarvito, A. L. Rheingold and K. H. Theopold, *Polyhedron* **2004**, *23*, 439.

This page intentionally left blank.

Molecular Precursor Methods for the Control of Structure in Heterogeneous Catalysts

Students: Furdala, K.L., Jarupatrakorn, J., Brutchey, R.L., Sadow, A.D., Gavenonis, J.
Collaborators: Bergman, R.G.; Bell, A.T.; Oliver, A., Hollander, F.J., Zettl, A., Hess, C.

Division of Chemical Sciences, Lawrence Berkeley National Laboratory, Berkeley, CA
94720
tdtilley@socrates.berkeley.edu

Goals

The primary goal of this project is to develop molecular chemistry that allows atomic-level and nanoscopic control over the structures of heterogeneous catalysts. Much of this work has targeted the production of multi-component oxides for which high dispersions are expected to give desirable catalytic properties.

Recent Progress

Molecular Precursor Routes to Heterogeneous Catalysts. The synthesis of a variety of multi-component oxide materials with tailored properties employed a molecular building-block approach referred to as the *thermolytic molecular precursor* (TMP) method. This molecular precursor approach employs metal complexes containing oxygen-rich ligands, such as those with the general formulas $L_nM[\text{OSi}(\text{O}^i\text{Bu})_3]_m$ and $L_nM[\text{O}_2\text{P}(\text{O}^i\text{Bu})_2]_m$, where L_n = alkoxide, amide, alkyl, etc. Such compounds function as excellent single-source precursors to carbon-free, homogeneous mixed-element oxide materials of the types M/Si/O and M/P/O, respectively. Although the sol-gel process and the TMP method both represent low-temperature routes to metastable materials, the TMP method offers several advantages. Firstly, the use of high purity and well-defined species allows accurate control over the stoichiometry of the final material. Also, the preexistence of M-O-E groups maximizes the homogeneity of the final material and leads to a high concentration of heterolinkages. The TMP method also offers benefits with respect to surface properties, since the use of nonpolar solvents minimizes pore collapse upon drying, thus providing high pore volumes and surface areas. Additionally, the use of nonaqueous media prevents M-O-E cleavage via hydrolytic means, a common occurrence in sol-gel processes that leads to inhomogeneity. Finally, the precursor complexes may serve as soluble molecular models for single-site catalysts involving a metal center on the surface of an oxide support.

Studies on aluminosilicate materials obtained by the TMP route indicate that the molecular precursor method results in a higher dispersion of Al and Si, and therefore a greater surface acidity, than related aluminosilicates obtained by sol-gel methods. Related investigations targeted vanadia-silica materials, and determined that precursors with the lower oxidation state (+4) gave more homogeneous structures. Routes to boron-containing materials were enabled with the synthesis of a rare example of a boronous acid, $\text{HOB}[\text{OSi}(\text{O}^i\text{Bu})_3]_2$. This species was used to obtain various metal-containing precursors. Molybdenum-containing precursors to Mo/P/O, Mo/P/Si/O, Mo/P/B/O and Mo/Bi/Si/O catalysts for oxydehydrogenation were investigated. Along similar lines, the new precursor $(^i\text{BuO})_3\text{CrOSi}(\text{O}^i\text{Bu})_3$ was used to obtain chromium-containing catalysts of the type Cr/Si/Al/O and Cr/Si/Zr/O. Upon calcinations, these materials contain mostly Cr^{6+} centers. These exhibit modest activities for propane ODH, and excellent activities and selectivities for the dehydrogenation of propane.

Production of Well-Defined, Single-Site Catalysts. Attempts to develop general routes to catalysts with tailored and improved properties are based on the application of molecular chemistry in the fine control of structures for the catalyst active site. Single-site titanium catalysts are the most active and selective for various hydrocarbon oxidation reactions. $\text{Ti}[\text{OSi}(\text{O}^t\text{Bu})_3]_4$ serves as an excellent reagent for introduction of isolated, surface-bound titanium sites for epoxidation. Results suggest that the siloxide ligands provide an important and beneficial effect on the structure of the supported catalytic site. Precursors with various Ti:Si ratios, $\text{Ti}[\text{OSi}(\text{O}^t\text{Bu})_3]_4$, $(^i\text{PrO})\text{Ti}[\text{OSi}(\text{O}^t\text{Bu})_3]_3$ and $(^t\text{BuO})_3\text{TiOSi}(\text{O}^t\text{Bu})_3$, were supported onto MCM-41 and SBA-15, and the structures of the active sites were probed via spectroscopic methods. These catalysts give the best results reported so far for the epoxidation of cyclohexene with titanium-based catalysts.

Molecular Precursor Route to Hybrid Inorganic/Organic Materials. It was shown that new types of hybrid inorganic-organic materials (which are promising as new catalyst supports) may be obtained by the thermolytic molecular precursor approach. Cothermolyses of $\text{Zr}[\text{OSi}(\text{O}^t\text{Bu})_3]_4$ with various organosilanes (e.g., $(\text{EtO})_3\text{SiC}_6\text{H}_4\text{Si}(\text{OEt})_3$) gave these materials, which were thoroughly characterized.

Homogeneous Catalysis with Methane. A new effort in this program targets the homogeneous, catalytic functionalization of methane. This chemistry takes advantage of the ability of early transition metal, d^0 complexes to mediate σ -bond metathesis chemistry. The scandium neopentyl derivative Cp^*_2ScNp ($\text{Np} = \text{CH}_2\text{CMe}_3$) is highly reactive toward C-H bond activation processes. For example, it reacts with benzene to produce neopentane and the phenyl derivative Cp^*_2ScPh . In addition, it reacts more rapidly with methane than does the methyl derivative Cp^*_2ScMe . The mechanism of this activation has been explored, and the chemistry involving the non-degenerate exchange of alkyl groups at scandium has been extended to the design of catalytic cycles.

DOE Interest

The programs described above provide a useful vehicle for the training of students and postdocs in technologies that impact the fields of catalysis, materials chemistry, and reaction chemistry/dynamics. In particular, it provides a rare opportunity for coworkers to gain experience in application of the diverse fields of inorganic synthesis, materials characterization, and reaction engineering in solving problems in catalysis. Most of this work has targeted the development of new catalysts for the selective conversions of hydrocarbons to more valuable products. Since such processes contribute significantly to the world economy, the potential impact is large. Our studies should lead to superior catalysts for various hydrocarbon transformations, including selective oxidations and carbon-carbon bond formations.

Future Plans

Molecular Precursor Routes to New Catalytic Materials. The use of molecular design concepts will be employed in studies to develop routes to new, catalytically active compositions such as VP_xO_y and VSb_xO_y . In addition, we will continue studies toward the achievement of control over the surface structures of heterogeneous catalysts. In one aspect of this work, molecular precursor species will be used to carry metal-based functional groups onto the surface of a support. This method will be explored in the context of extending the structural control that is currently available, by use of new copolymer templates. There is also a strong need for new synthetic methods for producing catalytic, oxide nanoparticles of controlled size and shape. Initial results indicate that the thermolytic molecular precursor route may be useful in this regard. We will also continue to investigate the use of this method in the preparation of isolated,

single-site catalysts on the surface of an oxide support. Recently prepared precursors, such as $V[\text{OSi}(\text{O}^t\text{Bu})_3]_2(\text{O}^t\text{Bu})_2$ and $\text{O}_2\text{Mo}[\text{OSi}(\text{O}^t\text{Bu})_3]_2$, are being studied in the synthesis of well-defined single sites involving vanadium and molybdenum. Such catalysts may prove to be selective hydrocarbon oxidation catalysts.

Transformations of Hydrocarbons via σ -Bond Metathesis. The homogeneous methane activation chemistry described above will be pursued further with attempts to obtain more active catalysts via manipulation of ligands on Sc and related metals. We will probe the mechanisms of methane activations in related systems, to learn as much as possible about the factors that influence activity and selectivity. Since there are a number of possible competing reactions (e.g., beta-hydrogen elimination and sp^2 C-H activation in the olefin), the influence of catalyst structure, and the electronic properties of ancillary ligands, will be extensively explored with respect to their influence on reactivity. We intend to examine these effects in complexes involving Lu, Y, and Sc, and for cationic complexes of Zr and Hf.

Publications (2002-04)

1. "Molecular Design and Synthesis of Heterogeneous and Single-Site, Supported Catalysts." T. D. Tilley. *J. Molec. Catal. A: Chem.* **2002**, 182-183, 17.
2. "New Tris(tert-butoxy)siloxy Complexes of Aluminum and Their Transformation to Homogeneous Aluminosilicate Materials via Low Temperature Thermolytic Pathways." C. G. Lugmair, K. L. Furdala and T. D. Tilley. *Chem. Mater.* **2002**, 14, 888.
3. "Iridium-Catalyzed H/D Exchange into Organic Compounds in Water." S. R. Klei, J. T. Golden, T. D. Tilley, and R. G. Bergman. *J. Am. Chem. Soc.* **2002**, 124, 2092.
4. "New Vanadium Tris(tert-butoxy)siloxy Complexes and Their Thermolytic Conversions to Vanadia-Silica Materials." K. L. Furdala and T. D. Tilley. *Chem. Mater.* **2002**, 14, 1376.
5. "Silica-Supported, Single-Site Titanium Catalysts for Olefin Epoxidation. A Molecular Precursor Strategy for Control of Catalyst Structure." J. Jarupatrakorn and T. D. Tilley. *J. Am. Chem. Soc.* **2002**, 124, 8380.
6. "Reactions of $\text{Cp}^*(\text{PMe}_3)\text{Ir}(\text{Me})\text{OTf}$ with Silanes: Role of Base-Free Silylene Complexes in Rearrangements of the Resulting Silicon-Based Ligands." S. R. Klei, T. Don Tilley and R. G. Bergman. *Organometallics* **2002**, 21, 3376.
7. "Stoichiometric and Catalytic Behavior of Cationic Silyl and Silylene Complexes." S. R. Klei, T. D. Tilley and R. G. Bergman. *Organometallics* **2002**, 21, 4648.
8. "Iridium(III) and Rhodium(III) Complexes Bearing Chelating Cyclopentadienyl-Phosphine Ligands as C-H Activation Catalysts for the Deuteration of Hydrocarbons in D_2O ." S. R. Klei, T. D. Tilley and R. G. Bergman. *Organometallics* **2002**, 21, 4905.
9. "Tris(tert-butoxy)siloxy Derivatives of Boron, Including the Boronous Acid $\text{HOB}[\text{OSi}(\text{O}^t\text{Bu})_3]_2$ and the Metal (Siloxy)boryloxy Complex $\text{Cp}_2\text{Zr}(\text{Me})\text{OB}[\text{OSi}(\text{O}^t\text{Bu})_3]_2$. A Remarkable Crystal Structure with 18 Independent Molecules in its Asymmetric Unit." K. L. Furdala, A. G. Oliver, F. J. Hollander and T. D. Tilley. *Inorg. Chem.* **2003**, 42, 1140.

10. "Nonaqueous, Molecular Precursor Route to Hybrid Inorganic/Organic Zirconia-Silica Materials Containing Covalently Linked Organic Bridges." R. L. Brutchey and T. D. Tilley. *Chem. Mater.* **2003**, *15*, 1040.
11. "Rhodium(III) and Rhodium(II) Complexes of Novel Bis(Oxazoline) Pincer Ligands." M. Gerisch, J. R. Krumper, R. G. Bergman and T. D. Tilley. *Organometallics* **2003**, *22*, 47.
12. "Design and synthesis of heterogeneous catalysts: the thermolytic molecular precursor approach." K. L. Fuldala and T. D. Tilley. *J. Catal.* **2003**, *216*, 265.
13. "Thermolytic Molecular Precursor Routes to Cr/Si/Al/O and Cr/Si/Zr/O Catalysts for the Oxidative Dehydrogenation and Dehydrogenation of Propane." K. L. Fuldala and T. D. Tilley. *J. Catal.* **2003**, *218*, 123.
14. "Homogeneous Catalysis with Methane. A Strategy for the Hydromethylation of Olefins Based on the Nondegenerate Exchange of Alkyl Groups and σ -Bond Metathesis at Scandium." A. D. Sadow and T. D. Tilley. *J. Am. Chem. Soc.* **2003**, *125*, 7971.
15. "Tailoring Properties of Silicon-Containing Oxide Catalysts via the Thermolytic Molecular Precursor Route." In *Organosilicon Chemistry V - From Molecules to Materials*, N. Auner and J. Weis, Eds.; K. L. Fuldala and T. D. Tilley; Wiley-VCH, Weinheim, Germany, p. 379-388.
16. "Monomeric Rhodium(II) Catalysts for the Preparation of Aziridines and Enantioselective Formation of Cyclopropanes from Ethyl Diazoacetate at Room Temperature." J. R. Krumper, M. Gerisch, J. M. Suh, R. G. Bergman and T. D. Tilley. *J. Org. Chem.* **2003**, *68*, 9705.
17. "Activated Boron Nitride Derived From Activated Carbon." W.-Q. Han, R. Brutchey, T. D. Tilley and A. Zettl. *Nano Lett.*, **2004**, *4*, 173.
18. "Synthesis and reactivity of bis(heptamethylindenyl)yttrium (Ind*₂Y) complexes containing alkyl and hydride ligands: crystal structure of Ind*₂YCl(THF)." J. Gavenonis and T. D. Tilley. *J. Organomet. Chem.* **2004**, *689*, 870.
19. "Dimolybdenum(III) Complexes of -OSi(O^tBu)₃, -O₂P(O^tBu)₂ and -OB[OSi(O^tBu)₃]₂ as Single-Source Molecular Precursors to Molybdenum-Containing, Multi-Component Oxide Materials." K. L. Fuldala and T. D. Tilley. *Chem. Mater.*, in press.
20. "Spectroscopic Characterization of Highly Dispersed Vanadia Supported on SBA-15 Silica." C. Hess, J. D. Hoefelmeyer and T. D. Tilley. *J. Phys. Chem. B*, submitted.

Well-Defined, Single Site Iron Centers and Heterobimetallic Systems for Catalytic Transformations of Hydrocarbons

Postdocs: Pak, C., Nozaki, C., Evans, O. R.
Students: Karshedt, D.

Division of Chemical Sciences, Lawrence Berkeley National Laboratory, Berkeley, CA 94720
tdtilley@socrates.berkeley.edu; bell@cchem.berkeley.edu

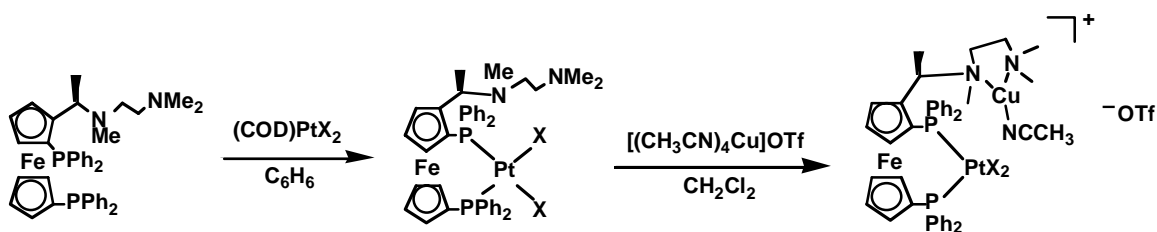
Goals

The iron-containing zeolite FeZSM-5 has attracted considerable attention due to its high activity as a catalyst for the selective oxidation of hydrocarbons with nitrous oxide as the oxidant. Although there is no consensus on the nature of the iron centers in this catalyst, it seems clear that some type of isolated iron site plays an important role in the selective processes catalyzed by FeZSM-5. Given the increasing interest in the structure and catalytic chemistry of supported iron centers, and related chemistry observed for iron-containing enzymes, we are pursuing the development of reliable routes to stable, well-defined inorganic iron species bound to an oxide support. A second aspect of this program involves attempts to develop new homogeneous catalysts based on heterobimetallic systems.

Recent Progress

Routes to Single-Site Iron Catalysts. For the introduction of single-site iron species onto silica, the precursor molecule $\text{Fe}[\text{OSi}(\text{O}^t\text{Bu})_3](\text{THF})$ is bonded to the surface of SBA-15 via protonolysis, which occurs with loss of $\text{HOSi}(\text{O}^t\text{Bu})_3$. Calcination then leads to stable, isolated inorganic Fe sites. The new site may be partially supported by the few equivalents of silica that are introduced by the molecular precursor, and in this way, stabilized. The resulting materials are catalysts for selective oxidations of alkanes, alkenes, and aromatic compounds with hydrogen peroxide as the oxidant.

Bifunctional Ligand for Pd/Cu and Pt/Cu Complexes. In designing the ligand framework for these catalysts, our attention was drawn to Kumada's ferrocene-based ligand (shown below). This ligand had previously been used for monometallic asymmetric catalysis. We reasoned that bimetallic complexes supported by this ligand might be readily synthesized in a stepwise fashion via the initial formation of a bisphosphine-Pd or -Pt complex and subsequent chelation of Cu(I) by the diamine moiety (see below; X = Me, Cl).



We have prepared bimetallic Pt-Cu complexes, and have devised a means for activating the Pt center toward the binding of organic substrates by abstracting the CH₃ groups with $[\text{Ph}_3\text{C}][\text{PF}_6]$. In attempting to prepare Pd-Cu complexes, we discovered an interesting

isomerization process in which the initially formed (P,P)-Pd complex was converted predominantly to the (P,N)-Pd complex over time. We have further probed the coordination chemistry of this ligand system by preparing a bimetallic Pd-Mg complex, in which Pd is (P,P)-bound and Mg is (N,N)-bound.

Heterobimetallic Pt/Ag System for the Hydroarylation of Alkenes. A new methodology for the hydroarylation of simple olefins (propylene, 2-butene, norbornene) with benzene and other arenes was developed. This process exhibits high yields and mild reaction conditions (80 °C, 2 h). The catalyst systems consist of a Pt(II) complex and a Ag(I) salt, such as AgOTf or AgBF₄. A variety of Pt precursors can participate in this process, including the complexes [2-(2-pyridyl)indolyl]PtCl(C₂H₄), containing a bidentate nitrogen donor ligand, and (1,5-cyclooctadiene)Pt(OTf)₂, containing a diolefin ligand. Control experiments demonstrate that the role of the Ag(I) salt extends beyond halide abstraction, and possibly involves arene activation. Pt complexes, on the other hand, may act as Lewis acids toward olefin substrates, as demonstrated by the exclusive formation of the branched product cumene from benzene and propylene. The potential catalytic role of strong protic acids, which could be formed via hydrolysis of metal triflates by adventitious water, has been ruled out with mechanistic experiments.

DOE Interest

These projects represent challenging research problems that are relevant to issues in biology, and to development of chemical processes that could have a significant impact on the economy. Hydrocarbons are an important source of chemical feedstocks, and their selective reactions with oxygen have the potential to provide valuable chemicals. In addition, an increased understanding of the reactivity of oxygen in catalytic oxidation processes should aid in the elimination of wastes and in maximizing the efficiency of hydrocarbon utilization to provide transportation fuels and chemicals. The training of students and postdocs in this field should add to the technological capability of the nation.

Future Plans

Routes to Single-Site Iron Catalysts. Our initial focus has been on mononuclear single-site catalysts that activate oxygen. We would like to like to expand this effort by looking at support (i.e., "ligand") effects on the reactivity of the isolated iron sites. For example, the FeZSM catalysts of Panov appear to contain iron in an aluminosilicate framework. We would therefore like to generate well-defined, single iron sites on high-surface-area aluminosilicates. It is also of interest to develop routes to diiron sites, since these have been implicated in the Panov chemistry and are clearly important for selective oxidation catalysis in biology. Initial efforts in this direction have produced molecular precursors to diiron species, including [NEt₄]₂{[(^tBuO)₃SiO]₃Fe-O-Fe[OSi(O^tBu)₃]₃}.

Heterobimetallic Catalyst Systems for Transformations of Hydrocarbons. Further investigations with the new homogeneous Pd/Cu and Pt/Cu complexes will focus on the role of these species as olefin oxidation catalysts. Studies will be designed to probe the ability of the copper center to activate oxygen, and the activation of olefins by the other metal center. Later work will also involve redesigns of the ligand platform, as appropriate, and immobilization of the catalytic centers. The new Pt/Ag catalyst system will be studied in detail. Considerable effort will be devoted to establishment of the mechanism of this bimetallic system. In addition, we intend to explore the generality of this transformation, and the use of this catalysis in hydroarylations with functionalized substrates.

Publications (2002-04)

1. "Oxidative Dehydrogenation of Propane over Vanadia-Magnesia Catalysts Prepared by Thermolysis of $\text{OV}(\text{O}^t\text{Bu})_3$ in the Presence of Nanocrystalline MgO ." C. Pak, A. T. Bell and T. D. Tilley. *J. Catal.* **2002**, 206, 49.
2. "Synthesis, Characterization, and Catalytic Performance of Single-Site Iron(III) Centers on the Surface of SBA-15 Silica." C. Nozaki, C. G. Lugmair, A. T. Bell and T. D. Tilley. *J. Am. Chem. Soc.* **2002**, 124, 13194.
3. "Synthesis and Study of Heterobimetallic Complexes Supported by a Ferrocene-Based Bisphosphine-Diamine Ligand." D. Karshtedt, A. T. Bell and T. D. Tilley. *Organometallics* **2003**, 22, 2855.
4. "Oxidative Dehydrogenation of Propane over Vanadia Based Catalysts Supported on High-Surface-Area Mesoporous MgAl_2O_4 ." O. R. Evans, A. T. Bell and T. D. Tilley. *J. Catalysis*, submitted.
5. "A Platinum-Silver catalyst System for the Hydroarylation of Unactivated Olefins." D. Karshtedt, A. T. Bell and T. D. Tilley. *J. Am. Chem. Soc.*, submitted.

This page intentionally left blank.

Probing Surface Chemistry under Catalytic Conditions: Hydrogenation and Cyclization

Postdocs: Dario Stacchiola

Students: Tao Zheng, Florencia Calaza

Collaborators: Dilano Saldin, H.C. Poon, Matthew Neurock

Department of Chemistry, University of Wisconsin-Milwaukee, Milwaukee, WI 53211
wtt@uwm.edu

Goal

To obtain a fundamental understanding of the catalytic reaction pathways for palladium-catalyzed hydrocarbon conversion reactions by relating the chemistry observed in ultrahigh vacuum to processes occurring under catalytic conditions.

Recent Progress

Ethylene and acetylene hydrogenation and acetylene cyclotrimerization provide ideal candidates for fundamental mechanistic studies since these reactions occur both in ultrahigh vacuum, where products are formed in temperature-programmed desorption, and also at high pressures where the catalytic reaction kinetics of the supported systems are mimicked by a model Pd(111) single crystal catalyst. The nature of the surface is monitored under reaction conditions using photoelastic modulation reflection-absorption infrared spectroscopy (PEM-RAIRS) where we have demonstrated that the infrared spectrum of a monolayer of CO can be measured in the presence of over 200 Torr of gas-phase CO. A method has also been developed for measuring the structures of disordered overlayers using low-energy electron diffraction (LEED) by measuring the I/V curves of the substrate (1×1) Bragg spots of disordered overlayer-covered surfaces. It has been shown theoretically that the effect of an adsorbate on the substrate diffraction spots is about two orders of magnitude larger than the diffuse background scattering and is therefore much easier to measure. The resulting I/V data are analyzed using conventional LEED methods and the method has been tested by comparing the structure measured from both disordered and ordered overlayers of acetylene on Pd(111) with identical structures being obtained by both methods

Both LEED and RAIRS measurements show that ethylene adsorbs on clean Pd(111) in a di-**F** configuration in a structure that is in good agreement with DFT results. A significant improvement in Pendry R-factor was found for a surface containing ~15% of a tilted species with a geometry that is in excellent agreement with the calculated structure for vinyl species on Pd(111) suggesting that some dehydrogenation takes place following ethylene adsorption in clean Pd(111). Vinyl species grafted onto Pd(111) using vinyl iodide either hydrogenate to yield ethylene or react to form ethylidyne on Pd(111) suggesting a possible route for ethylidyne formation.

Ethylene adsorption on hydrogen-saturated Pd(111) has also been studied using RAIRS and LEED revealing the formation of a **B**-bonded species, which is oriented with the C=C axis parallel to the surface and adsorbed on an atop site. Again, the measured structure is in excellent agreement with the results of DFT calculations. The proportion of **B**- and di-**F**-bonded ethylene varies with hydrogen coverage such that only di-**F**-bonded ethylene is present on the clean surface, while

ethylene is exclusively **B**-bonded on a hydrogen-saturated surface. Since hydrogen can adsorb both on and below the surface, the question of whether surface or subsurface hydrogen affects the nature of adsorbed ethylene was investigated. The ratio of surface to subsurface hydrogen depends on temperature and it was clearly demonstrated that subsurface hydrogen is exclusively responsible for inducing the formation of **B**-bonded ethylene. TPD experiments revealed that **B**-bonded ethylene desorbs with an activation energy of 50 kJ/mol compared with 79 kJ/mol for di-**F**-bonded ethylene so that the adsorption of ethylene is substantially weakened by the presence of subsurface hydrogen.

The chemistry of the ethyl intermediate to ethylene hydrogenation was also investigated on Pd(111) to identify the rate-limiting step in the sequential addition of hydrogen. In this case, the adsorbed ethyl group, formed by exposing the surface to ethyl iodide, reacted with hydrogen to form ethane in TPD at ~160 K compared to the desorption peak temperature for the hydrogenation of ethylene itself of ~270 K. This indicates that the addition of the first hydrogen to (**B**-bonded) ethylene is the rate-limiting step, and that the resulting ethyl group reacts rapidly once it is formed.

Strongly bound ethylidyne species are present on the surface during ethylene hydrogenation. In spite of the presence of this ethylidyne overlayer it has been shown that ethylene, acetylene and CO all adsorb onto ethylidyne-saturated Pd(111). Ethylene is di-**F**-bonded on ethylidyne-covered Pd(111) and **B**-bonded on ethylidyne-covered Pd(111) pre-dosed with hydrogen indicating that ethylidyne acts as a spectator species.

The kinetics of ethylidyne formation from ethylene have been measured on Pd(111), with an activation energy to ethylidyne formation of 92 ± 4 kJ/mol and a formation rate constant k_1 at 300 K of $\sim 7.1 \times 10^4 \text{ s}^{-1} \text{ Torr}^{-1}$. The ethylidyne removal kinetics by high pressures of hydrogen were measured, both on clean Pd(111) as well as on alumina supported palladium and showed that the initial removal rate is first order in hydrogen pressure for both a Pd(111) single crystal and alumina-supported palladium. Assuming that the initial rate of ethylidyne removal is given by $k_2 \text{P(H}_2\text{)}$ (ethylidyne) yields a value of $k_2 = 3.1 \pm 0.3 \times 10^{-2} \text{ Torr}^{-1} \text{ s}^{-1}$ at 300 K. The activation energy for ethylidyne removal varies between ~150 and 200 kJ/mol, depending on coverage.

The ethylidyne coverage on Pd(111) was measured under reaction conditions, using PEM-RAIRS, as a function of $\text{P(H}_2\text{)}/\text{P(C}_2\text{H}_4\text{)}$, the ratio of the hydrogen to ethylene pressure and showed that the ethylidyne coverage decreases from 0.25 in pure ethylene ($\text{P(H}_2\text{)}/\text{P(C}_2\text{H}_4\text{)} = 0$) to ~0.08 as the ethylene to hydrogen ratio increases to ~2, and remains constant for higher hydrogen to ethylene ratios. Since the rates of ethylidyne removal and formation have been measured independently, assuming that these rates are identical under reaction conditions, and that the system is at steady state yields a relative ethylidyne coverage under reaction conditions given by $\theta(\text{ethylidyne}) = (k/r)/(1+(k/r))$ where r is the ratio $\text{P(H}_2\text{)}/\text{P(C}_2\text{H}_4\text{)}$ and $k = k_1/k_2$. Using the values of k_1 and k_2 measured above suggests that the ethylidyne coverage should be constant over the range of $\text{P(H}_2\text{)}/\text{P(C}_2\text{H}_4\text{)}$ used experimentally, in contrast to what was found experimentally. Possible origins for the apparently lower value of k_1 are first that the presence of subsurface hydrogen results in the formation of **B**- rather than di-**F**-bonded ethylene and second, that saturation of the surface by hydrogen limits the surface sites available to accept hydrogen and lowers the extent of vinyl formation.

DOE Interest

These results provide a deeper understanding of the nature and reactivity of the surface species that participate in palladium-catalyzed hydrogenation and cyclization reactions. A combination of LEED intensity versus energy measurements of disordered overlayers with infrared spectroscopy has allowed us to measure the structures and reactivities of the key intermediates and identify rate-limiting steps in the reaction pathway. In particular, we have identified the complex role of hydrogen in these reactions, which can act to modify the nature of the strongly bound carbonaceous layer (consisting of ethylidyne or vinylidene) or the nature of the reactant by converting di-**F** into **B**-bonded ethylene. Measurements of the nature of the model catalyst surface under reaction conditions will allow a close connection to be made between the surface species and reaction steps identified in ultrahigh vacuum with the catalytic pathway occurring under realistic conditions.

Future Plans

Surface Structure Determination: The structures of surface species, particularly ethylidyne and vinylidene will be measured using LEED methods. We will examine the structure of vinylidene species as a function of surface coverage since the saturation coverage of these species ($\theta_{\text{sat}} = 1$) suggests that their geometry may change as a function of coverage. The method we have developed for examining disordered overlayers is ideally suited for examining such coverage dependent structural changes. We are collaborating with Professor Matthew Neurock who is carrying out DFT calculations for these structures as a function of coverage to compare with these structural measurements.

Analysis of Surfaces Under Reaction Conditions: We will continue to measure the composition of the Pd(111) single crystal under reaction conditions using PEM-RAIRS initially focusing on the behavior of ethylidyne species since the strong infrared absorbance of the methyl bending mode makes this an ideal candidate for such studies, and also on the more crowded surface formed from propylene. The surface structure will be measured as a function of pressure and temperature.

Modeling of Elementary Reaction Steps: The measured ethylidyne coverage under during ethylene hydrogenation cannot be reproduced using the individually measured ethylidyne formation and removal rates indicating that the rate of ethylidyne formation is substantially lowered by the presence of surface hydrogen. This effect will be explored by measuring the rate of ethylidyne formation on hydrogen-covered surfaces. We will collaborate with Professor Neurock, who has already carried out and published the results of DFT and Monte Carlo calculations on Pd(111)-catalyzed hydrogenation reactions, to model the elementary reactions steps to compare with the experimental data. Such a close interplay between experiment and theory will provide a framework for fully understanding catalytic reaction pathways.

Recent Publications

1. Ethylene Adsorption on Pd(111) Studied Using Infrared Reflection-Absorption Spectroscopy, D. Stacchiola, L. Burkholder and W.T. Tysoe, *Surf. Sci.*, **511**, 215 (2002)
2. The Adsorption of Ethylene on Ethylidyne-covered Pd(111), D. Stacchiola and W.T. Tysoe, *Surf. Sci.*, **513**, L431 (2002)
3. Photoelastic Modulation-Reflection Absorption Infrared Spectroscopy (PEM-RAIRS) of CO on Pd(111), D. Stacchiola, A.W. Thompson, M. Kaltchev and W. T. Tysoe, *Journal of Vacuum Science and Technology*, **A20**, 2101 (2002)
4. An Infrared Spectroscopic and Temperature-programmed Desorption Study of Methyl Iodide Hydrogenation on Pd(111), D. Stacchiola, Y. Wang and W.T. Tysoe, *Surf. Sci.*, **524**, 173 (2003)
5. The Effect of Subsurface Hydrogen on the Adsorption of Ethylene on Pd(111), D. Stacchiola and W.T. Tysoe, *Surface Science*, **540**, L600 (2003)
6. Structure and Reactivity of Propylene on Clean and Hydrogen-covered Pd(111), D. Stacchiola, L. Burkholder and W.T. Tysoe, *Surface Science*, **542**, 129 (2003)
7. Structural Determination of Ordered and Disordered Organic Molecules on a Surface from the Substrate Diffraction Spots in Low Energy Electron Diffraction: ($\sqrt{3}\times\sqrt{3}$)R30°-C₂H₂ and disordered CH₃OH on Pd(111), T. Zheng, W.T. Tysoe, H.C. Poon and D.K. Saldin, *Surface Science*, **543**, 19 (2003)
8. Kinetic and Reactive Properties of Ethylene on Clean and Hydrogen-covered Pd(111), L. Burkholder, D. Stacchiola and W.T. Tysoe, *Surface Review and Letters*, **10**, 909 (2003)
9. Structure Determination of Disordered Organic Molecules on Surfaces from the Bragg Spots of Low Energy Electron Diffraction and Total Energy Calculations, H. C. Poon, M. Weinert, D. K. Saldin, D. Stacchiola, T. Zheng and W. T. Tysoe, *Phys. Rev. B.*, **69**, (2004)
10. Measurement of the Structure of Disordered Overlayers of Ethylene on Clean and Hydrogen-covered Pd(111) by Low Energy Electron Diffraction, T. Zheng, D. Stacchiola, H.C. Poon, D.K. Saldin and W.T. Tysoe, *Surf. Sci.*, submitted
11. Hydrocarbon Conversion on Palladium Catalysts, D. Stacchiola, F. Calaza, T. Zheng and Wilfred T. Tysoe, *J. Mol. Catal. A, Chemical*, submitted

Potentially Catalytic and Conducting Polyorganometallics

Postdoctoral Fellows: Cremer, J.; Oertling, H.; Roeder, J.; Yu, Y.
Students: Leonard, P. W.; Whitener, G. D.; Windler, G. K.

Department of Chemistry, University of California at Berkeley, and the Chemical Sciences Division, Lawrence Berkeley National Laboratory, Berkeley, California 94720-1460

kpcv@berkeley.edu

Goal

To design and execute synthetic routes to novel oligometallic arrays held in unprecedented configurations and to explore their physical and chemical, particularly potentially catalytic properties.

Recent Progress

Molecular Synthesis of Carbon Nanotubes from Alkyne–Metal

Complexes

A method for the quantitative solid-state conversion of Co and Ni alkyne and biphenylene complexes at 550-700 °C for 0.5 to 3 hours into freestanding films of multiwalled carbon nanotubes has been developed. The process is unique in its use of defined molecular entities with controlled metal to carbon ratio as starting materials, the avoidance of specialized apparatus, the locospecific coverage of other structures, the emerging control of morphology of the produced ordered carbon, and the relatively mild conditions employed. The assembly of a library of structurally similar (oligo)alkynyl-arene transition metal complexes has been completed, including the metals Fe, Co, Ni, Pd, Pt, and Mo. A novel approach for the synthesis of complex alkyne ligands was developed based on tungsten catalyzed alkyne metathesis. The catalytic activity of the as-produced metal encapsulating carbon nanotubes in the Pauson-Khand reaction, Fischer-Tropsch synthesis, and shape-selective hydrogenation of nitroarenes is notable.

To probe the scope and limitations of the transition metal catalyzed side hydration of alkyne starting materials, when moist, in this synthesis, a study of their controlled reaction with water to give ketones was completed. This transformation depended strongly on the steric and electronic nature of the alkynes and other attached ligands (e.g. phosphines).

To probe the occurrence and fate of potential hydrocarbon intermediates, a FVP investigation of a biphenylene analog was concluded, leading to the isolation of five isomeric PAHs. Their mechanism of formation was probed in detail by extensive ¹³C labeling experiments.

Potentially Catalytic Oligocyclopentadienylmetals

The total synthesis of (pentaferrocenyl)CpMn(CO)₃ and its (C₅H₄Mn/Re)₅CpMn(CO)₃ congeners was accomplished (X ray structures), reaching the long sought goal of making permethylated (pentacyclopentadienyl)cyclopentadienyl complexes. The key was the use of (C₅H₄M)₂Zn reagents that could be induced to undergo fivefold Pd-catalyzed coupling with C₅I₅Mn(CO)₃ in up to 58% yield. Access to these remarkable hexanuclear clusters held in “unnatural” configurations, has opened up their exploration as potential catalysts and other functional materials. The generality of the method was demonstrated in the pericyclopentadienylmetalation of tetraiodocyclobutadieneFe(CO)₃ and hexaiodobenzene. The X-ray structures of the complexes reflect the extremely crowded nature of the persubstituted periphery of the core. Access to these remarkable clusters held in “unnatural” configurations has opened up their exploration as potential catalysts and other functional materials. The investigation of their chemistry has begun and has led to novel chemistry and structural configurations. Thus, [C₅H₄Mn(CO)₃]₅CpMn(CO)₃ undergoes photodecarbonylation to render the first stable and structurally characterized [CpMn(CO)₂]₂(CO) fragment, held together by the rigid ligand frame. In addition, (pentaferrocenyl)CpMn(CO)₃ can be selectively demanganesylated in high yield providing the novel potential ligand (pentaferrocenyl)cyclopentadiene, a highly crowded assembly endowed with five strongly electron donating substituents. Finally, single and double annealing of the Cp-substituents in (pentaferrocenyl)CpMn(CO)₃ can be effected by Lewis acids to generate intermediates on route to metallated semibuckminsterfullerene, C₃₀H₁₀, critical milestones in a projected rational synthesis of endohedral metallafulerenes.

A study of the metallomeric equilibrium between (η⁵:η⁵:η⁵-1,1':3',1''-terCp)[M¹M²(CO)₆][M³(CO)₃]⁻ X⁺ and (η⁵:η⁵:η⁵-1,1':3',1''-terCp)[M³M²(CO)₆][M¹(CO)₃]⁻ X⁺ has yielded a first X-ray structure of a heterotrimetallic (W-W-Mo) anion system and quantitative activation and equilibrium parameters. The data allow an estimation of relative metal–metal bond strengths in cyclopentadienylmetals, leading to a revision of the literature values for the W-W bond. The investigations feature the system as uniquely suitable for the study of such hitherto mechanistically inaccessible manifolds that represent, in essence, molecular wires and models for minisurfaces.

The photochemistry of FvRu₂(CO)₄ with dimethyl *cis*- or *trans*-butene- and butynedioate has been detailed, leading to the isolation of novel complexes FvRu₂(μ-η²:η⁴-CRCRCRCR)₂(L) (R = CO₂CH₃, L = CO, THF, *cis*-CHR=CHR, thiophene, PPh₃, DMSO). Kinetic experiments point to dissociative substitution of L.

Experimental and structural details of a range of fulvalene(Fv)W₂sulfur complexes have been determined, including the bridging disulfide FvW₂(μ-S₂)(CO)₆ and the monosulfide FvW₂(μ-S)(CO)₆.

Finally, the search for a synthetically conveniently accessible fulvalene* analog of Cp* (i.e. Me₅Cp) has led to syntheses of tetrakis(*tert*-butyl)- and tetrakis(trimethylsilyl)fulvalene. These ligands should enable the isolation of and structural characterization of previously observed FvM₂-CH activation products and open up the potential for catalytic transformations.

Future Plans

Metal-Catalyzed Routes to Carbon Nanotubes: A library of organometallic homo- and heterobinuclear complexes of $(C_6H_5)_2C_2(C_6H_5)_2$ will be screened for selectivity in defined wall, especially single wall, nanotube assembly. Efforts will be initiated in the construction of devices using this methodology. Extensions to the synthesis of BN and other heterotubes will be sought.

Potentially Catalytic Oligocyclopentadienylmetals: The electrochemical properties of radial CpM clusters, in particular the series based on cyclopentadienyl as the core, will be subject to continuing investigation. The ability of these potentially multichelating assemblies to provide the first isolable and structurally characterizable C-H σ -complexes of, e.g., methane will be tested. Preliminary observations of multiple C-H activations will be subject to scrutiny. Further effort will be made to effect complete annealing to the semibuckminsterfullerene core. Extensions of the synthetic methodology to decahaloferrocene and ruthenocene should provide access to decametallated metallocenes containing the topology of C_{60} and thus constituting excellent precursors to endohedral metallofullerenes. The novel free ligand pentaferrocenyl(cyclopentadiene), a highly electron rich (by virtue of the five Fc substituents) analog of Cp*, suggests an extensive exploration of its potential in the construction of electronically stabilized cationic and/or electron poor (16 or 14e) metals for catalysis (e.g. titanocenes for olefin polymerization, 16e-Cp*RuL⁺ for a large range of catalytic C-C bond formations).

Future work on the tercyclopentadienyl trimetallic core is directed toward manipulation of the ligand (e.g. a central indenyl fragment, to probe potential ring slippage) and the trimetallic array (e.g. rendition of an M-M'-M sequence for consonance with Marcus theory) for mechanistic purposes, and the juxtaposition of metal pairs judiciously chosen to allow for the determination of their relative intermetallic bond strengths.

Publications (2002-2004)

Chen, M.-C.; Eichberg, M. J.; Vollhardt, K. P. C.; Sercheli, R.; Wasser, I. M.; Whitener, G. D., "Photosubstitution of (Fulvalene)tetracarbonyldiruthenium by Alkenes and Alkynes: First Observation of Alkyne Coupling on Fulvalene Dimetals and Synthesis of a (Fulvalene)dimetallacyclopentadiene(alkene) Complex," *Organometallics* **2002**, *21*, 749; LBNL-49448.

De Azevedo, C. G.; Vollhardt, K. P. C., "Oligocyclopentadienyl Transition Metal Complexes," *Synlett* **2002**, 1019; LBNL-49449.

Israelsohn, O.; Vollhardt, K. P. C.; Blum, J., "Further Studies on Hydration of Alkynes by the PtCl₄-CO Catalyst," *J. Mol. Cat.* **2002**, *184*, 1; LBNL-49451.

Capps, K. B.; Whitener, G. D.; Bauer, A.; Abboud, K. A.; Wasser, I. M.; Vollhardt, K. P. C.; Hoff, C. D., "Synthesis and Crystal Structures of (Fulvalene)W₂(SH₂(CO))₆, (Fulvalene)W₂(μ -S₂)(CO)₆, and (Fulvalene)W₂(μ -S)(CO)₆-Low Valent Tungsten Carbonyl Sulfide and Disulfide Complexes Stabilized by the Bridging Fulvalene Ligand," *Inorg. Chem.* **2002**, *41*, 3212; LBNL-49452.

Whitener, G. D., "1. The Chemistry of Group IV Metals Supported by Nitrogen Bearing Ligands. 2. Late Metal Chemistry Supported by the Fulvalene Ligand," PhD Thesis, **2002**; LBNL-51973.

Iyer, V.; Vollhardt, K. P. C., "Fabrication of Carbon Nanotube Films from Alkyne-Transition Metal Complexes," *United States Patent Application*; US 2003/0175199 A1; Sep. 18, 2003; IB-1719P.

Miljanić, O. Š.; Vollhardt, K. P. C. ; Whitener, G. D., "An Alkyne Metathesis-Based Route to ortho-Dehydrobenzannulenes," *Synlett* **2003**, 29; LBNL-51972.

Iyer, V.; Vollhardt, K. P. C.; Wilhelm, R., "Near-quantitative Solid State Synthesis of Carbon Nanotubes from Homogeneous Diphenylethyne Cobalt and Nickel Complexes," *Angew. Chem.* **2003**, *115*, 4515; *Angew. Chem. Int. Ed.* **2003**, *42*, 4379; LBNL-54268.

Amouri, H.; Cammack, J. K.; Leonard, P. W.; Myrabo, R. L.; Vollhardt, K. P. C., "Electron Exchange Along the Tercyclopentadienyltrimetallic Scaffold: Kinetics, Equilibria, and Bond Strengths," *Angew. Chem.* **2004**, *116*, 1417; *Angew. Chem. Int. Ed.* **2004**, *43*, 1393; LBNL-54269.

Propane Oxidation/Amoxidation Reactions over Mixed Metal Oxide Catalysts: Nature of Surface Sites and Their Relationships to Reactivity/Selectivity Properties

Students: X. Gao*, P. Saunders*, H.S. Hong*, T. Kim, C. Zhao, E. Lee *graduated
Post-Doctoral Fellow: Z. Zhao+ +departed
Collaborators: L.E. Briand (U. Nacional La Plata, Argentina), W. Gruenert (Ruhr-U. Bochum, Germany), J.-M. Jehng (National Chung Hsing University, Taiwan), G. Deo (IIT-Kanpur, India)

Operando Molecular Spectroscopy and Catalysis Laboratory, Department of Chemical Engineering, Lehigh University, Bethlehem, PA 18015 USA iew0@lehigh.edu

Goals: Determination of the (1) nature of surface sites (surface composition, molecular structures, oxidation states and redox/acidic/basic sites) for mixed metal oxide catalysts (bulk mixed metal oxides and model supported metal oxides), (2) influence of the reaction environments on the active surface sites, and (3) molecular structure-reactivity/selectivity relationships for propane reactions oxidation, amoxidation and autothermal reactions.

Recent Progress: There is currently much interest in the activation of propane over mixed metal oxide catalysts to numerous reaction products: propylene, acrolein, acrylic acid, acrylonitrile and generation of H₂. However, there is currently very limited fundamental information about the nature of these active surface sites, especially under reactions conditions, and their relationships to the catalytic activity and selectivity. Two methods have been advanced and developed to obtain information about the surface composition of mixed metal oxides: low energy low energy ion scattering spectroscopy (LEISS) and CH₃OH-temperature programmed reaction (TPSR) spectroscopy. The elemental surface composition of mixed metal oxides was determined with a special LEISS procedure and revealed, *for the first time*, that bulk mixed metal oxides can exhibit surface segregation of certain elements (especially oxides of Mo and V). Additional information about the surface composition and reactivity was provided by CH₃OH-TPSR experiments that revealed the nature of the active surface sites (elemental composition, oxidation states, participation of surface and bulk lattice oxygen, redox/acidic/basic sites and their reactivity/selectivity relationships).

Molecular structural and oxidation state information about the active surface sites and surface reaction intermediates under reaction conditions were determined with *in situ* Raman, IR and UV-Vis spectroscopy for the model supported metal oxide catalyst systems. For propane oxidation reactions to propylene over supported vanadium oxide catalysts, the surface metal oxide species retained their fully oxidized dehydrated molecular structures with only a minor fraction becoming reduced by the reaction conditions. Under these reaction conditions, the surfaces exhibit no detectable surface reaction intermediates. For propane autothermal reforming to H₂ over supported Rh/Al₂O₃ catalysts, the development of UV Raman spectroscopy with a special *in situ* cell was required to be able to monitor the catalysts, *for the first time*, at temperatures of 1000 °C. The active surface species under these severe reaction conditions was rhodium oxide. No surface reaction intermediates were present at 1000 °C, but surface carbonaceous deposits were present on the catalyst at lower reaction temperatures.

Propane oxidative dehydrogenation was found to require one redox surface metal oxide site and was promoted by the specific oxide support (Zr > Ti > Nb > Al > Si) due to the participation of the bridging V-O-Support bond. Propane oxidation to acrolein, via propylene

oxidation, was found to require two surface sites and was also promoted by the specific oxide support (Zr > Ti > Nb > Al > Si) due to the participation of the bridging M-O-support bond. Thus, it appears that the promotion by the specific oxide support is a general phenomenon for oxidation reactions over supported metal oxide catalysts and that the number of required active surface sites is specific to each reactant molecule and product. These conclusions are also expected to play a role during oxidation reactions over bulk mixed metal oxide catalysts.

DOE Interest: The efficient use of natural gas hydrocarbon feedstocks for production of chemicals and energy over mixed metal oxide catalysts is of great interest to many catalytic applications. The more selective the chemical oxidation reactions, the smaller will be the amounts of environmentally undesirable by-products. The more selective the autothermal reactions to produce hydrogen, the more energy efficient will be the technology and by-product formation minimized. The key to achieving these goals is the establishment of molecular structure-reactivity/selectivity relationships for various mixed metal oxide catalysts employed for such oxidation reactions. Such fundamental molecular level information is needed for the development of theoretical models of mixed metal oxide catalysts for numerous alkane hydrocarbon oxidation reactions.

Future Plans:

1. Investigate propane/propylene oxidation to acrylic acid with well-defined bulk and supported mixed metal oxide catalytic materials.
2. Investigate propane/propylene oxidation to acrylonitrile with well-defined bulk and supported mixed metal oxide catalytic materials.
3. Continue to advance spectroscopic techniques that can provide composition and oxidation state information about the outermost surface of bulk mixed metal oxides.
4. Continue to advance molecular spectroscopic techniques that can provide molecular structures and oxidation states under reaction conditions.

Publications:

1. M.A. Banares and I.E. Wachs, "Molecular Structures of Supported Metal Oxide Catalysts Under Different Environments," *Journal of Raman Spectroscopy* **33** (2002) 359.
2. X. Gao and I.E. Wachs, "Molecular Engineering of Supported Vanadium Oxide Catalysts Through Support Modification," *Topic in Catalysis* **18** (2002) 243.
3. X. Gao, J.M. Jehng and I.E. Wachs, "In Situ UV-Vis-NIR Diffuse Reflectance and Raman Spectroscopic Studies of Propane Oxidation over ZrO₂-Supported Vanadium Oxide Catalysts," *Journal of Catalysis* **209** (2002) 43.
4. D. Kulkarni and I.E. Wachs, "Isopropanol Oxidation by Pure Metal Oxide Catalysts: Number of Active Surface Sites and Turnover Frequencies," *Applied Catalysis A: General* **237** (2002) 121.
5. M. Cherian, M. S. Rao, A.M. Hirt, I.E. Wachs and G. Deo, "Oxidative Dehydrogenation of Propane over Supported Chromia Catalysts: Influence of Oxide Supports and Chromia Loading," *Journal of Catalysis* **211** (2002) 482.
6. L.E. Briand, J.-M. Jehng, L. Cornaglia, A.M. Hirt and I.E. Wachs, "Quantitative Determination of the Number of Surface Active Sites and the Turnover Frequency for Methanol Oxidation over Bulk Metal Vanadates," *Catalysis Today* **78** (2003) 257.
7. I.E. Wachs, Y. Chen, J.-M. Jehng, L.E. Briand and T. Tanaka, "Molecular Structure and Reactivity of the Group V Metal Oxides," *Catalysis Today* **78** (2003) 13.

8. Z. Zhao, X. Gao and I.E. Wachs, "Comparative Study of Bulk and Supported V-Mo-Te-Nb-O Mixed Metal Oxide Catalysts for Oxidative Dehydrogenation of Propane to Propylene," *Journal of Physical Chemistry B* **107** (2003) 6333.
9. L.E. Briand, O.P. Tkachenko, M. Guraya, X. Gao, I.E. Wachs and W. Gruenert, "Surface Analytical Studies of Supported Vanadium Oxide Monolayer Catalysts," *Journal of Physical Chemistry* **108** (2004) 4823.
10. T.V.M. Rao, G. Deo, J.-M. Jehng and I.E. Wachs, "In Situ UV-Vis-NIR Diffuse Reflectance and Raman Spectroscopy and Catalytic Activity Studies of Propane ODH over Supported CrO₃/ZrO₂ Catalysts, *Langmuir* (accepted).

This page intentionally left blank.

Catalytic Hydrogenation of Carbon Monoxide

PI: Wayland, B. B. GS: Fu, X., Cui W., and Scricco, J.

Department of Chemistry, University of Pennsylvania, Philadelphia, PA 19104-6323

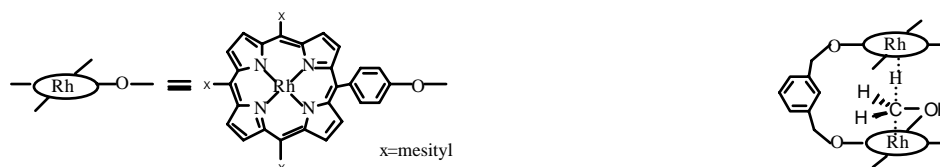
Abstract

This program encompasses a series energy research issues associated with conversion of carbon monoxide and hydrocarbons to organic oxygenates from reactions of CO, H₂, CH₄, C₂H₄, O₂, and H₂O. Diverse substrate reactions of group nine (Co, Rh, Ir) metalloporphyrins including formation of metallo-formyl complexes, methane and water activation are guiding the design of new catalyst materials with properties modified for improved rates and selectivity for applications in both organic and aqueous media. One of the current focus areas is the design and synthesis of diporphyrin ligands that form dimetal complexes capable of preorganizing transition states for substrate reactions that involve two metal centers. Dimetallo radical diporphyrin complexes are observed to manifest large rate increases over mono-metalloradical reactions of H₂, CH₄, CO and other small molecule substrates. One particularly important result is that bimetallo radical carbon-hydrogen bond activation can be designed to give kinetic preference for methane activation over that of both methanol and ethanol¹. Another current focus of this program is to explore the range of organometallic transformations that can be achieved in aqueous media. Water soluble group nine metalloporphyrins manifest remarkably versatile substrate reactivity in aqueous media which includes producing rhodium formyl (Rh-CHO) and hydroxy methyl (Rh-CH₂OH) species.² One of the most complete descriptions of equilibrium thermodynamics for organometallic reactions in water is emerging from the study of rhodium porphyrin substrate reactions in aqueous media.^{2,3} Current directions for this program include developing new strategies to obtain anti-Markovnikov addition of water, amines and alcohols with olefins, and evaluating catalytic reactions of CO that yield formamides and formic esters.

Overview of recent progress

m-xylyl tethered dirhodium(II) biporphyrins

Bimetallo-radical complexes of rhodium (II) have been prepared and evaluated with porphyrin units that prohibit intermolecular and intramolecular Rh(II)-Rh(II) bonding and a tether unit that has an appropriate size and flexibility to permit the two metal centers to reach the transition states for intramolecular substrate reactions.

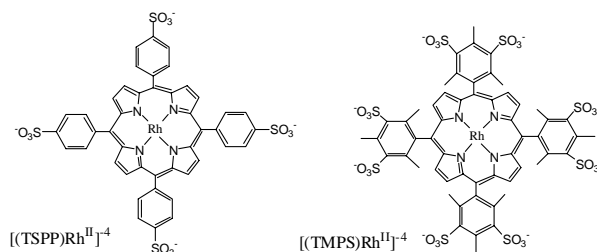


The primary initial objectives for designing bimetallo-radical species were to test the strategy to obtain rate enhancements for metallo-radical substrate reactions by converting termolecular metallo-radical processes to bimolecular reactions with reduced activation entropy while retaining selectivity. These objectives have been realized in the reaction of $\cdot\text{Rh}(\text{m-xylyl})\text{Rh}\cdot$ with methane, which occurs as a bimolecular process with reduced activation entropy compared to the reaction of methane with $(\text{TMP})\text{Rh}\cdot$. Realization of additional rate enhancements and substrate selectivity in this system requires reducing the activation enthalpy through designing bimetallo-radical structures that more closely emulate the transition state structures.

Organometallic Reactions of Group 9 Porphyrins in Water

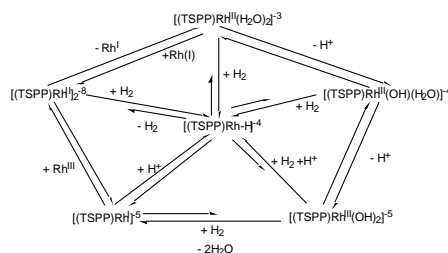
Studies of rhodium porphyrins in aqueous solution

Growing interest in applying organometallic reactions for processes in water and the utilization of water as a substrate are primary motivations for the study of rhodium porphyrin chemistry in aqueous media. Sulfonation of tetraphenyl porphyrin derivatives provides a convenient entry point into water-soluble porphyrin complexes.



Reaction of (TSPP) Rh^{III} species with H₂ in H₂O

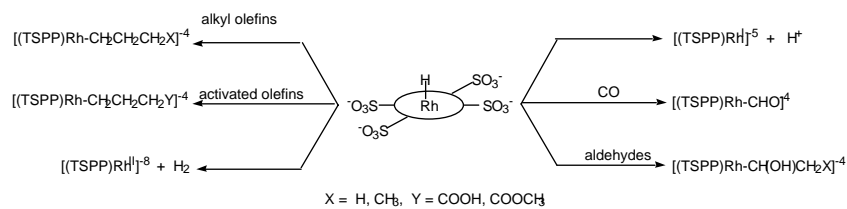
The set of species formed in aqueous solution in the reactions of H₂ with rhodium(III) porphyrins is illustrated in Scheme I.



Scheme I: Interrelationships of reactive Rh(I), Rh(II) and Rh(III) species

Reaction of [(TSPP)Rh-H]⁻⁴ with CO, aldehydes and olefins in H₂O

Reactions of (TSPP)Rh-H with CO, aldehydes and olefins that produce formyl, α -hydroxy alkyl and alkyl derivatives are summarized in Scheme II.



Scheme II: Reactivity patterns of [(TSPP)Rh-H]⁻⁴ species

(TSPP)Rh-H reacts rapidly with a wide range of olefins ($\text{CH}_2=\text{CHX}$; X = H, R, C₆H₅, CN, CO₂R) to give anti-Markovnikov addition of the Rh-H unit. This set of olefin reactions establishes the foundation to obtain anti-Markovnikov addition of H₂O to alkenes by addition of (por)Rh-H to the olefin to form (por)Rh-CH₂CH₂R and then nucleophilic displacement of (por)Rh⁻ by OH⁻ to produce the primary alcohol (HO-CH₂CH₂R).

Thermodynamic studies in water

Equilibrium constants have been evaluated for a wide variety of substrate reactions of rhodium porphyrins in water. Most of the reactions in Scheme I and Scheme II have been studied and many additional reactions of (por)Rh-H and (por)Rh-OH are currently being evaluated. This research will provide an unprecedented range of metal-substrate (M-H, M-R, M-OR) thermodynamic measurements. Reactivity and thermodynamic studies are currently being extended to the (TMPS)Rh and electron withdrawing porphyrin systems.

Publications:

- 1) “Bimetallo-Radical Carbon-Hydrogen Bond Activation of Methanol and Methane”, Weihong Cui, X. Peter Zhang, and Bradford B. Wayland, *J. Am. Chem. Soc.* **2003**, *125*, 4994.
- 2) “Aqueous Organometallic Reactions of Rhodium Porphyrins: Equilibrium Thermodynamics”, Xuefeng Fu, Leah Basickes and Bradford B. Wayland, *Chem. Commun.* **2003**, 520.
- 3) “Equilibrium Thermodynamic Studies in Water (1): Reactions of Dihydrogen with Rhodium(III) Porphyrins Relevant to Rh-Rh, Rh-H and Rh-OH Bond Energetics”, Xuefeng Fu and Bradford B. Wayland, *J. Am. Chem. Soc.* **2004**, *126*, 2623-2631.

This page intentionally left blank.

Non-Thermal Reactions of Gas-Phase Oxygen Atoms with Atoms Adsorbed on Transition Metal Surfaces

Postdocs: none currently

Students: Alex Gerrard, Brad Shumbera

Department of Chemical Engineering, University of Florida, Gainesville, FL 32611

weaver@che.ufl.edu

Goal

The reactions of gas-phase oxygen atoms at transition-metal surfaces are important in catalytic oxidation processes occurring at high temperature and with plasma activation. Due to the strong bonding of oxygen on metals, the collision of an oxygen atom with a metal surface results in significant energy release that can stimulate a variety of non-thermal reactions, including direct atom abstraction and collision-induced reactions. Such processes could play a central role in the surface chemistry occurring in extreme environments and are therefore important to understand. The goal of this project is to elucidate the mechanisms and to quantify the kinetics of non-thermal reactions between gas-phase oxygen atoms and atoms adsorbed on transition-metal surfaces, and to advance the fundamental understanding of the effects of adsorbate and surface properties on the predominant non-thermal processes.

Recent Progress

The initial focus of this project has been to design, assemble and test an apparatus for generating beams of thermal energy oxygen atoms that will be used in reactive scattering experiments in ultrahigh vacuum (UHV). The beam system consists of a plasma source that is mounted in a two-stage differentially-pumped chamber and coupled to an UHV chamber (Figure 1). Gaseous oxygen atoms are produced in this system by dissociating O₂ in a microwave plasma that is confined to a small volume at the end of the plasma source. Species exit the plasma volume through small holes at the end of the source, thus forming a beam that is directed toward the sample surface held in the UHV chamber. In the first pumping stage, the beam passes between charged parallel plates that deflect ions from the beam flux. After flowing through a thin-walled orifice separating the first and second pumping stages, the species travel down a quartz tube before entering the UHV chamber. The purpose of the quartz tube is firstly to collimate the beam so that the atomic oxygen flux can be confined to the sample surface. In addition, collisions at the inner walls of the tube are known to significantly reduce the fraction of atoms and molecules in vibrationally and electronically excited states. Thus, the beam flux reaching the sample should consist almost exclusively of thermal energy (~0.05 eV), ground-state atomic and molecular oxygen, with the fraction of oxygen atoms in the flux expected to lie between 45 and 65%. The quadrupole mass spectrometer (QMS) shown in the figure is available for characterizing the beam flux and

composition. Finally, a shutter is located in the first pumping stage to enable control over beam introduction into the main UHV chamber.

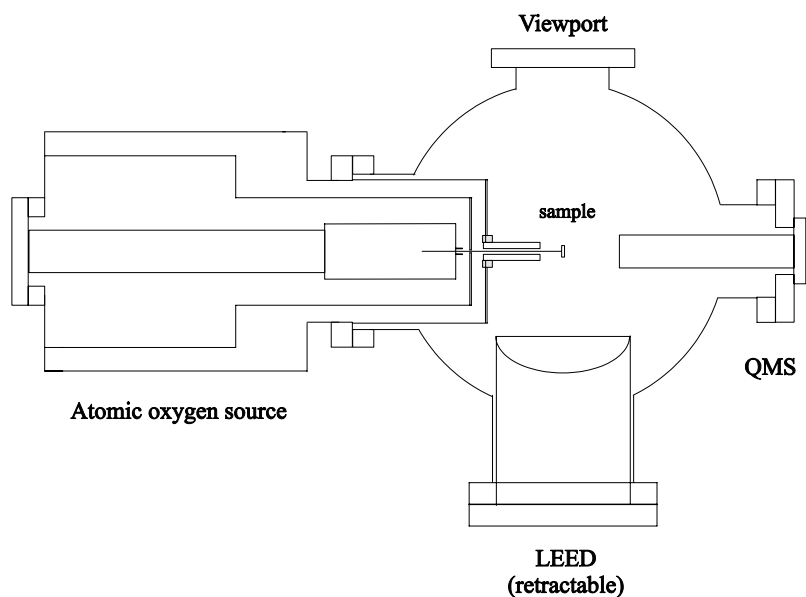


Figure 1. Schematic of atomic oxygen beam source attached to UHV system.

The new beam source was installed at the end of 2003 and its performance has recently been benchmarked by examining the oxidation of Si(100). Using X-ray photoelectron spectroscopy, the uptake of oxygen by Si(100) was measured as a function of exposure to oxygen beams generated with and without plasma activation. As expected, the rate of oxygen uptake was significantly enhanced when the plasma was activated. In addition, the saturation oxygen coverage that could be reached on Si(100) held at room temperature was about twice that achieved by exposing the surface to a pure O₂ beam. Analysis of the uptake results obtained with and without plasma activation indicates that the atomic oxygen flux at the sample location was in the range of 0.4 to 1.2 x 10¹⁴ atoms/cm² sec for the beam conditions employed. This range is ideal for measuring atom abstraction rates using direct mass spectrometric analysis of the desorbing products. Experiments using appearance potential mass spectrometry are currently underway to further characterize the atomic oxygen content of the beam.

DOE Interest

Understanding of the mechanisms that govern the surface reactions of gaseous oxygen atoms, and quantification of the associated reaction cross sections, is important to the design and modeling of catalytic processes that occur under extreme conditions, including processes such as surface combustion and plasma-assisted catalysis.

Future Plans

Atom abstraction from Pt(111). We have recently begun an investigation of the interactions of thermal-energy oxygen atoms with clean and adsorbate-modified Pt(111). The exposure of clean Pt(111) to atomic oxygen is expected to generate high coverage adsorbed phases and possibly oxide structures that will be characterized using several surface analysis techniques. We then plan to investigate the non-thermal reactions that occur between gas-phase oxygen atoms and various atoms (O, C, N, H) adsorbed on the Pt(111) surface. The general aim is to elucidate the mechanisms for these reactions and to investigate how adsorbate-surface bond strengths and interactions between adsorbates affect the kinetics for the non-thermal reactions that occur.

Hyperthermal oxygen atoms. We also plan to investigate the surface reactions induced by oxygen atoms generated with hyperthermal kinetic energies (~ 5 eV). Our approach for producing hyperthermal atomic oxygen involves the continuous permeation of oxygen atoms through a silver membrane followed by electron stimulated desorption of the oxygen atoms as they emerge on the vacuum side of the membrane. By investigating the surface reactions induced by both thermal and hyperthermal oxygen atoms, we seek to determine the main effects that incident energy has on the mechanisms and kinetics of the surface reactions of gas-phase oxygen atoms.

Substrate-mediated effects. The reactions between gas-phase oxygen atoms and atoms adsorbed on different metal surfaces will be investigated to determine how the non-thermal surface reactivity of oxygen atoms is influenced by the metal substrate. The reaction kinetics and branching among reaction channels may vary from metal to metal due to changes in the efficiency of energy exchange between energetic oxygen atoms and the surface.

Publications (2003-4)

No publications have yet resulted from this work.

This page intentionally left blank.

Polymer Supported Palladated Pincer Ligands in Catalysis

Postdoctoral Fellows: Holbach, M.; Ji, Y.; Yu, K.

Students: Jain, S.; Richardson, J.; Sears, J.; Sommer, W.; Swann, A.

Collaborators: Davis, R.; Jones, C.; Ludovice, P.; Sherrill, D.

School of Chemistry and Biochemistry and School of Chemical and Biomolecular Engineering, Georgia Institute of Technology, Atlanta, GA 30332
Department of Chemical Engineering, University of Virginia, Charlottesville, VA 22904
marcus.weck@chemistry.gatech.edu

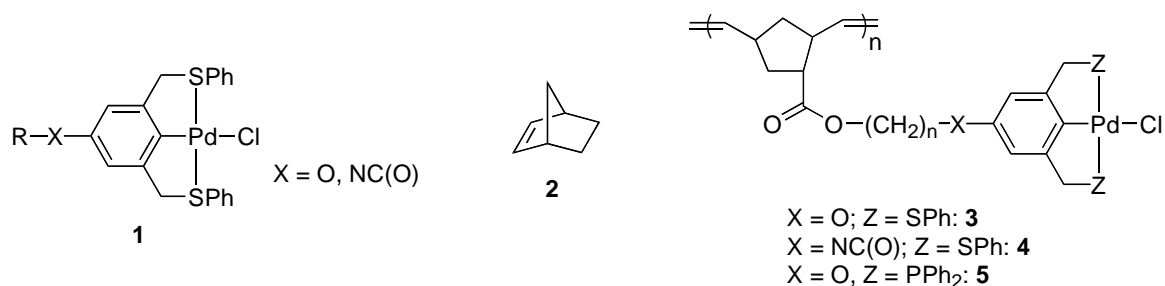
Goal

To develop a fundamental understanding of the interactions between soluble catalyst supports such as polymers and soluble nanoparticles and well-defined transition metal catalysts, in particular catalysts for organic transformations such as carbon-carbon bond formations and epoxidations.

Recent Progress

This project is part of a larger DOE funded initiative to elucidate the basic design principles that govern the interactions between well-defined transition metal catalysts and supports ranging from polymers to porous silica. Initially, we focused our efforts on the synthesis of polymer supported palladium/pincer complexes and studied their catalytic activity as well as their potential catalyst decomposition.

Heck Couplings with Pd-SCS pincer complexes: Supported palladated pincer complexes have been identified in the literature as potential well-defined catalysts for a variety of carbon-carbon bond formations including the Heck reaction. In particular so called Pd(II) SCS pincer complexes (**1**) have been described as outstanding Heck catalysts by a number of groups in the literature. Over the last six months, we have synthesized a variety of novel polymer supported Pd(II) pincer complexes. In contrast to previously published polymer supports that contain only one or two catalytic active moieties per polymer strand, our polymers are based on norbornene as polymerizable unit (**2**) thereby allowing for the controlled polymerization via ring-opening metathesis polymerization. The resulting polymers contain one catalytic site per repeating unit creating the highest supported Pd(II) pincer catalyst loading reported to date. A variety of poly(norbornene)s containing different supported Pd(II) pincer complexes were synthesized (compounds **3** - **5**). These polymer-supported catalysts vary slightly in their attachment of the catalytic moiety to the monomer unit and/or the elements that undertake the dative bonds to the palladium center.



Using a variety of characterization methods including NMR spectroscopy, targeted catalyst poisoning and IR, we have unequivocally determined that the supported polymer/Pd(II) pincer catalyst system **3** decomposes under standard reaction conditions for the Heck catalysis of iodo-arenes with acrylates. Furthermore, we were able to identify that the active catalytic species is a homogeneous molecular Pd(0) source. These findings are in contrast to reports in the literature and clearly demonstrated that these catalysts are not reusable and/or recoverable. Interestingly, preliminary investigations on the use of **4** as Heck catalyst suggest that this polymer Pd(II) system does not decompose or only partially decompose under standard reaction conditions. Investigations into the true nature of the catalytic species of **4** are currently being carried out.

Synthesis of Poly(norbornene)s Containing Terminal N-heterocyclic Carbenes as Ligands in Catalysis. We started on the synthesis of norbornene-based monomers containing terminal N-heterocyclic carbene ligands. These carbenes have been identified as outstanding ligands for a variety of catalysts for organic transformations including carbon-carbon bond formations such as olefin metathesis and the Heck reaction. Initially, we have synthesized a number of novel carbene ligands with a variety of alkyl spacers containing terminal functional groups such as thiols, alcohols, and olefins. Currently, we are actively pursuing the attachment of these carbenes onto norbornenes and soluble gold nanoparticles.

DOE Interest

A detailed understanding of the underlying design principles that dictate the interactions between a supported catalyst and its support are of utmost importance in catalysis. This research will improve the rational design of reusable and recyclable supported catalysts that are able to use the current basic carbon-hydrogen feedstock to create complex molecules and important precursors for drugs and polymers and it is therefore of general interest to the DOE.

Future Plans

Elucidating the Catalytic Species of Different Polymer Supported Pd(II) Pincer Catalysts. Using polymers **3** - **5** and similar polymers, we hope to identify the catalytic species of polymer supported Pd(II) pincer catalysts. Furthermore, we will investigate which factors influence the formation of the catalytic species using a combination of computational methods and experiments.

Influence of Polymer Backbone Structure on Catalyst Accessibility: We are investigating the role of the polymer backbone, its structure in solution (rigid rod versus

random coil) and ultimately the accessibility of the catalyst using poly(norbornene)s and poly(octene)s via a combination of computational methods and experimental characterizations such as two-dimensional NMR spectroscopy.

Investigations into the Use of Soluble Nanoparticles as Catalyst Support. Soluble gold and silver nanoparticles will be functionalized with thiol containing Pd(II) pincer complexes and their catalytic activity will be investigated. In a second step, these activities will be compared to the analogous polymer supported Pd pincer complexes and again, using a combination of computational methods and experiments the underlying design motifs will be elucidated.

Publications (September 2003-present)

1) Yu, K.; Sommer, W.; Weck, M.; Jones, C. W.; Silica and Polymer-Tethered Pd-SCS-Pincer Complexes: Evidence for Precatalyst Decomposition to Form Homogeneous Catalytic Species in Mizoroki-Heck Chemistry, manuscript submitted, March 12 2004.

This page intentionally left blank.

Morphological and Kinetic Aspects of Surface Processes

Postdocs: Huang, W.X., Ni, J.

Students: Fitts, W., Yan, X.M., Robbins, M, Park, H, Wang, Q., Lee, I., Compagna, J.

Collaborators: Sun, Y.-M., Zhao, W., Henderson, M., Szanyi, J., Onishi, H., Uetsuka, H.

Department of Chemistry and Biochemistry, University of Texas, Austin, TX 78712

<mailto:jmwhite@mail.utexas.edu>

Goals

Using model systems, our goals are to prepare and characterize intermediates postulated to play important roles in heterogeneously catalyzed reactions, to characterize ordered overlayers of organic species chemisorbed on single crystal metals, and to prepare and characterize the structural and chemical properties of metal nanoparticles on planar model oxide substrates.

Recent Progress

Thermodynamics of decanethiol on gold. The coverage-dependent phase behavior of the thiolate formed from decanethiol, $\text{CH}_3(\text{CH}_2)_9\text{SH}$, on Au(111) was studied at 0°C using variable-temperature scanning tunneling microscopy and compared to analogous results for temperatures between 25 and 65 °C.^{1,2} The effects that a reconstructed (herringbone) and stepped Au(111) surface have on the structure of submonolayers of decanethiolate were also studied between 25 and 60 °C.² At 25 °C, formation of lattice gas (α) species at low coverages alters the herringbone structure by shortening the periodicity of the elbows from 25 to 15 nm. In addition, small β phase islands nucleate and grow anisotropically in regions of fcc stacking. These domains grow by incorporating nearby lattice gas species, consuming herringbone ridges and altering the remnant ridges that surround them. For a coverage that saturates the β -phase (~0.25 of the closest packing achievable), raising the temperature to 30 or 40 °C increases the average size of the β -phase islands by condensation of neighboring islands with no evidence, at the selected coverage, for the presence of any other thiolate phase. At 60 °C, well above the thiolate melting point to form the ϵ -phase, small β -phase domains remain.

Electron-induced dissociation of tert-butyl nitrite adsorbed on Ag(111). Non-thermal methods for generating catalytically interesting intermediates is a sug-goal of our project. The electron-induced chemistry of *tert*-butyl nitrite (TBN, $(\text{CH}_3)_3\text{CONO}$), adsorbed on Ag(111), or over a CH_3OH spacer layer, was studied at 90 K using three kinds of measurements—the time dependence of ejected fragments during 70 eV electron irradiation, temperature-programmed desorption (TPD) after irradiation, and X-ray photoelectron spectroscopy before and after irradiation.³ Only NO is detected during 70 eV electron irradiation, and the initial total cross-section for loss of TBN is quite large,

$3.3 \times 10^{-15} \text{ cm}^2$. Post-irradiation TPD, after dissociating ~90% of a saturated TBN monolayer, reveals residual TBN and a number of products, including NO, C₄H₈ (isobutene), CH₃COCH₃ (acetone), (CH₃)₃COH (*t*-butyl alcohol), CO and H₂O. Interestingly, there is no evidence for H₂ in TPD. Illustrating a central role for the Ag(111) substrate, electron-induced dissociation of monolayer TBN adsorbed over 10 ML of methanol was less efficient, by a factor of 4, than 1 ML TBN on clean Ag(1 1 1).

Reactions of hydrocarbon species on silver. Silver is an ideal substrate for modeling many aspects of heterogeneous reactions of hydrocarbons, e.g., partial oxidation of propene. The interactions of propene, itself, with Ag(111) were examined using TPD and RAIRS.⁴ At 100 K, propene reversibly adsorbs, with chemisorbed desorption peaks at 161, (α_1) and 145 K (α_2), and a multilayer peak at 123 K (α_3). Repulsive interactions drive a change from α_1 - to α_2 -propene during adsorption and desorption. The three adsorption states are distinguished by RAIRS on the basis =CH₂ wagging vibration frequencies at 924, 918 and 908 cm⁻¹, respectively. Vibrational spectroscopic and thermal desorption evidence describing the behavior of propene on oxygen-modified Ag(111) at 100 K indicates a gradual transition from π -bonded to *di*- σ -bonded propene as the oxygen adatom coverage increases.⁷

Reactions of propene on oxygen modified Ag(111) surface were also investigated.⁵ In the presence of oxygen adatoms, interactions of propene with the substrate are strengthened. The reaction between propene and oxygen adatoms (0.086 ML) produces not only total oxidation products (CO₂ and H₂O), but also partial oxidation products (CO and acetone). The formation of chemisorbed hydroxyl groups is identified by RAIRS when coadsorbed propene and oxygen adatoms are annealed to 200 K. The formation of hydroxyl is ascribed to the abstraction of methyl hydrogen by oxygen adatoms.

Nitrogen oxides on silver. The interactions of NO₂ with Ag(111) at various temperatures were investigated by means of temperature programmed desorption and reflection-adsorption infrared spectroscopy and found to be sensitively coverage- and temperature-dependent.⁹ During dosing at 508 K, NO₂ decomposes into NO(g) and O(a) whereas at 215 K NO and O remain adsorbed. The NO(a) occupy threefold-bridged sites and atop sites in sequence. Orientations of the NO(a) axes are affected by neighboring O(a).

Cross-coupling of C₁ groups on silver. The cross-coupling reaction between CH₂ and CF₃ on Ag(111) to form adsorbed CF₃CH₂(a) was, for the first time, spectroscopically identified as an intermediate in the reaction to form CF₂CH₂.¹⁰ It is formed by migratory methylene insertion into Ag-CF₃. CF₃CH₂(a) undergoes β -fluoride elimination to form CF₂CH₂. These results provide direct new fundamental insight into Fischer-Tropsch synthesis.

Chemistry of carboxylates on TiO₂. In collaboration with scientists at Pacific Northwest National Laboratory, the thermal and photochemical properties of trimethyl acetate (TMA) on TiO₂(110) have been examined.¹¹⁻¹³ Deprotonation occurs at or below 300 K to form trimethyl acetate, (CH₃)₃CCOO⁻, is bound to exposed Ti⁴⁺ cations, and

OH^- involves a bridging oxygen atom of the substrate. On the basis of temperature-programmed desorption and isothermal reaction mass spectrometry, the desorbing products include $(\text{CH}_3)_3\text{CCOOH}$, isobutene ($i\text{-C}_4\text{H}_8$), carbon monoxide, and water. Much of the $(\text{CH}_3)_3\text{CCOO}^-$ is relatively stable and decomposes to release mainly carbon monoxide and isobutene above 550 K with a maximum rate at 660 K. Thermal desorption to 750 K leaves a carbon-free surface that is indistinguishable from the initially clean surface. During dosing at 550 K, a steady-state reaction condition is realized with about half the adsorption sites being occupied at any instant.

The behavior of H_2O on clean and trimethyl acetate (TMA)-covered $-(1 \times 1)$, prepared with or without oxygen vacancies and associated Ti^{3+} , reveals the hydrophilic nature of clean surfaces and the hydrophobic nature of TMA-covered surfaces. UV irradiation of a hydrophobic surface in the presence of 10^{-6} Torr of O_2 removes TMA and rapidly restores hydrophilicity. The presence of oxygen atom vacancies does not detectably alter the hydrophilicity of either clean or TMA-covered $\text{TiO}_2(110)$.

Metal nanoparticle synthesis. As a strategy for synthesizing metal nanoparticles, thermally evaporated Ag was deposited onto a thin (~ 1.2 nm) crystalline ice layer on an inert oxide substrate--hafnia (HfO_2) at 100 K.⁸ The Ag atoms penetrate into the ice matrix but do not reach the underlying HfO_2 substrate. After controlled thermal desorption of water by heating to 300 K, atomic force microscopy reveals Ag particle formation. Figure 1 illustrates for one set of preparation conditions.

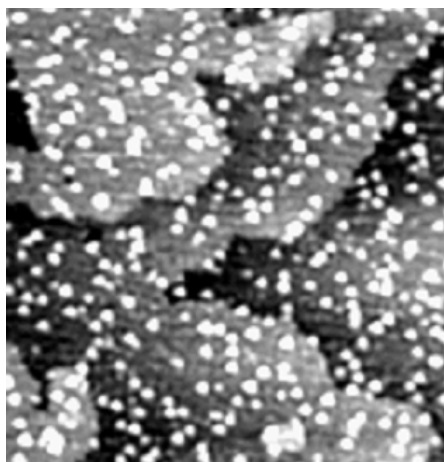


Figure 1. 200 x 200 nm image of Ag nanoclusters on a $\text{TiO}_2(110)$ surface. The sample was prepared by dosing 0.2 ML (effective) on solid water film (~ 10 ML thick). Water and Ag were deposited on 100 K surface. Water was then desorbed by warming to 300 K.

Instrumentation. As an integral part of this project, we have made improvements to standard UHV surface analysis tools that allow *in-situ* elevated temperature real time analysis of insulator substrates. For real-time analysis during thermal annealing, a continuous wave CO_2 infrared laser was coupled to a surface analysis system equipped

for x-ray photoelectron spectroscopy (XPS) and ion scattering spectroscopy (ISS).⁶ The laser beam was directed into the vacuum chamber through a ZnSe window to the back side of the sample. With 10 W laser output, the sample temperature reached 563 K. The chamber remained below 10^{-8} Torr during annealing and allowed XPS and ISS data to be gathered as a function of time at selected temperatures. As a test example, real time Cu₂O reduction at 563 K was investigated.

Future plans.

Ir nanoclusters. Motivated to develop the basic science of catalytically activating C-H and C-halogen bonds at the surfaces of metal nanoclusters, we plan to prepare surfaces comprising size-selected Ir nanoclusters, some involving other metals, supported on planar oxide supports; to characterize the surfaces structurally using scanning tunneling microscopy; and to study the chemical properties of the supported clusters employing molecular beam reactive scattering techniques, complemented, as needed, by electron microscopy and standard surface science spectroscopies.

DOE Interest

Controlled deposition and characterization of metal nanoclusters are central issues in developing the basic science of highly selective catalytic systems that involve C-H and C-X bond activation.

Publications (2002-3)

1. W.P. Fitts, J.M. White and G. E. Poirier, "Thermodynamics of Decanethiol Adsorption on Au (111): Extension to 0°," *Langmuir*, **18**(6), (2002) 2096-2102.
2. W.P. Fitts, J.M. White and G.E. Poirier, "Low coverage decanethiolate structure on Au(111): Substrate effects," *Langmuir*, **18**(5), (2002) 1561-1566.
3. Ilkeun Lee, S. K. Kim, Wei Zhao, and J. M. White, "Electron-induced dissociation of *tert*-butyl nitrite adsorbed on Ag(111)," *Surface Sci.*, **499** (2002) 53-62.
4. W.X. Huang and J.M. White, "Propene Adsorption on Ag(111): a TPD and RAIRS Study," *Surf. Sci.*, **513** (2002) 399-404.
5. W.X. Huang and J.M. White, "Propene Oxidation on Ag(111): Spectroscopic Evidence of Facile Abstraction of Methyl Hydrogen," *Catal. Lett.*, **84** (2002) 143.
6. Q. Wang, Y.-M. Sun, W. Zhao, J. Campagna and J.M. White, "In-situ Laser Annealing System for Real Time Surface Kinetic Analysis," *Rev. Sci. Instr.*, **73** (2002) 3916.
7. W.X. Huang and J.M. White, "Transition from π -bonded to di- σ metallacyclic

propene on O-modified Ag(111) *Langmuir*, **18**(25), (2002) 9622-9624.

8. X.-M. Yan, J. Ni, M. Robbins, H. Park, W. Zhao and J.M.White, "Silver nanoparticles synthesized by vapor deposition onto an ice matrix", *Journal of Nanoparticle Research* **4**(6), (2002) 525-533.

9. W.X. Huang, J.M. White, "Revisiting NO₂ on Ag(111): a detailed TPD and RAIRS study", *Surface Science*, **529** (2003) 455-470.

10. W.X. Huang and J. M. White, "Direct Spectroscopic Evidence of the Cross-Coupling Reaction between CH₂(a) and CF₃(a) on Ag(111)", *J. Am. Chem. Soc.*, **125**(36), (2003) 10798-10799.

11. White. J.M., Szanyi, J., and Henderson, M.A., "The Photo-Driven Hydrophilicity of Titania: A Model Study Using TiO₂(110) and Adsorbed Trimethyl Acetate", *J. Phys. Chem. B.*, **107** (2003) 9029-9033.

12. Henderson, M., White, J., Uetsuka, H., Onishi, H., "Photochemical Charge Transfer and Trapping at the Interface Between an Organic Adlayer and an Oxide Semiconductor", *J. Am. Chem. Soc.*, **125** (2003) 14974-14975.

This page intentionally left blank.

Catalysis on the Nanoscale: Preparation, Characterization and Reactivity of Metal-Based Nanostructures

Postdocs: Cai, T., Liu, P., Kim, Y., Potapenko, D., Wang, X.

Students: Horn, J., Mann, H., Lightstone, J.

Collaborators: Beuhler, R., Hanson, J., Rodriguez, J., Sears, T.

Department of Chemistry, Brookhaven national Laboratory, Upton, NY 11973

hrbek@bnl.gov, muckerma@bnl.gov, mgwhite@bnl.gov

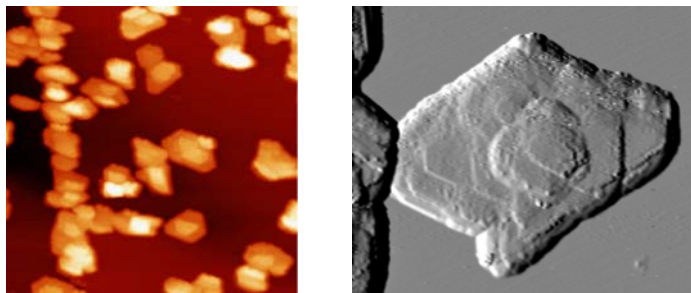
Goal

Explore and manipulate the size, morphology and chemical environment of metal-containing nanoparticles with the goal of modifying their reactivity.

Recent Progress

Model Ru/C catalyst for ammonia synthesis: New-generation ammonia-synthesis Ru catalysts are more active at lower temperatures and pressures than iron-based catalysts used worldwide in this large-scale industrial process. Industrial Ru catalysts are synthesized using a carbonyl precursor and oxide, nitride or graphite substrates. To prepare a model Ru catalyst, we have grown Ru particles using chemical vapor deposition of $\text{Ru}_3(\text{CO})_{12}$ as a precursor on a highly oriented pyrolytic graphite (HOPG) surface. HOPG has been modified with one-atomic-layer-deep holes mimicking an activated carbon support by mild sputtering and oxidation in air. At low Ru surface concentrations, the Ru particles (~ 2 nm) have a round shape, while at higher Ru surface concentrations, the Ru forms flat layered crystallites (~ 3 nm high and ~ 40 nm wide) with the (0001) facet parallel to the graphite surface (see Figure).

A reactivity study of a model Ru/C catalyst was carried out to advance the understanding of this structure sensitive reaction where dinitrogen dissociation is the rate-limiting step. The N_2 desorption maximum occurs at ~ 650 K for the small particles and 500 K for the larger crystallites. The higher temperature desorption has its origin at opened Ru surfaces which dominate the small round particles; the lower temperature desorption comes from terraces of the Ru(0001) surface, which



Crystalline Ru nanoparticles on HOPG (200 nm x 200 nm) [left]; morphology of a single Ru nanoparticle (73 nm x 50 nm) [right].

are predominant for the large flat crystallites. The initial sticking coefficient for N₂ dissociative adsorption on the Ru/HOPG model catalyst is 1×10^{-7} , ~4-5 orders of magnitude larger than Ru single crystal surfaces.

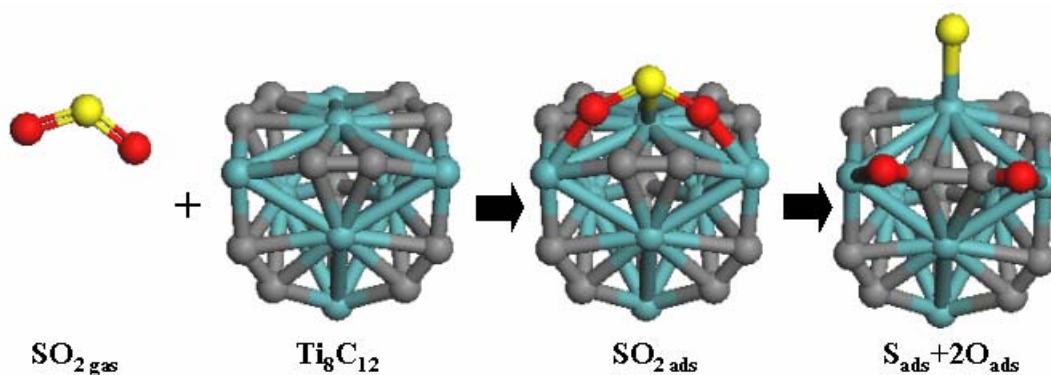
Activation of gold nanoparticles on oxide surfaces: Gold nanoparticles deposited on metal oxides display an unexpected high reactivity. A priori, it is not clear if this phenomenon is a consequence of the size of the nanoparticles or the result of interactions with the oxide support. To address this issue we examined and compared the destruction of SO₂ on Au/Ti(110) and Au/MgO(100) surfaces. Synchrotron-based high-resolution photoemission and first-principles density-functional slab calculations were used in the studies. We found that the dissociation of SO₂ on Au/MgO(100) is very limited due to weak Au↔MgO interactions. On the other hand, the deposition of Au nanoparticles on TiO₂(110) produces a system with an extraordinary ability to adsorb and dissociate SO₂. Neither MgO(100) nor TiO₂(110) are able to dissociate SO₂ on their own. On both oxide supports, the largest activity for the full dissociation of SO₂ is found in systems that contain Au coverages smaller than 1 ML when the size of the Au nanoparticles is below 5 nm. The data clearly show how important can be the effects of the oxide support for the activation of Au nanoparticles.

M_mX_x nanoparticle formation and deposition: Our recent laser ablation studies on the Mo_nX_m (X= C, N, S) clusters suggest that gas-phase cluster methods can generate an extensive array of transition metal compounds with a wide range of particle size, stoichiometry and structure. Our ultimate goal is to use such a source to deposit mass-selected nanoparticles onto a substrate, e.g., graphite or TiO₂, and thereby prepare a model catalyst system whose particle size distribution is precisely known. Much of the effort this year has been spent on constructing a deposition apparatus and characterizing the magnetron sputtering cluster source which will be used in place of laser ablation in the first generation instrument. Using a high-mass quadupole spectrometer, we have demonstrated the ability to form a wide range of bare metal, metal carbide and metal sulfide cluster ions with resolvable masses up to 10,000 amu, e.g., Mo₁₀₅. Transition metals studied include Ti, V, Zr, Nb and Mo. Of significant interest is the observation of “magic number” Metcar clusters (M₈C₁₂, M≡Ti, Zr) as well the observation of nearly stoichiometric niobium carbide nanocrystallites, e.g., Nb₁₄C₁₃. For molybdenum, a “magic number” sulfide cluster, Mo₃S₉, was also observed. The Mo₃S₉ cluster has been implicated as a structural unit in amorphous phase of molybdenum sulfide which is particularly active for desulfurization. Future work will focus on the deposition of size-selected clusters onto well-defined substrates under UHV conditions for characterization by thermal desorption and photoemission.

Theoretical studies of the structure and properties of M₈C₁₂ metallocarbohedrenes (metcars): We have extensively studied the geometric and electronic structure of the “metallocarbohedrenes” (metcars) Ti₈C₁₂ and Mo₈C₁₂ using fully *ab initio* and density functional methods. We were particularly interested in how these systems might serve as model heterogeneous nanocatalysts with precisely defined size and active sites. We examined these issues through calculations employing a hierarchy of levels of theory and the correlation of the molecular orbitals as the symmetry of the cluster is systematically reduced.

Our most important discovery in these calculations was that it required the highest levels of theory to identify the correct electronic ground state (1A_1), symmetry group in its equilibrium geometry (D_{2d}) and principal orbital configuration of the Ti_8C_{12} metcar. The structure consists of an outer tetrahedron of Ti atoms (formal oxidation state “+1”) connected by C_2 units, and a smaller inverted tetrahedron of Ti atoms (formal oxidation state “+2”) bound directly to each other and with each of them η^2 -bonded to three of the C_2 units comprising the outer tetrahedron.

Density functional theory was also employed to study the interaction of SO_2 with the Ti_8C_{12} and Mo_8C_{12} metcars. The S – O bonds of SO_2 spontaneously break on Ti_8C_{12} ($\Delta E \approx 3.8$ eV) and Mo_8C_{12} ($\Delta E \approx 2.9$ eV). The products of the decomposition reaction (S, O) interact simultaneously with metal and C sites. The C atoms are not simple spectators and they play an important role in the energetics for the dissociation of SO_2 . The theoretical calculations indicate that the metcars are more reactive towards small molecules (CO , NH_3 , H_2O and SO_2) than $TiC(001)$ and $MoC(001)$ surfaces. The particular geometry of the metcar attenuates the ligand effects of C on Ti and Mo.



Dissociation of SO_2 on a Ti_8C_{12} metcar. Ti atoms are shown as blue spheres, while gray spheres represent C atoms.

Future Plans

Future work will focus on nanostructured carbides, nitrides and sulfides of the Group 4-6 transition metals (*e.g.*, Ti, V, Nb, Mo, Zr), which have been observed to exhibit catalytically active bulk surfaces and/or unique gas-phase cluster structures. Such materials may offer advantages over supported noble metal catalysts in terms of selectivity and resistance to poisoning and sintering. A major objective is to understand how nanoparticle size, support and alloy formation effect the electronic environment of the metal active sites and their chemical reactivity.

DOE Interest

Understanding how to modify the metal active site through manipulation of nanostructured materials can provide a basis for development of new catalytic materials.

Publications 2002-2003

1. Z. Chang, Z. Song, G. Liu, J. A. Rodriguez, J. Hrbek, *Synthesis, Electronic and Chemical Properties of MoO_x Clusters on Au(111)*, *Surface Science* **512**, L353 (2002).
2. K. Kobayashi, G. E. Hall, J. T. Muckerman, T. J. Sears, A. J. Merer, *The E³Π - X³Δ Transition of Jet-Cooled TiO Observed in Absorption*, *J. Molec. Spectroscopy* **212**, 133 (2002).
3. J. A. Rodriguez, G. Liu, T. Jirsak, J. Hrbek, Z. Chang, J. Dvorak, A. Maiti, *Activation of Gold on Titania: Adsorption and Reaction of SO₂ on Au/TiO₂(110)*, *J. Am. Chem. Soc.* **124**, 5242 (2002).
4. T. Cai, Z. Song, Z. Chang, G. Liu, J. A. Rodriguez, J. Hrbek, *Ru Nanoclusters Prepared by Ru₃(CO)₁₂ Deposition on Au(111)*, *Surf. Sci.* **538**, 76 (2003).
5. H. Hou, J. T. Muckerman, P. Liu, J. A. Rodriguez, *A Computational Study of the Geometry and Properties of the Metcars Ti₈C₁₂ and Mo₈C₁₂*, *J. Phys. Chem. A* **107**, 9344 (2003).
6. J. M. Lightstone, H. Mann, M. Wu, P. M. Johnson, M. G. White, *Gas-Phase Production of Molybdenum Carbide, Nitride and Sulfide Clusters and Nanocrystallites*, *J. Phys. Chem.* **107**, 10359 (2003).
7. P. Liu, J. A. Rodriguez, *Interaction of Sulfur Dioxide with Titanium-Carbide Nanoparticles and Surfaces: A Density Functional Study*, *J. Chem. Phys.* **119**, 10895 (2003).
8. P. Liu, J. A. Rodriguez, H. Hou, J. T. Muckerman, *Chemical Reactivity of Metcar Ti₈C₁₂, Nanocrystal Ti₁₄C₁₃ and A Bulk TiC(001) Surface: A Density Functional Study*, *J. Chem. Phys.* **118**, 7737 (2003).
9. P. Liu, J. A. Rodriguez, J. T. Muckerman, J. Hrbek, *Interaction of CO, O and S with Metal Nanoparticles on Au(111): A Theoretical Study*, *Phys. Rev. B* **67**, 155416 (2003).
10. P. Liu, J. A. Rodriguez, J. T. Muckerman, J. Hrbek, *The Deposition of Mo Nanoparticles on Au(111) from a Mo(CO)₆ Precursor: Effects of CO on Mo-Au Intermixing*, *Surf. Sci.* **530**, L313 (2003).
11. A. Maiti, J. A. Rodriguez, M. Law, P. Kung, J. R. McKinney, P. Yang, *SnO₂ Nanoribbons as NO₂ Sensors: Insights from First-principles Calculations*, *Nanoletters* **3**, 1025 (2003).
12. J. A. Rodriguez, X. Wang, J. C. Hanson, G. Liu, A. Iglesias-Juez, M. Fernandez-Garcia, *The Behavior of Mixed-Metal Oxides: Structural and Electronic Properties of Ce_{1-x}Ca_xO₂ and Ce_{1-x}Ca_xO_{2-x}*, *Journal of Chemical Physics* **119**, 5659 (2003).
13. J. A. Rodriguez, M. Perez, T. Jirsak, J. Evans, J. Hrbek, L. Gonzalez, *Activation of Au Nanoparticles on Oxide Surfaces: Reaction of SO₂ with Au/MgO(100)*, *Chem. Phys. Lett.* **378**, 526 (2003).
14. J. A. Rodriguez, J. C. Hanson, J.-Y. Kim, G. Liu, A. Iglesias-Juez, M. Fernandez-Garcia, *Properties of CeO₂ and Ce_{1-x}Zr_xO₂ Nanoparticles: XANES, Density Functional, and Time-Resolved XRD Studies*, *Journal of Physical Chemistry B* **107**, 3535 (2003).

15. Z. Song, T. Cai, Z. Chang, G. Liu, J. A. Rodriguez, J. Hrbek, *Molecular Level Study of the Formation and the Spread of MoO₃ on Au(111) by STM and XPS*, J. Am. Chem. Soc. **125**, 8059 (2003).
16. Z. Song, T. Cai, J. A. Rodriguez, J. Hrbek, A. S. Y. Chan, C. M. Friend, *A Novel Growth Mode of Mo on Au(111) from a Mo(CO)₆ Precursor: An STM Study*, J. Phys. Chem. B **107**, 1036 (2003).
17. J. X. Wang, S. R. Brankovic, Y. Zhu, J. C. Hanson, R. R. Adzic, *Kinetic Characterization of PtRu Fuel Cell Anode Catalysts Made by Spontaneous Pt Deposition on Ru Nanoparticles*, J. Electrochem. Soc. **150**, A1108 (2003).
18. D. Mahajan, C. L. Marshall, N. Castagnola, J. C. Hanson, *Sono Synthesis and Characterization of Nanophase Molybdenum-Based Materials for Catalytic Hydrodesulfurization*, Applied Catalysis A **258**, 83 (2004).
19. P. Liu, J. A. Rodriguez, *Effects of Carbon on the Stability and Chemical Performance of Transition Metal Carbides: A Density Functional Study*, J. Chem. Phys. (in press).
20. J. A. Rodriguez, *Activation of Gold on Nanoparticles on Titania: A Novel Desox Catalyst*, (in press).
21. J. A. Rodriguez, *Gold Nanoparticles on Titania: Activation and Behavior* in *Dekker Encyclopedia of Nanoscience*, Dekker Publishing (in press).

This page intentionally left blank.

Chemical Transformation Mechanisms

Principal Investigators: K. A. Carrado, G. Sandi, N. A. Tomczyk

Postdocs: N. Castagnola

Graduate Students: R. Fernandez-Saavedra, R. Kizilel

Collaborators: R. Cook, L. Curtiss, J. Hessler, R. Klingler, C. Marshall, J. Rathke, E. Ruiz-Hitzky, S. Seifert, C. Song, P. Stair, S. Vajda

Chemistry Division, Argonne National Laboratory, Argonne, IL 60439

rewinans@anl.gov

Goal

The three programs described here seek to elucidate mechanisms pertinent to both the synthesis and deactivation of catalysts. The chemistry of synthetic clays is being studied to understand how a particular heterogeneous nanoporous catalyst is formed, and to exploit this knowledge for tailoring the characteristics of the catalytic material. Mechanisms of the formation of aromatic precursors that can lead to carbonaceous deposits on acidic catalysts, on nano-sized metal clusters on surfaces, and on metal nanoparticles within synthetic clays are being explored.

Recent Progress

The first subtask has been an on-going program in DOE for several years, whereas the second and third are new programs this year. As a result, the first subtask has had significant progress whereas the second and third subtasks have only preliminary data at this time.

Fundamental Studies of the Design of Nanoporous Silicate Catalysts. Several new mesostructured synthetic clay (MSC) materials were prepared and evaluated for their potential use as catalysts. Textural porosity was determined as a vital parameter to understand for catalytic, as well as for polyelectrolyte, applications. It was found previously that using a silica sol creates a MSC with high surface area morphological features (textural porosity), whereas use of other silicon sources creates a more traditional layered clay catalyst that is not as active. After extensive characterization, it was determined that the unique features of the MSCs, including especially their thermally stable mesoporosity, would lend themselves to selective catalysis. One area where selectivity could be crucial is the efficient hydrodesulfurization (HDS) of low-quality hydrocarbon feedstocks. In order to make strides towards this goal, we have begun with model compound studies.

New MSCs were prepared as a function of the size, pH, and counterion (and therefore the surface chemistry) of various silica sol precursors. XRD showed slight differences in crystallinity, surface areas ranged from 195-293 m²/g with either H2 or H3 hysteresis loops, pore volumes varied from 0.31-0.49 cc/g, and TEM showed sol particle sizes slightly different in some cases from values provided by the manufacturer. For HDS, the conversion of dibenzothiophene (DBT) to biphenyl was examined using Co/Mo/S-loaded MSC supports. The catalysis was accomplished in collaboration with C. Marshall of the Chemical Engineering Division at ANL. The most active clay was derived from silica sol AS30, with an activity of 65% DBT conversion (vs. 86% for a commercial alumina catalyst). This sol has a nominal particle diameter of 22 nm and it

yields the highest observed synthetic clay pore volume at 0.49 cc/g, which may be related to the high activity.

For deep HDS activity, the conversion of 4,6-dimethyldibenzothiophene (DMDBT) was tested in collaboration with C. Song at Pennsylvania State University. A commercial catalyst displays 11.4% conversion. This value is nearly attained (10.5%) for the Co/Mo/S-loaded mesostructured clay derived from AM30 silica sol. A Co/Mo/S clay catalyst made from laponite, a hectorite clay of typical platelet morphology, has very low activity (3.0%), indicating that the unique morphology of the mesostructured clays is important. Contrary to the HDS data above, the most active deep HDS catalyst is derived from AM30 silica sol, which has a 12 nm size and yields a synthetic clay with the lowest pore volume observed (0.31 cc/g). Deep HDS data nearly as good were obtained with the AS30 sol described above, with DMDBT conversion at 9.5%. The one feature that clays from both AS30 and AM30 sols share is an H3 N₂ isotherm hysteresis loop, whereas the rest have H2 loops. The importance of this textural porosity feature to catalytic activity will be examined in future studies.

The sol of smallest particle size (7 nm, SM30) showed poor results in both HDS tests, although we had expected that the smaller size would allow more dissolution and perhaps more incorporation into the matrix. Upon close examination of the x-ray powder diffraction (XRD) results, it appears that the most crystalline clays are AM30, AS30, and HS30, which are also the most active. The materials were also provided to G. Sandi for testing as polymer-clay nanocomposite membranes for lithium ion transport in secondary batteries.

Aromatic Molecule Formation Mechanisms on Homogeneous and Heterogeneous Acidic Catalysts: New proposal.

Aromatic Formation Mechanisms on Metal Nanoclusters: New proposal.

DOE Interests

The chemistry of synthetic clays is being studied to understand how a particular heterogeneous nanoporous catalyst is formed, and to exploit this knowledge for tailoring the characteristics of the catalytic material. In terms of catalyst deactivation processes, the formation of polycyclic aromatic compounds is a key step. Our studies probe both homogeneous and heterogeneous catalysts, initially polyphosphoric acid and zeolites, which are active for such transformations as methanol to hydrocarbons. This will provide detailed information regarding mechanisms of reaction for a specific substrate initially; however, these methods are applicable to a number of mechanistic problems in catalysis.

Future Plans

Fundamental Studies of the Design of Nanoporous Silicate Catalysts. We have had enormous success in the past exploiting solid-state ²⁹Si and ¹³C NMR to examine formation of the synthetic clay catalysts. We will again make use of these methods to probe the crystallinity of the various silica sol samples made for HDS and compare the results with those from XRD. The issue to determine is why certain silica sols foster greater crystallinity in the clay catalysts. Another important question to address is whether the absence of silica impurity hastens or otherwise affects the clay crystallization mechanism and subsequent porosity and catalytic behavior. A complete understanding of such mechanisms leads to better catalyst design. In situ SAXS experiments using a new flow cell are underway in order to aid in this understanding.

We will exploit our prior knowledge gained from mechanistic determinations to synthetic clays that contain a catalytically active metal component. Bifunctional catalysts contain both an acidic component (typically for hydrocarbon cracking) and a metal

component. We will probe the mechanism of formation of clay catalysts, including metal-lattice substituted materials and nanocomposites created with small metal and metal oxide particles, via NMR, in situ time-resolved small angle X-ray scattering (SAXS), anomalous SAXS, microscopy, and other techniques. A comparison of the clay catalysts after a catalytic reaction will then be made in order to assist in understanding the role of the metal nanoclusters in the particular catalytic reaction.

Organosilanes are of special interest because of their now demonstrated ability to be incorporated into the framework of clay as it is crystallizing. One natural extension of this process for us to study is the simultaneous incorporation of templating molecules such as polymers, and their effect on porosity or network structures. We will also compare and contrast the mechanism of formation of organo-grafted clays with silane-derived hectorite and silica sol-derived hectorite.

Aromatic Molecule Formation Mechanisms on Homogeneous and Heterogeneous Acidic Catalysts. This program has four main objectives: (1) to elucidate the mechanisms of aromatic hydrocarbon formation that are often the first step in catalyst deactivation in important industrial processes (2) to probe the aromatic species formed in both heterogeneous and homogeneous acidic catalysis of methanol to hydrocarbons (3) to develop an approach for studying the mechanisms of catalyst deactivation that will be applicable to other important systems and (4) to advance the use of in situ methods (including UV-Raman, NMR and SAXS) for these pioneering studies. Initially, the methanol to hydrocarbon reaction in polyphosphoric acid solution and on acidic zeolites will be compared and contrasted. The approach will take information defined on the homogeneous system and compare and contrast it with comparable experimental and computational data measured on the heterogeneous systems. Note that this approach does not presume that the two systems have much in common; it simply makes use of the homogeneous system as a definable and logical basis for comparison of results and a reasonable preliminary guide to experimentation on the heterogeneous process. In this approach, how the systems differ from each other is as important as features they might have in common.

Aromatic Formation Mechanisms on Metal Nanoclusters. This program encompasses several primary objectives: (1) to elucidate mechanisms of aromatic formation on metal catalysts in deactivation reactions involving olefins (2) to study nano-sized metal catalytic clusters from micelle directed synthesis in terms of formation and reactivity (3) to elucidate the mechanisms of deactivation of well-defined metal clusters supported on acidic surfaces (4) to study the deactivation of metal nanoparticles on polymer-clay nanocomposite membranes, and (5) to bridge the gap between homogeneous and heterogeneous catalysis in terms of synthesis and functionality. Initially, the metal of choice for all of these studies will be Pt(0) and propene will be the carbon source. Techniques including TEM, NMR, SAXS, and GISAXS will be used to follow the preparation of the clusters and to characterize them prior to the reactivity studies. These methods, plus Raman spectroscopy and *ex situ* MS, will be used to elucidate the mechanism of aromatic formation on the catalyst.

Publications (2002-2004)

1. K. A. Carrado, Introduction: clay structure, surface acidity and catalysis, in *Handbook of Layered Materials for Catalytic Applications*, S. M. Auerbach, K. A. Carrado, P. K. Dutta, Eds.; Marcel-Dekker: NY, 2004, in press.
2. *Handbook of Layered Materials Science & Technology*, S. M. Auerbach, K. A. Carrado, P. K. Dutta, Eds.; Marcel-Dekker: NY, 2004, in press.

3. K. A. Carrado, A. Decarreau, F. Bergaya, G. Lagaly, Synthetic clay minerals and purification of natural clays, in *Handbook of Clay Science*, F. Bergaya, B.K.G. Theng, G. Lagaly, Eds., Elsevier: Amsterdam, in press.
4. *Handbook of Zeolite Science and Technology*, S. M. Auerbach, K. A. Carrado, P. K. Dutta, Eds.; Marcel-Dekker: NY, 2003.
5. G. Sandi, H. Joachin, R. Kizilel, S. Seifert, K. A. Carrado, In situ SAXS studies of the structural changes of polymer nanocomposites used in battery applications, *Chem. Mater.*, 2003, *15*, 838.
6. L. J. Smith, J.-M. Zanotti, G. Sandi, K.A. Carrado, P. Porion, A. Delville, D. L. Price, M. L. Saboungi, Characterization of polymer clay nanocomposite electrolyte motions via combined NMR and neutron scattering studies, *Solid-State Ionics—2002*, Eds: P. Knauth, J-M. Tarascon, E. Traversa, H.L. Tuller (MRS Symp. Proc., Vol. 756), 2003, 339.
7. G. Sandi, K. A. Carrado, H. Joachin, W. Lu, J. Prakash, Polymer nanocomposites for lithium battery applications, *Journal of Power Sources*, 2003, *119-121C*, 492.
8. S. R. Segal, K. A. Carrado, C. L. Marshall, K. B. Anderson, Catalytic decomposition of alcohols, including ethanol, for in situ hydrogen generation in a fuel stream using a layered double hydroxide-derived catalyst, *Appl. Catal. A: Gen.*, 2003, *248*, 33.
9. G. Sandi, H. Yang, H. Joachin, K. A. Carrado, R. E. Winans, J. Prakash, Determination of the hydrogen storage capacity of novel sepiolite-derived carbonaceous materials, *J. New Mater. Electrochem. Syst.*, 2003, *6*, 169.
10. T. Kupka, B. Ruscic, and R. E. Botto, Hartree-Fock and density functional complete basis-set (CBS) predicted nuclear shielding anisotropy and shielding tensor components, *Solid State Nucl. Magn. Reson.*, 2003, *23*, 145.
11. D. M. Gregory and R. E. Botto, Pore structure and sorption properties of silica aerogels studied by magnetic resonance imaging and pulsed-field gradient spectroscopy, *Appl. Spectroscopy*, 2003, *57*, 245.
12. F. Kenig, D.-J. H. Simons, D. Crich, J. P. Cowen, G. T. Ventura, T. Rehbein-Khalily, T. C. Brown, K. B. Anderson, Branched aliphatic alkanes with quaternary substituted carbon atoms in modern and ancient geologic samples, *Proc. Natl. Acad. Sci.*, 2003, *100*, 12554.
13. Tanaka, R.; Hunt, J. E.; Winans, R. E.; Thiyagarajan, P.; Sato, S.; Takanohashi, T. Aggregates structure analysis of petroleum asphaltene with small-angle neutron scattering, *Energy & Fuels*, 2003, *17*, 127.
14. J. P. Hessler, R. E. Winans, S. Seifert, Spatially resolved small-angle X-ray scattering studies of soot inception and growth, *Proc. Combustion Institute*, 2002, *29*, 2743.
15. G. Sandi, R. E. Winans, S. Seifert, K. A. Carrado, In situ SAXS studies of the structural changes of sepiolite clay and sepiolite-carbon composites with temperature, *Chem. Mater.*, 2002, *14*, 739.
16. S. R. Segal, K. B. Anderson, K. A. Carrado, C. L. Marshall, Low temperature steam reforming of methanol over layered double hydroxide-derived catalysts, *Appl. Catal. A: Gen.*, 2002, *231*, 215.
17. K. A. Carrado, R. Csencsits, P. Thiyagarajan, S. Seifert, S. M. Macha, J. S. Harwood, Crystallization and textural porosity of synthetic clay minerals, *J. Mater. Chem.*, 2002, *12*, 3228.
18. Calo, J. M.; Hall, P. J.; Houtmann, S.; Lozano-Castello, D.; Winans, R. E.; Seifert, S. "Real time" determination of porosity development in carbons: A combined SAXS/TGA approach. *Stud. Surf. Sci. Catal.*, 2002, *144*(Characterization of Porous Solids VI), 59.

Surface Bonding of Molecules, Their Reaction and Confinement Effects in the Chemisorbed Layer

Postdocs: Lee, Junseok

Students: Zubkov, Tykhon; Morgan, Gregg; Lee, Jae-Gook

Department of Chemistry, Surface Science Center, University of Pittsburgh, Pittsburgh, PA 15260; jyates@pitt.edu

Goal

To understand the role of surface defects on the reactive chemistry of chemisorbed molecules of interest in heterogeneous catalysis.

Recent Progress

A. Adsorption and Dissociation of CO on the Atomic Step Sites on Ru(109).

Metallic Ru surfaces are known to effectively catalyze the production of linear alkanes from CO and H₂ in the Fischer-Tropsch reaction [1,2]. It is very likely that the first step of this process is the dissociation of the CO bond in chemisorbed CO. We have studied the Ru(109) single crystal surface using reflection IR, temperature programmed desorption, isotopic mixing, and low energy electron diffraction methods with a special aim to evaluate the role of the atomic step sites which this crystal presents.

The Ru(109) surface formally possesses single atomic height step edges separating Ru(001) terraces of 5 Ru atom width. Our LEED investigations have shown that step doubling in fact occurs, yielding double atom-height step sites separated by 10 atom-wide terrace sites [3]. Figure 1 shows a portion of the LEED pattern, generated by stacking LEED

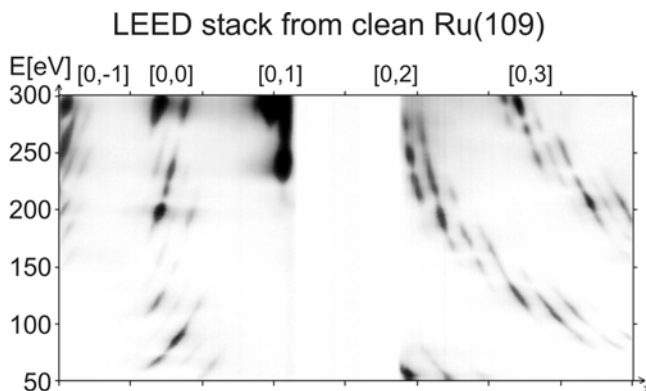


Figure 1. LEED Stack Measurement of the Ru(109) Surface. The [0,0] beams are identified by the lack of horizontal displacement as the electron energy is changed.

measurements at different primary electron beam energies. These measurements are compared with dynamical simulations of the LEED patterns for both single atom-height step sites and for double atom-height step sites, shown in Figures 2 and 3.

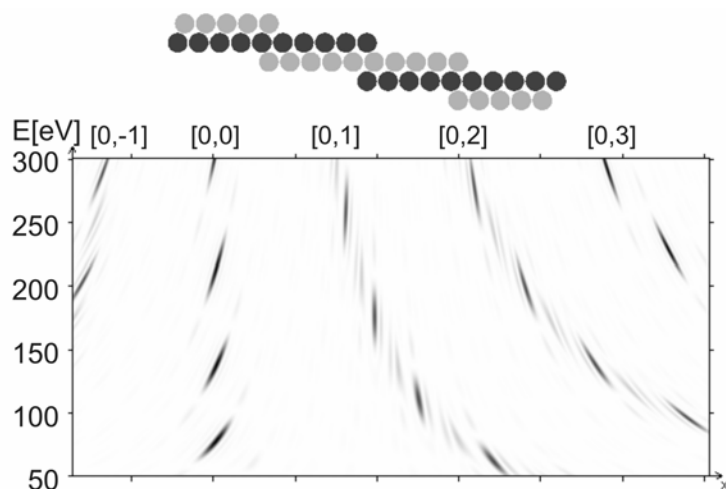
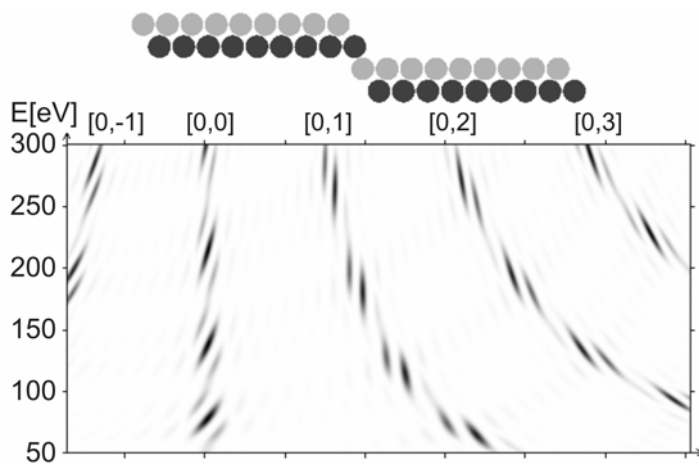


Figure 2. Kinematic LEED Simulations of the Ru(109) Surface with Single-Height Steps as Shown.

Figure 3. Kinematic LEED Simulation for Ru(109) Surface with Double-Height Steps as Shown. Comparison with the experiment in Figure 1 strongly favors the double height step geometry for the Ru(109) surface.



A model of the stepped Ru(109) surface is shown in Figure 4. The orientation of the trigonally-arranged step atoms is $\langle 101 \rangle$.

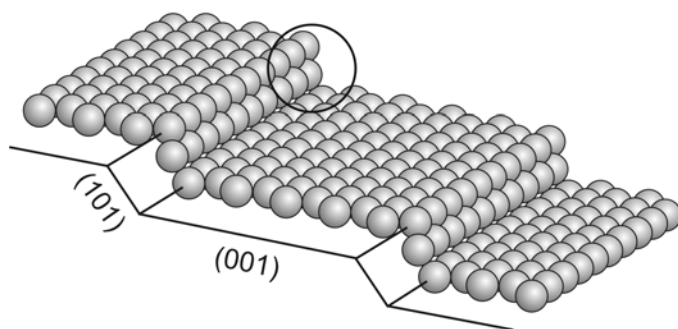


Figure 4. Structure of the Ru(109) Surface

The kinetics of adsorption of CO on the Ru(109) surface has been studied using the collimated and absolutely calibrated capillary array doser, and the results

are shown in Figure 5. At 88 K, an initial sticking coefficient of unity is measured, and most importantly, the sticking coefficient remains above 0.9 for the main range of adsorption. This behavior suggests that adsorption occurs via a mobile precursor mechanism up to near saturation coverage of 0.5 CO/Ru.

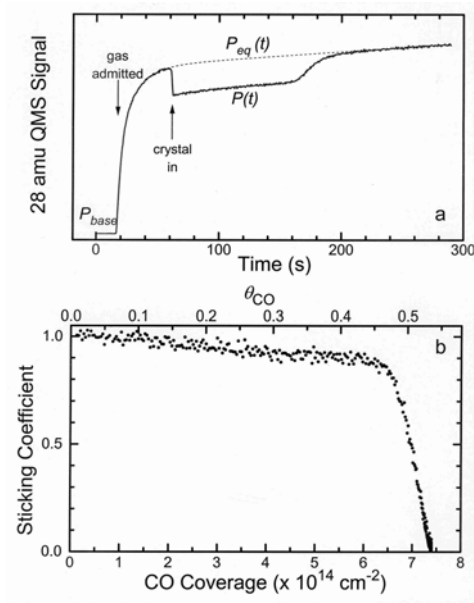


Figure 5. Uptake Curve for CO Adsorption on Ru(109) and Sticking Coefficient Derived from the Uptake Curve.

The reflection IR spectral developments during CO adsorption are shown in Figure 6. A C-O stretching mode, initially observed at 1973 cm^{-1} intensifies and shifts to higher wavenumber. There is an uncanny resemblance between this family of infrared spectra and those obtained on the flat Ru(001) crystal surface by others [4-6], suggesting that the 10 Ru atom wide terraces are similar to the infinitely wide Ru(001) plane in-so-far as the vibrational behavior of chemisorbed CO is concerned. One might ask why specific CO modes associated with the step sites are not seen, and we believe that these modes are invisible because of strong intensity sharing effects with the dominant CO phase on the terraces.

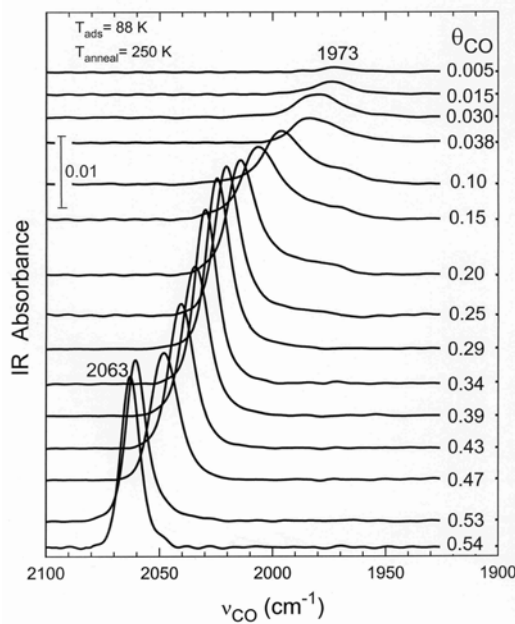


Figure 6. IR Spectral Development for $^{12}\text{C}^{16}\text{O}$ Chemisorption on Ru(109).

In contrast to the similarity between Ru(109) and Ru(001) when viewed from the infrared behavior of chemisorbed CO, the temperature programmed desorption spectra for the two surfaces differ markedly. Figure 7 shows the results for Ru(109).

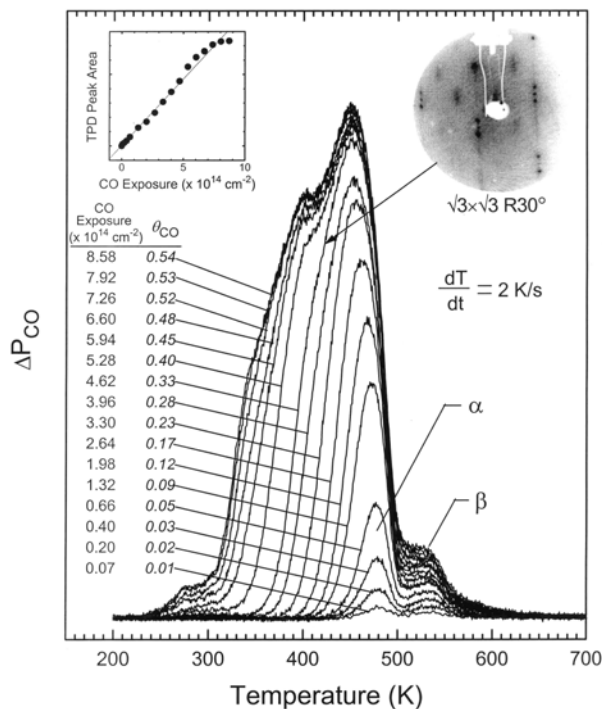


Figure 7. TPD Spectra for CO on Ru(109). The insert shows the LEED pattern obtained for 1/3 monolayer coverage on the Ru(109) terraces.

The TPD spectra reveal that a high temperature CO desorption state (β -CO) is dominant at lower CO coverages, and persists up to saturation coverage. A lower temperature state (α -CO) dominates the desorption process at higher CO coverages, and ultimately is composed of several features. The behavior in the coverage region where α -CO dominates is very different from that observed on Ru(001), where the classic studies of the Menzel group show that a CO-surface phase transition causes dramatic variations in the rate of CO desorption in the temperature range of α -CO desorption.

The unique β -CO desorption process (Figure 7) is of special interest since it is produced as a result of chemical processes at the atomic step sites on the Ru(109) surface. The β -CO state begins to desorb near 480 K; **careful studies by reflection IR indicate that at this temperature, all observable CO has disappeared from the surface, yet CO is observed to desorb in the range 485 K - ~580 K.** The β -CO desorption process is not observed on the smooth Ru(001) surface [4-6]. Thus, we infer that β -CO results from recombination of dissociated fragments of C(a) and O(a) which have been produced on the step sites. This postulate was confirmed by studies of isotopic mixing between doubly-labeled CO isotopomers, and as shown in Figure 8, isotopic mixing is indeed a process which occurs solely in the temperature range of the β -CO desorption process.

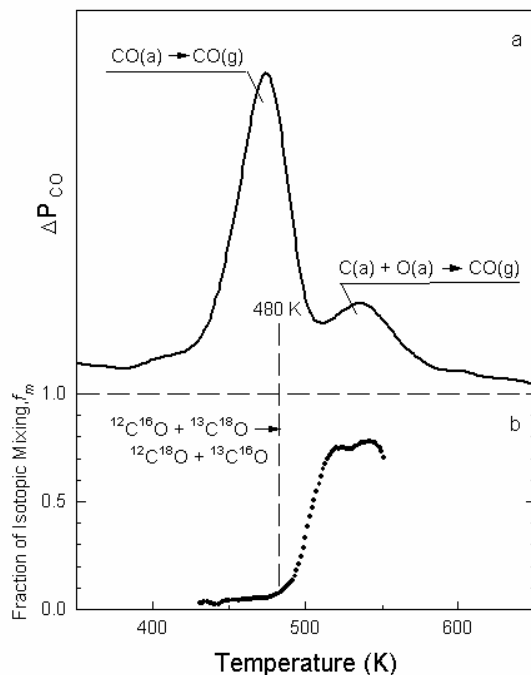


Figure 8. CO Isotopic Mixing During TPD from Ru(109).

These results suggest that the classic Fischer-Tropsch catalytic activity of Ru is a specific property of the defect sites on this element. The "nascent" carbon produced by low temperature CO dissociation on defect sites is likely to participate in reaction with hydrogen to initiate alkane synthesis. The carbon produced on the defect sites

can also recombine with oxygen atoms at very low temperatures on the surface due to the mobility of one or both of these species. These observations suggest that preparative procedures for high area Ru catalysts, which enhance the fraction of low Ru-Ru coordination at defect sites, will probably show enhanced catalytic activity in the Fischer-Tropsch reaction.

References

1. H.H. Storch, N. Golumbic and R.B. Anderson, *The Fischer-Tropsch and Related Syntheses*, John Wiley and Sons: New York: Chapman and Hall, London, 1951; pp. 309-312.
2. R.B. Anderson, *The Fischer-Tropsch Synthesis*, Academic Press, 1984; p. 110.
3. T. Zubkov, G.A. Morgan, Jr., J. T. Yates, Jr., O. Kuhlert, M. Lisowski, R. Schillinger, D. Fick, H.J. Jansch, submitted to *Surface Science*.
4. H. Pfnür, D. Menzel, F.M. Hoffmann, A. Ortega and A.M. Bradshaw, *Surf. Sci.* **93**, 431 (1980).
5. R.L. Wang, H.J. Dreuzer, P. Jacob and D. Menzel, *J. Chem. Phys.* **111**, 2115 (1995).
6. G.E. Thomas and W.H. Weinberg, *J. Chem. Phys.* **70**, 1437 (1979).
7. T. Zubkov, G. Morgan and J. T. Yates, Jr., *Chem. Phys. Lett.*, **362**, 181 (2002).

DOE Interest

Because of the widespread use of Ru catalysts in the Fisher Tropsch synthesis we decided to try to learn something about the atomic details of the key reaction necessary for the FT synthesis- the dissociation of CO. We found, interestingly, that atomic step defect sites on Ru are much more active for CO dissociation than smooth surfaces. Thus, for maximum kinetic rate, the practical Ru catalyst should be prepared to expose a maximum fraction of defect sites.

Future Plans

The role of Pt adatoms on the chemisorption behavior of the atomically-stepped Ru(109) surface will be investigated by reflection IR and by thermal desorption kinetics. The goal is to determine whether the Pt atoms (probably located at atomic step sites) behave as isolated atomic sites with their own electronic character, or whether they behave as more delocalized electronic entities. Understanding this will aid in understanding alloy catalysts as often used, for example, in Ru/Pt fuel cell electrodes.

Publications (2002-04)

1. J.-G. Lee, J. Ahner and J. T. Yates, Jr., "Adsorption Geometry of 4-Picoline Chemisorbed on the Cu(110) Surface: A Study of Forces Controlling Molecular Self-Assembly," *J. Am. Chem. Soc.* 124, 2772 (2002). Erratum: 124, 13636 (2002).
2. T. Zubkov, G. Morgan, Jr. and J. T. Yates, Jr., "Spectroscopic Detection of CO Dissociation on Defect Sites on Ru(109): Implications for Fischer-Tropsch Catalytic Chemistry," *Chem. Phys. Lett.*, 362, 181 (2002).
3. J-G. Lee, S-H. Hong, J. Ahner and J. T. Yates, Jr. "Surface Aligned Ion-Molecule Reaction: Direct Observation of Initial and Final Ion Momenta," *Phys. Rev. Lett.* 89, 253202-1 (2002).
4. L. Thompson, J-G. Lee, P. Maksymovych, J. Ahner and J. T. Yates, Jr. "Construction and Performance of a UHV-Compatible High Temperature Vapor Dosing System for Low Vapor Pressure Compounds," *J. Vac. Sci. Technol. A* 21, 491 (2003).
5. T. Zubkov, G.A. Morgan, Jr., J. T. Yates, Jr., O. Köhlert, M. Lisowski, R. Schillinger, D. Fick, H.J. Jansch "The Effect of Atomic Steps on Adsorption and Desorption of CO on Ru(109)" *Surface Science*, 526, 57 (2003).
6. J.-G. Lee and J. T. Yates, Jr., "Methanethiol Chemisorption on Cu(110): Chemical and Geometrical Issues Related to Self-Assembly," *J. Phys. Chem. B.* 107, 10540 (2003).
7. J-G. Lee, J. Lee and J. T. Yates, Jr., "Non-dissociative Chemisorption of Methanethiol on Ag(110)-A Critical Result for Self-Assembled Monolayers," *J. Am. Chem. Soc.* 124, 440 (2004).
8. J.-G. Lee, J. Lee and J. T. Yates, Jr., "Comparison of Methanethiol Adsorption on Ag(110) and Cu(110)-Chemical Issues Related to Self-Assembled Monolayers," *J. Phys. Chem. B.* 108, 1686 (2004).
9. G. A. Morgan, Jr., D. C. Sorescu, T. Zubkov and J. T. Yates, Jr., "The Formation and Stability of Adsorbed Formyl as a Possible Intermediate in Fischer-Tropsch Chemistry on Ruthenium," *J. Phys. Chem. B* 108, 3614 (2004).
10. J.-G. Lee and J. T. Yates, Jr., "Surface-Aligned Ion-Molecule Reaction in the Surface of a Molecular Crystal- $CD_3^+ + CD_3I \rightarrow C_2D_5^+ + DI$," submitted to *J. Am. Chem. Soc.*

Molecular Design of Hydrocarbon Oxidation Catalytic Processes

Postdocs: Qing Zhao, Hansheng Guo

Students: Min Shen

Department of Chemistry, University of California, Riverside, CA 92521

francisco.zaera@ucr.edu

Goal

To understand the molecular-level mechanistic factors that define selectivity in the catalysis of oxidation of hydrocarbons, of alkanes and alcohols in particular.

Recent Progress

Our past research has relied on a combination of modern surface-characterization techniques with well-defined surfaces under ultrahigh vacuum (UHV) conditions to look into the elementary steps that comprise catalytic oxidations. Our general conclusion based on that work is that the selectivity of those reactions is defined by the regioselectivity of dehydrogenation steps from alkyl and alkoxide surface intermediates. Figure 1 illustrates the reaction diagram underpinning this central hypothesis. Two sets of reactions are presented in this diagram to account for both oxidative coupling and chain growth in alkanes (left) and oxidation and dehydrogenation of alkanes and alcohols (right), and a common alkoxide intermediate, the result of either oxygen insertion into alkyl-surface bonds or α -dehydrogenation from adsorbed alcohols, is also indicated. In terms of dehydrogenation versus dehydration in alcohols, direct β -hydride elimination to aldehydes or ketones (the dehydrogenation product) was determined to be the preferred pathway on late transition metals. On the other hand, promotion of γ -hydride elimination may lead to the production of an oxametallacycle instead. That intermediate can then undergo oxygen extrusion to the olefin (the dehydration product). Some of our recent studies have focused on this idea.

This project was initiated with the use of 2-propyl iodide to prepare 2-propyl surface groups on a Ni(100) single crystal surface. It was found that 2-propyl moieties can easily incorporate oxygen atoms to form 2-propoxide groups, even if only on surfaces with submonolayer oxygen coverages emulating defective oxides. It was also shown that similar 2-propoxide species can be prepared by decomposition of 2-propanol. The resulting 2-propoxide moieties are stable on both clean and oxygen-treated Ni(100) surfaces up to ~ 325 K, but decompose via β -hydride elimination above that temperature to yield acetone. Additional temperature programmed desorption (TPD) experiments indicated that propene does not convert directly to acetone on these O/Ni(100) surfaces, a thought-provoking conclusion given that alkene partial oxidation is in fact performed industrially by using oxide catalysts. Our results suggest that such a process may occur via an initial hydrogenation of the alkene to an alkyl intermediate on a metal center followed by a sequence of oxygen migratory insertion and β -hydride elimination steps.

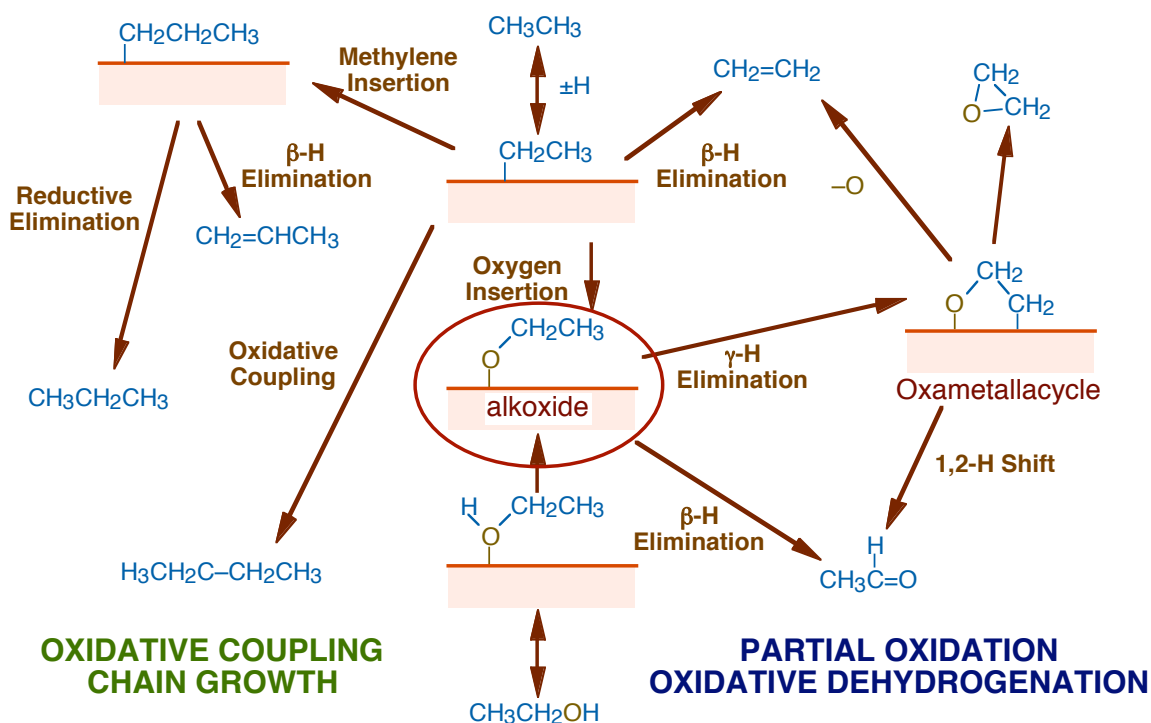


Figure 1

The chemistry of $\text{HOCH}_2\text{CH}_2\text{I}$, a precursor to surface oxametallacyclobutane, was also studied on $\text{Ni}(100)$. It was determined that a low-temperature decomposition channel of the adsorbed $\text{HOCH}_2\text{CH}_2\text{I}$ produces small amounts of ethylene (together with water) around 140 K. The activation of the remaining species occurs around 150 K to yield $-\text{O}(\text{H})\text{CH}_2\text{CH}_2-$ and 2-hydroxyethyl intermediates. The $-\text{O}(\text{H})\text{CH}_2\text{CH}_2\text{I}-$ intermediate dehydrogenates around 160 K to produce the desired $-\text{OCH}_2\text{CH}_2\text{I}-$ surface oxametallacycle, and that later isomerizes via a 1,2 hydrogen shift to yield acetaldehyde. The 2-hydroxyethyl intermediate, on the other hand, reacts around 160 K via two competing steps, a reductive elimination with surface hydrogen to produce ethanol, and a β -hydride elimination to yield surface vinyl alcohol. The vinyl alcohol converts further on the surface either by losing its oxygen atom to produce ethylene or by tautomerizing to acetaldehyde. Overall, these studies have proved that oxametallacycles may be intermediates towards the production of alcohol dehydration products (olefins), but could also lead to dehydrogenation (aldehydes and ketones).

In a separate study, the possibility of activating γ hydrogens in surface alkoxides was explored. Preliminary work using tert-butyl alcohol on $\text{Ni}(100)$ has suggested that, indeed, γ -H elimination may occur in those systems. Alternatively, the β carbon of the alkoxide may be deactivated via inductive substitutions. TPD results from studies with 1,1,1-trifluoro-2-propanol have shown an increase in activation energy for β -hydride elimination of approximately 10 kcal/mol, and the opening up of a second dehydration pathway for the adsorbed alcohol, which results in a desorption peak for 3,3,3-trifluoropropene at 437 K in TPD experiments.

DOE Interest

The combination of the results from our reactivity studies with additional work on the nature of the catalytic surface has provided us with a tentative list of characteristics for the active sites involved in hydrocarbon oxidation catalysis: (1) the need for surface metal atoms to induce the initial bond-activation of the reactant; (2) the need of a proximity between the resulting alkyl/alkoxide intermediates and oxygen surface atoms, which may require unique unsaturated coordination to be reactive; (3) the tuning of the electronic properties of the metal site to set the relative rates of β - versus γ -dehydrogenation steps, and with that the selectivity between dehydrogenation and dehydration reactions; and (4) the enhancing ability of surface hydroxides toward oxygen insertion reactions (and possibly dehydrogenation steps) on surface alkoxides. A more detailed list of this sort, which we are in the process of developing, should be helpful for the design of specific and selective hydrocarbon oxidation catalysts.

Future Plans

Regioselectivity of dehydrogenation steps as they relate to hydrocarbon oxidation processes. New experiments will involve tert-butyl species to characterize γ -H eliminations, 2-bromo-1-propanol, 1-bromo-2-propanol, and 1-chloro-2-methyl-2-propanol to test the reactivity of oxametallacycle intermediates as a function of the extent of substitutions at particular locations within the carbon backbone, allyl alcohol to explore changes in selectivity due to the weakening of the C–O bond, and propene and propyl halides to investigate the reactivity of allylic hydrogens.

Chemical reactivity on oxide and oxygen-treated metal surfaces toward chain growth processes. Experiments will be carried out with mixtures of methylene and methyl precursors and with coadsorbed ethylene to explore the potential insertions into metal-carbon bonds in competition with alkyl coupling and oxygen insertion steps. Selective deuterium isotope labeling will be employed to differentiate among the different possible mechanisms. Systematic studies will be carried out as a function of the coverages of each of the surface species involved as well.

Reactivity of different types of oxygen-based surface sites. Different preparations will be tried on several crystallographic orientations and by modifying NiO films via sputtering and/or annealing. The nature of the resulting sites will be characterized by chemical titrations and physical (XPS, PAX) methods. Their reactivity towards hydrocarbon surface species will be probed, and their effect on modifying the surface mobility of the reactants will be tested using selective isotope labeling. Differentiation among the different oxygen species will be attempted by oxygen isotope labeling. The reactivity of surface hydroxide species will be probed.

Contrasting of the chemistry on nickel versus vanadium oxides. Oxygen treatments for the preparation of different oxygen sites on vanadium will be developed, and the resulting surfaces characterized by using methodology similar to that developed for nickel. The reactivity of those surfaces toward different reactions with alkyls, allyls, alkenes and alcohols will be tested. Vanadium oxides are central components in many oxidation catalysts. Nickel and vanadium oxides are expected to represent opposite extremes within the range of oxides available for hydrocarbon oxidation catalytic applications.

Publications (2002-4)

1. Ali H. Ali and F. Zaera, Kinetic Study on the Selective Catalytic Oxidation of 2-Propanol to Acetone over Nickel Foils, *J. Mol. Catal. A*, **177**, 215-235 (2002).
2. F. Zaera, Surface Characterization and Structural Determination: Optical Methods, in *The Encyclopedia of Chemical Physics and Physical Chemistry*, J. Moore and N. Spencer, editors, Institute of Physics Publishing (UK), Vol. 2, pp. 1563-1581 (2001).
3. F. Zaera, The Surface Chemistry of Catalysis: New Challenges Ahead (Invited contribution for the special 500th issue of Surface Science), *Surf. Sci.*, **500**, 947-965 (2002).
4. F. Zaera, Kinetics of Chemical Reactions on Solid Surfaces: Deviations from Conventional Theory, *Acc. Chem. Res.*, **35**, 129-136 (2002).
5. F. Zaera, Outstanding Mechanistic Questions in Heterogeneous Catalysis, *J. Phys. Chem. B*, **106**, 4043-4052 (2002).
6. F. Zaera, Infrared and Molecular Beam Studies of Chemical Reactions on Solid Surfaces, *Int. Rev. Phys. Chem.*, **21**, 433-471 (2002).
7. H. Guo, D. Chrysostomou, J. Flowers and F. Zaera, The Effect of Coadsorbed Oxygen on the Chemistry of Ammonia over Ni(110) Single Crystal Surfaces, *J. Phys. Chem. B*, **107(2)**, 502-511 (2003).
8. H. Guo and F. Zaera, The Reactivity of Hydroxyl Groups towards Ammonia on Ni(110) Surfaces, *Surf. Sci.*, **524/1-3**, 1-14, (2003).
9. F. Zaera, The Surface Chemistry of Hydrocarbon Partial Oxidation Catalysis, *Catal. Today*, **81(2)**, 149-157 (2003).
10. H. Guo and F. Zaera, Reactivity of Hydroxyl Species from Coadsorption of Oxygen and Water on Ni(110) Single-Crystal Surfaces, *Catal. Lett.*, **88(3-4)**, 95-104 (2003).
11. Q. Zhao and F. Zaera, Switching of Alcohol Oxidation Mechanism on Nickel Surfaces by Fluorine Substitution, *J. Am. Chem. Soc.*, **125(36)**, 10776-10777 (2003).
12. Q. Zhao and F. Zaera, Adsorption and Thermal Conversion of 2-Iodoethanol on Ni(100) Surfaces: Hydroxyalkyls and Oxametallacycles as Key Intermediates during the Catalytic Oxidation of Hydrocarbons, *J. Phys. Chem. B*, **107(34)**, 9047-9055 (2003).
13. N. Gleason, J. Guevremont and F. Zaera, Thermal chemistry of 2-Propanol and 2-Propyl Iodide on Clean and Oxygen-Pretreated Ni(100) Single Crystal Surfaces, *J. Phys. Chem. B*, **107 (40)**, 11133-11141 (2003).
14. H. Guo and F. Zaera, Thermal Chemistry of Diiodomethane on Ni(110) Surfaces: I. Clean and Hydrogen Predosed, *Surf. Sci.*, **547(3)**, 284-298 (2003).
15. H. Guo and F. Zaera, Thermal Chemistry of Diiodomethane on Ni(110) Surfaces: II. Effect of Coadsorbed Oxygen, *Surf. Sci.*, **547(3)**, 299-314 (2003).
16. F. Zaera, Surface Chemistry of Hydrocarbon Fragments on Transition Metals: Towards Understanding Catalytic Processes (2003 North America Catalysis Society Paul H. Emmett Award Lecture), *Catal. Lett.*, **91(1-2)**, 1-10 (2003).
17. F. Zaera, Mechanistic Requirements for Catalytic Active Sites, *J. Phys.: Cond. Matter*, in press.
18. Z. Ma and F. Zaera, Heterogeneous Catalysis by Metals, in *Encyclopedia of Inorganic Chemistry*, Second Edition, R. B. King, editor-in-chief, John Wiley & Sons, in press.
19. F. Zaera, Mechanisms of Hydrocarbon Conversion Reactions on Heterogeneous Catalysts: Analogies with Organometallic Chemistry, *Top. Catal.*, in preparation.

Molecular Level Design of Chiral Heterogeneous Catalysts

Students: Rees Rankin, Joanna James, Layton Baker, Ye Huang, Luke Burkholder,
Tao Zheng
Postdocs: Dario Stacchiola, J. Kubota

Goal

To prepare surfaces having chiral structures of different origin and optimize their enantioselectivity for adsorption and catalysis.

Recent Progress

Surfaces having chiral structures at the atomic scale can catalyze reactions enantioselectively. Naturally chiral surfaces can be created either by starting with a chiral bulk structure or by taking an achiral bulk structure such as that of a metal and cleaving along a plane that exposes a chiral surface. Chiral surfaces can also be made by templating an otherwise achiral surface with chiral organic molecules. The enantioselectivity of surfaces prepared in these ways is being explored through the use of a number of chiral molecular probes.

Previous work has shown that the adsorption of R- or S-2-butanol on the Pd(111) surface can be used to create an enantioselective, templated chiral surface. The enantioselectivity has been probed by the adsorption of R- or S-propylene oxide where coverages are measured from both its desorption spectrum and its infrared-absorption spectrum. Enantioselective adsorption of the propylene oxides is observed over a narrow range of the 2-butanol coverage near $\Theta_{2\text{-ButO}} \sim 1/2$ monolayer. The enantioselective ratio for adsorption of the propylene oxides on the templated surface is defined as

$$ER_{2\text{-ButO}} = \frac{\Theta_{\text{R-PropyleneOxide}}}{\Theta_{\text{S-PropyleneOxide}}}$$

and can reach a value as high as $ER_{2\text{-Butanol}} = 2$.

Recent work has made use of R- and S-2-methyl butanoic acid as the chiral template on Pd(111) and has shown that for this templating agent there is no enantioselective adsorption of propylene oxides ($ER_{2\text{-Methyl Butanoic Acid}} = 0$). This may arise from the fact that the chiral butyl group is now located further away from the surface than in the case of the 2-butanol templates and can rotate more freely, thus reducing its chirality. Functionalizing the butyl group with an amine (2-amino butanoic acid) anchors the butyl group to the surface and restores enantioselectivity for the adsorption of propylene oxide,

$ER_{2\text{-Amino Butanoic Acid}} = 1.75 \pm 0.15$. Using amino acids of various types it has been possible to observe enantioselectivity ratios as high as $ER_{\text{Amino Acid}} \approx 2$ on Pd and Pt surfaces. Initial work with other amino acids suggests that the ER value decrease as the size of the functional group on the amino acid increases. This may be due to the formation of larger “chiral” pockets.

Initial work using Density Functional Theory (DFT) to explore the structures of adsorbed amino acids has begun with the Cu(110) and Cu(100) surfaces in order to resolve known issues regarding the structures of the ordered overlayers that they form on these surfaces. Earlier experimental studies of glycine and alanine adsorption on these surfaces showed that both molecules form highly structured adlayers, but the determination of the structures of these adlayers from experimental data was controversial. For glycine/Cu(110), the existence of two distinct adlayer domains, one heterochiral and one homochiral, was suspected based on STM images. This conclusion has been called into question by x-ray photoelectron diffraction (XPD) data that did not support the existence of multiple distinct adlayers. DFT calculations show unequivocally that the heterochiral adlayer is the only structure that appears on Cu(110), and that the multiple domains observed with STM can be understood as rotationally equivalent domains of this single adlayer. In contrast, calculations for glycine on Cu(100) show that two structurally distinct adlayers appear with essentially equal energies. Both of these structures are consistent with the extant XPD data from glycine/Cu(100). Similar calculations for alanine adlayers on Cu(110) and Cu(100) have shown that the binding footprint of glycine on Cu surfaces provides an excellent starting point for describing the binding of alanine and other amino acids.

The most widely studied enantioselective heterogeneous catalyst is based on the templating of Pt with cinchonidine. This catalyst is used in solution for the enantioselective hydrogenation of ketoesters. Infrared spectroscopy has been used to study the adsorption of cinchonidine, lepidine and other small models of cinchonidine on Pt surfaces. The properties of the template are influenced by the solvent. For example, the thermal stability of cinchonidine adsorbed from CCl_4 is increased by dissolution of hydrogen into the solution. The solvent also has a strong influence on the enantioselectivity of templated hydrogenation catalysts. The polarity of the solvent has been found to influence the kinetics of cinchonidine desorption into solution in a manner that is correlated to its influence on the enantioselectivity of the templated catalyst.

Adsorption of the cinchonidine template on Pt is very sensitive to the concentration in solution. At low concentrations little cinchonidine is adsorbed. At intermediate concentrations the cinchonidine is adsorbed with the quinoline ring parallel to the surface while at high concentrations the ring is tilted away from the surface. The optimum enantioselectivity occurs under conditions that are consistent with a template adsorption geometry having the quinoline ring parallel to the surface.

Finally, naturally chiral surfaces have been prepared by exposing high Miller index planes of fcc metals such as Cu. Electron diffraction has shown that these are indeed chiral and desorption studies have shown that their enantioselectivity originates with kinks on the surfaces. The most recent work has extended this work to studies of reactivity on these surfaces. Using chiral 2-bromobutane it has been possible to create chiral 2-butyl groups on naturally chiral Cu surfaces. The kinetics of their -hydride elimination has been found to be enantioselective.

DOE Interest

Enantioselectivity is perhaps the most subtle form of chemical selectivity. Understanding enantioselective surface chemistry can have broad impact on our understanding of selectivity in many other heterogeneous catalytic processes. Enantioselectivity is critical to the production of numerous fine chemicals used for bioactive applications such as pharmaceuticals. Heterogeneous catalysis has a number of attractive features that offer opportunities for its use in fine chemical synthesis.

Future Plans

Future work is centered on exploration of the enantioselectivity of surfaces templated with amino acids, related compounds, and naphthylethylamine (a model for cinchonidine). Pt, Pd and Cu surfaces will be templated with these chiral compounds in order to explore the influence of substrate on their enantioselectivity. In addition, efforts will be made to explore the use of new chiral probes such as 3-methylcyclohexanone, 2-chlorobutane, and 2-aminobutane. DFT calculations will be used to model the interaction of these probes with amino acids in the gas phase and with amino acids on Cu surfaces. Amino acids are also known to induce the reconstruction of Cu surfaces to expose high Miller index facets which are naturally chiral. Efforts are being made to develop a process to prepare high surface area Cu powders with surfaces that are homochiral and thus can be used at a macroscopic level for enantioselective separations and catalysis.

Relevant Publications

1. F. Zaera, Kinetics of Chemical Reactions on Solid Surfaces: Deviations from Conventional Theory, *Acc. Chem. Res.*, **35**, 129-136 (2002).
2. J. Kubota, Z. Ma and F. Zaera, In-Situ Characterization of Adsorbates in Solid-Liquid Interfaces by Reflection-Absorption Infrared Spectroscopy, *Langmuir*, **19**(8), 3371-3376 (2003).
3. Z. Ma, J. Kubota and F. Zaera, The Influence of Dissolved Gases on the Adsorption of Cinchonidine from Solution onto Pt Surfaces: An In-Situ Infrared Study, *J. Catal.*, **219**(2), 404-416 (2003).
4. W. Chu, R. J. LeBlanc, C. T. Williams, J. Kubota and F. Zaera, Vibrational Band Assignments for the Chiral Modifier Cinchonidine: Implications for Surface Studies, *J. Phys Chem. B*, **107**(51), 14365-14373 (2003).
5. D. Stacchiola, L. Burkholder and W.T. Tysoe, Enantioselective Chemisorption on a Chirally Patterned Surface in Ultrahigh Vacuum: Adsorption of Propylene Oxide on 2-butoxy-Covered Pd(111), *J. Am. Chem. Soc.*, **124**, 8984 (2002)
6. Dario Stacchiola, Luke Burkholder and Wilfred T. Tysoe, Enantioselective Chemisorption on a Chirally Modified Surface in Ultrahigh Vacuum: Adsorption of Propylene Oxide on 2-butoxy-Covered Pd(111), *J. Mol. Catal A: Chemical*, in press
7. F. Roma, D. Stacchiola, G. Zgrablich and W. T. Tysoe, Theoretical Analysis of the Coverage Dependence of Enantioselective Chemisorption on a Chirally Patterned Surface, *Journal of Chemical Physics*, **118**, 6030 (2003)
8. F. Romá, D. Stacchiola, W.T. Tysoe and G. Zgrablich, Lattice-gas Modeling of Enantioselective Adsorption by Template Chiral Substrates, *Physica A.*, in press
9. H. C. Poon, M. Weinert, D. K. Saldin, D. Stacchiola, T. Zheng and W. T. Tysoe, Structure Determination of Disordered Organic Molecules on Surfaces from the Bragg Spots of Low Energy Electron Diffraction and Total Energy Calculations, *Phys. Rev. B.*, **69**, 35401 (2004)

This page intentionally left blank.